

A life-cycle approach to optimise Higher Education building design strategies for future UK climate projections

Submitted to
the University College London
in Fulfilment of the Requirements for the Degree of
Doctor of Philosophy

by

Eleni Davidson

to

**BARTLETT SCHOOL OF ENVIRONMENT, ENERGY AND RESOURCES
INSTITUTE FOR ENVIRONMENTAL DESIGN AND ENGINEERING**

Supervisors: Dejan Mumovic, Yair Schwartz

November 13, 2025

DECLARATION

“I, Eleni Davidson confirm that the work presented in my thesis is my own. Where information has been derived from other sources, I confirm that this has been indicated in the thesis.”

University College London
November 13, 2025

ABSTRACT

Refurbishment of higher education buildings offers potential for substantial carbon savings but involves complex trade-offs between embodied and operational emissions, often evaluated using static assumptions over the building’s life-cycle. This research develops a dynamic Life-Cycle Assessment and Climate Change Adaptation (LCA-CCA) optimisation methodology to assess refurbishment strategies under future climate and grid decarbonisation scenarios. The approach was applied to three mixed-use urban university buildings, evaluating life-cycle carbon and life-cycle cost impacts over a 60-year period using the multi-objective genetic algorithm, NSGA-II, to identify Pareto-optimal solutions.

Findings demonstrated that air-source heat pumps (ASHPs) had a far greater influence on life-cycle carbon reduction than fabric upgrades, with all three case studies exhibiting baseline airtightness and thermal performance suitable for efficient ASHP operation. Despite higher embodied impacts from refrigerant leakage and end-of-life recovery, ASHPs consistently delivered the greatest overall carbon savings, reinforcing the cumulative life-cycle benefits of system electrification, particularly under faster grid decarbonisation scenarios. Mixed-mode ventilation also emerged as a key driver of both carbon and cost savings. Overall, system upgrades and control strategies were found to offer greater benefits than extensive fabric interventions.

The analysis also demonstrated an increasingly nuanced balance between embodied and operational carbon when aligned with system electrification and grid decarbonisation. Measures such as triple glazing or insulation additions beyond regulatory standards provided limited or adverse effects on life-cycle carbon when coupled with ASHPs, despite benefits under gas-based systems. Finally, long-term stability in annual building life-cycle carbon emissions was achieved only when rapid grid decarbonisation was paired with full electrification of heating systems. Under slower pathways, all other design combinations showed continued increases in carbon impact over the buildings’ 60-year lifespan. Overall, these findings emphasise the need to consider dynamic uncertainties in LCA, incorporating changing interactions between building design, wider energy systems, and climate conditions to ensure refurbishment strategies remain robust throughout the transition to net zero.

IMPACT STATEMENT

This thesis advances the academic field of non-domestic refurbishment techniques by incorporating dynamic considerations of future climate and decarbonisation pathways into the life-cycle assessment of Higher Education buildings. The case study findings help to progress understanding of how design preferences for typologically diverse HE buildings change under different decarbonisation scenarios. Learnings from applying this methodology using advanced techniques, such as genetic algorithm optimisation, also have the potential to influence curriculum development in courses at the intersect of architecture and engineering. By providing real-world examples of integrating climate change adaptation and LCA into the design process, this thesis offers a replicable methodology for examining other non-domestic building typologies, fostering cross-disciplinary research collaboration.

In professional and industry contexts, the adopted methodology provides strategic solutions for refurbishment projects to align more closely with net-zero carbon targets. The approach adopts practical and applied design solutions, equipping architects, engineers, and sustainability consultants with tools to balance operational and embodied carbon impacts while maintaining cost-effectiveness. These findings align closely with the goals of certification systems like LEED, BREEAM and WELL, providing opportunities to enhance the climate-resilience criteria in these standards. Additionally, the proposed framework for integrating LCA and CCA into the design process could be further developed, with the potential to inform design protocols for refurbishment projects.

From a policy perspective, this work improves understanding of how decarbonisation pathways, largely shaped by national and regional policy frameworks, influence optimal building design and retrofit strategies. The research highlights the importance of aligning building intervention strategies with future energy grid scenarios and policy-driven decarbonisation targets, supporting the development of informed, adaptive policies across the HE sector and beyond.

From a societal perspective, this research contributes to improving the environmental quality within HE buildings by promoting climate-resilient and sustainable environments for students and staff. By offering insights into achieving an optimal balance between carbon reductions and cost-effectiveness, the findings provide universities with actionable strategies to enhance environmental performance. This presents opportunities for institutions to demonstrate corporate responsibility and ethical leadership in sustainability.

The findings have already begun to generate impact through dissemination

at academic and industry events. Presentations at Energy Resilience and the Built Environment Centre for Doctoral Training (ERBE CDT) research events, the Building Research Establishment (BRE), and the Annual Symposium of Architectural Research (ATUT) 2022 conference have shared the research outcomes with key stakeholders and researchers. Regular engagement with the industry sponsor, Feilden Clegg Bradley, provided valuable feedback and ensured practical relevance.

ACKNOWLEDGEMENT

This research would not have been possible without the support and contributions of many individuals and institutions. I am deeply grateful to the Energy Resilience and the Built Environment Centre for Doctoral Training (EP/S021671/1), funded by the UK Engineering and Physical Sciences Research Council, with additional financial support from Feilden Clegg Bradley Studios. Their resources and network provided a strong foundation for this work and made the program an enriching experience.

I extend my heartfelt thanks to my academic supervisors, Professor Dejan Mumovic and Dr. Yair Schwartz, at the Bartlett School of Environment, Energy, and Resources, for their invaluable guidance, encouragement, and expertise throughout this journey. I am also thankful to my industrial supervisors, Joe Jack Williams and Ian Taylor, at Feilden Clegg Bradley Studios, whose expert insights have been instrumental in shaping this research.

Special thanks to Dr. Yi Zhang for guidance with JEPlus software and to Dr. Ivan Korolija and Dr. Nishesh Jain for providing valuable modelling assistance. Their technical expertise have been greatly appreciated.

I am profoundly thankful to my friends and family for their unwavering support and encouragement, which kept me motivated through the most challenging moments.

Finally, to my husband, Hugh Larkin, your constant support and ability to help me keep perspective have been a source of strength throughout this process.

Contents

Contents	vii
List of Figures	xi
List of Tables	xiv
1 Introduction	1
1.0.1 Context	1
1.0.2 Higher Education Sector	1
1.0.3 Life-Cycle Analysis	2
1.0.4 Building Performance Under a Changing Climate	3
1.1 Research Hypothesis, Questions, and Objectives	4
1.2 Contribution to Knowledge	6
2 Literature Review	8
2.1 Overview: Energy and Carbon Performance of the UK Higher Education Sector	8
2.2 Embodied carbon in building redevelopment	15
2.2.1 Embodied Carbon as a Life-Cycle Component	15
2.2.2 Calculation Methods and Protocols	16
2.2.3 Drivers for Embodied Carbon Reduction	17
2.2.4 Challenges and Limitations of Embodied Carbon Assessments	18
2.3 Life cycle carbon in higher education building redevelopment	21
2.3.1 Non-recurring emissions	21
2.3.2 Repair and maintenance	22
2.3.3 Operational carbon impacts	22
2.4 Future considerations	23
2.4.1 Cost implications	23
2.4.2 Climate change impacts	24
2.4.3 Grid Decarbonisation	26
2.5 Computational methods for reducing life-cycle carbon and life-cycle cost	28
2.5.1 Case studies and applications	30
2.6 Knowledge Gap	36

3	Methodology	38
3.1	Methodological Development	38
3.2	Methods Overview	40
3.3	Methods 1: Framework Development	41
3.3.1	Framework Principle	41
3.3.2	Life-cycle Objective Functions	41
3.3.3	Framework Optimisation Strategy	42
3.3.4	Modelling tools	45
3.3.5	Summary of framework inputs & outputs	45
3.3.6	LCA Standards & Calculations	48
3.3.7	Scenario Analysis	55
3.4	Methods 2: Case Study Development	59
3.4.1	Principle	59
3.4.2	Case Study Selection	59
3.4.3	Modelling, Calibration & Validation	60
3.4.4	ECM selection process	62
3.5	Results Reporting and Visualisation	66
3.6	Summary of Methods	68
4	Case Study 1	69
4.1	Overview	69
4.2	CS1: Model Development and Validation	70
4.2.1	Secondary Dataset Analysis	70
4.2.2	Model development	73
4.2.3	Calibration Results	76
4.3	CS1: Framework Development	78
4.3.1	Preliminary testing	78
4.3.2	ECM selection	79
4.3.3	Modelling Inputs: Carbon Calculations	80
4.3.4	Modelling Inputs: Cost Calculations	84
4.4	CS1: Framework Implementation	86
4.4.1	Life-cycle optimisation results	86
4.4.2	Scenario analysis	92
5	Case Study 2	98
5.1	Overview	98
5.2	CS2: Model Development and Validation	99
5.2.1	Secondary Dataset Analysis	99
5.2.2	Model development	100
5.2.3	Calibration Results	101
5.3	CS2: Framework Development	102
5.3.1	ECM selection	102
5.3.2	Modelling Inputs: Carbon Calculations	104
5.3.3	Modelling Inputs: Cost Calculations	108

5.4	CS2: Framework Implementation	110
5.4.1	Life-cycle optimisation results	110
5.4.2	Scenario analysis	115
6	Case Study 3	120
6.1	Overview	120
6.2	CS3: Model Development and Validation	121
6.2.1	Secondary Dataset Analysis	121
6.2.2	Model development	122
6.2.3	Calibration Results	124
6.3	CS3: Framework Development	125
6.3.1	ECM selection	125
6.3.2	Modelling Inputs: Carbon Calculations	127
6.3.3	Modelling Inputs: Cost Calculations	130
6.4	CS3: Framework Implementation	132
6.4.1	Life-cycle optimisation results	132
6.4.2	Scenario analysis	139
7	Discussion	144
7.1	Overview	144
7.2	Synthesis of case study findings	144
7.2.1	Future Energy, Carbon, and Cost in HE Building Design . .	144
7.2.2	Aggregated Impact over Time	149
7.3	Responding to Research Questions	150
7.4	Scaling-up and Methodological Development	153
7.4.1	Scaling-up	153
7.4.2	Methodological Development	156
7.5	Integrating CCA-LCA Framework into the Design Process	157
8	Conclusion	161
8.1	Summary of Key Findings	161
8.2	Final Remarks	163
8.3	Limitations and Further Development	164
8.3.1	Framework Development	166
8.3.2	Case Study Application	169
	References	170
	Appendices	193
A	ASHP EMS script	193
B	Preliminary Testing: Roof Albedo	195
C	CS1 Preliminary Testing: North window-to-wall ratio (WWR)	197

D	Embodied Carbon (A1-A3) Material List	198
E	CS1 LCA Calculations: Supplementary detail	200
F	CS2 LCA Calculations: Supplementary detail	205
G	CS3 LCA Calculations: Supplementary detail	213
H	Build-up schematics and calculations	218
I	CS1 results	220
	I.0.1 Scenario 1: Linear Regression Statistical Output	220
J	CS2 Results	225
	J.0.1 Scenario 1: Linear Regression Statistical Output	225
K	CS3 Results	228
	K.0.1 Scenario 1: Linear Regression Statistical Output	228

List of Figures

2.1	Timeline of UK HE sector development.	9
2.2	Breakdown of scope 1, 2 and 3 carbon emissions across the tertiary education sector in academic year 2020-21 [13].	11
2.3	Modular components of the various whole life carbon building assessment, according to BS EN 15978 [17].	15
2.4	Typical procedural steps involved in GA optimisation, from [126].	29
2.5	Character string representation of building design characteristics as genes within the GA optimisation process.	29
3.1	Simplified overview of research process.	40
3.2	Rapid data-driven optimisation framework for CCA and LCA. LHS=Latin Hypercube Sampling.	44
3.3	Overview of CCA-LCA framework including all stages, inputs and outputs.	47
3.4	Electricity carbon emission factor scenarios, adapted from [158, 157].	55
3.5	Predicted share of green gas in the gas network, extrapolated from National Grid ESO FES: ‘Falling Short’ pathway [157].	56
3.6	Electricity and gas fuel price pathways.	57
3.7	CS1 EMS scripted ASHP operation compared to baseline district energy network (DEN) consumption for a week in February.	64
3.8	Structure of results leading into CS synthesis in the discussion.	66
3.9	Key methodological steps, interrelationships and outputs in line with core study objectives.	68
4.1	CS1 profile.	69
4.2	CS1 measured and extrapolated low-temperature hot water and domestic hot water values for 2018.	72
4.3	CS1 measured vs simulated calibrated outputs for 2018.	77
4.4	Assembly section: CS1 external wall build-up demonstrating all elements included in embodied carbon (EC) calculations and the position of additional internal mineral wool (MW) insulation (@@ins1@@).	81
4.5	Correlation between rated capacity (RC), mass and refrigerant mass established from ASHP manufacturers’ specifications [188].	83

4.6	DEN carbon factor forecast based on changing gas and electricity CEF projections.	84
4.7	Optimised LCCF and LCC values.	86
4.8	NSGA-ii optimisation results for CS1 scenario 1.	87
4.9	Weighted coefficients (β) of categorical variables in linear regression analysis for Scenario 1.	89
4.10	Comparison of pareto optimal solutions across decarbonisation scenarios. Points represent group averages; ranges depict variance of LCCF and LCC across pareto optimal solutions.	92
4.11	Average share of embodied versus operational carbon components across pareto solutions for scenarios 1 and 2.	94
4.12	CS1 change in LCCF of pareto optimal solutions over time for S1 and S2.	95
5.1	CS2 profile.	98
5.2	CS2: End-use disaggregated metered monthly electricity consumption data for Aug 2016 - Jul 2017.	100
5.3	Assembly section: CS2 external wall build-up demonstrating the position of additional internal MW insulation (@@ins1@@).	106
5.4	Correlation between RC, mass and refrigerant mass established from literature and VRF specifications by manufacturers Carrier and Daikin [193, 194].	107
5.5	NSGA-ii optimisation results for CS2 scenario 1.	111
5.6	Weighted coefficients (β) of categorical variables in linear regression analysis for Scenario 1.	112
5.7	LCCF vs. LCC Comparison of pareto optimal solutions across decarbonisation scenarios. Points show group averages; error bars represent ranges.	116
5.8	Average share of embodied versus operational carbon components across pareto solutions for scenarios 1 and 2.	117
5.9	CS2 change in LCCF of pareto optimal solutions over time for scenario 1 and 2.	118
6.1	CS3 profile.	120
6.2	CS3: End-use disaggregated metered monthly energy consumption data for 2021-2022.	122
6.3	Assembly section: CS3 external wall build-up demonstrating all elements included in EC calculations and the position of additional internal MW insulation (@@IWI@@).	129
6.4	Optimised LCCF and LCC values.	132
6.5	NSGA-ii optimisation results for CS3 scenario 1.	133
6.6	Weighted coefficients (β) of categorical variables in linear regression analysis for Scenario 1.	135

6.7	LCCF vs. LCC Comparison of pareto optimal solutions across decarbonisation scenarios. Points show group averages; error bars represent ranges.	139
6.8	Average share of embodied versus operational carbon components across pareto solutions for scenarios 1 and 2.	141
6.9	CS3 change in LCCF of pareto optimal solutions over time for scenario 1 and 2.	142
7.1	Case study comparison of metrics under current and future climates.	145
7.2	Ranges from Pareto-front values for EC and OC across three case studies and various decarbonisation pathways.	147
7.3	Aggregated LCCF over 60 year period across case studies for S1 and S2.	150
7.4	CIBSE TM46 current and predicted benchmarked EUI, simulated under 2022 and 2050 weather data [190].	155
7.5	Suggested framework for integration of LCA-CCA into wider design process.	158
F.1	Relationship between natural gas boiler capacity and mass, extrapolated from manufacturers specifications [213, 214, 215].	207
H.1	Schematic demonstrating the calculation of volumes per FU used in EC calculations for PIR insulation and plasterboard.	218
H.2	Assembly section: PIR insulated plasterboard reveal detailing from the Zero Carbon Hub thermal bridging guide [186].	219
I.1	CS1 DEN scenario 1 linear regression model statistics for LCCF. . .	221
I.2	CS1 DEN scenario 1 linear regression model statistics for LCC. . .	222
I.3	CS1 ASHP scenario 1 linear regression model statistics for LCCF. .	223
I.4	CS1 ASHP scenario 1 linear regression model statistics for LCC. . .	224
J.1	CS2 scenario 1 linear regression model statistics for LCCF.	226
J.2	CS2 scenario 1 linear regression model statistics for LCC.	227
K.1	CS3 NGB scenario 1 linear regression model statistics for LCCF. . .	229
K.2	CS3 NGB scenario 1 linear regression model statistics for LCC. . .	230

List of Tables

2.1	Life-cycle optimisation case studies of non-domestic buildings: Location, building typologies and optimisation parameters.	31
2.2	Methods, frameworks, objectives and assumptions used in optimisation studies in the non-domestic sector. NA = not applicable, NS = not stated.	33
3.1	Key methodological challenges, principles, and implementation in this study. .	38
3.2	BS EN 15978:2011 life-cycle stages and calculation assumptions adapted from RICS [17, 19].	50
3.3	Scope of analysis: Inclusions and exclusions.	53
3.4	Summary of adopted scenarios with 60 year average carbon factors and fuel prices.	58
3.5	Summary of the case study building characteristics.	59
3.6	Categories, types, and sources of secondary data used for the development and calibration of building-level case study models. . . .	60
3.7	Acceptable CV(RMSE) and NMBE tolerances for monthly calibration as stated by ASHRAE (2014) [176].	62
3.8	energy conservation measure (ECM) toolkit.	65
4.1	Workshop (WS) lighting and power densities and schedules obtained from sub-metered data for annual period of 2018.	71
4.2	CS1 operational stage observations from sub-metered data.	72
4.3	CS1 primary constructions and thermal properties of existing building.	73
4.4	Flow and return set-point temperatures for CS1 low-temperature hot water and chilled water circuits. (MSCB: multi-service chilled beam; FCU: fan-coil unit; AHU: air-handling unit; DH: district heating).	74
4.5	Calibration results for CS1. Target monthly validation criteria: $C_v(\text{RMSE}) < 15\%$, $\text{NMBE} \pm 5\%$ [176].	76
4.6	Summary of findings from preliminary studies for CS1.	78
4.7	Assigning genes and possible values for implementing into multi-objective optimisation framework.	79

4.8	Calculated EC of construction elements for CS1, including materials, volume per functional unit (FU), assumptions impacting the calculations, and total EC for each element. Items shown in red are interventions. Waste rates obtained from [163]; expected lifespan from [77, 19]. Manufacture location: Local (L), National (N), European (E).	80
4.9	EC calculation assumptions for ASHP.	83
4.10	Calculated carbon emission factors for the DEN from 2013-2020. . .	84
4.11	Calculated capital expenditure (CapEx) of construction elements for CS1, including materials, volume per FU and replacement costs. Items shown in red are interventions. Expected lifespan from [77, 19].	85
4.12	Summary of grid decarbonisation rate scenario alternatives; both S1 and S2 adopt the fluctuating fuel price pathways described in section 3.3.7.	92
4.13	Recurring pareto optimal solutions across S1 and S2.	96
5.1	CS2 operational stage observations from sub-metering campaign. . .	99
5.2	CS2 primary constructions and thermal properties of existing building.	100
5.3	Calibration results for CS2. Target monthly validation criteria: $C_v(\text{RMSE})$ 15%, $\text{NMBE} \pm 5\%$ [176].	101
5.4	Assigning genes and variable alterantives for implementation into the multi-objective optimisation framework.	102
5.5	Calculated EC of construction elements for CS2, including materials, volume per FU, assumptions impacting the calculations, and total EC for each element. Items shown in red are interventions. Waste rates obtained from [163]; expected lifespan from [77, 19]. Manufacture location: Local (L), National (N), European (E). . . .	105
5.6	EC calculation assumptions for ASHP versus VRF, obtained from literature, manufacturers' specifications and government guidelines [189, 195, 196].	107
5.7	Calculated CapEx of construction elements for CS2, including materials, volume per FU and replacement costs. Items shown in red are interventions. Expected lifespan from [77, 19].	109
5.8	Summary of grid decarbonisation rate scenario alternatives; both S1 and S2 adopt the fluctuating fuel price pathways described in section 3.3.7.	115
6.1	Data cleaning rules dependant on number of consecutive missing data points for the CS3 metered hourly dataset.	122
6.2	CS3 primary constructions and thermal properties of existing building.	123
6.3	CS3 operational energy use dataset observations.	124

6.4	Calibration results for CS3. Target monthly validation criteria: $C_v(\text{RMSE})$ 15%, $\text{NMBE} \pm 5\%$ [176].	124
6.5	Assigning genes and variable alternatives for implementation into the multi-objective optimisation framework.	125
6.6	Calculated EC of construction elements for CS3, including materials, volume per FU and assumptions impacting the calculations. Items shown in red are interventions. Waste rates obtained from [163]; expected lifespan from [77, 19]. Manufacture location: Local (L), National (N), European (E).	128
6.7	Calculated CapEx of construction elements for CS3, including materials, volume per FU and replacement costs. Items shown in red are interventions. Expected lifespan from [77, 19].	131
6.8	Summary of grid decarbonisation rate scenario alternatives; both S1 and S2 adopt the fluctuating fuel price pathways described in section 3.3.7.	139
B.1	Metrics and values adopted to represent high albedo properties. . .	195
B.2	CS1 simulated annual energy consumption for baseline and high albedo roof.	195
C.1	Impact of varying the N-facade WWR on annual normalised energy consumption by end-use and total operational carbon.	197
D.1	A1-A3 emissions per kg of material; most values modified by the densities provided.	199
E.1	air source heat pump (ASHP) specifications for various models manufactured by Carrier [188].	200
E.2	Calculated EC of construction elements for CS1, including materials, volume per FU and assumptions impacting the calculations. For manufacture, L=local, N=national, E=European.	201
E.3	E.2 (continued)	202
E.4	E.3 (continued)	203
E.5	Cost of two stage air-to-water heat pump for low-temperature hot water use, based on data from [212] and extrapolated based on calculated output capacity from each simulation run. Initial price discounted by two years to reflect estimated costs for 2022 starting year.	204
E.6	MVHR unit and ductwork costs, discounted based on price from Stage D appendices from 2014. Life-spans obtained from [77]. . . .	204
F.1	variable refrigerant flow (VRF) specifications for various models manufactured by (1) Daikon and (2) Carrier [194, 193].	205
F.2	NGB specifications for various models manufactured by [213, 214, 215].	206

F.3	MVHR components by weight, according to [198]. From ProAir PA600PLI EPD: “C3. Waste processing: In the C3 phase, it is assumed that the HRV units and the installed components (such as: ducting, wiring, switches, etc.) are shredded for recycling or landfilling. It is assumed that 100% of the metals, plastics and PCBs are recycled. The remaining materials are assumed to be landfilled. C4. Disposal: In C4, the mass of material per unit that goes to landfill is the mass of the HRV units, less the mass of recyclable materials (metals, plastic and PCBs) per unit” [198].	207
F.4	Calculated EC of construction elements for CS2, including materials, volume per FU and assumptions impacting the calculations. For manufacture, L=local, N=national, E=European.	208
F.5	F.4 (continued)	209
F.6	Extrapolation of two stage air-to-water heat pump for low-temperature hot water use, based on data from [212], and extrapolated based on calculated output capacity from each simulation run. Initial price discounted by two years to reflect estimated costs for 2022 starting year.	210
F.7	MVHR unit and ductwork costs, discounted based on price from Stage D appendices from 2014. Life-spans obtained from [77]. . . .	210
F.8	VRF unit costs obtained from manufacturers specifications [193], and extrapolated based on calculated output capacity from each simulation run.	211
F.9	NGB unit costs obtained from [212], and extrapolated based on rated capacity from each simulation run. Description: Commercial; Condensing Gas boiler; Low Nox floor standing condensing boiler with high efficiency modulating premix burner; Stainless steel heat exchanger.	212
G.1	Calculated EC of construction elements for CS3, including materials, volume per FU and assumptions impacting the calculations. For manufacture, L=local, N=national, E=European.	214
G.2	G.1 (continued)	215
G.3	Cost of two stage air-to-water heat pump for low-temperature hot water use, based on data from [212], and extrapolated based on calculated output capacity from each simulation run. Initial price discounted by two years to reflect estimated costs for 2022 starting year.	216
G.4	MVHR unit and ductwork costs, discounted based on price from Stage D appendices from 2014. Life-spans obtained from [77]. . . .	216
G.5	NGB unit costs obtained from [212], and extrapolated based on rated capacity from each simulation run. Description: Commercial; Condensing Gas boiler; Low Nox floor standing condensing boiler with high efficiency modulating premix burner; Stainless steel heat exchanger.	217

List of Abbreviations

ASHP air source heat pump	xvi
BAU Business-as-usual	92
BEM building energy modelling	30
BL baseline	195
CapEx capital expenditure	xv
CCA climate change adaptation	2
CCS carbon capture and storage	56
CEF carbon emission factor	27
COP coefficient of performance	64
CVRMSE Coefficient of Variation of Root Mean Square Error	61
DEC Display Energy Certificate	12
DEN district energy network	70
DTS dynamic thermal simulation	59
EC embodied carbon	xi
ECM energy conservation measure	xiv
EMS energy management system	63
EOL end-of-life	82
EPD Environmental Product Declarations	17
EUI energy use intensity	4
FES Future Energy Scenarios	55
FCU fan coil unit	103
FU functional unit	80
GA genetic algorithm	4
GHG greenhouse gas	1
GIA gross internal area	1
GWP global warming potential	20
HA high albedo	195
HE higher education	1
HEI higher education institutions	8

HVAC heating, ventilation and air conditioning	16
IEQ indoor environmental quality	2
IWI internal wall insulation	91
LCA life-cycle analysis	2
LCC life-cycle cost	3
LCCF life-cycle carbon footprint	2
MOO multi-objective optimisation	28
MVHR mechanical ventilation with heat recovery	43
MW mineral wool	xi
NCM National Calculation Methodology	60
NGB natural gas boiler	99
NPV net present value	32
NV natural ventilation	35
NMBE Nominal Mean Bias Error	61
NSGA-ii Non-dominated Sorting Genetic Algorithm II	29
OC operational carbon	30
ODBT outdoor dry-bulb temperature	193
OpEx operating expenditure	3
PIR polyisocyanurate	79
PSO Particle Swarm Optimisation	30
RC rated capacity	xi
RCP representative concentration pathway	165
SHGC solar heat gain coefficient	90
SP set-point	101
SR solar reflectivity	195
TE thermal emissivity	195
UHI urban heat island	1
UKCP09 UK Climate Projections 2009	25
UKCP18 UK Climate Projections 2018	25
XPS extruded polystyrene	91
VRF variable refrigerant flow	xvi
WWR window-to-wall ratio	ix

Chapter 1

Introduction

1.0.1 Context

Strong evidence suggests that a continued upward trend in greenhouse gas (GHG) emissions could see global temperatures rise in excess of 1.5°C above 1850-1900 levels before the end of the century [1]. Since the spatial distribution of warming is non-uniform, a 1.5°C rise in global mean surface temperature is associated with substantially higher temperature increases in many land regions, with the urban heat island (UHI) effect further exacerbating the warming impact experienced in large cities [1]. Despite global efforts to stabilise GHG emissions, atmospheric carbon dioxide (CO₂) continues to rise [2], and the warming effect will continue for several centuries following stabilisation due to the inertia of the planet's climate system [3].

In the UK, under a high emission scenario, temperatures experienced on hot summer days are projected to increase between 3.7°C to 6.8°C by 2070, accompanied by a greater frequency of hot spells [4, 5]. Thermal discomfort can result in acute subclinical health symptoms, such as headache, fatigue, and difficulty concentrating [6], and correlations have been identified between heat stress, productivity and cognitive performance [7, 8, 9]. Many naturally ventilated buildings have been designed to only just adhere to national guidance on overheating, so a significant increase in external temperature may cause shifts in thermal operating conditions [10, 11].

1.0.2 Higher Education Sector

The UK higher education (HE) sector represents a substantial and distinct component of the national building stock, with a total gross internal area (GIA) exceeding 22 million m² in 2021/22 [12]. It accounts for roughly 2% of the UK's overall carbon footprint, with the built environment contributing around one-fifth of sectoral emissions [13]. University estates are therefore an important testbed for decarbonisation and climate adaptation strategies.

HE buildings are particularly challenging to decarbonise due to their diverse age, form, and function. Approximately 40% of UK university buildings were constructed between 1940 and 1980, when energy efficiency standards were limited [14]. Many older structures are protected heritage assets, limiting options for envelope upgrades. In parallel, the modern university estate incorporates energy-intensive research laboratories, 24-hour IT infrastructure, and mixed-use teaching and accommodation spaces, leading to highly variable occupancy patterns and energy demands. These operational complexities create barriers to standardised retrofit solutions and make HE estates vulnerable to climate-induced overheating and energy performance risks.

Financial constraints further exacerbate these challenges. While sector capital investment in estates has regularly exceeded £2.5 billion per year, a significant proportion is directed toward maintenance and expansion rather than deep refurbishment [12]. Yet, given that the majority of the 2050 building stock already exists, refurbishment represents the most immediate and scalable route to carbon reduction. Improving the environmental and energy performance of existing HE buildings is therefore critical - not only to reduce emissions and improve resilience under a warming climate - but also to safeguard indoor environmental quality (IEQ), which is essential for learning and cognitive performance [15, 16].

1.0.3 Life-Cycle Analysis

Life-cycle analysis (LCA) is a crucial tool for understanding the environmental impacts of building design, construction, and operation [17, 18]. The integration of LCA into climate change adaptation (CCA) frameworks can allow for a comprehensive assessment of both embodied and operational carbon emissions. Embodied carbon, associated with manufacturing, transportation, and construction of building materials and systems, is projected to contribute towards a greater share of life-cycle carbon footprint (LCCF) as the grid becomes less carbon-intensive [19]. This shift necessitates a balanced approach to building design that considers both emission types under various decarbonisation pathways.

Although LCA has been widely applied in evaluating energy-efficient and low-carbon building design, its integration within climate change adaptation studies, particularly for non-domestic refurbishment, remains limited. Most existing research focuses on mitigation measures to reduce energy consumption, often assuming static climate and grid conditions throughout the building life cycle. Adaptation-related impacts, such as increased cooling demand, overheating risk, and equipment degradation under future climates are rarely quantified within life-cycle boundaries. In non-domestic buildings, the complexity of use patterns, diverse construction typologies, and extended service lives further complicate dynamic LCA modelling under changing climate conditions. These chal-

allenges, combined with uncertainties in future weather projections and changing carbon emission factors, have restricted the wider adoption of integrated LCA-CCA approaches in this domain [20, 21].

In addition to environmental impacts, some life-cycle frameworks also evaluate economic implications of design decisions through assessment of life-cycle cost (LCC), referring to the initial costs associated with construction, including the selection of materials and technologies (CapEx), and ongoing operational and maintenance costs over the building’s life-cycle (operating expenditure (OpEx)). The integration of CapEx and OpEx within the LCA framework provides an indication of the financial trade-off for different design strategies. By considering both the environmental (LCCF) and economic (LCC) impacts, LCA assessments can support the development of sustainable and cost-effective building design strategies. This approach aims to ensure that decisions are made with a full understanding of their long-term implications, balancing the requirement for financial viability with the overarching goal of reducing carbon emissions and enhancing sustainability.

1.0.4 Building Performance Under a Changing Climate

Assessing the thermal and energy performance of buildings under future climates involves predicting how they will respond to changing climate conditions over their lifecycle. Probabilistic climate projections provide a range of possible future scenarios, helping to account for uncertainty. By incorporating these projections, building designers can develop strategies that are resilient to a variety of future climate conditions, ensuring that buildings remain comfortable, efficient, and sustainable throughout their lifecycle.

Climate change mitigation and adaptation are often presented as two distinct causes for action. *Mitigation* refers to the reduction of atmospheric GHGs to slow or stop global climate change, whilst *adaptation* refers to adjusting to the impacts of a climate change through enhanced resilience. Existing climate change impact studies demonstrate that there is a clear interdependency between the two concepts, with the degree of resilience and choice of adaptation strategies strongly influencing future demand and energy system sizing [22]. Some mitigation strategies also provide adaptive capacity, such as the installation of PVs with the dual benefits of reduced emissions and reduced reliance on the grid in the event of failure during extreme weather events.

1.1 Research Hypothesis, Questions, and Objectives

The hypothesis of this research is that integrating a [LCA](#) approach with [CCA](#) strategies can reduce both carbon and cost efficiencies for [HE](#) buildings under future climate scenarios.

To test this hypothesis and address identified research gaps, the following research questions are defined:

Research Questions:

1. How will future climate projections affect the predicted operational energy performance of higher education buildings?
2. What are the life-cycle carbon and life-cycle cost implications of adopting climate change adaptation strategies in the design of urban higher education buildings?
3. What trade-offs and synergies exist between embodied and operational carbon when applying climate change adaptation strategies in the higher education sector?
4. How do uncertainties in grid decarbonisation trajectories impact the selection of optimal climate change adaptation strategies?

Research Objectives:

To address these questions and explore the complex relationships between building design strategies, future energy systems, and the environmental and economic outcomes within the [HE](#) sector, the study pursues the following specific objectives:

- Develop an original integrative assessment model that combines [LCA](#) with [CCA](#) strategies tailored for the [HE](#) sector, capturing long-term impacts of refurbishment design decisions under various future climate scenarios.
- Quantify design intervention impacts on key metrics such as energy use intensity ([EUI](#)), [LCCF](#), and [LCC](#) to measure carbon and cost efficiency under changing climate conditions.
- Analyse the effects of varying grid decarbonisation rates on the suitability of building adaptation strategies, identifying how shifts in energy sources influence the environmental and economic viability of different approaches.
- Apply a multi-objective genetic algorithm ([GA](#)) to identify a set of Pareto-optimal solutions that achieve an optimal balance between carbon reductions and cost-effectiveness, providing a structured approach for decision-making.

- Generate significant practical recommendations for policymakers and practitioners, aiming to enhance the climate resilience of [HE](#) buildings through actionable insights on design and retrofit strategies that align with long-term carbon reduction objectives.

1.2 Contribution to Knowledge

This research aims to advance the understanding of sustainable refurbishment practices by addressing critical gaps in integrating [LCA](#) and [CCA](#) specifically within the [HE](#) building sector. Based on an extensive literature review, this study identifies and responds to the limited scope of existing research on the long-term impacts of climate resilience strategies when applied to non-domestic buildings. The contributions presented here build on previous work by offering a robust and comprehensive approach that not only quantifies the carbon and cost trade-offs associated with climate-adapted design but also considers the future dynamics of energy systems and carbon trajectories. These original contributions are outlined below:

Development of an Integrated CCA-LCA Approach for HE Building Refurbishment

The study develops and applies an integrated methodology that combines [CCA](#) strategies with [LCA](#), tailored specifically for [HE](#) buildings. It incorporates future climate projections and addresses uncertainties in grid decarbonisation, allowing for a more nuanced analysis of [HE](#) building design. Through a multi-objective [GA](#) optimisation approach, the research identifies Pareto-optimal solutions that balance energy efficiency, carbon reduction, and cost-effectiveness. This allows for a rapid and robust evaluation of numerous design permutations, providing a set of optimal solutions that can guide decision-making in the context of [HE](#) building refurbishment and adaptation. The integration of these techniques enables a multi-dimensional evaluation of building design strategies, balancing energy efficiency, life cycle carbon emissions and life cycle costs.

Climate Change Impact Assessment on HE

By incorporating future climate projections, this research provides an indication of how future climate scenarios affect energy performance, highlighting the varying impacts across different [HE](#) building typologies. This original analysis provides insight into scaled-up impacts and possible needs for reassessment of energy benchmarks as climate conditions evolve, offering significant implications for building design and operation standards.

Assessment of LCCF and LCC Impacts on HE

The research provides a robust examination of how operational efficiency and fuel sources affect the [LCCF](#) of [HE](#) buildings, evaluating a range of design variables and combinations. By modelling [LCCF](#) over the building's life cycle using dynamic decarbonisation pathways, the study indicates how design decisions might vary based on different projected scenarios.

The study addresses various potential challenges in achieving significant [LCC](#) reductions while pursuing low-carbon design strategies. It provides insight into the implications of projected operational costs associated with electricity-based technologies and natural gas on [LCC](#) outputs. The findings highlight important trade-offs between economic and environmental factors.

Evaluation of Embodied vs. Operational Carbon Trade-offs in HE Design

Trade-offs between embodied and operational carbon emissions are explored in case study [HE](#) buildings, particularly in the context of insulation and material choices, with reference to the net carbon impact of interventions beyond current building standards. The research also considers the quantified benefits of using renewable construction materials, with respect to design flexibility.

Contributions to Policy and Practice

The research offers significant actionable insights and recommendations for practitioners and policymakers aiming to enhance building resilience under future climates. By demonstrating the benefits of integrating [CCA](#) and [LCA](#) approaches and highlighting the key trade-offs and synergies under different decarbonisation pathways, the study provides a practical methodology that can inform policy development and guide the design and refurbishment of sustainable [HE](#) buildings.

Overall, this research advances the understanding of how to effectively integrate [LCA](#) and [CCA](#) methodologies within the [HE](#) building sector, taking into account the uncertainties associated with future grid decarbonisation. It provides a comprehensive and robust approach for evaluating and optimising building design strategies, balancing energy use, carbon emissions, and costs. By applying this life-cycle optimisation methodology to three existing [HE](#) buildings, specific case-based recommendations for refurbishment are also provided. The findings and methodologies developed in this study contribute to the broader efforts to create sustainable and resilient built environments in the face of climate change.

Chapter 2

Literature Review

2.1 Overview: Energy and Carbon Performance of the UK Higher Education Sector

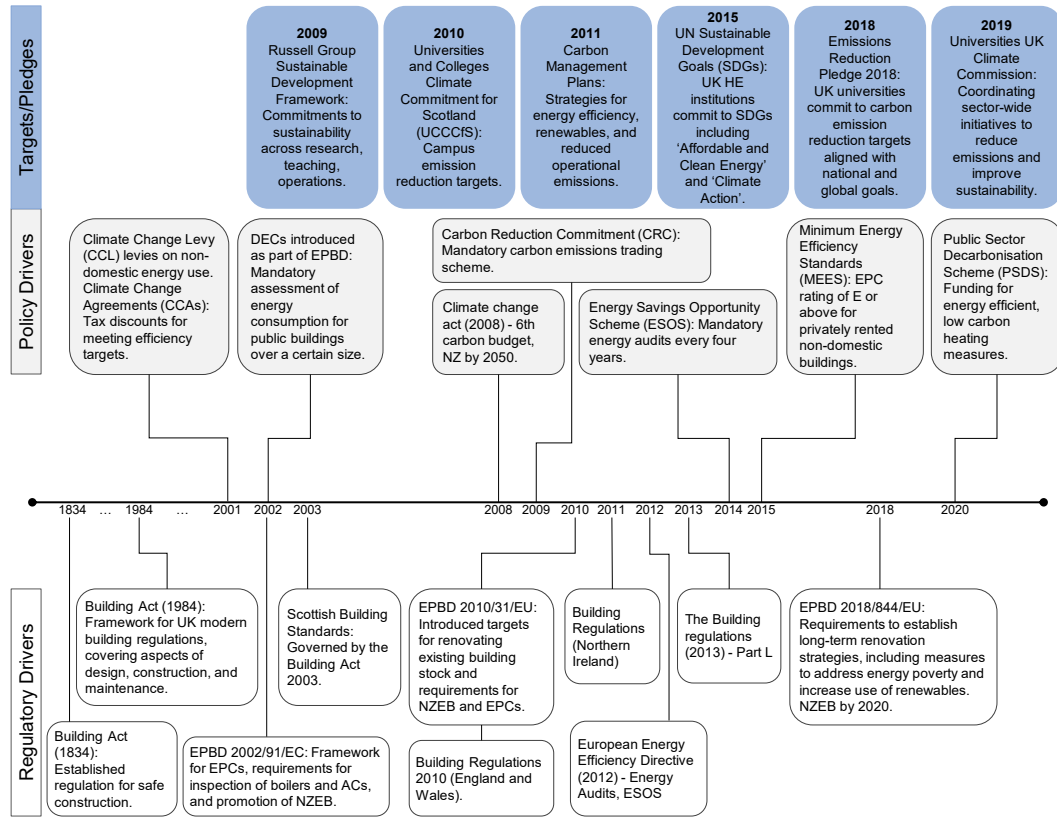
The UK HE estate has undergone significant transformation over past decades, strongly influenced by a shift towards institutional autonomy and increased stakeholder importance [23]. This section examines the history, evolution, and energy performance monitoring of university buildings in the UK, highlighting key developments and their impact on the sector’s overall carbon emissions. It also explores the drivers and interventions aimed at reducing energy and carbon emissions, providing a comprehensive understanding of how the UK HE sector is addressing environmental sustainability in the context of institutional growth and regulatory changes.

Historical Context and Evolution

The architectural landscape of academic institutions reflects the changing regulatory and technological advancements of each era. The UK HE estate consists of buildings dating back several centuries, with some institutions tracing their origins to the medieval period and as early as the 12th century [27]. Many historic university buildings can be characterised by the enduring influence of styles such as Gothic and Collegiate Gothic, becoming emblematic of traditional higher education institutions (HEI). Post World War II construction practices in the UK shifted towards robust concrete structures, reflecting a trend influenced by brutalist architectural principles [28]. Subsequent to the Building Act of 1984 [29], efforts in university architectural development started to concentrate on enhancing thermal energy efficiency through improved airtightness, glazing and envelope properties.

During the late 20th and early 21st centuries, HEIs transitioned from ‘elitist’, with less than 15% participation amongst the age group, to ‘mass’ (15-50% participation) to ‘universal’ majority participation, responding to growing economic

(a) Timeline of UK HE sector relevant regulatory and policy drivers and key pledges.



(b) UK HE estate GIA vs. energy consumption; estimates from [24, 25, 26].

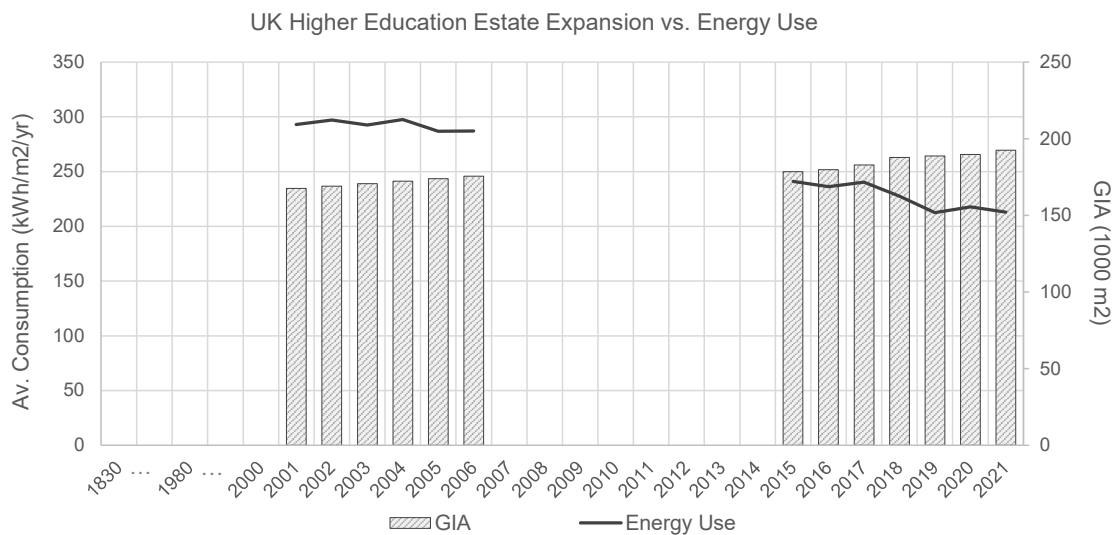


Figure 2.1: Timeline of UK HE sector development.

demands and social aspirations [30]. This resulted in a gradual expansion of UK university estates by approximately 15% from 2001 to 2021, to accommodate burgeoning student enrollments [24], as depicted in Figure 2.1. In academic year 2021/22 the total GIA of UK estates reached over 22 million m², increasing by approximately 403 thousand m² in a single year [12]. The post-millennial period also saw increased competition amongst global universities for students, staff, and research funding [23]. In 2021/22 total capital investment across HEI estates was £2.5 billion, with repairs and maintenance accounting for approximately 30% of property costs, reflecting substantial investment in modern infrastructure to sustain competitiveness in the international academic arena [12].

Energy and Carbon Emissions Breakdown

The energy consumption across the UK HE sector has seen significant changes over recent years. From 2001 to 2006, annual reported energy consumption fluctuated, influenced by various factors including the expansion of facilities, implementation of energy efficiency measures and adoption of renewable energy sources [26]. As of the latest reports, the sector's energy consumption has decreased; according to HESA, the total energy consumption of UK universities was approximately 7.2 terawatt-hours (TWh) in 2021/22, a decline from around 7.6 TWh in 2015/16 [25]. This correlates to an approximate average campus consumption of 213 kWh/m²/yr in 2021/22, as depicted in Figure 2.1 [25]. This reduction can be attributed to various energy efficiency initiatives and the implementation of sustainability strategies across campuses [31]. Similarly, reported onsite and off-site renewable energy generation has increased by nearly three fold over this same period [25].

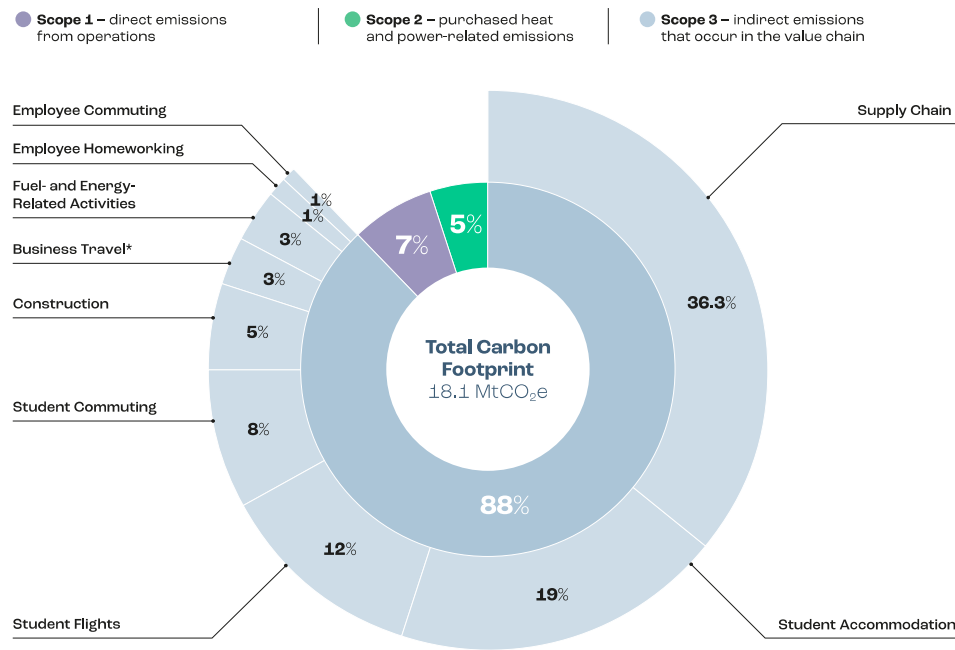


Figure 2.2: Breakdown of scope 1, 2 and 3 carbon emissions across the tertiary education sector in academic year 2020-21 [13].

The tertiary education sector contributes a significant portion of the UK's total carbon emissions [13]. In 2020/2021, direct and indirect emissions from the sector totalled 18.1 MtCO₂e, as depicted in Figure 2.2, accounting for approximately 2.3% of the UK's overall carbon footprint [13, 32]. HEIs are responsible for 86% of these emissions, with Further Education institutions contributing the remaining 14% [13]. The built environment contributes 19.1% of the sector's total emissions across Scopes 1-3, with Scope 1 and Scope 2 emissions accounting for 2.1 MtCO₂e (12%) of the sector footprint [13]. Supply chain emissions from construction projects in 2020/2021 contributed approximately 4.7%. However, substantial variability in construction-related emissions can be observed across different years, and was nearly three times greater two years prior [13]. Whilst deployment of energy efficiency measures across UK universities is estimated to have saved 2.21 MtCO₂e of Scope 1 emissions between 2008–2019, it is also noted that per capita emissions do not decline in direct proportion to energy efficiency improvements [33]. This is due to the rebound effect, where factors such as expanding operations and changing economic activities offset some of the gains from efficiency measures [33]. As a result, efficiency improvements alone are insufficient to meet net-zero targets, and accelerated adoption of renewable energy sources is essential.

Sustainability Drivers in HEIs

The evolution of UK university estates reflects an ongoing transition towards sustainable building practices and improved energy efficiency [12]. This trajectory has

been propelled by regulatory and policy drivers that collectively seek to optimise operational efficiency and environmental stewardship within HE infrastructure. A timeline of relevant drivers is presented in Figure 2.1. These measures can be broadly classified as regulation, funding initiatives, and legislative frameworks, as outlined below.

Regulatory Drivers

The regulatory framework for building design and construction in the UK has advanced energy efficiency and sustainability, with relevance to the design of HEIs. The Building Regulations 2010 established more stringent energy performance standards for new constructions and renovations [34]. The Energy Efficiency Directive 2012 reinforced these measures, setting out measures to promote energy efficiency across various sectors including HEIs [35]. Subsequent updates to the Energy Performance of Buildings Directive (EPBD) in 2010 and 2018 introduced requirements for nearly zero-energy buildings, furthering sustainable building practices [36]. Additionally, the introduction of Display Energy Certificate (DEC)s in 2002 under the EPBD has been pivotal for performance monitoring, providing transparency and accountability by assessing buildings' energy performance based on actual consumption.

Financial Drivers

Government-led schemes can incentivise energy efficiency and investment in HEIs. For example, the Public Sector Decarbonisation Scheme provides financial support for universities to invest in low-carbon heating systems and energy efficiency measures, facilitating the transition to sustainable campuses by enabling significant energy efficiency upgrades [37]. Additionally, the introduction of the Climate Change Levy (CCL) and the Carbon Reduction Commitment (CRC) trading schemes aimed to regulate energy and carbon through fiscal measures [38, 39].

Legislative Drivers

While not exclusively focused on HEIs, the Climate Change Act 2008 established legally binding targets for reducing GHG emissions, with the aim to achieve net-zero emissions in the UK by 2050 [40]. Similar legislative trend have been observed across devolved administrations; the Climate Change (Scotland) Act 2009 introduced mandatory climate change reporting for public bodies [41], and the Future Generations Act 2015 sets out obligations for the Higher Education Funding Council for Wales (HEFCW) to deliver a sustainable development plan [42, 43]. This legislation has been pivotal in driving sustainability efforts across various sectors, including higher education.

Sustainability Initiatives and Carbon Management

Many UK universities have pledged to align carbon reduction targets with national and global climate imperatives [31]. The Emissions Reduction Pledge 2020

provided a government framework for public sectors to declare intentions to reduce GHG emissions by 30% by 2020/21 relative to a 2009/10 baseline [44]. HECFE set additional sector targets of 43% and 83% reductions by 2020 and 2050 respectively, against a 2005 baseline, focusing on direct (Scope 1) and indirect (Scope 2) emissions [45]. Universities were required to develop five-year Carbon Management Plans (CMPs) to achieve this target, setting out how carbon emission reductions will be achieved within the CMP period. The Universities and Colleges Climate Commitment for Scotland (UCCCfS) promoted transparency in progress reporting and carbon-reduction intentions via Climate Change Action Plans (CCAPs) [46]. These initiatives align with broader national objectives, emphasising the important role of the HE sector in practicing sustainability and reducing their carbon footprints.

Despite these efforts, recent statistics indicate that many institutions are struggling to meet these targets. According to the University Carbon Progress Report 2018, UK universities are projected to achieve only a 13% reduction in emissions by 2020 [47]. Of the 127 institutions that initially committed to the 43% reduction, only 52 are on track to meet or exceed this target. Additionally, about a third of these institutions have lowered their initial targets set in 2008 [47]. The 20 Russell Group universities account for more than half of the sector’s emissions, with only two HEIs reportedly on track to meet their emission reduction targets [47]. Moreover, carbon-reduction commitments vary across institutions [31], with no mandated implementation or monitoring of energy efficiency measures across the whole sector. Therefore, achieving carbon neutrality by 2050 remains a significant challenge for the sector, requiring increased uptake of renewable energy sources and improved energy efficiency measures. This highlights the challenges faced by the sector in achieving its sustainability goals and the need for more rigorous implementation and monitoring.

Challenges in Reducing Campus Emissions

Reducing campus emissions in HEIs presents several significant challenges, despite proactive measures and ambitious targets set by many universities. These barriers can be broadly categorised as technical, financial, organisational, and behavioral.

Technical Challenges A key complication in reducing operational energy and carbon emissions within the HE sector is the diversity and complexity of university estates. Older buildings, often with historical and architectural significance, pose particular challenges for energy efficiency upgrades; retrofitting these structures to meet modern energy standards whilst retaining heritage attributes can be technically complex and costly [48]. Furthermore, HE buildings constructed between 1940 and 1980 account for approximately 40% of the UK stock [14], representing a major energy challenge due to typically high U-values and infiltration rates [49, 50, 51]. Retrofitting leaky, international style buildings can achieve high thermal

performance during the heating season but often intensifies overheating during summer months [52].

Financial Challenges The capital costs required for implementing carbon reduction programmes and technologies in HEIs can compromise progress [43]. While these investments may pay off in the long run, the initial outlay can be prohibitive, especially for institutions with limited budgets [43]. Securing funding and grants for sustainability projects can be competitive and uncertain, and increased commercialisation of the sector has reduced the financial sway of public organisations in encouraging carbon reduction practices [43]. Additionally, the financial benefits of energy-saving measures often do not align with the short-term financial planning horizons of many institutions.

Operational Challenges UK universities face a significant challenge in balancing commercial growth with emissions reduction [43]. The sector's success has driven increases in revenue, student numbers, and campus expansion, both domestically and internationally. Additionally, the rise in energy-intensive research activities and the investment in new student facilities, including on-site accommodation, further complicate efforts to reduce carbon emissions [43]. The varied nature of campus activities can complicate efforts to implement uniform energy-saving measures [53]. Furthermore, effective implementation of sustainability initiatives requires coordination across various departments, including facilities management, finance, and academic departments. Organisational silos can hinder the cohesive efforts required to reduce emissions.

Behavioral Challenges Engaging the campus community, including students, faculty, and staff, in sustainability efforts is crucial for success. Changing behavior and fostering a culture of sustainability can be slow and challenging. There is often a gap in awareness and understanding of the importance and impact of sustainability measures. Educational programs and awareness campaigns are needed to motivate and actively involve the campus community.

Section Summary

The historical evolution of university estates has led to significant growth and architectural developments shaped by regulatory changes and institutional autonomy. This expansion has been accompanied by substantial investments in modern infrastructure to support increasing student enrollments and global competitiveness. Despite the sector's proactive measures to reduce energy consumption and carbon emissions, challenges persist, particularly in retrofitting older buildings and securing the necessary funding for sustainability initiatives. As the UK HE sector continues to evolve, it faces the dual challenge of maintaining growth while achieving long-term sustainability and carbon reduction targets.

2.2 Embodied carbon in building redevelopment

2.2.1 Embodied Carbon as a Life-Cycle Component

Embodied carbon is a term frequently adopted in building construction research and practice. It typically refers to the carbon emissions associated with the manufacture, transport, installation, and disposal of building materials and systems [19, 17]. This life-cycle component aligns with Scope 3 emissions as defined by the GHG Protocol, which includes all indirect emissions that occur in the value chain of a building, outside of its direct operations [54]. ‘Upfront’ embodied carbon impacts refer to emissions occurring during product manufacture and construction, whilst downstream impacts occur during the building use stage and end-of-life.

Evaluations of the embodied carbon component can vary significantly depending on the defined boundary conditions and the scope of the analysis [17]. Typically, the scope of analysis includes stages from raw material extraction (cradle) to the building’s end-of-life (grave), often termed ‘cradle-to-grave’ analysis. This intends to capture the entire lifecycle of building materials, depicted by the modular components shown in Figure 2.3.

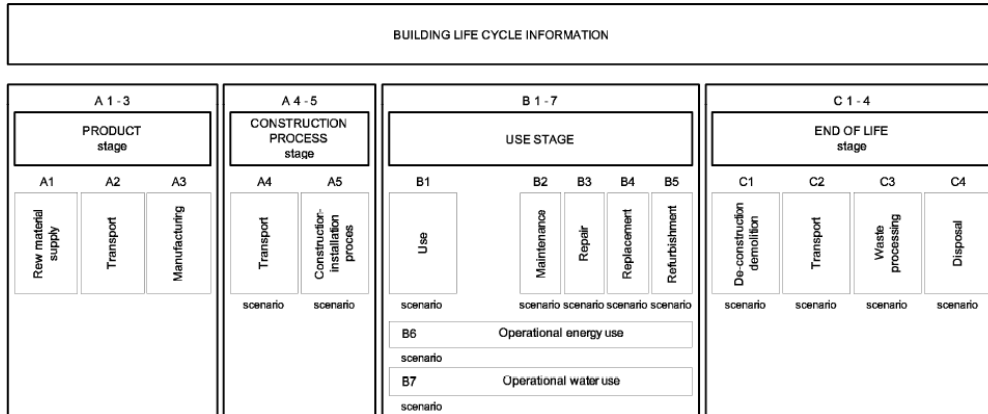


Figure 2.3: Modular components of the various whole life carbon building assessment, according to BS EN 15978 [17].

In BS EN 15978, the life-cycle is divided into four main stages. The product stage (A1-A3) includes the extraction and processing of raw materials, transportation to manufacturing sites, and the production of construction products, representing the initial EC burden. The construction stage (A4-A5) accounts for the transport of materials to site and on-site construction or installation processes. The use stage (B1-B7) represents the building’s operational life, including maintenance, repair, replacement and refurbishment, as well as the energy and water use associated with the building’s operation. Finally, the end-of-life stage (C1-C4) includes demolition or deconstruction, transport of waste materials, processing for recycling or reuse, and final disposal. Together, these stages intended to provide

a comprehensive framework for assessing whole-life carbon impacts.

Beyond these, Module D accounts for potential benefits and burdens that occur outside the system boundary, such as the reuse, recovery, or recycling of materials once the building has reached the end of its life. These avoided impacts recognise the potential for materials or components to offset emissions in future product systems, although their inclusion and quantification can vary across studies. By contrast, cradle-to-gate boundaries capture only the emissions up to the point a product leaves the factory gate (A1–A3), omitting downstream construction, use, and end-of-life impacts [17].

The scope of analysis definition can also have a strong influence on [LCA](#) results, with respect to the inclusion and exclusion of materials and systems. Whilst defining the scope can be more straightforward when applied in practice, building refurbishment research which is not applied through real-world application often involves many assumptions surrounding retained and replaced components. Typically, key structural elements such as piles, pile caps, columns and beams are assumed to be retained through redevelopment scenarios, although this should be assessed on case-by-case basis depending on the building’s prior condition. In addition, studies often focus on the embodied carbon of the building fabric without accounting for building services, such as heating, ventilation and air conditioning ([HVAC](#)) systems. This omission is often due to limited data availability concerning their embodied carbon. However, some research highlights the substantial embodied carbon potential of certain [HVAC](#) systems, particularly those based on refrigerant technologies [55].

2.2.2 Calculation Methods and Protocols

[LCA](#) is a systematic method used to evaluate the environmental impacts of a product or system throughout its entire lifecycle, from raw material extraction to disposal [56]. It involves compiling an inventory of relevant energy and material inputs and environmental releases, evaluating the potential impacts associated with identified inputs and releases, and interpreting the results to help decision-makers. According to ISO 14040, the [LCA](#) process is divided into four main stages: goal and scope definition, inventory analysis, impact assessment, and interpretation [56]. Each stage plays a crucial role in ensuring the comprehensiveness and accuracy of the assessment.

Standards such as BS EN 15978 and industry guidance, such as RICS whole life carbon assessment, provide frameworks for applying [LCA](#) in the built environment context [17, 19]. These standards cover the environmental performance of buildings, including their embodied carbon, and aim to ensure that assessments are carried out in a consistent and reliable manner, promoting transparency and comparability across different case studies [17].

Data Sources

The reliability of input data can have a strong influence on [LCA](#) calculation outputs [57]. Industry supplied Environmental Product Declarations ([EPD](#))s are commonly utilised to supply data for A1-A3 stages of building components. Whilst production of these environmental declarations follow a standardised protocol (EN 15804) [58], several limitations exist in pertaining to the reliability of data. For example, [EPDs](#) are only relevant to the specific product under investigation; without comparative analysis it is not possible to tell if they are statistically representative of the wider product range. Since participation in the [EPD](#) process is voluntary, the data may not be representative of products at an industry-wide scale. Additionally, [EPDs](#) are supplied by the manufacturers themselves, which can introduce questions regarding impartiality and potential bias.

The Inventory of Carbon and Energy (ICE) V3.0 database compiles embodied energy and carbon data from a wide range of peer-reviewed literature and verified sources [59]. Values in this dataset were selected according to five criteria, ensuring consistency of data within the inventory [60]. In this study, preferences were given to data sources that complied with accepted methodologies or standards e.g. ISO 14040. The ICE values represent selected or recommended best estimates derived from available literature, informed by professional feedback and assessment of data quality [60]. Similar databases, such as the Embodied Carbon in Construction Calculator (EC3) [61], One Click LCA [62], and Ökobaumat [63], provide additional resources for embodied carbon assessments, often integrating regionalised data. However, the effectiveness of such databases relies heavily on the availability of [EPDs](#). Data pertaining to certain product types, particularly in relation to building system services, can be limited, posing significant constraints.

2.2.3 Drivers for Embodied Carbon Reduction

Regulatory Drivers

Policies and regulations in the UK increasingly mandate the consideration of embodied carbon in construction, often in line with industry-led initiatives. At the regional level, the London Plan requires Whole Life-Cycle Carbon assessments for all major developments referable to the Mayor, effectively mandating embodied carbon reporting for large new-build schemes and significant refurbishments within Greater London [64]. However, requirements are typically stricter and more consistently applied to new developments than to redevelopment or retrofit projects, where embodied carbon reduction is encouraged but less formally regulated. Emerging policy discussions, such as proposals for mandatory Whole Life-Cycle Carbon reporting and embodied carbon limits in building regulations (e.g. Part Z), demonstrate a growing consensus around the need for consistent enforcement [65]. Currently, the absence of a UK-wide regulatory requirement for

embodied carbon reporting represents a policy gap.

At the national level, the *Construction 2025* government strategy sets broad targets for halving carbon emissions across the construction sector by 2025, promoting supply-chain decarbonisation and material efficiency [66]. More broadly, the Climate Change Act of 2008 establishes legally binding legislation for GHG emissions reductions, influencing policies that address embodied carbon in building materials and practices [40]. Participation in the UK Emission Trading Scheme and the implementation of carbon pricing mechanisms also indirectly incentivise the reduction of embodied carbon within construction practice [67].

Industry Drivers

Alongside regulatory mandates, sustainability assessments and certifications incentivise and promote the consideration of embodied carbon across industry. BREEAM, tailored to UK standards, assesses building sustainability across various criteria, including embodied carbon reduction strategies [68]. LEED, an internationally recognised certification methodology, also addresses embodied carbon through credits focused on material selection and life-cycle assessment [69]. These certifications can offer strong motivational factors, enhancing reputation and credibility of stakeholders involved in the building supply chain. Industry collaboration and initiatives, as exemplified by the London Energy Transformation Initiative (LETI), provide further guidance for achieving low-carbon building practices through embodied carbon assessment within the UK construction sector [70]. These elements collectively contribute to the framework for evaluating and managing embodied carbon in building construction practices and life-cycle carbon assessments within the UK regulatory context.

2.2.4 Challenges and Limitations of Embodied Carbon Assessments

Embodied carbon assessments face several challenges that can impact accuracy and consistency. It is important to consider these upon evaluation of the environmental impacts of building materials and systems.

Data Availability and Quality

A primary challenge is the variability in data sources and the quality of data available for embodied carbon assessments, as previously discussed. While databases such as Bath ICE and EPDs provide valuable information, there are often gaps, especially concerning the embodied carbon of complex building systems and less commonly utilised building materials. Additionally, uncertainties within EPDs, such as variability in manufacturing energy use, material sourcing, and transport emissions, also limit assessment consistency. Ensuring accurate data on material

properties and manufacturing processes is crucial but can be challenging due to inconsistencies across different sources and life-cycle inventory methodologies [58, 56, 57].

Model Accuracy

The accuracy of embodied carbon assessments is also influenced by the modelling tools used and the expertise of the modeller. Errors can arise due to the freedom of boundary conditions and assumptions of the assessor [71]. Simplifications embedded within LCA software, incorrect system boundary assumptions and user misinterpretation can all lead to inconsistencies reporting [71]. Furthermore, distinctions between design-stage estimates and actual procurement decisions can introduce discrepancies, as final material selections, supplier choices, and real-world construction practices often deviate from initial assumptions. Addressing these challenges requires greater transparency in modelling assumptions and more standardised calculation methodologies.

System Boundaries

System boundary definition can have significant influence on the results of embodied carbon assessments, both with respect to included stages (cradle-to-gate vs. cradle-to-grave) and scope (included building components). Excluding certain materials or stages of the lifecycle may result in underestimations of the total environmental impact associated with building materials and systems [58, 56].

Regional Variability

Embodied carbon varies significantly based on regional factors such as local manufacturing practices, energy sources, and transportation distances. These regional variations can impact the overall environmental performance of buildings and must be considered to provide accurate assessments [58, 56].

Timely Relevance

The dynamic nature of new building materials and technologies necessitates continuous updates to embodied carbon data to ensure relevance and accuracy over time. New materials, manufacturing processes, and technologies emerge regularly, requiring ongoing efforts to update embodied carbon databases and incorporate these developments into life-cycle assessments effectively.

Scope of Environmental Impact

Several research initiatives have attempted to expand the scope of life-cycle assessments to include additional environmental impacts, such as resource depletion,

water usage, and biodiversity loss [72, 73]. However, most building-level case studies continue to focus on global warming potential (GWP) as measured by CO₂-equivalent emissions, as this is the most consistently measurable and standardised environmental metric in construction industry practices [74]. Assessing the overall environmental impact of buildings can be challenging due to differing units of measurement across impact categories. Metrics must first be normalised to a common scale and then weighted to reflect their relative significance [74]. Whilst guidance exists on reducing various impact categories to a single dimension, the complexity of acquiring data from many different process flows can result in these studies typically being applied to individual building materials or to high-level, simplistic models [74]. Applying a wider environmental impact methodology to detailed building models can become very complex. Furthermore, factors such as long-term resource availability are often excluded from current assessment frameworks, highlighting a need for developing new metrics and methodologies to capture these aspects effectively.

2.3 Life cycle carbon in higher education building redevelopment

A growing body of evidence indicates relative benefits of refurbishment scenarios over new construction in terms of embodied energy and carbon impact [57, 75]. While new-build scenarios can significantly enhance the operational efficiency of HE buildings, structural retention and refurbishment can reduce embodied carbon impacts [76]. Studies with a strong emphasis on reducing operational over embodied energy for minimising life-cycle carbon often overlook the impacts of grid decarbonisation, with an increasing need to consider the diminishing proportion of operational carbon emissions over time [76]. Consequently, there can be a trade-off between these options in building redevelopment; both AUDE and HEFCE have stated that this trade-off should be carefully considered during the planning stages of higher education building redevelopment projects [45].

2.3.1 Non-recurring emissions

The proportion of carbon emissions relating to ‘one-off’ embodied carbon impacts, including product manufacture, construction and demolition, varies across HE case studies. Hawkins and Mumovic found that in existing UK HE buildings, the embodied carbon ranged between 200 and 300 kgCO₂e/m², accounting for up to 6% of the total life cycle carbon impact [76]. A study on a mixed-use HE building in Michigan indicated that material production contributed 3% of life-cycle GWP, whereas construction, transportation and decommissioning combined contributed only 0.5% [77]. Junnila et al. observed that the sum of materials, construction and end-of-life phase contributed 11.7% and 9.97% for a European and US office building respectively [78]. Whilst values across these studies indicate a relatively low proportion of these embodied components to LCCF, findings also suggest that as operational efficiency improves, the embodied carbon impact may reach parity [76].

Differences in boundary conditions, scope, and life-cycle inventories can significantly influence assessment outcomes [57]. The LCA studies described differ in the timeframe of analysis, ranging from 50 to 75 years. Some studies advise the utilisation of lower average lifespans for non-residential buildings due to increasing frequency of redevelopment to meet modern functional and aesthetic standards [78]. Consequently, the significance of the materials, construction, maintenance, and end-of-life stages relative to the use phase may be expected to grow as functional obsolescence becomes more common. On the other hand, increasing awareness around the relative benefits of refurbishment and low-embodied carbon building practices across industry may simultaneously drive reductions in material, construction and demolition related emissions [70].

2.3.2 Repair and maintenance

Recurring emissions in HE buildings typically refer to repair, maintenance and replacement of building fabric and services. This component also varies widely across studies based on their definition of boundary conditions. Studies considering more intricate details such as furnishing and fittings often note significant contributions to the total embodied energy from frequent replacement of internal finishes, such as carpets and ceiling tiles [77, 78]. Whilst this level of detail can offer greater accuracy for evaluation of LCCF in existing HE buildings, where no changes are assumed through replacement cycles, it can also accentuate uncertainties when assessing LCCF of design alternatives at early design or refurbishment stage.

Relatively few LCA studies consider the EC associated with building services due to limited data availability [79]. Research suggests that, whilst the initial impact of services may be comparatively minor, the recurring associated EC impacts can be significant over a building’s lifetime, due to the high replacement rates [80, 79]. Furthermore, studies including refrigerant-based HVAC components, such as ASHP and VRF systems, have indicated substantial recurring EC impacts due to refrigerant leakage and end-of-life rates [55]. Yet, refrigerants are considered in a low proportion of carbon footprint assessments within the HE sector [81]. Better integration of CIBSE TM65 could improve refrigerant tracking in LCA [80]. Mandated disclosure of refrigerant inventories within institutional reporting frameworks may also support more transparent embodied emission estimates.

2.3.3 Operational carbon impacts

Operational carbon impacts are a critical component of the life cycle carbon footprint of HE buildings. Static LCA studies that utilise fixed assumptions relating to the carbon intensity of energy use consistently show that the use phase dominates life cycle carbon emissions [76, 77, 78]. For example, Scheuer et al. found that the operations phase alone accounted for 96.5% of the total life cycle GWP in a mixed-use higher education building [77]. Similarly, Junnila et al. observed that the use phase contributed 83-85% of the total CO₂ emissions in offices sharing similar functional characteristics with HE buildings [78]. Operational carbon has also been noted to vary widely across HE end-use typologies. Higher education buildings with laboratories and medical research facilities have been shown to have relatively high operational carbon impacts due to specialised equipment and climate control requirements [76]. However, changing grid carbon intensity can significantly alter LCA outcomes and has been recommended for construction industry inclusion by the Royal Institution of Chartered Surveyors (RICS) since 2017 [19]. The implications of such assumptions are discussed in Section 2.4.3, with relevant studies provided in Section 2.5.1.

2.4 Future considerations

Life-cycle carbon and cost assessments in building refurbishment can be influenced by a number of ‘future considerations’, such as product and fuel price variability, changing climate factors and grid decarbonisation. These aspects are discussed in the following sections.

2.4.1 Cost implications

Optimal strategies for reducing life-cycle cost in building refurbishment are subject to dynamic market impacts. Costs associated with products, services, and labour can vary in line with market conditions, technological advancements, and regulatory changes. Moreover, operational costs incurred during the usage phase of the building can be significantly impacted by fluctuating fuel prices. Both components can affect the long-term economic feasibility of construction projects and can be challenging to predict with accuracy due to inherent uncertainties.

Upfront Costs Projections

Market volatility, driven by supply chain disruptions, geopolitical factors, and demand fluctuations, can lead to significant variation in the construction material costs [82, 83]. For instance, recent evidence highlighted how global events, such as the COVID-19 pandemic and international conflicts, can cause significant increases in material costs due to manufacture and supply chain disruptions [84, 85]. Regulatory changes, such as new building codes and environmental regulations, can also affect costs by requiring additional compliance measures [86]. Whilst integrating energy efficient technologies and low-carbon materials can offer long-term savings potential, they often involve higher upfront costs or perceived financial risks [87]. Future cost reductions typically correlate with the rate of deployment of a new technology; for example, widespread adoption of heat pumps could drive down costs, but depend on policy support to strengthen their economic competitiveness [88]. Additionally, uncertainty pertains to the long-term futures of carbon-intensive industrial sub-sectors, such as steel and concrete [89], with potentially significant implications on predicting future market prices in the construction industry.

Labour costs typically constitute between 20-40% of total construction project expenses [90]. Factors influencing labour costs include wage rates, productivity levels, and labour availability [91]. The construction industry often faces challenges related to labour shortages and skills gaps, which can drive up wages and delay projects. The adoption of automation and prefabrication techniques has been proposed as a solution to mitigate labour costs, though these technologies also require initial capital investment.

Operational Costs Projections

Fuel price projections are influenced by global market dynamics, geopolitical events, and policy decisions. The shift towards renewable energy sources and advancements in energy storage technologies are anticipated to stabilise and potentially reduce fuel prices in the long term, provided that they are successfully decoupled from fossil fuel market prices. However, short-term projections indicate potential volatility due to factors such as fluctuations in oil prices and changes in energy policies. Implementing energy efficiency measures and adopting renewable energy systems can mitigate the impact of this volatility on operational costs. Buildings equipped with energy-efficient technologies and powered by renewable sources are less susceptible to fluctuations in conventional fuel prices, resulting in more predictable and potentially lower operational costs.

Cost of Environmental Impacts

The construction industry must increasingly account for the cost of carbon, driven by policies like carbon taxes and cap-and-trade systems. These mechanisms aim to internalise the environmental costs of carbon to incentivise reductions in GHG emissions [92, 93]. Carbon taxes directly impose fees on carbon emissions, significantly impacting the cost structure of projects that use high-embodied carbon materials. Meanwhile, cap-and-trade systems set emission limits and create a market for trading emission permits, encouraging the adoption of low-carbon technologies and materials. The introduction of these pricing mechanisms can stimulate innovation and sustainable practices within the construction sector, yet they also introduce financial complexities and uncertainties [94].

In conclusion, understanding future cost implications of construction projects requires a comprehensive analysis of upfront and operational costs, as well as additional factors like the cost of carbon. Incorporating future cost assessments into life-cycle costing can be highly complex and uncertain, hence the common adoption of constant future rate discount factors [95].

2.4.2 Climate change impacts

Changing climate conditions are expected to alter the operational energy component of buildings over their lifetime. Shifting temperature patterns and the increased frequency of extreme weather events can impact heating and cooling loads, leading to variations in energy demand and associated emissions. Incorporating climate change projections and scenarios into life-cycle assessments can help to ensure carbon and cost reduction strategies remain effective under evolving climatic conditions.

Development of UK Climate Projections

Climate projections are widely adopted in building performance research to understand potential future climate risks and inform adaptation strategies [96, 97, 98]. In the UK, substantial efforts have been made to develop comprehensive climate projections through initiatives such as UK Climate Projections 2009 (UKCP09) and UK Climate Projections 2018 (UKCP18) [5]. These datasets were developed by the Met Office Hadley Centre and aim to incorporate the latest scientific understanding and climate modeling techniques [99].

UKCP09 introduced a probabilistic approach to climate projections, offering a range of alternative possible futures rather than a single deterministic outcome. This was achieved through a large ensemble of model runs, which allowed for the exploration of uncertainties inherent in climate projections [100]. UKCP09 used downscaling techniques to refine the global climate model outputs to a higher resolution suitable for regional and local impact assessments. The key outputs were available at a 25 km grid scale, enabling stakeholders to better assess and plan for climate impacts at a local level [101].

UKCP18 provided increased spatial resolution, with outputs available at 12 km and finer scales for specific applications [5]. This allowed for more precise assessments of climate impacts, particularly in urban areas where microclimate effects can be critical [99]. New downscaling approaches were also introduced, integrating regional climate models and statistical techniques to better capture local variations and extremes. This improved the representation of phenomena such as heatwaves and heavy rainfall events, which can be of important relevance for impact and adaptation studies. Furthermore, UKCP18 expanded the range of scenarios considered, reflecting various GHG concentration pathways and socio-economic developments [99].

Climate Scenarios

Climate projections typically adopt scenarios to represent different GHG emission and socio-economic pathways. Representative Concentration Pathways (RCPs) describe varying trajectories in GHG concentrations, ranging from low (RCP2.6) to high (RCP8.5) emission pathways [102]. Shared Socioeconomic Pathways (SSPs) complement RCPs by presenting various socio-economic futures, including factors such as population growth, economic development, and technological advancements. This combination allows for a more comprehensive exploration of a range of potential climate futures and their impacts on society [103].

Percentile Projections

Percentile projections provide a range of possible outcomes based on different confidence levels [5]. These projections present climate variables, such as tem-

perature and precipitation, as percentiles, indicating the probability of different climate impacts. The 50th percentile projection represents the median outcome, and is prioritised in building thermal performance assessment methodologies [104]. However, consideration of upper (90th) and lower (10th) percentiles can help to convey the uncertainty associated with climate projections and allows decision-makers to consider a range of possible futures in their planning [105].

2.4.3 Grid Decarbonisation

Over the past few decades, the UK grid has experienced a significant reduction in carbon emissions from electricity generation. Since 1990, emissions from the power sector have dropped by approximately 70% [106, 107], primarily attributed to the decline in coal-fired power and the rise of renewable energy sources [108]. Grid decarbonisation has major implications for the construction sector, influencing multiple life-cycle stages, including product manufacture and operational carbon emissions. The key impacts are discussed below.

Process Decarbonisation within the Construction Industry

Embodied energy in construction material production accounts for approximately 43–62 MtCO_{2e} annually [109], representing over 10% of the UK’s total emissions [106]. Factors such as the energy supply mix, future infrastructure demand, and efficiency gains substantially impact emission levels [110, 89]. Reducing emissions from the manufacture of widely-used, carbon-intensive materials such as steel, cement, aluminium, and glass remains a challenge, with processes typically reliant on fossil fuels [89, 111]. Cement production alone accounts for approximately 7% of global CO₂ emissions, with 30 to 40% of these emissions derived from fuel combustion [112, 89]. Research suggests that, even under predictions of lower demand and slower rates of grid decarbonisation, additional emission reduction strategies will be required for the construction sector to meet national carbon targets [110].

Uncertainty surrounding process decarbonisation within the construction industry necessitates greater consideration of design and material choices [110]. Material substitution using low EC alternatives such as timber, recycled metals and geopolymer concrete, is critical for a quicker transition to a low-carbon built environment [113, 114, 59]. However, overcoming perceived industry barriers, such as high costs and poor product availability, is essential for adoption [115]. Reducing material usage through design optimisation and material efficiency, including ‘lightweighting’ strategies further contributes to emission reductions [113, 89]. Additionally, the re-use of materials and components, including integration of modular assemblies, supports the principles of a circular economy, reducing demand for new materials whilst extending the lifecycle of existing ones [89]. Integrating these strategies (material substitution, reduction, and re-use) advances progress towards sector-wide process decarbonisation [113]. However, early supply

chain engagement with industry professionals, improved accuracy and availability of carbon data, and effective use of whole life costing is required to encourage wide-spread adoption [115].

Operational Decarbonisation

Operational decarbonisation within the built environment encompasses changes to the fuel supply mix, operational energy demand, and system efficiencies. Whilst the carbon intensity of electricity generation in the UK has decreased significantly, from 705 gCO₂e/kWh in 1990 to 238 gCO₂e/kWh in 2023 [116], fossil fuel carbon emission factor (CEF)s are unlikely to undergo significant decline [117]. Despite this, high-efficiency gas boilers are still considered viable for retrofit under current building regulations, with no definitive phase out date set from existing non-domestic buildings [118]. Consequently, buildings reliant on fossil thermal energy, such as natural gas, are likely to contribute disproportionately to carbon emissions over their operational lifetimes.

The rate of decarbonisation can impact the viability of retrofit measures from a life-cycle carbon perspective [119]. Several studies indicate variability in the carbon payback times of retrofit measures owing to different grid energy mix pathways [119, 120, 121, 122]. Whilst it can be argued that a more sustainable grid mix will reduce the effectiveness of some retrofit measures, in terms of carbon payback [120, 121], other measures, such as systems upgrades from gas to electric heating, are inherent to buildings achieving low-carbon energy in the first place and are thought to be beneficial across a range of decarbonisation scenarios and wider climate impacts [122]. Incorporating alternative future energy scenarios can be important in determining the cumulative impact of a building operating into the future, ensuring long-term effectiveness of retrofit strategies in contributing to overall carbon reduction goals [119].

2.5 Computational methods for reducing life-cycle carbon and life-cycle cost

Various methodologies are adopted in building research to reduce the life-cycle carbon and cost impact of refurbishments. Parametric modelling is a widely-adopted technique that facilitates the systematic variation of design parameters within predefined ranges, often used to assess influence on environmental and economic performance over the building’s lifespan [123]. This method can provide detailed insights into the effects of individual parameters. However, as the number of parameters and their possible combinations increase, this approach can become computationally expensive and time-consuming, particularly when employing brute force methods to exhaustively analyse all possible scenarios [123, 124].

Algorithms in building research

The complexity of balancing multiple, often conflicting objectives, such as LCCF and LCC, necessitates more efficient search techniques. Among the various mechanisms for multi-objective optimisation (MOO), GAs stand out due to their adaptability and effectiveness [123]. Unlike the scalarisation approach, which combines multiple objectives into a single weighted sum and struggles with accurate estimation of weighting factors, GAs inherently accommodate the complexity and diversity of objectives without requiring such conversions [123].

GAs are metaheuristic algorithms inspired by the process of natural selection and a sub-set of the class of evolutionary algorithms [125]. The mechanism operates via manipulation of character strings (a.k.a. chromosomes) by genetic operators and the selection of solutions according to their “fitness” level [126]. Through operations, such as crossovers and mutations, the algorithm iteratively evolves a population of potential solutions towards an optimum [126]. This heuristic method enables GAs to efficiently navigate large and complex search spaces, making them particularly suitable for problems with multiple, competing objective functions. The typical procedural steps involved in GA optimisation are shown in Figure 2.4.

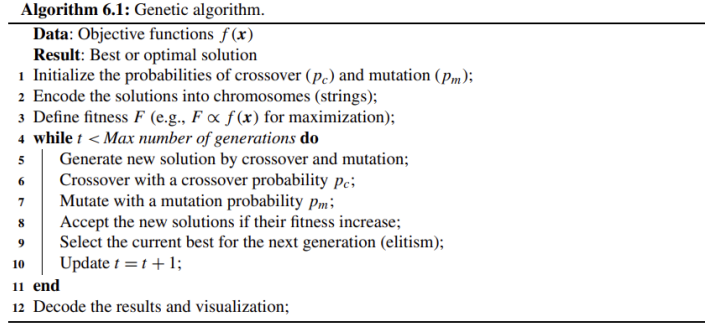


Figure 2.4: Typical procedural steps involved in GA optimisation, from [126].

In the context of building research, the character strings are represented by a specific combination of building design characteristics, as depicted in Figure 2.5. Each unique attribute is presented as a gene with multiple variants. For instance, consider the measure of reducing the U-value of the building’s thermal envelope through additional insulation. Here, the energy conservation measure - adding an insulation layer - serves as the gene, while the different thicknesses of the insulation layer represent the variants of this gene. The crossover process refers to the exchange of *genetic material* between parent chromosomes to create new offspring solutions, potentially combining the advantages of different configurations to find better-performing solutions in relation to the specified performance criteria. This approach mimics evolutionary principles to efficiently search for optimal or near-optimal solutions in complex design spaces.

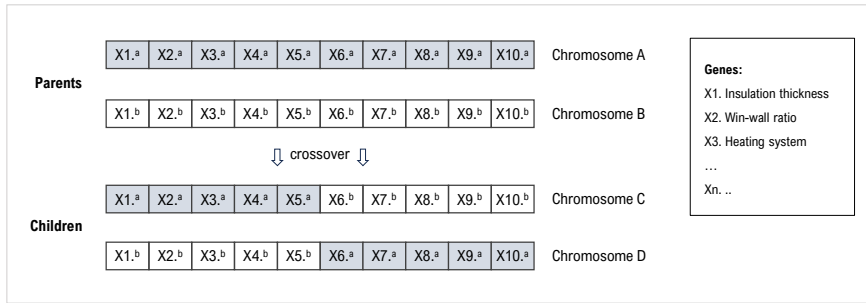


Figure 2.5: Character string representation of building design characteristics as genes within the GA optimisation process.

A significant advantage of **GAs** is their ability to generate a Pareto front, a collection of solutions where no single solution is superior across all objectives [123]. This provides flexibility to building stakeholders to weigh-up the relative benefits and drawbacks across a selection of viable solutions rather than a singular point [127]. Mechanisms, such as Non-dominated Sorting Genetic Algorithm II (**NSGA-ii**) exemplify the power of **GAs** in efficiently navigating the complex trade-offs inherent in **MOO** problems [127]. Furthermore, **GAs** have been integrated into various optimisation platforms, such as Matlab, modeFRONTIER, and JEPlus

[123, 128], enhancing the practical applicability of GAs in building performance optimisation.

2.5.1 Case studies and applications

Life-cycle optimisation of non-domestic buildings

Optimisation Techniques

LCA in the non-domestic building sector has increasingly incorporated advanced optimisation techniques [123]. The most common algorithms used include Particle Swarm Optimisation (PSO) and single and multi-objective GA [123]. PSO is particularly effective for continuous optimisation problems [20], whilst GAs are capable of handling combinations of discrete and continuous variables [123]. Other methods such as mixed integer zero-one programming have been used for minimising single environmental indicators or costs [129]. In general, the selection of optimisation technique is driven by the number of objectives, the type and scale of variables (discrete or continuous), speed and accuracy of search mechanisms, and the integration capability with building energy modelling (BEM) platforms [129, 130, 131].

Optimised Parameters

Whilst a range of optimisation parameters have been explored in relation to non-domestic building retrofit (see Table 2.1), active and passive measures are often considered in isolation [131, 132, 133, 134]. For example, Osman et al. explored the life-cycle GWP impacts of cogeneration technologies, demonstrating up to a 38% reduction in carbon emissions with microturbine or internal combustion engine combined heat and power systems [129]. Bull et al. adopt a primarily fabric-based approach for the retrofit of UK school buildings, with findings indicating a carbon payback period less than the building's lifespan (<60 years) for all considered measures [135]. Similarly, Mendez Echenagucia et al. optimise aspects of the building envelope only, finding WWR reductions to be the most influential factor in reducing both EC and operational carbon (OC) emissions [130]. While these studies all contribute towards the evidence base for non-domestic life-cycle retrofit, it is important to consider fabric and system measures in combination, as their interactions are typically non-additive (agnostic); total savings from combined measures are less than the sum of individual savings [135]. Moreover, under limited investment, prioritisation of system over fabric upgrades has been indicated for non-domestic UK studies [20].

Investigated Typologies

In the context of building refurbishments, the specific characteristics of existing structures can have a strong influence on optimisation outcomes [20, 139]. Despite this, LCA optimisation studies have primarily focused on residential and office buildings. There is a lack of detailed investigation across a broader range

Table 2.1: Life-cycle optimisation case studies of non-domestic buildings: Location, building typologies and optimisation parameters.

		Passive strategies													Active strategies							
Location	Typology	Roof thermal properties	Wall thermal properties	Floor thermal properties	Glazing conductivity	Glazing SHGC	Frame conductivity	Roof solar reflectance	Airtightness	Night ventilation	Shading	Win-wall ratio	Win opening ratio	Facade orientation	Occupancy behaviour	Heating system	Cooling system	Lighting + equipment	Temp SP	Mech Vent System	On-site renewables	Ref
UK	HE (teaching, office)	x	x	x									x			x					x	[20]
US	Office		x		x				x		x	x		x								[130]
US	Commercial															x					x	[129]
Turkey	School	x	x	x	x	x	x														x	[136]
UK	School	x	x	x					x							x						[135]
US	Office	x	x		x	x			x	x			x			x	x	x	x			[21]
UK	HE (various)	x	x		x				x		x					x	x	x	x	x		[76]
Korea	HE (residential)																				x	[131]
Shanghai	Office		x		x	x			x						x	x	x	x	x	x	x	[137]
UK	Office	x	x		x																x	[138]
South Africa	NS															x	x	x				[132]
Spain	Office	x	x		x	x	x		x						x	x		x		x		[139]
Norway	Office	x	x	x	x							x							x	x		[140]
France	School	x	x	x	x	x					x											[141]
Hong Kong	Exhibition space																				x	[133]
US	Office	x	x		x	x																[134]
Serbia	School		x																x			[142]
South Korea	HE (library)					x	x			x									x	x		[143]
Finland	Office	x	x		x	x						x				x	x	x		x	x	[144]

of building typologies and functions, including the diverse and complex building types found within HEIs [20]. Luo and Oyedele optimised an office building, finding that renewable energy and active system upgrades should be prioritised over insulation due to the building’s high electricity-to-heat demand ratio [20]. By comparison, a HE teaching building, with a relatively lower electricity-to-heat demand ratio, did not optimise towards the adoption of on-site renewables under limited investment [20]. Gangolells et al. discovered that optimal environmental measures varied depending on the office typology, with building age being a significant determinant of the efficacy of energy retrofitting strategies [139]. Thus, it is important to consider the contextual aspects of pre-existing designs when defining optimisation problems, and to expand research across a broader range of building typologies.

LCA Standards and Scope

Life-cycle optimisation studies in the non-domestic sector show significant discrepancies in the adopted standards and scope of analysis, impacting the comparability of results [20, 136, 21, 129, 135]. Many studies do not explicitly state adherence to international or national standards, resulting in variability in assumptions, life-cycle calculation protocols and assumed time frames [131, 132, 140]. The assumed

lifespan for **LCA** ranges from 10 to 60 years, affecting the assessment of long-term sustainability measures [129, 135]. Ganoellis et al. found that generally, optimal measures from an environmental perspective were not optimal from an economic perspective within a 20-year period [139]. However, many retrofit strategies may become more lucrative when assessing over a longer time-frame that more closely resembles the lifespan of a typical non-domestic building. Contrasting findings from a UK school building study indicate that the carbon payback is shorter than financial payback, and all measures and combinations of measures repaid the carbon invested in them [135]. These inconsistencies highlight the need for standardisation in life-cycle definitions to enhance comparability.

LCA Objective Functions

Variability in objective functions and life-cycle definitions further complicates the comparison of studies. Energy savings potential and overheating are commonly considered alongside the ‘payback period’ or net present value (NPV) [145, 146, 147, 148]. In addition, several studies focus on **LCC** against operational **GWP**, disregarding the embodied emissions associated with implementing, maintaining, and replacing retrofit measures [21, 131, 137]. Some research indicates that cost-effective measures almost always provide life-cycle **GHG** emission reductions, but not vice-versa [139]. However, this relationship will be distorted by the expected changes in grid-related carbon emissions over time, as discussed in section 2.4.3. The majority of studies do not account for expected changes in **OC** emissions over time, and often do not state the **CEF** assumptions associated with operational energy use. This omission can significantly impact optimal outcomes due to variations in energy grid **CEFs** [130].

Summary of dynamic LCA studies

In recent years, **LCA** studies have increasingly incorporated dynamic characterisation factors to account for temporal changes in environmental impacts, particularly in relation to decarbonising energy networks. This approach aims to provide a more realistic and adaptive understanding of the sustainability of buildings and technologies over their entire life spans. Table 2.2 shows various studies that incorporate dynamic characterisation factors into life-cycle assessments methodologies and a comparison of the assumptions adopted. A discussion of key study outputs is provided below.

For example, Mendez-Echenagucia et al. examined the balance between embodied and operational carbon in the context of energy grid changes [130]. Their study demonstrated how both under- and over-investment in building envelope performance can lead to avoidable emissions over the building’s lifespan, driven by grid carbon intensities and local climates. In regions with low-carbon intensity energy grids, excessive investment in building envelope improvements can result in up to 10 kgCO₂e/m² of unnecessary emissions over 30 years, whereas under-

Table 2.2: Methods, frameworks, objectives and assumptions used in optimisation studies in the non-domestic sector. NA = not applicable, NS = not stated.

Method	LCA Framework	Objective Functions	Climate Projection(s)	CEF Assumption	Fuel Price Projection	Ref
PSO	ISO 14040	1: LCC 2: LCCF	1981-2000, 2021-2040, 2061-2080	static	static	[20]
Multi-objective GA	NA	1: Overheating hours 2: Heating energy 3: Lighting energy	2020, 2044, 2090	NA	NA	[145]
Parametric (brute force)	ISO 14040 ISO 14044 EN 15978	1: EC emissions 2: OC emissions	historic	dynamic	dynamic	[130]
Mixed integer programming	NS	1: LCC 2: GWP 3: TOPP ¹	historic	static	static	[129]
Parametric	ISO 14040 EN 15643	1: LCCF 2: Life-cycle energy 3: Embodied energy	historic	static	NA	[136]
Parametric	EN 15804	1: Heating energy 2: EC emissions 3: LCCF 4: NPV 5: Payback times	historic	static	dynamic	[135]
JMIM feature selection	NA	1: NPV 2: Energy savings	2100	NA	NA	[21]
Parametric (brute force)	EN 15978	1: EC emissions 2: OC emissions	historic	static	static	[76]
Parametric	NS	1: Electricity use 2: OC emissions 3: Cost effectiveness	1981-2000, 2031-2050, 2081-2100	dynamic	dynamic	[148]
Multi-objective GA	NS	1: LCC 2: Energy savings	historic	NA	dynamic	[131]
Parametric	NS	1: Energy consumption 2: LCC 3: CO ₂ savings	historic	static	static	[137]
PSO	ISO 14040	1: LCC 2: Life-cycle energy 3: LCCF	historic	static	static	[138, 149]
Multi-objective GA	NS	1: Energy savings 2: NPV 3: Payback period	historic	NA	static	[132]
Parametric	EN 15804 EN 15978	1: LCCF 2: OE savings 3: Initial investment 4: Payback period	historic	static	static	[139]
PSO-Generalized Pattern Search	NS	1: LCC 2: Energy consumption	historic	NA	dynamic	[140]
Single and multi-objective GA	NS	1: EC emissions 2: CapEx 3: Energy consumption 4: Thermal comfort	historic	NS	NS	[141]
Single and multi-objective GA	NS	1: Total cost 2: OC emissions 3: Grid Interaction Index	historic	dynamic	dynamic	[133]
PSO	NS	1: LCC	historic	NA	dynamic	[134]
Single-objective optimisation	NS	1: Total cost 2: PMV ²	historic	NA	static	[142]
Multi-objective GA	ISO 14040	1: PMV ² 2: Initial investment 3: Heating energy 4: NPV 5: GWP	historic	NS	dynamic	[143]
Multi-objective GA	NS	1: OC emissions 2: NPV of LCC	historic	NA	dynamic	[144]

¹Tropospheric ozone precursor potential (TOPP); ²Predicted mean vote (PMV).

investment in high-carbon intensity grids could lead to more than 150 kgCO₂e/m² of wasted emissions [130]. Moreover, findings indicated that under-investment was more likely in harsh climates with high carbon grids and over-investment more likely in moderate climates with low carbon grids. Results show how the relationship between embodied and operational carbon is highly localised, with optimal design variables varying significantly between locations. This study underscores the importance of aligning investment strategies with the anticipated decarbonisation trajectory of energy grids and local climates.

Similarly, Collinge et al. applied dynamic characterisation factors to the [LCA](#) of an educational building, demonstrating how the environmental impacts over the building’s lifetime vary significantly from what would be predicted if temporal changes were not taken into account [150]. The results suggest changes in external conditions such as energy mixes or environmental regulations during a building’s lifetime, can influence the [LCA](#) results to a greater degree than the material and construction phases. Sensitivity analysis indicated robustness in the considered scenarios, with static results lying within the upper and lower bounds of dynamic [LCA](#) scenarios. Correspondingly, adapting [LCA](#) to a more dynamic approach seems likely to increase the usefulness of the method in assessing the environmental performance of buildings and other complex systems in the built environment. While dynamic characterisation factors were considered, the temporal aspect of climate change was not addressed in either study [130, 150].

Shibuya and Croxford further investigated the implications of dynamic factors in [LCA](#), focusing on carbon and cost considerations under future climate scenarios for office buildings in Japan [148]. Although their study did not encompass all life-cycle stages as per BS EN 15978 [17], focusing on in-use emissions only, it demonstrated the potential impact of dynamic factors on operational carbon emissions and cost-effectiveness, highlighting variations across different locations and time periods. Additionally, the research takes into account contextual implications of the Fukushima nuclear accident on Japan’s energy policy, which may affect the country’s ability to meet CO₂ reduction targets through changes in electricity generation [148]. Findings emphasise the need for comprehensive approaches that integrate situational considerations into [LCA](#) methodologies. Unlike the aforementioned studies, future climate data was incorporated into this analysis, however parametric techniques were adopted limiting the breadth and granularity of optimisation parameters assessed.

Coupling optimisation and climate change adaptation

Recent studies have increasingly focused on integrating climate change adaptation within multi-objective optimisation frameworks for building retrofitting, particularly in non-domestic settings. These efforts aim to create a combined optimisation-adaptation approach that can address the challenges posed by future

climate conditions.

For instance, a study on Canadian school buildings employs [NSGA-II](#) to optimise thermal comfort, lighting, and heating energy performance, using future climate projections [\[145\]](#). The study explores various thermo-physical building characteristics, including U-values, [WWR](#), shading, and cool roofs, to determine the most effective retrofit strategies under changing climate conditions [\[145\]](#). Findings support a phased approach: energy-efficient envelopes and natural ventilation with night cooling for present climates, adding cool roofs and overhangs in the medium term, and movable screen shading in the long term [\[145\]](#). Another study assesses the life-cycle performance of retrofitting [HE](#) buildings under climate change conditions, using a Genetic Algorithm-Artificial Neural Network (GA-ANN) approach to predict future energy demand and production [\[20\]](#). Findings illustrate evolving investment priorities over time, with changes to building energy demand end-uses and renewable energy production. The authors estimate up to a 4.7% over-estimation or 54.7% under-estimation of lifetime cost, energy and carbon if optimal retrofitting solutions from current weather conditions are adopted under climate change conditions [\[20\]](#). However, changes to the carbon intensity and cost of the power grid, natural gas and biomass production under future years were not considered [\[20\]](#).

Further exploration by Shen et al. examines the impact of global climate change from 2020 to 2060 on the effectiveness of [ECMs](#) in office buildings across various U.S. climates [\[21\]](#). The authors note variability of optimal retrofit strategies, and their ranking in the combinatorial space, based on pre-existing building characteristics and changing climate conditions. The economic benefits of natural ventilation ([NV](#)) under future climates are highlighted, reducing cooling loads through removal of redundant heat during suitable outdoor conditions. Additionally, it was found that optimal airtightness and glazing properties differ across U.S. climate zones, suggesting that retrofit strategies must be tailored to local conditions to remain effective under changing climate scenarios. A final study evaluates contemporary energy-optimised office buildings in Southeast Asia, focusing on passive measures to mitigate overheating and reduce energy consumption [\[146\]](#). This study uses [GA](#) optimisation to compare the performance of energy-optimised designs under current and future climates.

2.6 Knowledge Gap

In this section, a synthesis of the literature review is presented to define the knowledge gaps leading to research questions central to this study.

Despite advancements in the optimisation of climate change adapted building design, notable gaps remain for the non-domestic building sector. Studies indicate that future climate change will impact building energy demand. However, most existing research focuses on immediate or short-term impacts, limiting understanding of how probabilistic climate predictions will influence long-term operational energy performance in the UK HE sector and consequences for building design. This gap suggests a need for more detailed investigations into the changing climate impacts on energy demands for HE buildings, particularly with respect to heating and cooling loads. This work aims to address this research gap by examining the impacts of future climate projections on operational energy performance within the HE sector. This leads to the first research question: *How will future climate projections affect the predicted operational energy performance of higher education buildings?*

Life-cycle analyses are increasingly utilised in building design research. However, there remains a lack of cohesive approaches that consider both LCCF and LCC metrics within CCA strategies, particularly for non-domestic settings. Most studies consider these metrics individually, limiting understanding of the trade-offs and synergies between economic and environmental targets. Furthermore, the integration of a combined systems-fabric approach within LCA across a wider range of non-domestic building typologies, including HE buildings, remains under-explored. Future efforts should also aim to standardise approaches using established protocols and guidelines to improve the comparability and reliability of LCA outcomes. Addressing this research gap, this study aims to examine how these metrics can impact design decisions for HE building refurbishment under climate change. This leads to the second research question: *What are the life-cycle carbon and life-cycle cost implications of adopting climate change adaptation strategies in the design of urban higher education buildings?*

In terms of carbon emissions, the literature identifies a gap in understanding the relationship between embodied and operational carbon within the HE sector, especially in the context of climate adaptive strategies. Existing studies often isolate these factors, without accounting for the potential trade-offs and synergies that could arise from a combined approach to carbon management. This is particularly relevant to HE buildings, where structural and operational features can vary widely. EC and OC emissions are often analysed separately and relatively few studies consider how material choice and systems interact across a building's life cycle under climate change. This knowledge gap informs the third research question: *What trade-offs and synergies exist between embodied and operational carbon*

when applying climate change adaptation strategies in the higher education sector?

Grid decarbonisation trajectories can introduce additional uncertainties in the design of low-LCCF adaptation strategies, yet most current analyses assume static grid conditions. HE buildings can have long lifespans and unique energy demands, requiring a more dynamic understanding of how variable decarbonisation rates affect long-term energy resilience and adaptation strategies. There is a need to consider dynamic characterisation factors for a more realistic assessment of carbon and cost investment trade-offs and payback periods. This research incorporates diverse decarbonisation pathways to address this gap, leading to the fourth research question: *How do uncertainties in grid decarbonisation trajectories impact the selection of optimal climate change adaptation strategies?*

Overall, the study aims to capture temporal changes and future scenarios to provide a more long-term understanding of the carbon and cost impacts of HE building refurbishment strategies.

Chapter 3

Methodology

3.1 Methodological Development

The research methodology was developed to address theoretical and practical challenges associated with conducting life-cycle assessments in the [HE](#) sector under long-term projection uncertainty. The approach balances data limitations, model complexity, and computational efficiency with the need for robust, transparent, and adaptable methods. Table [3.1](#) summarises these challenges, outlines the adopted methodological principles, and specifies how each was implemented in this study.

Table 3.1: Key methodological challenges, principles, and implementation in this study.

Challenge	Methodological Principle	Implementation
Time resolution: Hourly simulations vs. annual grid decarbonisation data	Hourly resolution enables simulation of dynamic occupancy and load patterns, while annualised grid data manages long-term uncertainty in decarbonisation and pricing trajectories.	Hourly simulations were performed in EnergyPlus to capture load variability (section 3.4.3). Annual fuel price and grid decarbonisation data were integrated from government and industry projections, ensuring consistency with long-term pathways (section 3.3.7).
Robust detailing vs. simplified assumptions	Balance detailed thermal and systems modelling with pragmatic simplifications for uncertain future parameters.	Detailed envelope and HVAC system models were calibrated using construction records and site data, while grid-level and macroeconomic assumptions were simplified to scenario-based inputs (section 3.4.3 vs. 3.3.7).
Capital and operating cost data reliability	Integrate CapEx and OpEx while considering the volatility of energy and commercial markets.	Material and system cost data were obtained from up-to-date market databases (section 3.3.6 , Appendix E-G), and electricity and gas price projections. The time value of money was represented through applying a discount rate to estimate the present value of future cash flows (section 3.3.6).

Challenge	Methodological Principle	Implementation
Architecturally-driven approach	Reflect diverse typologies and operational patterns in HE buildings.	Three real-world case studies were selected to represent different typologies (architectural school, heritage office, residential halls). Each model incorporated validated occupancy schedules and operational data from Estates teams (sections 4.1 , 5.1 , 6.1).
Defining system boundaries	Set clear, building-focused boundaries to prioritise operational and direct impacts, while acknowledging excluded upstream impacts.	The assessment encompassed material production to end-of-life disposal (Modules A–C) and benefits beyond the system boundary (Module D). Costs and emissions associated with wider infrastructure transitions associated with a changing energy system (e.g. hydrogen or ‘green gas’ networks) were excluded in accordance with BS EN 15978 conventions, ensuring methodological consistency and maintaining relevance to building-scale decision-making (section 3.3.6).
Long-term climate projection uncertainty	Integration of future climate scenarios to capture changing thermal loads while balancing model complexity and simulation scope.	A high-emission 2050s climate scenario was applied to represent a conservative outlook on overheating risk, capturing the potential upper bound of climate impacts relevant to refurbishment decision-making. Focusing on mid-century projections (2050s) instead of end-of-century (2080s) introduces slightly more certainty and aligns design decisions more closely with the building’s practical life-cycle. The analysis was limited to a single climate scenario to reduce computational demand but the approach remains adaptable to a range of potential future conditions (section 3.3.5).
Detailed modelling vs. scalability	Detailed, context-specific models capture the unique characteristics of HE buildings but can limit scalability.	Results from each case study were analysed for cross-case patterns and compared against the wider HE building stock (section 7), enabling broader sectoral interpretation.

Overall, the methodological framework ensures that each challenge is explicitly addressed within the modelling, data integration, and scenario analysis process, reinforcing transparency and reproducibility.

3.2 Methods Overview

The approach taken to address these research questions is based on the concept of Design Science Research [151]. The core research principles involved are detailed case study modelling analysis, and the simulation and rapid assessment of multiple design alternatives. A comparison of outputs from each design solution aims to identify the most favourable (‘optimal’) design scenarios. A simplified overview of the research design is presented in Figure 3.1, demonstrating the two main methodological domains of the work.

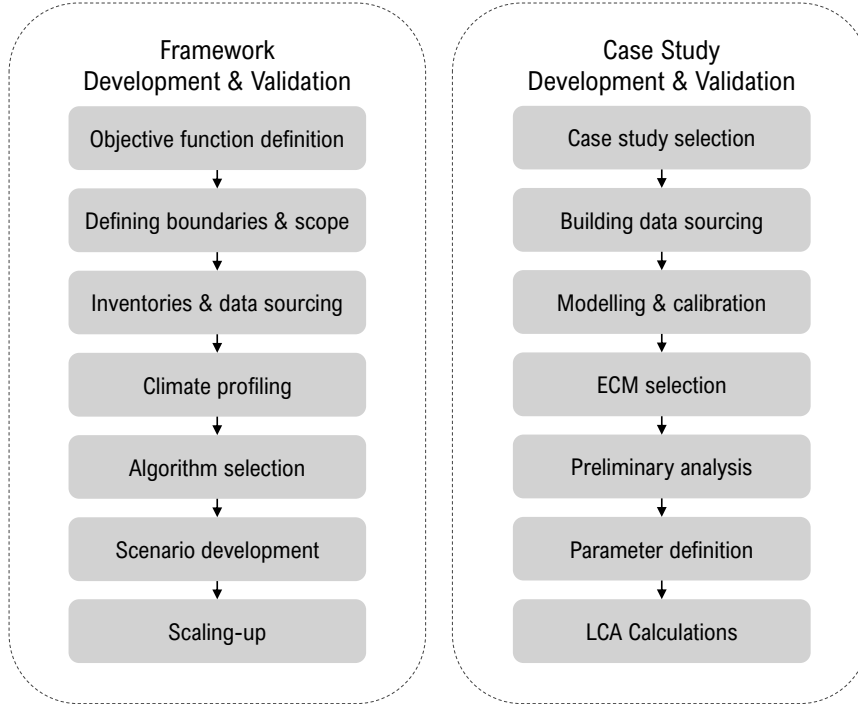


Figure 3.1: Simplified overview of research process.

Although each stage can be broadly classified into the development of either framework or case study, the flows of work interact at several stages and are mutually dependent. The two scopes of work form the main sub-chapters of the methodology; the first section focusing on the establishment of the future climate LCA framework, the second providing a detailed account of case study development, validation and pre-processing prior to application within the framework.

3.3 Methods 1: Framework Development

3.3.1 Framework Principle

The first stage of the methodology is to develop a framework that can subsequently be applied to and validated through real-world case studies. Responding to the objectives identified in 1.1, the framework has been developed with the following inclusions:

- The ability to handle detailed building energy models, characterising the [HE](#) building stock at a sufficient level of detail.
- Simulates and post-processes combinations of multiple design alternatives.
- Calculates the [LCCF](#) and [LCC](#) at each design iteration.
- Incorporates changing climate assumptions over the building's life cycle.
- Operates as a feedback loop, understanding the impact of various scenarios relating to grid decarbonisation on design output.

The methods and tools used to achieve each of these framework elements are discussed in the following sections.

3.3.2 Life-cycle Objective Functions

The objective functions used in the optimisation framework are to minimise both life-cycle carbon and life-cycle costs through a combination of design improvements.

Objective Function 1: Minimise LCCF Reduce total carbon emissions over the building's life cycle, including both embodied and operational carbon. In the context of a changing climate, this objective seeks to balance these two components to achieve the lowest overall carbon footprint, recognising the trade-offs between initial construction impacts and long-term operational efficiency.

Objective Function 2: Minimise LCC Reduce total cost incurred over the building's life cycle, accounting for both [CapEx](#) and [OpEx](#). In the context of a changing climate, this objective addresses the balance between upfront investment and long-term operational savings, aiming to achieve the most cost-effective building over its entire lifespan.

Where active [HVAC](#) systems are present, operational components of life cycle carbon and life-cycle cost become a function of the heating and cooling energy loads and mechanical ventilation requirements. As such, the thermal operating

conditions must be controlled within certain boundary conditions that are considered “acceptable” to the occupant. The assumptions made to control this dynamic variable are considered on a case-by-case basis, depending on the building’s systems thermal regulation strategy and historical set-point data.

3.3.3 Framework Optimisation Strategy

Optimisation Strategy

The aim of implementing multi-objective optimisation is to find a set of solutions that define the optimal trade-off between multiple, competing objective functions. As discussed in section 2.5, conventional, iterative techniques can be used to test adaptation strategies via *brute-force*. However, the time and labour intensity of this approach often limits its application to a relatively small search space. Harnessing the use of GAs is a more efficient method for investigating numerous variable options in combination.

Algorithm Selection

The selection of NSGA-ii to drive the optimisation framework is grounded in its effectiveness in handling multi-objective optimisation problems efficiently. NSGA-ii is widely adopted in building retrofit optimisation studies to reduce processing time and power [152], and offers the following relative advantages over other evolutionary algorithms:

Non-dominated Sorting NSGA-ii utilises non-dominated sorting to categorise solutions into Pareto fronts, ensuring that the algorithm maintains diversity across the population. This facilitates the exploration of trade-offs between multiple conflicting objectives, such as LCCF and LCC.

Diversity Preservation Through the incorporation of crowding distance, NSGA-ii promotes the spread of solutions across the Pareto front. This diversity preservation helps in avoiding premature convergence to a limited region of the solution space, thereby offering a wide range of optimal design alternatives for building refurbishments. It has been demonstrated to find a better spread of solutions and better convergence near the true pareto-optimal front than other evolutionary algorithms [127].

Elitism Mechanism NSGA-ii typically incorporates an elitism mechanism that ensures the best solutions from one generation are carried over to the next, thereby preventing the loss of good solutions and promoting faster convergence.

Efficient Pareto Front Approximation NSGA-ii provides a good approximation of the Pareto front in a single run, making it effective for problems with

multiple objectives where finding a representative set of trade-off solutions is crucial.

Application of NSGA-ii for optimisation under future climate scenarios has also previously been demonstrated [153].

NSGA-ii Mechanism

The multi-objective optimisation process, using NSGA-ii, is outlined in Figure 3.2, with detailed steps as follows:

1. Initial population generation:
An initial set of parameter values are generated using Latin hypercube sampling (LHS) [154]. LHS ensures a random yet well-distributed sample selection across the entire parameter space, representing a diverse configuration of adaptation strategies.
2. Future climate simulation: The initial sample is simulated with future climate weather projections to ascertain the operational energy performance of the various building configurations.
3. Objective function calculation: Aligning simulation results with carbon emission data and cost inputs, the LCCF and LCC objective functions are calculated for each design alternative. The algorithm assigned equal weighting to carbon and cost in the simulation.
4. Selection and crossover: The algorithm identifies the best-performing solutions from the initial population based on their non-domination rank and crowding distance. These selected solutions undergo crossover operations to generate offspring for the next generation, promoting the exchange of valuable traits between solutions.
5. Mutation: To maintain genetic diversity and prevent premature convergence to suboptimal solutions, mutations are applied to some offspring. This introduces random variations, helping the algorithm explore new regions of the solution space.
6. Populate next generation: The resulting solutions, after crossover and mutation, form the next generation of CCA strategies. Through continuation of this iterative process, each new generation should perform better than the previous.
7. Handling constraints: Constraints are implemented into the framework to avoid hybrid systems being formed from incompatible variables. For example, the use of nightpurge ventilation in combination with mechanical ventilation with heat recovery (MVHR) nightcycle operation are operational incompatible, and as such, these parameters are flagged as mutually exclusive.

The population size, maximum number of generations, mutation rate and cross-over rate were determined based on best-practice according to literature. Unlike brute force methods, **GAs** can rapidly process multiple variables without exploring the entire design space. The limitation is that locating the global optima is not always guaranteed. In addressing this limitation, multiple runs are conducted for each model to verify that the **GA** consistently reaches the same optimum, thereby increasing confidence in the presence of a global optimum.

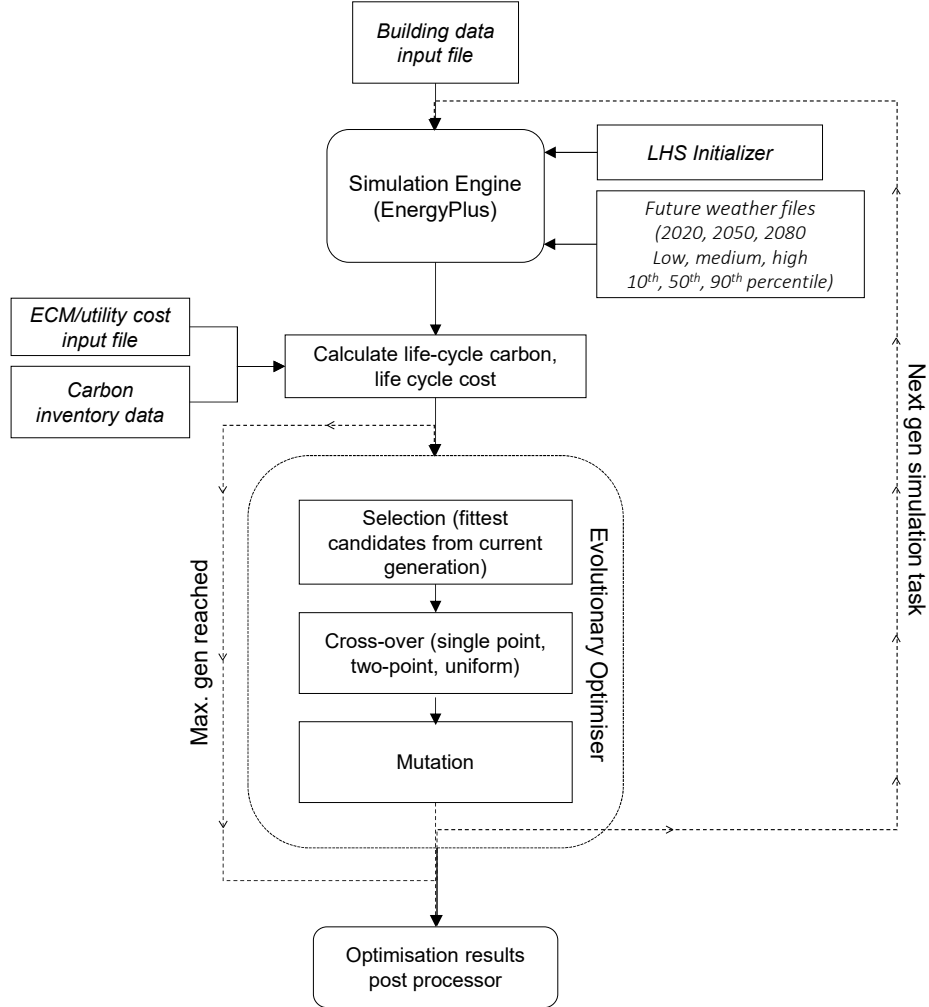


Figure 3.2: Rapid data-driven optimisation framework for CCA and LCA. LHS=Latin Hypercube Sampling.

In this study, no pre-defined weights or priorities were assigned to the objective functions; instead, the **NSGA-ii** algorithm fully explored the Pareto front, identifying a set of non-dominated solutions that represent optimal trade-offs between **LCCF** and **LCC**. This allows for decision-making to occur post-optimisation, where solutions along the Pareto front are evaluated according to decision-makers (e.g. estates teams) preferences.

3.3.4 Modelling tools

EnergyPlus

Case study models are developed using a whole-building energy modeling software and simulated with EnergyPlus [155]. EnergyPlus is the most widely used building energy simulation tool in building retrofit optimisation research. Developed by the U.S. Department of Energy, it has undergone numerous reliability tests and validations, ensuring it meets the accuracy requirements necessary for building design and performance analysis [156]. EnergyPlus simulates dynamic, operational energy flows, such as heating, cooling, lighting and power and ventilation in the context of specified external climatic conditions. This makes it an essential tool for evaluating the energy efficiency and environmental impact of building retrofit strategies under various climate conditions.

jEPlus+EA

To integrate dynamic thermal simulation modelling within the [NSGA-II](#) mechanism, an advanced building performance optimisation tool was utilised. JEPlus varies input parameter values to automate the generation and execution of multiple EnergyPlus simulations for complex parametric studies [128]. By coupling JEPlus with [GAs](#), JEPlus+EA enables the efficient exploration of a vast search space to facilitate multi-objective optimisation [128].

Integrations

Several integrations were necessary for the extraction and post-processing of data in the optimisation framework. [EC](#) and [CapEx](#) data were processed using regular expressions to identify the relevant values based on the input parameters. Additionally, Python scripts were integrated into the platform to calculate custom [EC](#) and [CapEx](#) values during post-processing. This was particularly important for components like [HVAC](#) systems, whose sizes and associated carbon and cost values were dependent on the simulated capacities and thus could only be determined after the simulation run was completed.

3.3.5 Summary of framework inputs & outputs

A more detailed overview of the [CCA-LCA](#) optimisation framework is presented in Figure 3.3, with input and output flows. These are outlined below with further detail available in the following sections.

Inputs

Calibrated EnergyPlus File: Detailed building energy simulation models, calibrated against actual measured energy consumption data to ensure accuracy in

predicting building performance.

Climate Projections: Climate data from the UK Climate Projections 2009 (UKP09) are adopted to simulate future weather scenarios [96]. These projections include temperature, precipitation, and other climate variables that affect building energy performance.

Refined Adaptation Measure Alternatives: Measures are tailored from the broader **ECM** toolkit, adapted to address the unique characteristics of each building (see section 3.4.4).

CapEx Data: Initial costs associated with implementing the adaption measures and recurring costs due to replacement over the buildings life-span (see section 3.3.6).

EC Data: Data on the carbon associated with the materials and construction processes for each adaptation measure; includes emissions generated during the production, transportation, installation and replacement cycles (see section 3.3.6).

Carbon Emission Projections: Carbon emission factors associated with building operation under different energy mix and policy projections; derived from government and National Grid Future Energy Scenarios and outline a ‘best-case’ and ‘worst-case’ pathway (see section 3.3.7) [157, 158].

Fuel Price Projections: Future energy price forecast, based on government projections, adjusted to their **NPV** using the BRSIA methodology (see section 3.3.7) [95].

Outputs

Pareto Optimal Solution Sets: A set of solutions derived from the **CCA-LCA** optimisation process that represents the most efficient trade-offs between **LCCF** and **LCC** under projected future climates.

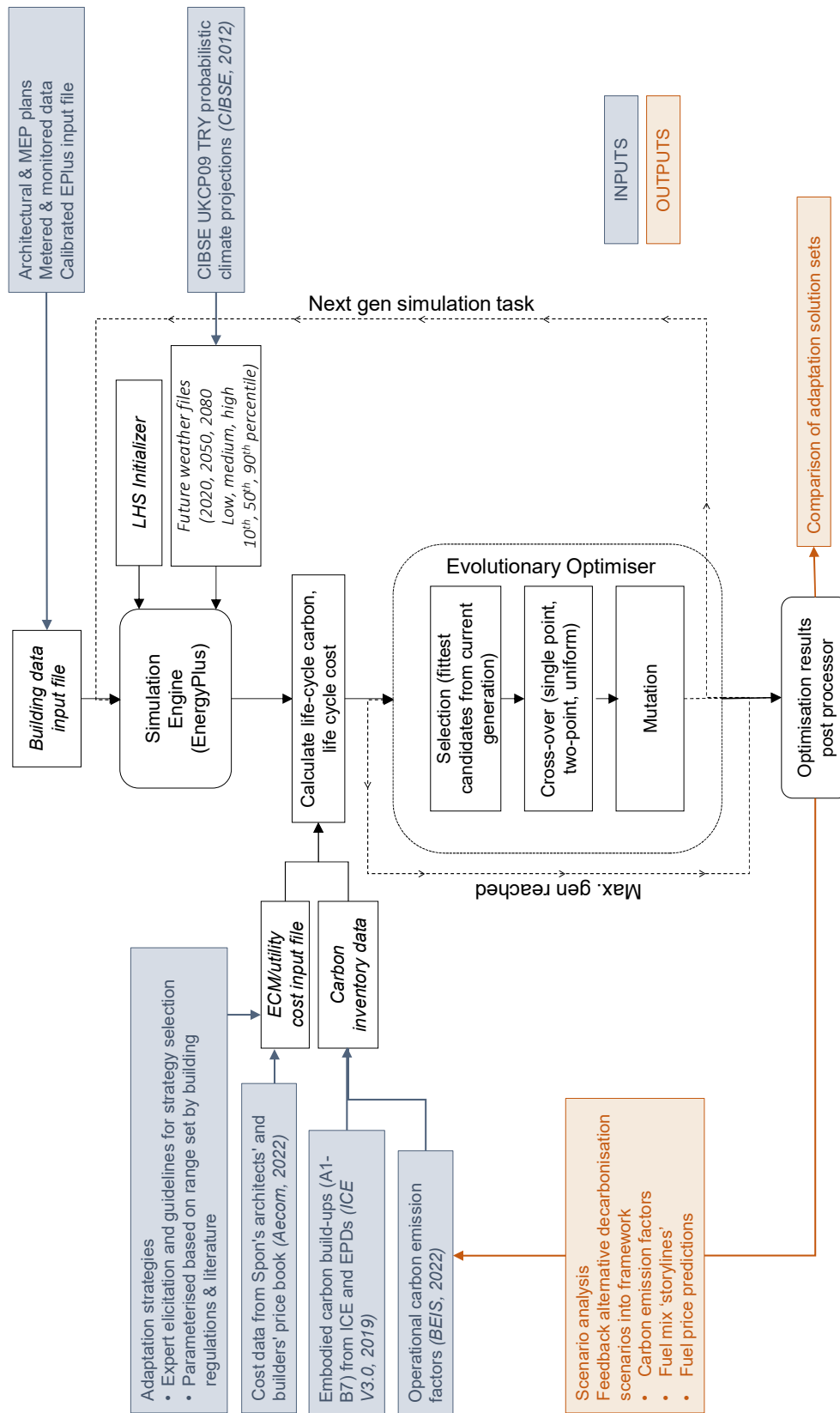


Figure 3.3: Overview of CCA-LCA framework including all stages, inputs and outputs.

3.3.6 LCA Standards & Calculations

Life-cycle assessment is an area of growing interest in building construction research, with several public and industry bodies providing guidance for conducting these studies [19, 18]. This section defines the standards adopted in this research and the various calculations, assumptions and conditions that have been used to conduct LCA. The BRE indicate that an expected 60 year building lifespan is appropriate for reporting purposes [159]. This aligns with CIBSE future weather data files for 2020, 2050 and 2080 [160], so is used as the assumed timeframe for life-cycle assessments. Following BS EN 15978:2011 the functional equivalent, which improves cross-study comparability, can be defined as: 1 m² of usable floor area of the relevant building type, based in the UK, over a 60-year reference period, providing the defined service levels. Service levels include thermal comfort and ventilation set-points, as specified in each building's operational stage data, which also align with UK Building Regulations and standards [17].

LCCF Standards

There are many ways in which the life-cycle carbon impact of a building can be defined and calculated based on study scope and boundary conditions. This work implements the most recent standard for life-cycle impact assessments in the built environment, BS EN 15978:2011 - Sustainability of construction works - Assessment of environmental performance of buildings [17]. The following sections outline the assumptions behind each life-cycle stage in the study context.

LCCF Scope

The standard defines the four main stages of a building's life cycle: Product, construction, use-stage and end-of-life, as depicted in Table 3.2. For most framework stages, assumptions used were based on RICS whole life carbon assessment for the built environment [19]. The primary assumptions for each life-cycle stage are outlined in Table 3.2. The following life-cycle stages are excluded from the assessment due to data limitations, methodological boundaries, or their relatively minor contributions to total life-cycle impacts:

- Repair and Maintenance (B2, B3): Products and systems are assumed to perform according to their defined service lives, with replacements captured under B4. This is considered appropriate since evidence suggests repair and maintenance impacts become more dominant over a very long life expectancy (e.g. 200 years), whereas embodied impacts from initial production typically dominate over a more moderate reference service life (e.g. 60 years) [161]. In addition, module B2 and B3 is not widely reported in databases and is highly project-specific - exclusion avoids introducing additional uncertainties and unverified bias towards certain design attributes.

- Operational Water Use (B7): Any energy use and associated emissions from water-related systems are captured under operational energy use (B6). Module B7, accounting for emissions from water supply and wastewater treatment, is excluded as the buildings studied are connected to mains water networks and public sewer system. This makes it difficult to attribute these centralised emissions to individual buildings.
- Demolition (C1): Deconstruction and demolition are omitted due to high variability in end-of-life practices and the lack of reliable data on equipment use and site-specific logistics. Whilst average rate figures (based on GIA) are provided in some LCA guidance [19], this is calculated to have relatively low impact on overall LCA results, and does not influence the selection of Pareto-optimal outputs, since GIA remains consistent throughout design alternatives.

LCCF Calculations

The LCCF in $\text{kgCO}_{2e}/\text{m}^2/60$ years is calculated for each model (i) within every generation of the framework. It is given by: The LCCF in $\text{kgCO}_{2e}/\text{m}^2/60$ years is calculated for each model (i) within every generation of the framework. It is given by:

$$\text{LCCF} = \sum_i (E_{ip} + E_{it} + E_{ic} + E_{iu} + E_{ir} + E_{io} + E_{ieol}) \quad (3.1)$$

where each component E_{ip} , E_{it} , E_{ic} , E_{iu} , E_{ir} , E_{io} , and E_{ieol} represents emissions associated with different stages of the building's life cycle:

E_{ip} Production and manufacturing (A1-A3)

E_{it} Transport to site (A4)

E_{ic} Construction works on site (A5)

E_{iu} In-use processes (B1)

E_{ir} Replacement works (B4)

E_{io} Operational energy use (B6)

E_{ieol} End-of-life and disposal (C2-C4)

Carbon Inventories

The relevant data for the different stages of a buildings life-cycle is obtained from literature and carbon inventories, primarily ICE V3.0 [59]. This database compiles embodied energy and carbon values from a wide range of peer-reviewed and verified sources, applying consistent selection criteria and professional input to

Table 3.2: BS EN 15978:2011 life-cycle stages and calculation assumptions adapted from RICS [17, 19].

Stage	Inclusion Assumptions
Product	A1 – Raw material supply x Cradle-to-gate (A1-A3) emissions scaled from material density or system mass. Supplied by Bath ICE V3, where available, and EPDs in accordance with BS EN/ISO standards in all other cases [59].
	A2 – Transport x
	A3 – Manufacturing x
Construction	A4 – Transport x Based on default local, national, European or global transport distances [19]. GHG transport emissions assumed 0.10614 kgCO ₂ e per tonne.km for HGV [162].
	A5 – Construction x Component-specific baseline wastage rates obtained from WRAP guide to reference data [163]. A5 GHG emissions established based on site waste disposal scenarios [19].
Use stage	B1 – Use x Included in relation to refrigerant emissions, where relevant, as can be a significant component of life-cycle GHG emissions [55].
	B2 – Maintenance
	B3 – Repair
	B4 – Replacement x Expected lifespan derived from multiple sources to calculate replacement emissions per reference study period [77], [19].
	B5 – Refurbishment x Single-step intervention - no planned alteration to fabric or systems during the service life of the building.
	B6 – Operational energy use x Calculated based on simulated EnergyPlus outputs [155]. Operational carbon emission factors developed based on BEIS projections and National Grid Future Energy Scenarios (see section 3.3.7).
	B7 – Operational water use
End-of-life	C1 – Demolition
	C2 – Transport x Average distance between two closest landfill sites obtained from government database [19], [164].
	C3 – Waste processing x Recovery rates of 90-96% for inorganic waste; 0.013 kgCO ₂ e/kg waste applied to remaining proportion for disposal. Organic waste (timber) assumes 25% landfilling at 2.13 kgCO ₂ e/kg and 75% incineration with emissions equal to sequestered carbon [19].
	C4 – Disposal x

recommend best estimates [60]. However, product data can be outdated and limited, particularly regarding the embodied carbon of systems. When ICE data was unavailable, alternative datasources, such as manufacturer’s specifications and literature, were used. This approach ensures that comprehensive assessments can still be conducted, albeit with a less rigorous methodological approach.

LCC Standards

Life-cycle cost frameworks account for costs related to the initial capital investment of construction and operational cash flows over a defined period of time [165]. The life-cycle costing framework used in this research is based on the current international standard ISO 15686-5:2017 Buildings and constructed assets - Service life planning - Part 5: Life-cycle costing [18]. The standard draws a boundary around construction, operation, maintenance, and end of life as the key components to be included in life cycle costing calculations.

LCC Scope

The scope of the LCC analysis is defined using the ‘Typical Scope of Costs’ framework outlined in ISO 15686-5:2017 [18]. This framework specifies the categories of costs that are considered within the boundary conditions of the analysis, as well as those that are excluded. Aligning with ISO 15686-5:2017 guidance, the scope of costs included in this study are:

Construction Costs Capital expenditure resulting from procurement, installation, and commissioning of building components and systems. This primarily refers to the costs of material and labour.

Operational Costs Operational expenses associated with activities and processes over the buildings life cycle. This research considers operating costs related to the use of energy utility.

Renewal Costs Costs associated with the replacement of building components or systems during their life cycle. In the study context, this refers to replacement of components at the end of their estimated life-span.

End of life costs, relating to the removal and disposal of building materials and components, were not included in this study. Disposal methods and associated costs can vary widely depending on local regulations, waste management practices and material type, and in many cases, constitute a relatively small portion of the overall LCC compared to initial and operational costs. Given the challenge of obtaining accurate and comprehensive data for this stage, the primary focus of the study was on the LCC of initial, operational and renewal costs only. These aspects are typically more directly relevant to decision-making during the design, construction, and operation phases of buildings.

LCC Calculations

The LCC is given by:

$$\text{LCC} = \sum_i^i (C_{ip} + C_{ir} + C_{io}) \quad (3.2)$$

C_{ip} Initial production and construction costs (A1-A5)

C_{ir} Replacement costs (B4)

C_{io} Operational costs (B6)

ISO 15686-5:2017 advise that discounted future costs and benefits should be converted to a NPV for a consistent comparison of alternatives [18]. NPV is calculated by discounting future cash flows to their present value using a discount rate, aiming to account for the time value of money. In this study all future costs are brought to their NPV through the following formula:

$$\text{NPV} = \sum_{i=0}^n \frac{V_i}{(1+r)^n} \quad (3.3)$$

n Period of analysis in years

i Present

V_i Cost in year i

r Real discount rate

A discount rate of 3% per annum was adopted in line with BSRIA Guide: Life Cycle Costing and HM Green Book [95, 166].

Cost inventories

Cost data was obtained from up-to-date literature, inventories, and industry specifications. Priority was given to data derived from Spon's Architects' and Builders' Price Book 2022 [167], providing relatively detailed, industry-relevant and up-to-date information on the prices of various building materials and labour costs. Utilisation of the 2022 edition aimed to capture relatively current market conditions at year 1 of the 60 year study period (2022-2082). Future costs were discounted from the 2022 baseline. Measured work rates consist of the following components [167]:

Labour: Calculated from gang wage rate (skilled or unskilled) and the time required, noting that large regular or continuous areas of work are more economical to install than smaller complex areas.

Plant: Machinery and running costs for construction, such as fuel, water supply, electricity and waste disposal.

Materials: Costs of ancillary materials, such as nails, screws, waste, required in association with the main material product.

Prime Cost: Actual price of the material, as sold by the suppliers, accounting for trade and quantity discounts and transport to site.

For HVAC systems, the equivalent process was adopted, prioritising the use of Spon’s Mechanical and Electrical Services Price Book for consistent reporting, where available [168].

Boundary Conditions

Boundary conditions are clearly defined to ensure a consistent and realistic scope for LCA calculations [19]. Building components included within this assessment are outlined in Table 3.3. The analysis includes an initial replacement cycle of the external envelope, since geometry adjustments (e.g., WWR changes) are included as variable parameters in the optimisation process, impacting external facades. However, sub-structural and super-structural elements, such as foundations, base-ment build-up, columns, beams, frames, and upper floors are assumed to be re-tained during all building refurbishment processes. This assumption focuses the analysis on elements with the most significant impact on operational performance.

Table 3.3: Scope of analysis: Inclusions and exclusions.

Element Group	Building Element	Inclusion
Substructure	Foundations	
Substructure	Basement build-up	
Superstructure	Columns & beams	
Superstructure	Frame	
Superstructure	Upper floors	
Superstructure	Roof	x
Superstructure	External walls	x
Superstructure	Stairs and ramps	
Superstructure	Openings: Windows	x
Superstructure	Openings: External Doors	
Superstructure	Internal walls and partitions	x
Superstructure	Internal doors and glazing	
Finishes	Wall, floor, ceiling finishes	
Fittings and furnishings		
Building services/MEP	Chillers	x
Building services/MEP	Heating systems	x
Building services/MEP	Ventilation systems	x
Building services/MEP	Distribution systems	x
Building services/MEP	Electrics	
Site external works		

The study scope does not consider on-site renewable energy generation technologies, such as roof-mounted photovoltaics. Within the interconnected urban context of the HE buildings under study, these technologies may not necessarily

serve the building in question and could introduce additional complexities and uncertainties regarding net operational energy use. As such, the emphasis remains on evaluating passive design and energy efficiency improvements rather than on-site energy generation.

3.3.7 Scenario Analysis

This section considers the alternative decarbonisation and fuel price pathways adopted in the [CCA-LCA](#) framework.

Carbon Emission Pathways

The projected rate of system decarbonisation is important in capturing the shifting ratio of embodied and operational carbon and may impact the choice of climate change adaptation measures selected for refurbishment. The UK energy generation sector has seen a significant reduction in carbon intensity, driven by the increasing share of renewable energy sources and the phasing out of coal [169]. However, uncertainty remains with respect to continued transformation, with future decarbonisation projections strongly influenced by policy, regulation and investment [157].

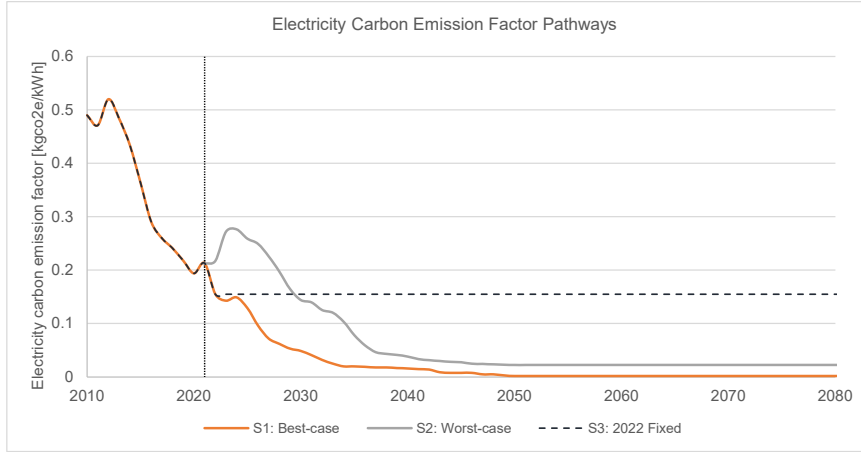


Figure 3.4: Electricity carbon emission factor scenarios, adapted from [158, 157].

Several sources of information were considered to develop scenarios relating to the rate of change of electricity CEFs over time. Future CEFs were projected based on UK Government carbon conversion factors and National Grid Future Energy Scenarios (FES) [157, 158]. The FES outline different pathways for delivering net zero carbon emissions in the UK by 2050, and one pathway that does not meet this target [157]. These pathways are presented as the CO₂ intensity of electricity generation, excluding negative emissions from bio-energy carbon, capture and storage, equal across all scenarios for the year 2021. A scaling factor was calculated by relating the measured carbon intensity of generation values to the grid average carbon intensity of supply, provided by the UK Government Green Book supplementary guidance, for the equivalent year [158]. This scaling factor (x1.363) accounts for factors such as losses due to transmission and distribution, assumed fixed over the 60 year reference period. Finally, a scenario was also considered where both electricity and gas CEFs are fixed at 2022 values, to understand the implications of this commonly used LCA assumption on optimisation

outputs. The resulting electricity CEF pathways for *S1:Best-case*, *S2:Worst-case* and *S3:2022 fixed* story-lines shown in Figure 3.4.

Decarbonisation pathways for the gas network are currently less defined, with the future of low-carbon hydrogen production, carbon capture and storage (CCS) and the integration of biomethane still under exploration. These technologies face significant technical, economic, and policy challenges, contributing to substantial uncertainty in long-term emission projections. In this research, carbon emissions from gas consumption were estimated based on the relative proportion of green to unabated natural gas [157]. This pathway predicts a relatively steady year-on-year increase in green gas penetration until 2050, which was extrapolated to 2080 to cover the 60-year study timeframe, as depicted in Figure 3.5. For consistency, the gas CEF projections were kept the same for both *S1:Best-case* and *S2:Worst-case* scenarios. This assumption is based on the premise that if the building configuration continues to rely on gas-based heating systems, widespread adoption of heating technologies is still being employed in the future, aligning with the ‘falling-short’ FES specified. Furthermore, alternative FES pathways actually show marginal decreases in the average share of green gas over the projected period; this highlights that faster energy transitions are predicted on the basis of reduced overall gas supply rather than increased reliance on green gas penetration.

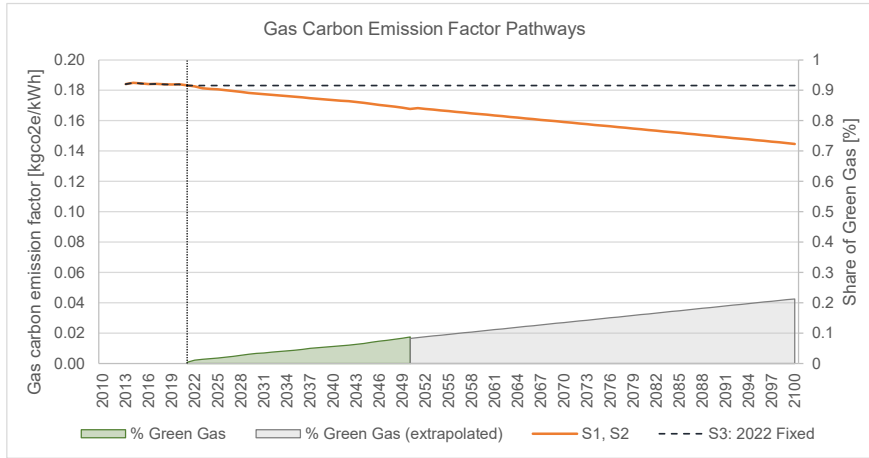


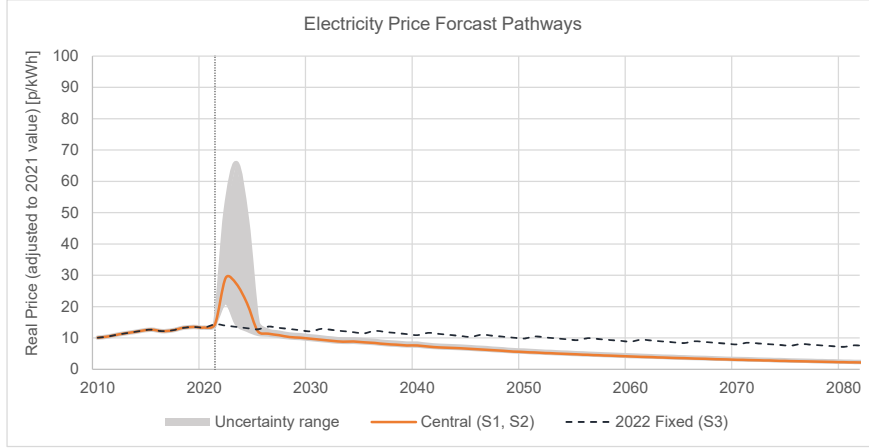
Figure 3.5: Predicted share of green gas in the gas network, extrapolated from National Grid ESO FES: ‘Falling Short’ pathway [157].

Fuel Price Pathways

Fluctuating fuel price projections were developed based on the UK Government Green Book central estimate for electricity and gas [158]. All of these projections (low, central, high) assume a gradual rebound from the sharp peak in energy costs seen from the period 2021-2023. The high-case scenario presented in the Green

Book shows a much sharper and more prolonged price peak; however, all scenarios share the underlying assumption that energy prices will eventually decline and steady as the energy transition progresses e.g. through the decoupling of renewable electricity prices from gas-fired generation and reduced exposure to external geopolitical price shocks as reliance on imported oil and gas decreases.

(a) Electricity Fuel Price Projections



(b) Gas Fuel Price Projections

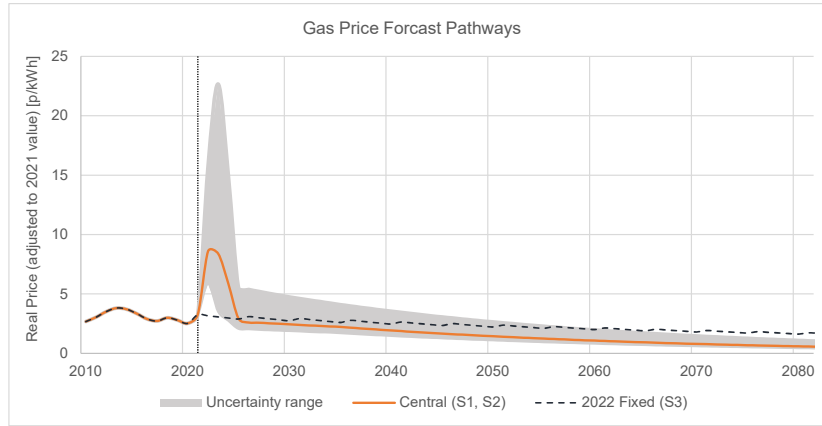


Figure 3.6: Electricity and gas fuel price pathways.

Given the difficulty of aligning fuel price signals with specific decarbonisation pathways (and the substantial associated uncertainties), a single (central) price trajectory was adopted for this study. This approach enables clearer interpretation of the results by isolating the effects of varying operational carbon intensities without conflating them with uncertainties in price projections. As such, the aim of this research was not to forecast precise market behaviour but to test the relative performance of design measures under consistent operational cost assumptions. Sensitivity to energy price uncertainty is acknowledged as a limitation, with future work recommended to incorporate probabilistic or range-based cost modelling.

Future costs were brought to the NPV using the same methodology outlined in section 3.3.6, with a 3% discount rate per annum applied in line with the BSRIA life-cycle costing methodology [95]. For S3, in-line with the fixed rate assumptions used for the carbon calculations, the 2022 fixed-price factors were adopted with assumptions and discounts applied in line with the BSRIA methodology [95]. The aim was to understand the implications of these commonly used fixed-rate assumptions, that do not consider situational context, on optimisation outputs. The average CEFs and operating costs for electricity and gas over the 60 year life-cycle are summarised in Table 3.4.

Table 3.4: Summary of adopted scenarios with 60 year average carbon factors and fuel prices.

Scenario No.	Description	Elec. (kgCO _{2e} /kWh)	Gas CF (kgCO _{2e} /kWh)	Elec. (£/kWh)	Gas (£/kWh)
S1	Best-case	0.021	0.168	0.066	0.017
S2	Worst-case	0.062	0.168	0.066	0.017
S3	2022 fixed	0.155	0.183	0.102	0.023

3.4 Methods 2: Case Study Development

3.4.1 Principle

Case study analyses are widely adopted in thermal and energy-related building research practice. The case study approach aims to understand the dynamics present within a single, real-world setting [170]. It is through this intimate connection with the empirical reality that testable, relevant and valid theories can be established [170, 171]. Specifically, the application of this research phenomenon was deemed appropriate due to the site-specific nature of this work. Building performance analysis is closely related to local climate factors, and properties of existing HE building design will vary by region. Furthermore, LCA is dependent on carbon emission factors, fluctuating fuel prices, product supply chains and distribution networks, all of which are highly specific to the location under consideration. The case study approach allows for various scenarios to be tested on a dynamic representation of real-world HE building design and operation.

3.4.2 Case Study Selection

Three case study HE buildings located in central London were selected for detailed dynamic thermal simulation (DTS) modelling to observe energy performance under future climates. These buildings represent a range of functions that are common to the UK HE building stock, consisting of offices, teaching spaces, study areas, laboratories and ICT facilities [172]. A variety of building geometries, thermo-physical properties, and systems configurations have also been identified. Crucially, the buildings are expected to experience high and intermittent internal heat gains that are typical of HE spaces and high EUIs associated with laboratories and ICT facilities [173]; factors that are likely to influence a buildings resilience to climate change. The final building selections were made based on secondary data availability. All three case studies underwent major refurbishments between 2010 to 2019, as presented in Table 3.5. Further details on each case study are provided in chapters 4.1, 5.1, and 6.1.

Table 3.5: Summary of the case study building characteristics.

	Primary Activity	DEC	EPC	Construction Year	Refurbishment Year	Approx. GIA (m ²)
CS1	Architectural school	D		1975	2016	8842
CS2	Post-graduate school	C		Early 1900s	2010	5365
CS3	Student accommodation		A	1960s	2019	7891

3.4.3 Modelling, Calibration & Validation

For the three case study buildings described in section 3.4.2, various data sources were acquired to develop, calibrate and validate the building energy models. The baseline simulation and operational stage data for model development and calibration purposes are presented in Table 3.6. The general approach taken is described in this section; this was refined and adapted on a case-by-case basis depending on specific data availability.

Model Development

The building data types listed in Table 3.6 were used to develop an initial baseline EnergyPlus model. These secondary data sources capture aspects of the building relating to physical geometries and properties. The composition, thickness and thermal bulk properties of all main construction materials were incorporated in to the model in attempt to capture the thermo-physical properties of the building. Model-estimated U-values were cross-referenced against the original construction specifications, where available. In response to the combined systems-fabric optimisation framework adopted in this research, it was considered necessary to also include detailed modelling of HVAC systems. Information on existing equipment and specifications were obtained from the designer’s as-built mechanical drawings.

Compact occupancy schedules were adapted from the UK National Calculation Methodology National Calculation Methodology (NCM) activity data for non-domestic buildings [174]. The NCM schedules were updated to reflect the buildings’ opening times, term dates and out-of-hour activities e.g., external courses held during reading weeks. Where available, sub-metered data for lighting and power and monitored CO₂ levels were used for further indication of occupancy use patterns. If zone-specific information was not available, the same NCM-adjusted profiles for occupancy, lighting and equipment were applied across zones of similar activities.

Table 3.6: Categories, types, and sources of secondary data used for the development and calibration of building-level case study models.

Data Category	Data Types	Data Source	Secondary Data
Baseline simulation building data	Location, orientation, geometry, Construction materials Glazing type, WWR, Systems design, Small power and lighting	Estates Teams Facilities Teams Industry partners ¹	Site plans Construction drawing specifications M&E drawings Building audits
Operational stage data	Electricity consumption data Fossil thermal consumption data Zone air temperature Zone CO ₂ levels	Estates Teams Internal sources ² Online data sources ³	Mains meters, Sub-metering, Utility data, Internal monitoring

Calibration & Validation

The models were calibrated according to the multi-level calibration framework presented by Jain et al. (2020), following whole-building calibrated performance paths defined in measurement and verification (M&V) protocols [175, 176]. The level of detail achieved through disaggregated calibration techniques varied model to model, depending on the availability and quality of metered data. As a minimum, the models were calibrated against historical monthly metered energy consumption over an annual period, disaggregated by electricity and gas consumption. Spatial and further end-use disaggregation was also applied, where possible. In accordance with the ASHRAE M&V protocol [176], two statistical metrics were adopted for validation of modelled energy consumption against actual metered data. Coefficient of Variation of Root Mean Square Error (**CVRMSE**) and Nominal Mean Bias Error (**NMBE**) are widely adopted statistical metrics for building calibration, used to enhance the predictive capability, robustness and credibility of modelling results.

NMBE (eq 3.4) evaluates average bias by calculating the deviation of simulated values from measured ones, identifying systematic over- and under-estimations of simulated data. A low **NMBE** indicates unbiased model predictions, accurately representing real energy consumption patterns [177]. **NMBE** is subject to cancellation errors, where positive and negative deviations offset each other.

$$NMBE = \frac{\sum_{n=1}^n (y_i - \hat{y}_i)}{(n - p)\hat{y}} \quad (3.4)$$

CVRMSE (eq 3.5) measures the variability of errors between measured and model-predicted values, providing an indication of the model's ability to estimate the overall load shape of the measured data [177]. A low **CVRMSE** indicates that the model is precisely predicting energy consumption patterns. Since it is not subject to cancellation errors, it is recommended to use this metric alongside **NMBE** for verification of model accuracy [176].

$$CV(RMSE) = \frac{1}{\hat{y}} \sqrt{\frac{\sum_{n=1}^n (y_i - \hat{y}_i)^2}{n - p}} \quad (3.5)$$

y_i = Actual metered energy consumption for the i -th data point

\hat{y}_i = Model-predicted energy consumption for the i -th data point

\hat{y} = Mean of the actual metered energy consumption

n = Total number of data points

p = Number of model parameters

These metrics serve distinct but complementary purposes in building model calibration, together ensuring both accuracy (NMBE) and precision (CVRMSE) in predictions of real-world energy consumption patterns [177, 176]. The monthly limits shown in Table 3.7 depict “acceptable” statistical tolerances for a calibrated model, as corroborated by multiple protocols [176, 178].

	CV(RMSE)	NMBE
Tolerance (%)	15	± 5

Table 3.7: Acceptable CV(RMSE) and NMBE tolerances for monthly calibration as stated by ASHRAE (2014) [176].

3.4.4 ECM selection process

Template Development

In response to the research questions specified in section 2.6, a combination of building fabric and systems interventions were considered for inclusion within the optimisation process, presented in Table 3.8. The specific measures were informed by review of relevant literature and government and industry publications, and validated through contribution and guidance from industry. The criteria for selection of these strategies was as follows:

Criterion 1. Demonstrating a high performance under future or extreme climate conditions.

Criterion 2. Demonstrating a high performance with HE building typologies.

Criterion 3. Aligning with principles of low-energy design and current building standards.

The initial combination of passive and active climate change adaptation strategies formed a generalised ECM template (Table 3.8), which was refined at the case study level to ensure compatibility with individual building design criteria. The process of refining the ECM selection to adhere with specific case studies was two-fold. Firstly, strategies were eliminated or adapted based on current best practice protocols and guidance. For example, options for HVAC replacement were guided by existing systems’ design, insulation thicknesses varied based on

existing thermo-physical properties, and materials differed to align with existing design features. This allowed for final solution sets that were design driven yet validated by principles of building physics. The parameter value ranges included for each variable were either discrete or continuous and were developed in-line with current standards, such as Part L [179]. The second stage of parameter refinement was through preliminary testing, discussed in the following section.

Preliminary testing

Since each additional parameter results in an exponential increase in the number of possible solutions, initial testing helped to reduce overall simulation time and costs. For example, sensitivity analysis was used to identify variables that had negligible or negative impact on building energy performance. The focus of these studies was to reduce the number of options, particularly where the potential variation in embodied carbon and upfront cost was insignificant e.g. temperature set-point changes. For these options, the optimisation would be largely driven by operational cost and carbon differences resulting solely from the variation in operational energy consumption, so sensitivity analysis was deemed sufficient to decide on the best options.

A detailed evaluation of configurations and settings also helped to ensure the models were operating as expected and to identify inputs that may significantly extend simulation time. For example, the use of calculated [NV](#) and infiltration significantly increases model complexity and simulation time, since time-step calculations are conducted based on multiple factors, such as buoyancy, wind driven pressure differences and crack dimensions. Due to the large number of model permutations being considered and the size and detail of the case study building under investigation, it was deemed appropriate to utilise a simplified scheduled [NV](#) option. Exclusion of ineffectual variables and/or parameters reduced the number of possible design combinations included in the [GA](#), thus increasing the speed of optimisation.

ASHP Operation

Across all case studies, low-temperature [ASHPs](#) were implemented as an alternative to the existing heating systems. Since no EnergyPlus template exists for modelling air-to-water heat pump operation, an energy management system ([EMS](#)) code was developed to replicate its operation, calculating heating electricity consumption at each time-step based on current conditions. The script is provided in [Appendix A](#). It utilises the capacity function of temperature curve to adjust nominal system capacity to rated capacity at each 10 minute interval, based on the outdoor dry bulb temperature and loop flow/return temperatures. At each time step, the calculated heat demand is adjusted based on available heat capacity to set the part-load ratio and corresponding output from the part-load fraction

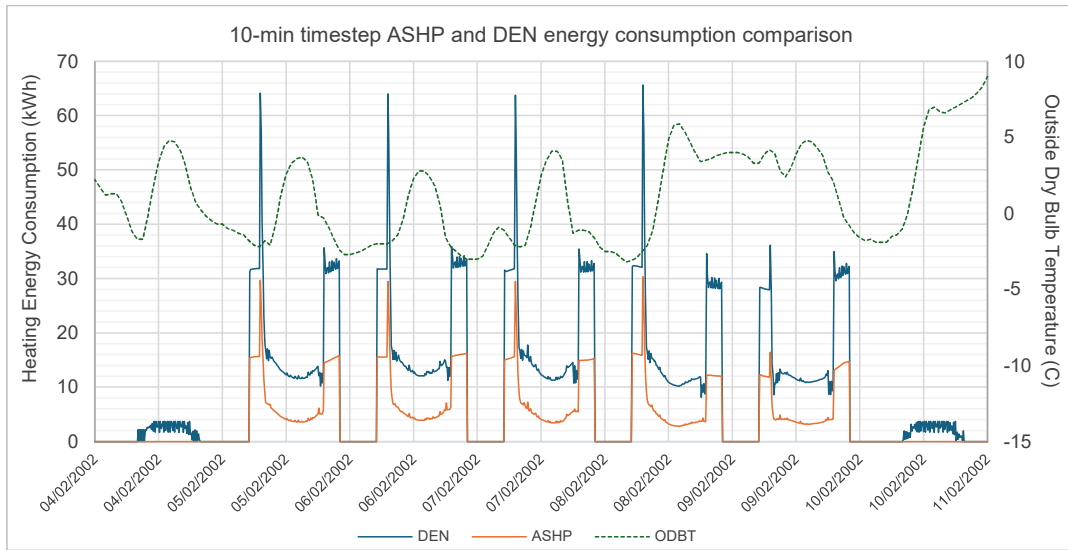


Figure 3.7: CS1 EMS scripted ASHP operation compared to baseline district energy network (DEN) consumption for a week in February.

correlation curve. The nominal coefficient of performance (COP) of 3.2 is adjusted based on time-step outdoor dry bulb temperature and flow/return temperatures, using the COP function of temperature curve. Finally, heat demand is modified according to the COP and part-load ratio output to provide estimated ASHP heating electricity consumption at each timestep. Simulated heating energy usage for a typical winter design week for CS1 is shown in Figure 3.7, with ASHP electricity consumption amounting to approximately 40% that of the district energy network heating loads.

Table 3.8: ECM toolkit.

Adaptation Strategy	Description	Metric	Standard Intervention	Possible Value Range
Double Glazing	Upgrade to low-e double glazing with argon filled cavity	U-value (W/m ² K)	1.3-2.0	1.5
Triple Glazing	Upgrade to triple glazing	U-value (W/m ² K)	0.6-1.1	0.8
Glazing SHGC	Decrease solar heat gain transmission with low-e film	g-value	0.3-0.7	0.3
N-façade WWR	Introduce smaller or larger windows into the North façade	% change	NA	-50, 0
S-façade WWR	Introduce smaller or larger windows into the South façade	% change	NA	-50, -30, 0, +30
E-façade WWR	Introduce smaller or larger windows into the East façade	% change	NA	-50, -30, 0, +30
W-façade WWR	Introduce smaller or larger windows into the West façade	% change	NA	-50, -30, 0, +30
Internal wall insulation	Add mineral wool insulation internally to external walls	thickness (mm)	100	0, 50, 80, 120
Roof albedo	Add high albedo white clay tiles to roof build-up	SR (%) / TE (%)	0.8/0.9	
Roof insulation	Add XPS polystyrene insulation to existing roof insulation	thickness (mm)	150	0, 120, 150, 180
Window frame material	Add frame-wrapped PUR insulation to reduce thermal bridging (Psi-value)	thickness (mm)	0	0, 50, 100
Infiltration	Reduce leakage through building fabric; assumed airtightness improved with additional frame-wrapped insulation	m ³ /m ² /hr @ 50 Pa	3	0.5, 1, 3
NV control strategy	Automatically open windows based on deltaT (constrained by SP temp)	dT (°C)	2	2
Nighttime purging	Open windows overnight when outside temp at least 2 degrees below inside; vary min. outdoor temperature 15-18C, constrained by SP temperature	OutdoorT (°C)	17	15, 16, 17, 18
E-shading	Add vertical external shading devices to E-façade	d/h ratio	0	0, 0.2, 0.4, 0.6
W-shading	Add vertical external shading devices to W-façade	d/h ratio	0	0, 0.2, 0.4, 0.6
S-shading	Add horizontal external shading devices to S-façade	d/h ratio	0	0, 0.2, 0.4, 0.6, 0.8
MV night cycle	MVHR on overnight (22:00-5:00) when outside air is cooler than inside air temperature and min ODBT > 18 degrees	on/off	0	0, 1
MV W/E cooling	MVHR on over weekend when outside air is cooler than inside air temperature and min ODBT > 18 degrees, constrained by AHU air supply SP temp	on/off	0	0, 1
ASHP	Upgrade heating and/or cooling system to more efficient ASHP	yes/no	0	0, 1

3.5 Results Reporting and Visualisation

This section outlines the structured approach taken to present and interpret the results generated by the **LCA-CCA GA** optimisation framework. Results were reported with the aim of effectively communicating the trade-offs and impacts of various design alternatives across different metrics and scenarios. A combination of visualisation techniques and sequential analysis were employed to highlight key insights relevant to decision-makers in sustainable building refurbishments.

The design alternatives derived from the optimisation process are initially presented as a Pareto front, illustrating the relative trade-offs between **LCCF** and **LCC**. These results are then analysed in sequential stages: Linear regression analysis offers a weighted evaluation of how each variable influences the life-cycle metrics. The **GA** outputs from alternative decarbonisation pathways are then presented, showing the range of **LCCF** and **LCC** values across Pareto-optimal solutions. Scenarios are further analysed to examine the breakdown of embodied and operational carbon contributions for each building component upgrade. Finally, the temporal evolution of **LCCF** is visualised to depict changes over time under various design and decarbonisation scenarios. A synthesis of findings from all case studies is provided in the discussion, offering overarching insights and practical implications.

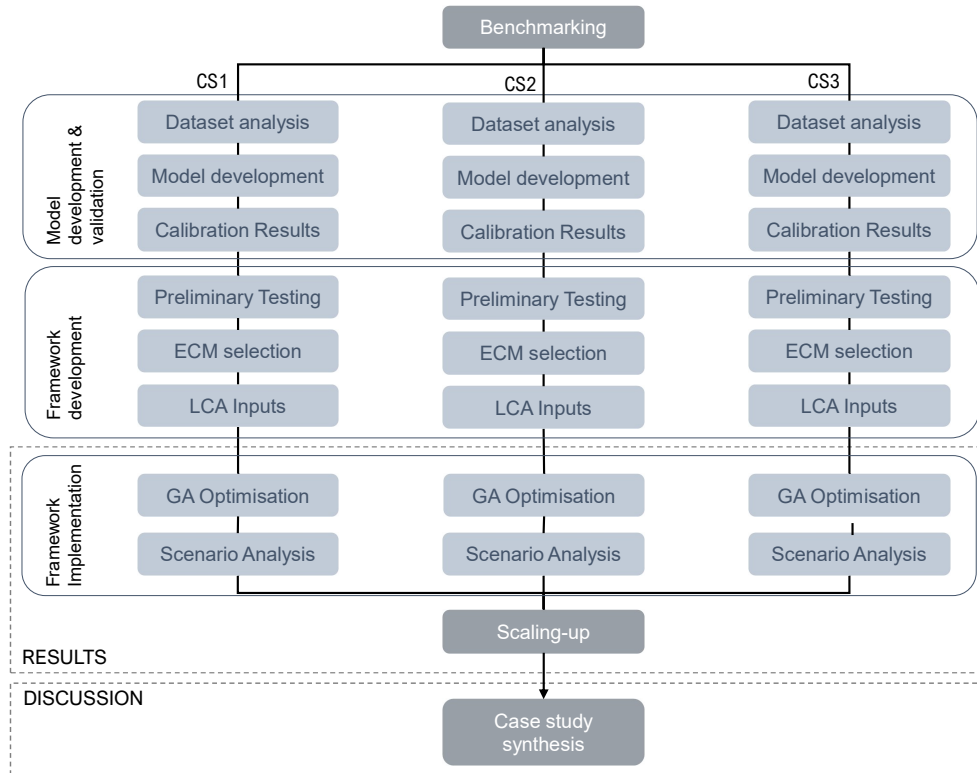


Figure 3.8: Structure of results leading into CS synthesis in the discussion.

The following chapters are structured around each case study, dividing the process into three main phases: (1) Model development and validation, (2) Framework development, and (3) Framework implementation. This approach aligns with the methodological framework detailed in sections 3.3 and 3.4, tailored to the specific requirements of each case study and framework component. Outputs from the framework, specifically the CCA-LCA optimisation results, are synthesised across all case studies in the Discussion (Chapter 7). The progression of results leading into the discussion is visually outlined in Figure 3.8.

3.6 Summary of Methods

The methods chapter outlines the steps for developing the Climate Change Adaptation (CCA) and Life Cycle Assessment (LCA) framework, along with the development and validation of case study models for its use. The conceptual flow diagram shown in Figure 3.9 outlines the key methodological steps, interrelationships and outputs.

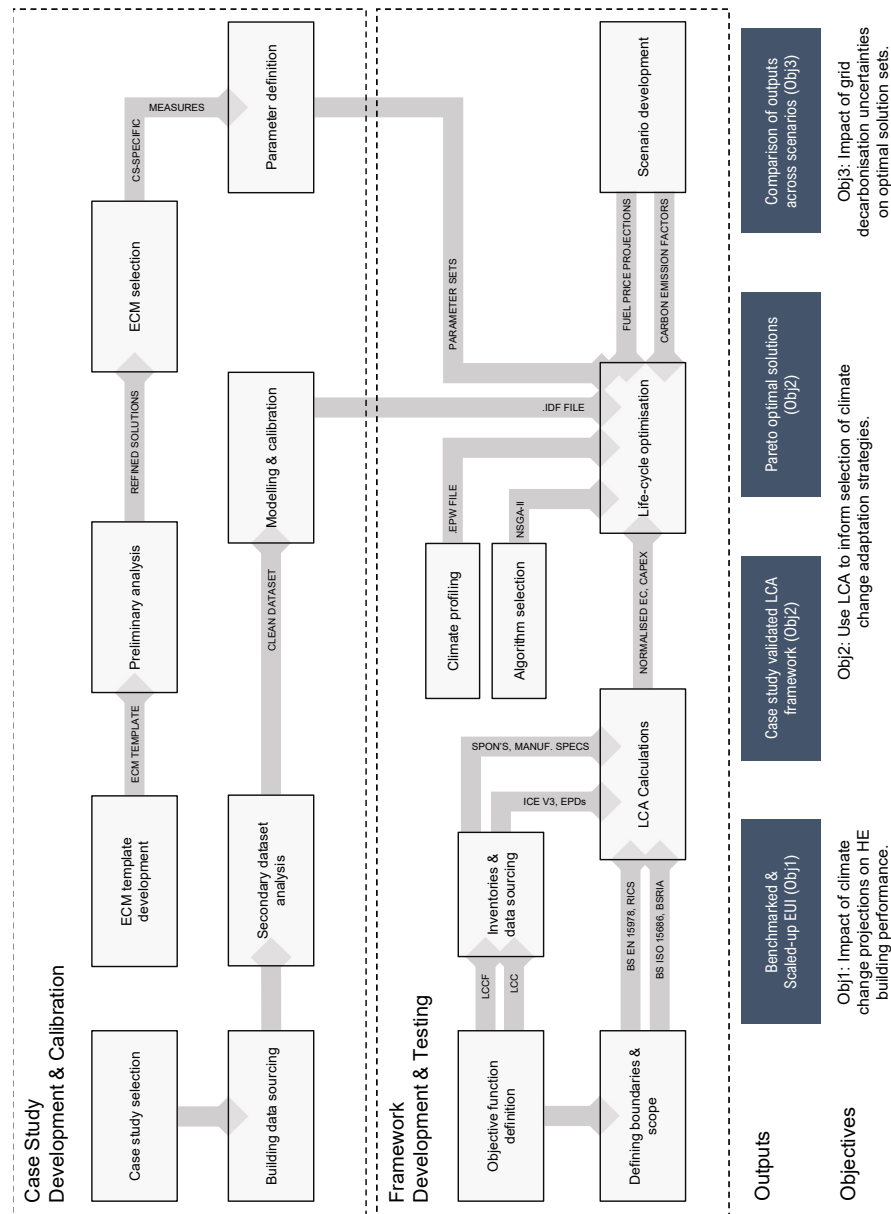


Figure 3.9: Key methodological steps, interrelationships and outputs in line with core study objectives.

Chapter 4

Case Study 1

4.1 Overview


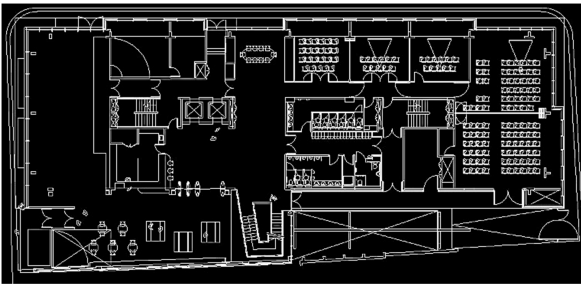
CS1	
<div>  <p>Source: https://www.ucl.ac.uk/bartlett/news/2017/jul/22-gordon-street-wins-new-london-architecture-award</p>  </div>	
Location	London (Euston)
CIBSE benchmarking classification	Academic - Art and Design
Gross floor area (m2)	8842
No. storeys/height (m)	8 (incl. basement) / 26 m
Space-use function (%) excluding circulation spaces	Studios (24%), workshops (10%), offices (10%), teaching (6%), meeting spaces (4%), café/exhibition/social spaces (10%), ICT (3%)
Envelope properties	Brick slip façade Aluminium-timber composite window frames Recessed double-glazing Green roof
Building service systems	District heating with CHP and NG boilers Multi-service chilled beams FCUs Air-cooled chillers AHU with heat recovery

Figure 4.1: CS1 profile.

CS1: Architectural School

Refurbished in 2016, CS1 saw a substantial increase in gross internal area, with extended workshop and studio spaces. A major refurbishment consisted of the replacement of external walls and windows, with the addition of a brick slip facade around the entire external envelope. Some elements of the original fabric were retained, such as concrete substructures, columns and beams. The building adopts mixed-mode ventilation strategies. Heating is supplied via a centralised district energy network (DEN), with gas-supplied combined heat and power plant operation. Cooling is supplied via air-cooled chillers. Multi-service chilled beams and fan-coil units serve heating and cooling to the zones.

4.2 CS1: Model Development and Validation

This section presents the pre-processing steps taken to prepare the secondary energy consumption datasets for use in model development and calibration.

4.2.1 Secondary Dataset Analysis

An initial analysis of the secondary dataset was conducted for assessment of data quality, imputation of missing data points and handling of non-typical consumption and use patterns. The annual period of 2018 was selected to allow occupants time to acclimate post-refurbishment, thus establishing more representative occupancy densities and use patterns. In addition, the period until March 2021 witnessed a notable decline in building energy demand due to the impact of the Covid-19 pandemic; calibration was performed outside of this timeframe to avoid deviations from typical consumption patterns.

Data Analysis and Cleaning: Electric Loads

High-resolution, quarter-hourly electricity consumption data was available for 2018 (98.5% completeness) to be used for model calibration, with missing values imputed using averages from adjacent time steps. Highly regular cyclic trends were observed from January to May, with increased consumption during the cooling season. Chiller electric loads remained high during the heating season with weekend operation, indicating out-of-hour usage and inefficiencies. Similarly, out-of-hours and weekend lighting and power electricity consumption was also noted, particularly in basement workshops. The summer exhibition period caused a significant peak in electricity consumption, driven by increased chiller and workshop use. Custom schedules were developed to accurately reflect these non-typical patterns, as exemplified in Table 4.1.

Table 4.1: Workshop (WS) lighting and power densities and schedules obtained from sub-metered data for annual period of 2018.

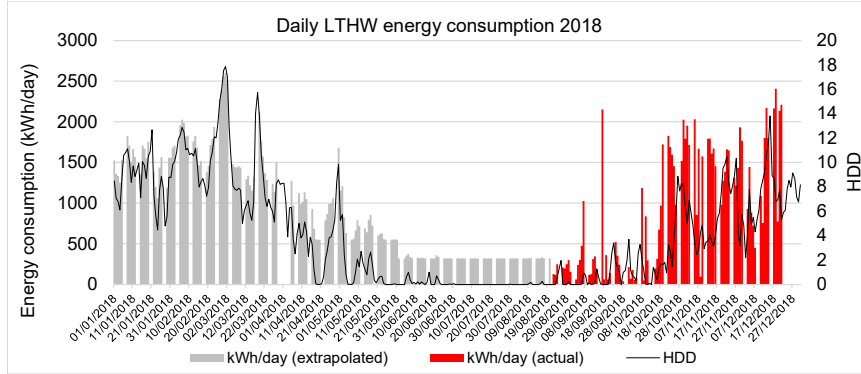
	WS1	WS2	WS3	WS4	WS5	WS6	WS7	WS8	WS9	WS10	WS11
L&P (W):	1250.42	885.69	484.71	1571.94	1172.79	5371.04	318.70	3631.14	6912.99	4532.40	2930.65
Floor area (m ²):	15.30	355.97	355.97	355.97	33.71	151.71	38.48	33.71	74.42	33.71	356.37
Power density (W/m ²):	81.73	2.49	1.36	4.42	34.79	35.40	8.28	107.72	92.89	134.45	8.22
Schedules:											
Mon-Fri, 09:30-17:00	0.74	0.92	0.82	1.00	1.00	0.69	1.00	0.81	1.00	0.91	0.95
Mon-Fri, 17:00-09:30	0.20	0.33	0.12	0.30	0.41	0.55	0.23	0.13	0.05	0.21	0.28
Sat-Sun, 09:30-17:00	0.19	0.27	0.06	0.29	0.36	0.48	0.14	0.11	0.01	0.18	0.25
Sat-Sun, 17:00-09:30	0.14	0.06	0.00	0.10	0.30	0.40	0.08	0.08	0.01	0.14	0.07
11 May -22 Jun											
Mon-Fri, 09:30-21:00	1.00	1.00	1.00	0.99	0.77	1.00	0.63	1.00	0.88	1.00	1.00
Mon-Fri, 21:00-09:30	0.17	0.21	0.07	0.21	0.24	0.79	0.06	0.23	0.08	0.24	0.19
Sat-Sun, 09:30-21:00	0.35	0.31	0.25	0.33	0.25	0.92	0.16	0.26	0.03	0.27	0.31
Sat-Sun, 21:00-09:30	0.09	0.00	0.00	0.05	0.18	0.66	0.00	0.18	0.03	0.19	0.03
23 Jun-7 Jul											
Mon-Fri, 09:30-21:00	0.64	0.90	0.74	0.77	1.05	0.86	0.85	0.89	0.99	0.98	0.81
Mon-Fri, 21:00-09:30	0.13	0.27	0.09	0.22	0.34	0.77	0.13	0.12	0.04	0.18	0.22
Sat-Sun, 09:30-21:00	0.12	0.10	0.04	0.23	0.32	0.66	0.13	0.07	0.02	0.13	0.16
Sat-Sun, 21:00-09:30	0.11	0.00	0.00	0.10	0.31	0.66	0.00	0.07	0.02	0.13	0.05

Data Analysis and Cleaning: Thermal Loads

The quality of thermal energy data for 2018 was poor by comparison, with daily low temperature hot water energy consumption data available from August 2018 to March 2019 only. In lieu of alternative data sources, the relationship between heating degree days and daily energy consumption over available periods was used to extrapolate data points to the rest of the year ($R^2=0.47$). For domestic hot water, daily consumption data was available from July 2018 to March 2019. Weekday, weekend and holiday averages of 230 kWh/day, 166 kWh/day and 55 kWh/day respectively were calculated to extrapolate this trend for the first part of 2018. The resulting measured and estimated daily low-temperature hot water and domestic hot water trends are shown in Figure 4.2a and 4.2b.

The operational-stage observations noted through analysis of monitored datasets are summarised in Table 4.2.

(a) LTHW



(b) DHW

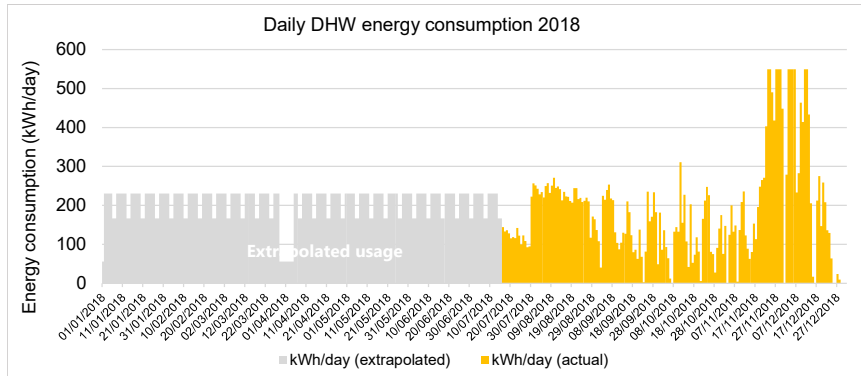


Figure 4.2: CS1 measured and extrapolated low-temperature hot water and domestic hot water values for 2018.

Table 4.2: CS1 operational stage observations from sub-metered data.

Category	Observations
Electricity Consumption	<ul style="list-style-type: none"> Regular electric load patterns from January to May, increasing during the cooling season Approximate baseload of 60 kWh maintained year-round Significant rise in consumption during summer exhibition (23rd June-7th July) High out-of-hours usage in workshops, especially during summer exhibition Continued building operation over summertime term closures
Chiller Consumption	<ul style="list-style-type: none"> High cooling loads during the heating season (January, October-December) Increased daily consumption by 406 kWh during cooling season (May-August) Weekend operation indicating inefficiencies Flat-line in consumption for one week in August and September

4.2.2 Model development

The baseline model was developed in line with the methodology outlined in section 3.4.3. Construction materials and thicknesses were interpreted from Stage D Appendices reports and validated through a combination of site visits and expert elicitation. The expert elicitation process involved direct engagement with estates teams, design engineers, and architects who were involved in the original building development. These discussions focused on clarifying key aspects of building operation, services configuration, and occupancy patterns, and were supplemented by secondary datasets provided by the estates team, including construction specifications and post-occupancy monitoring data. A low-risk ethical approval was obtained from UCL to undertake this engagement. The primary constructions adopted in CS1 and their thermal properties are presented in Table 4.3. A glazing light transmittance value of 0.7 and solar heat gain coefficient of 0.4 was implemented, aligning with the stage D part L2A assessment.

Table 4.3: CS1 primary constructions and thermal properties of existing building.

Construction	Description	Thickness (m)	U-value (W/m ² .K)
External wall	70mm brick slip with steel frame system, 1 layer 12.5mm cement board, 1 layer 12.5mm plaster board, mineral wool infill	0.385	0.2
External sedum roof	Full extensive roof system: vapour control layer, rigid insulation, waterproof capping sheet, mat, drainage layer and sedum blanket	0.551	0.13
External flat roof	New roof system: vapour control layer, rigid XPS insulation, 17.5mm cast concrete	0.476	0.13
Internal partitions	25mm heavyduty plasterboard on metal framing	0.120	1.56
External glazing	Double glazed timber and anodised aluminium composite windows	-	1.5
External glazing	Double glazed, timber framed curtain walling system	-	1.5

In response to the secondary dataset analysis in section 4.2.1, the following updates were made to the baseline model:

- NCM schedules for lighting, equipment and occupancy were adapted to account for extended building opening hours from 7:00 to 22:00 during weekdays and 9:00 to 18:00 on weekends at reduced occupancy.
- Seminars, tutorial spaces and computing zones were modelled as operational during university teaching hours only (9:00 to 18:00), without weekend activity, verified through disaggregated zonal energy consumption patterns and post-occupancy evaluation reports.
- Custom schedules were incorporated to account for out-of-hour workshop operations, with evidence of lighting and power operation overnight and schedule changes before and during the summer exhibition show (see Table 4.1).

- Expected metabolic rates were estimated based on typical activities in each zone using assumptions from ASHRAE 55 standard and CIBSE Guide A [180, 181].

Detailed HVAC modelling was implemented for a more accurate depiction of HVAC systems and processes. In accordance with details outlined in the post-occupancy evaluation, all main plant in the building was time-schedule operated to enable at 7am and disable at 7pm on weekdays, and disable during the weekends. Prolonged cooling was available from 17:00 to 22:00 during periods of extended summer exhibition activity, as indicated by chiller energy consumption data trends. Heating setpoint temperatures were set to 22.5 °C and cooling setpoint temperatures to 25 °C for most conditioned spaces, including studios, teaching spaces, offices and break-out spaces and workshops, according to building management system settings. The building operates with mixed-mode ventilation; MVHR is enabled to pre-condition zones from 05:00 and disabled at 22:00. MVHR operation schedules followed zonal occupancy patterns and a sensible heat recovery effectiveness of 0.75 was applied.

LTHW Circuit	Flow Temperature Set-Point [°C]	Return Temperature Set-Point [°C]
Secondary Side - MSCB	40	35
Secondary Side - FCU & AHU	80	60
Primary Side – Incoming DH	90	75

(a) Low-temperature hot water circuit

CHW Circuit	Flow Temperature Set-Point [°C]	Return Temperature Set-Point [°C]
MSCB	14	18
FCU & AHU	6	12

(b) Chilled water Circuit

Table 4.4: Flow and return set-point temperatures for CS1 low-temperature hot water and chilled water circuits. (MSCB: multi-service chilled beam; FCU: fan-coil unit; AHU: air-handling unit; DH: district heating).

Temperature regulation in conditioned spaces was primarily managed by active multi-service chilled beams. Should the zone operative temperature exceed the cooling setpoint, proportional integral control valves within the chilled water system facilitate additional chilled water flow through the multi-service chilled beam, cooling the zone. Conversely, if the temperature fell below the heating setpoint, pressure independent control valves in the low-temperature hot water system serving the multi-service chilled beam open to allow low-temperature hot water flow, maintaining thermal comfort. Conditioned zones on the lower ground floor and open lobby/exhibition spaces on the ground floor are served via fan-coil

units instead of multi-service chilled beam, with a similar control strategy. The flow and return temperatures for both circuits are shown in Table [4.4a](#) and [4.4b](#). The low-temperature hot water system is connected to the district energy network while cooling is provided by two roof mounted chillers. The various circuits were modelled in EnergyPlus and set-points were applied.

4.2.3 Calibration Results

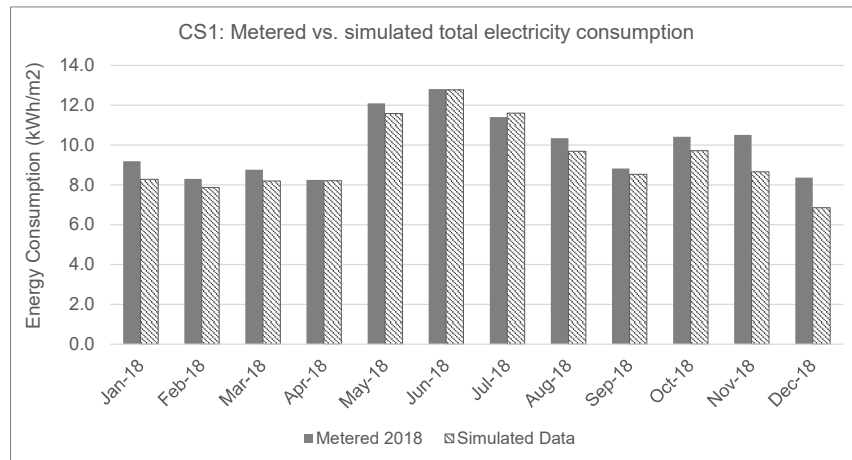
In accordance with the CIBSE TM63 calibration process [182], the model was refined to meet the calibration standards outlined by ASHRAE Guideline 14 and IPMVP [176, 183]. Real weather data from the London Weather Centre station from 2018 was used in the calibration process, aligning with the building monitoring period and proximate location. Employing iterative, evidence-based adjustments as outlined by Jain et al. (2020) [175], the model incorporated relevant weather data, schedules, loads, and system configurations. Table 4.5 provides a summary of the results, contrasting the calibrated model’s projections for heating, cooling and total electricity consumption with the monitored data described in 4.2.1. Compliance with ASHRAE Guideline 14 necessitates that monthly Coefficient of variation of the Root Mean Squared Error (CVRMSE) remains below 15% and Normalised Mean Biased Error (NMBE) within $\pm 5\%$ [176]. The model achieves monthly heat use errors of CVRMSE = 8% and NMBE = +4% and monthly electricity use errors of CVRMSE = 8% and NMBE = +5%. These findings demonstrate that the calibrated model sufficiently meets the ASHRAE Guideline 14 criteria.

Table 4.5: Calibration results for CS1. Target monthly validation criteria: $C_v(\text{RMSE}) < 15\%$, NMBE $\pm 5\%$ [176].

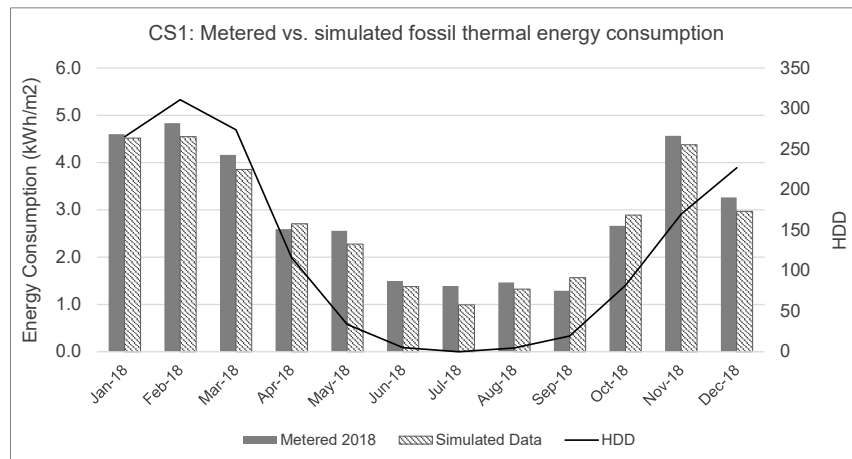
By Fuel Type	$C_v(\text{RMSE})(\%)$	NMBE(%)
Electricity	8	5
DEN	8	4
By End Use	$C_v(\text{RMSE})(\%)$	NMBE(%)
L&P	8	-5
LTHW	10	5
DHW	11	3
Cooling	38	25

The calibration results in Table 4.5 reveal end-use compliance for lighting and power, low-temperature hot water and domestic hot water. For cooling electricity consumption, the validation criteria were exceeded, indicating discrepancies between metered and simulated energy outputs. A comparison of monthly measured and simulated cooling electricity consumption is shown in Figure 4.3c. The chart shows a close similarity for all months with the exception of January, February and October to December, for which the monitored data significantly exceeds the simulated cooling energy consumption. Since data for these months had previously been identified as non-typical, confirmed through trends in cooling degree day and consumption patterns for 2021-22, it was considered reasonable to utilise the partially-calibrated model for further analysis.

(a) Electricity total



(b) Fossil thermal heat



(c) Cooling electricity

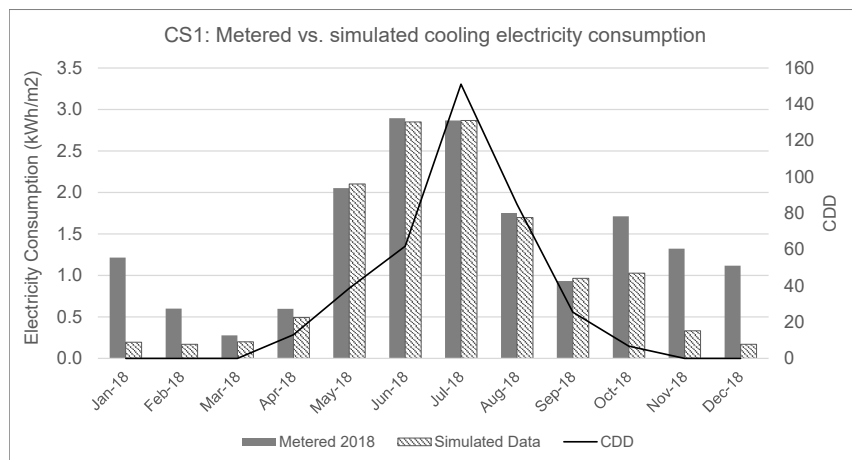


Figure 4.3: CS1 measured vs simulated calibrated outputs for 2018.

4.3 CS1: Framework Development

This chapter presents outputs from the implementation of various stages of the life-cycle optimisation framework on CS1 (outlined in Figure 3.8). Firstly, results from sensitivity analysis are summarised with reference to inclusions/exclusions from the subsequent GA optimisation process. Normalised functional unit LCA calculation results are then presented for the refined ECM solution set and integrated into the NSGA-ii GA. Section 4.4.1 discusses the life-cycle optimisation results for a single scenario. Finally, outputs are compared to findings from alternative grid decarbonisation and cost scenarios.

4.3.1 Preliminary testing

Sensitivity analysis was conducted as a preliminary step to the GA optimisation process, identifying parameters with negligible or negative impact on building energy performance. These were excluded from further investigation. Details and results from preliminary studies can be found in Appendix B and C, with outputs summarised in Table 4.6.

Table 4.6: Summary of findings from preliminary studies for CS1.

Parameter	Test	Findings
Roof Albedo	Outer surface replaced with high albedo material (SR 0.8, TE 0.9)	Marginal impact on energy savings (<1%), with EC substantially outweighing OC benefits. EC: +4.7 kgCO _{2e} /m ² /yr OC: -0.6 kgCO _{2e} /m ² /yr
North WWR	North facade WWR increase to +30%	Cooling loads: -0.09 kWh/m ² /yr (-0.01%) Heating loads: 0.3 kWh/m ² /yr (<0.01%) Net increase in energy use: +0.19 kWh/m ² /yr OC: +306 kgCO _{2e} /yr
Shading D/H Ratio	Varied from 0 to 1.2 for each facade orientation	Additional operational energy change beyond 0.8 d/h were minor. Optimal value ranges per facade shown in Table 4.7

4.3.2 ECM selection

In response to preliminary studies, the [ECM](#) toolkit was adapted for CS1, reducing the solution space from 424,673,280 to 21,676,032. Included parameter adaptations are presented in [Table 4.7](#) and detailed below.

Table 4.7: Assigning genes and possible values for implementing into multi-objective optimisation framework.

Gene	Parameter	Metric	Variants
x1.	Glazing U-value	W/m ² K	1.5, 0.8
x2.	g-value	SHGC	0.4, 0.3
x3.	North glazing area	%	0, -50
x4.	South glazing area	%	0, -50, -30, +30
x5.	East glazing area	%	0, -50, -30, +30
x6.	West glazing area	%	0, -50, -30, +30
x7.	S-louvre	D/H ratio	0, 0.4, 0.6, 0.8
x8.	E-louvre	D/H ratio	0, 0.2, 0.4, 0.6
x9.	W-louvre	D/H ratio	0, 0.2, 0.4, 0.6
x10.	Wall Insulation (MW)	mm	0, 50, 80, 120
x11.	Roof Insulation (XPS)	mm	0, 120, 150, 180
x12.	Frame U-value	W/m ² K	1.384, 0.378, 0.219
x13.	Infiltration Rate	m ³ /(m ² .h)@50Pa	3, 1, 0.5
x14.	NV control	-	None, dT, nightpurge
x15.	HVAC system	-	DH, ASHP
x16.	MVHR control	-	7-19 weekdays, nightcycle, weekends

Window-to-Wall Ratio (WWR)

Adjustments were made relative to the baseline geometries of the existing building, with variants ranging from a 50% reduction to a 30% increase in glazing area.

Shading Components

Shading included vertical devices on east and west facades, and horizontal louvres on north facades, varied by louvre depth to window height ratio (D/H)[[184](#), [185](#)].

Frame Thermal Conductivity

Assumed improvements through the addition of a polyisocyanurate ([PIR](#)) closer, consisting of an insulation layer (0.05-0.1m) and a plasterboard internal lining (see [Appendix H.2](#)) [[186](#)]. Frame U-values were updated to reflect this insulation addition (0.05m thickness; U=0.378 W/m²K, 0.1m thickness; U=0.219 W/m²K).

Infiltration Rates

Associated infiltration rates relating to [PIR](#) closers were estimated, correlating U-values and infiltration rates via a psi value calculator [[186](#), [187](#)].

4.3.3 Modelling Inputs: Carbon Calculations

Life-cycle EC emissions were calculated on a functional unit (FU) basis, accounting for the various life-cycle stages as specified in BS EN 15978:2011 [17]. For building fabric, the functional unit (FU) was 1m² of the respective building element. Where HVAC related EC emissions were included, the functional unit adopted was 1 unit of the relevant HVAC equipment. These values were scaled according to actual fabric/component sizes upon implementation of the CCA-LCA framework.

EC: Fabric

The embodied carbon associated with the primary building elements that change during the optimisation process are presented in Table 4.8. These were derived using the LCA stages and calculation methodology described in section 3.3.6. In accordance with RICS Professional Standard [19], assumptions were made relating to the typical location of manufacture (Local, National or European), the waste rate and expected lifespan of each building material. Whilst items shown in red represent alternative design interventions, the EC of the remaining items was still calculated for replacement cycles, where relevant. All values in Table 4.8 are presented with respect to a functional unit of 1m² equivalent surface area of the relevant building material. A more extensive list of LCA assumptions and results, and the sources used to develop these assumptions are provided in Appendix E.2 and D.

Element	FU	Build-up	Volume/FU (m ³ /FU)	Manu- facture (L/N/E)	Waste rate (%)	Lifespan (yrs)	EC (kgCO _{2e} /FU)	Total EC (kgCO _{2e} /FU)
Roof	m ²	Cast concrete	0.175	L	5	75	63.10	312.07-332.91
		Reinforcement mesh	0.003	N	15	75	43.07	
		EPS insulation	0.300	N	5	40	85.74	
		+/-XPS insulation	0.120-0.180	N	5	40	41.68-62.52	
		Metal deck	0.001	N	1	30	78.48	
External Wall	m ²	Brick slip	0.070	N	20	75	41.99	122.31-139.88
		MW insulation	0.050	N	15	75	10.85	
		Stainless steel brickties	1.2E-06	N	3	75	0.04	
		MW insulation	0.120	N	15	75	26.04	
		Gypframe	0.000	N	3	75	9.13	
		Cement board	0.013	N	5	75	5.61	
		+/-MW insulation	0.050-0.120	N	15	75	10.85-26.04	
		+/-Gypframe	0.000	N	3	75	6.75-9.13	
		Steel studs	0.000	N	3	75	3.85	
		Gypsum plasterboard	0.012	N	5	30	7.20	
Spandrel panel	m ²	Aluminium cladding	0.002	N	1	30	73.17	127.72
		MW insulation	0.170	N	15	75	36.89	
		Gypsum plasterboard	0.025	N	22.5	30	17.66	
Double glazing	m ²	-	0.003	E	5	40	24.72	24.72
Triple glazing	m ²	-	0.003	E	5	40	26.38	26.38
PIR closer	m ²	PIR insulation	0.05-0.1	N	15	75	12.56-25.12	35.67-48.23
		Gypsum plasterboard	0.039	N	5	30	23.11	
Louvre	m ²	Aluminium	0.002	N	1	30	73.17	73.17

Table 4.8: Calculated EC of construction elements for CS1, including materials, volume per functional unit (FU), assumptions impacting the calculations, and total EC for each element. Items shown in red are interventions. Waste rates obtained from [163]; expected lifespan from [77, 19]. Manufacture location: Local (L), National (N), European (E).

The embodied carbon of window glazing and frame elements was calculated separately, since changes to the win-wall ratio can impact the frame to glazing surface area ratio. The EC associated with the protruding aluminium timber composite frame build-up was consistent across both double and triple glazed systems, assuming the additional layer of glazing would not have a significant impact on the frame composition.

For the PIR closer, the plasterboard internal lining was assumed to protrude the depth of the reveal (0.107m) and close across the frame width of 0.05m. Since the calculation was on the basis of the functional unit of 1m² of frame, the total volume of each material was estimated by the calculations outlined in Appendix H.1. The resulting EC value in kgCO_{2e} was multiplied by the total frame area for each model iteration.

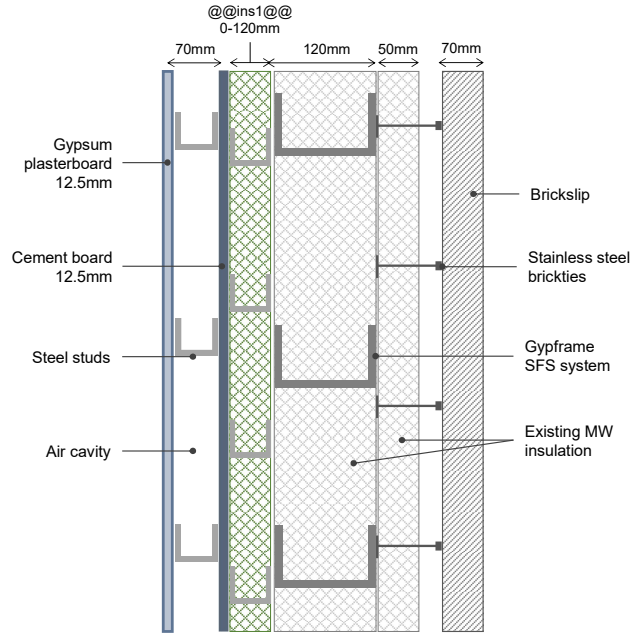


Figure 4.4: Assembly section: CS1 external wall build-up demonstrating all elements included in EC calculations and the position of additional internal MW insulation (@@ins1@@).

The modelled external wall build-up is depicted in Figure 4.4, aligning with the baseline U-values specified in architectural plans, and typical materials as guided by industry standards [179]. Despite the relatively small volumes, the high EC value associated with stainless steel brickets (4.41 kgCO_{2e}/kg) and galvanised steel gypframe and studs (2.76 kgCO_{2e}/kg) can be significant upon accumulation. Additional internal mineral wool insulation and gypframe were included in varying thicknesses of 0, 50, 80, 120mm and positioned behind the cement board layer. Typical sizing, frequencies and spacing of metal elements were established through expert elicitation.

EC: Systems

The existing heating system serving CS1 is a **DEN**, described in the following section. For design scenarios that utilise the **DEN**, as opposed to the **ASHP** alternative, it is assumed that existing **HVAC** equipment is sufficient to last the building's life-cycle. In reality, certain elements of the **DEN** system will likely be replaced, such as the gas boilers. However, the **DEN** serves a network of surrounding buildings so the relative share of carbon associated with this singular building would be minimal. In contrast, the **EC** associated with refrigerant-based HVAC systems can be substantial due to the typically high **GWP** of refrigerants [55]. The general procedure for calculating the **EC** associated with the **ASHP** followed the life-cycle stages used for all other building materials, described in section 3.3.6. However, several important additional stages were incorporated that are not deemed relevant for typical materials. This included 'in-use emissions' (B1) and 'refrigerant disposal' (CSR) [19]. These stages reflect the carbon emissions associated with refrigerant leakage during the use and end of life phases respectively.

ASHP rated capacity, extracted from each simulation run, was used to estimate system mass; extrapolation of manufacturers' specifications showed a strong linear correlation between **ASHP** mass and rated capacity ($R^2=0.97$) [188]. Therefore, it was considered reasonable to estimate system mass from capacity according to the linear equation shown in Figure 4.5a. A1-A3 emissions associated with the manufacture of **ASHP** materials were obtained from literature [55], and scaled by mass to achieve the industrial scale required for serving large **HE** buildings. Similarly, a strong correlation was observed between **ASHP** heating capacity and refrigerant mass ($R^2=0.98$), from manufacturers' specifications [188]. The linear expression shown in Figure 4.5b was used to predict the refrigerant mass of the system. **EC** calculations assumed a commonly used refrigerant, R-32, with a **GWP** of 675. A refrigerant leakage rate of 3.8% per year and end-of-life (**EOL**) recovery rate of 98% was obtained as the medium estimate from a synthesis of sources by George et al. [189], with an annual top-up to maintain refrigerant mass [55]. The material recovery rate of 96% was selected in-line with **RICS** suggested recovery rate for metals [19], since the composition breakdown from manufacturers' specifications shows a high proportion of metal content [188]. The various assumptions associated with the **EC** of **ASHPs** are summarised in Table 4.9.

OC emissions

The baseline scenario considers the **DEN** serving the existing building. The **DEN** is provided by a combination of gas boilers and combined heat and power plants. The nature of combined heat and power is such that gas inputted in to the system results in a combined electricity and heat/steam output. As such, the **CEF** is calculated based on the carbon associated with gas consumption minus the car-

Table 4.9: EC calculation assumptions for ASHP.

System type	ASHP
FU	unit
Manufacture	European
Expected lifespan	22 yrs
Refrigerant type	R-32
In-use refrigerant leakage rate	3.8% per yr
Refrigerant EOL recovery rate	98%
GWP	675
Material recovery rate	96%

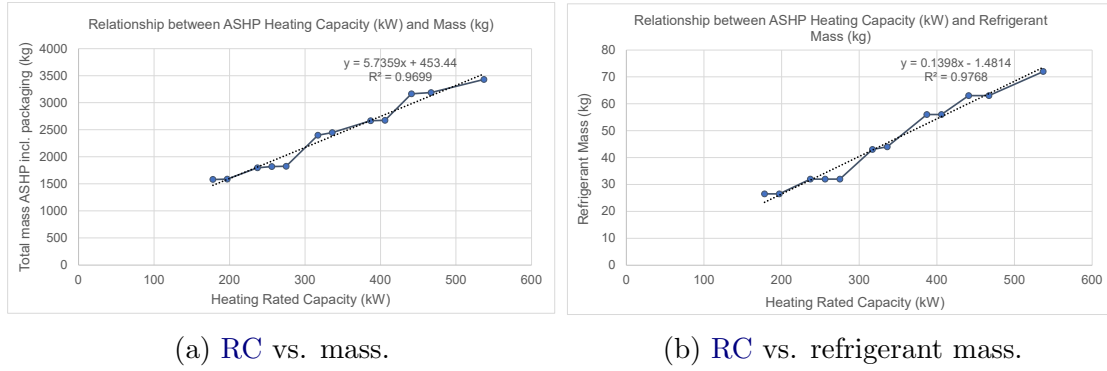


Figure 4.5: Correlation between RC, mass and refrigerant mass established from ASHP manufacturers' specifications [188].

bon savings associated with the electricity by-product, that would otherwise be sourced from the grid. The calculated equivalent CEF for the whole DEN system is shown in Table 4.10 for the years 2013-2020, based on measured DEN input and output consumption data. Assuming an average combined heat and power system efficiency ($\eta=60\%$) from measured data, the CEF of the overall DEN system was extrapolated to 2100, using the gas and electricity predicted CEF pathways described in section 3.3.6.

The resulting DEN CEF pathways associated with the various storylines are depicted in Figure 4.6. The general trend across scenarios shows a relatively sharp increase in CEF up to 2020, plateauing between 2030-2040, followed by a gradual decline. The initial increase is reflective of an increasing share of renewable electricity generation. As a result, the carbon savings associated with the combined heat and power electricity by-product decreases rapidly, representing the diminishing payback due to grid decarbonisation. Carbon emissions associated with gas consumption are also predicted to decrease due to an increasing penetration of green gas in to the network. The initial impact of this is relatively marginal in comparison to the much more rapidly declining electricity CEF. However, over time a gradual decrease in the overall DEN CEF can be expected; as electricity CEFs for most scenarios start to plateau around the year 2040, the decreasing

Table 4.10: Calculated carbon emission factors for the DEN from 2013-2020.

Year	2013-14	2014-15	2015-16	2016-17	2017-18	2018-19	2019-20
Grid CEF: gas (kgCO _{2e} /kWh)	0.20	0.18	0.18	0.18	0.18	0.18	0.18
Grid CEF: electricity (kgCO _{2e} /kWh)	0.52	0.46	0.41	0.35	0.28	0.26	0.23
Boiler: gas input (GWh)	18.4	19.6	25.7	30.7	26.5	29.6	29.1
CHP: gas input (GWh)	45.6	40.9	33.0	16.3	25.6	28.4	31.1
CHP: heat/steam output (GWh)	13.7	13.8	10.7	4.9	5.8	6.5	7.1
CHP: electricity output (GWh)	15.9	13.4	10.5	5.5	8.1	9.7	10.1
CHP: efficiency	65%	67%	64%	64%	54%	57%	55%
Boiler: gas input (kgCO _{2e})	3,643,022	3,614,224	4,734,236	5,652,706	4,869,117	5,433,831	5,348,789
CHP: gas input (kgCO _{2e})	9,023,054	7,545,741	6,073,119	3,009,367	4,713,570	5,212,756	5,719,519
CHP: electricity output (savings) (kgCO _{2e})	-8,237,701	-6,212,183	-4,321,306	-1,935,527	-2,279,194	-2,478,050	-2,364,722
net CO ₂ of system (kgCO _{2e})	4428375	4947782	6486049	6726547	7303492	8168537	8703586
System CEF (kgCO_{2e}/kWh)	0.16	0.17	0.21	0.23	0.27	0.27	0.29

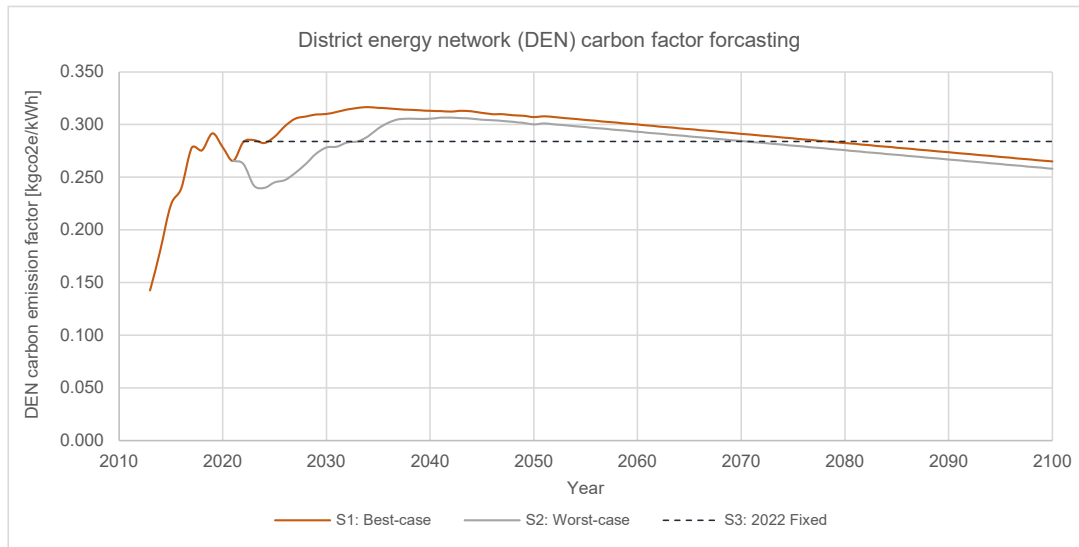


Figure 4.6: DEN carbon factor forecast based on changing gas and electricity CEF projections.

CEF associated with gas consumption becomes the predominant driving factor. It is apparent that the carbon associated with the alternative - an electrically-fuelled heating system with equivalent power requirements - would be less than that of the DEN over the building's life cycle, since the electricity CEF approaches zero. Thus, it is important to weigh up this OC savings against the EC associated with switching from the baseline DEN to alternative, electricity-based, heating systems.

4.3.4 Modelling Inputs: Cost Calculations

CapEx

The LCC of various building components are summarised in Table 6.7, calculated following the ISO 15686-5:2017 protocol described in section 3.3.6 [18]. All values were interpolated based on available data [167]; more extensive details of

interpolations, including material and labour costs, are provided in Appendices E.5 and E.6.

Element	FU	Build-up	Volume/FU (m ³ /FU)	Total Rate (£)	Replacement (yrs)	NPV- adjusted cost (£)	LCC (£)	Total LCC (£)
Roof	m ²	Cast concrete	0.175	100	-	-	100	227.13-259.91
		Reinforcement mesh	0.003	-	-	-	-	
		EPS insulation	0.300	85	40	-	85	
		+/-XPS insulation	0.120-0.180	32.24-57.33	40	9.88-17.58	42.13-74.91	
		Metal deck	0.001	-	30	-	-	
External Wall	m ²	Brick slip	0.070	61.96	-	-	61.96	179.2-183.85
		MW insulation	0.050	4.53	-	-	4.53	
		Stainless steel brickties	1.2E-06	-	-	-	-	
		MW insulation	0.120	8.17	-	-	8.17	
		Gypframe	0.000	61.52	-	-	61.52	
		Cement board	0.013	-	-	-	-	
		+/-MW insulation	0.050-0.120	4.79-8.17	-	-	4.79-8.17	
		+/-Gypframe	0.000	3.62-4.89	-	-	3.62-4.89	
		Steel studs	0.000	-	-	-	-	
		Gypsum plasterboard	0.012	24.51	30	10.10	34.61	
Spandrel panel	m ²	Aluminium cladding	0.002	202.35	30	83.37	285.72	320.81
		MW insulation	0.170	10.58	-	-	10.58	
		Gypsum plasterboard	0.025	24.51	30	10.10	24.51	
Double glazing	m ²	Double glazed casement aluminium window frame	-	609.07-652.06	40	186.71-199.89	795.78-851.95	795.78-851.95
Triple glazing	m ²	Triple glazed casement aluminium window frame	-	812.51-855.50	40	249.08-262.26	1061.59-1117.76	1061.59-1117.76
PIR closer	m ²	PIR insulation	0.05-0.10	43.56	-	-	43.56-52.25	152.23-161.92
		Gypsum plasterboard	0.0393	76.96	30	31.71	108.67	
Louvre	m ²	Aluminium	0.002	580.87	30	239.31	820.18	820.18

(a) Fabric

Element	FU	Total Rate (£)	Replacement (yrs)	NPV- adjusted cost (£)	Total LCC (£)
ASHP	387 kW* unit	164,473	22, 44	130,635	295,109
MVHR	14,690 m³/h unit	26,464	20, 40	22,765	49,230

(b) Systems *Extrapolated according to calculated rated capacity from each simulation run.

Table 4.11: Calculated CapEx of construction elements for CS1, including materials, volume per FU and replacement costs. Items shown in red are interventions. Expected lifespan from [77, 19].

OpEx

Fuel price pathways followed the fluctuating fuel price assumptions outlined in section 3.3.7.

4.4 CS1: Framework Implementation

4.4.1 Life-cycle optimisation results

Outputs from the life-cycle optimisation framework for the ‘S1: Best-case’ pathway are presented in this section. Alternative decarbonisation scenarios are explored in the subsequent section 4.4.2.

Pareto Optimal Solutions

The results of the NSGA-ii optimisation process for ‘S1: Best-case’ scenario are shown in Figure 4.7. Several runs were conducted to ensure the same pareto optimal solutions were reached each time, indicating the presence of global optima. Overall, for interventions and replacements, pareto optimal solutions range from 805-932 £/m² for LCC and from 342-725 kgCO₂e/m² for LCCF over the 60 year time frame. LCCF values appear to be considerably less than HE refurbishment studies from literature, due to the quantification of grid decarbonisation in lieu of fixed carbon factors [76]. In addition, CS1 recently underwent an extensive refurbishment with the resulting fossil thermal consumption significantly less than good practice benchmarks [190].

The presence of two distinct search regions represent heating system alternatives. LCCF sample variance is substantially lower amongst ASHP solutions (σ^2 : 17 kgCO₂e/m² vs. 450 kgCO₂e/m²). This indicates that additional design variations have less impact on OC savings once ASHP heating systems have been implemented, signifying greater design flexibility.

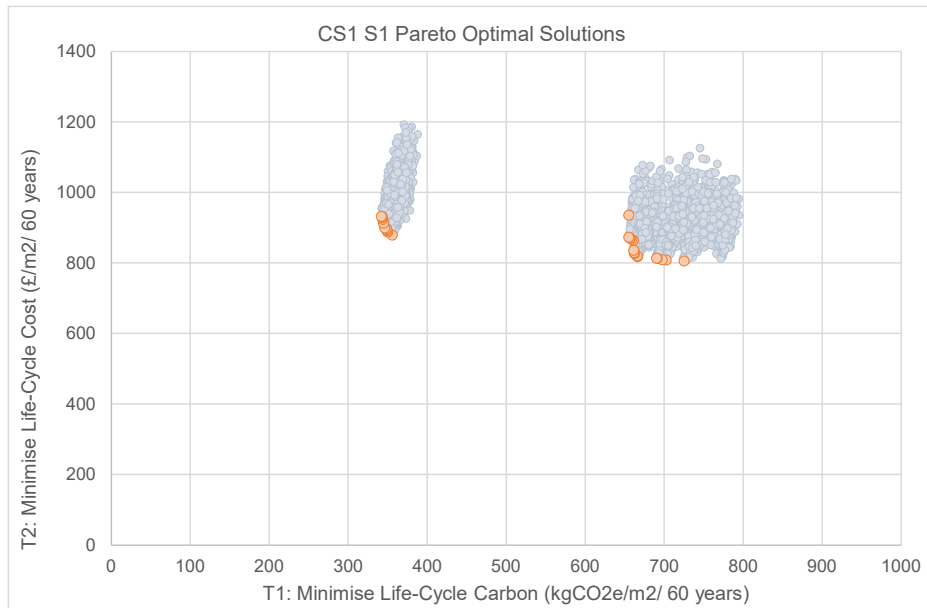
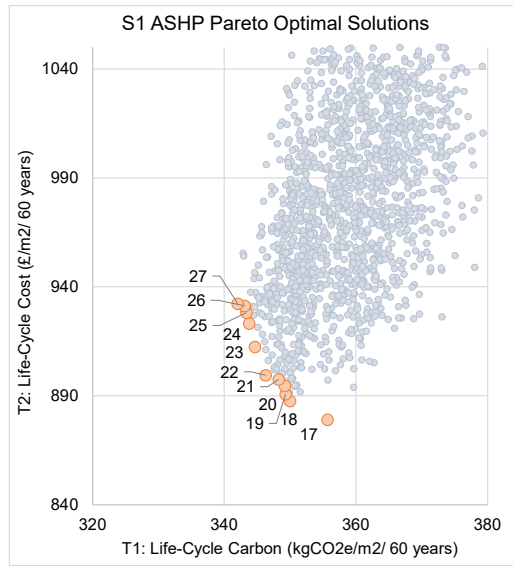
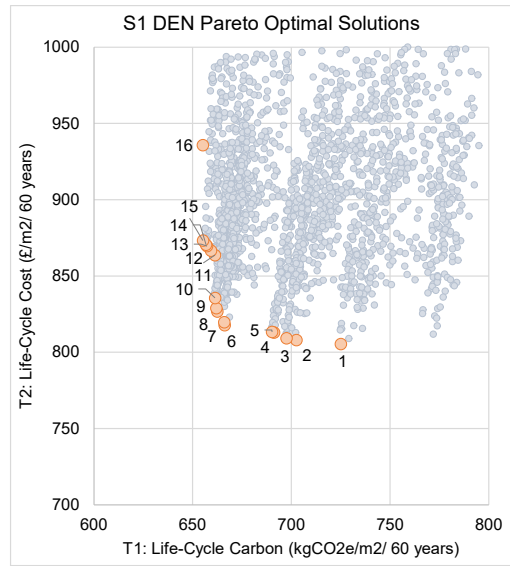


Figure 4.7: Optimised LCCF and LCC values.



(a) ASHP



(b) DEN

#	Heating System	Glazing Type	SHGC	North WWR	South WWR	South Louvre D/H	East WWR	East Louvre D/H	West WWR	West Louvre D/H	IWI Ins. +mm	Roof Ins. mm	Frame U-value W/m ² .K	Infiltr. Rate m3/m ² .h	MVHR Control Strategy	NV Control Strategy
1	DEN	Double	0.3	-50%	-50%	0	-50%	0.2	-50%	0	+0	+0	0.219	0.5	Weekday	Nightpurge
2	DEN	Double	0.4	-50%	-50%	0	-50%	0	0%	0	+80	+0	1.384	3	Nightcycle	Baseline
3	DEN	Double	0.4	-50%	-50%	0	-50%	0	-50%	0	+0	+0	1.384	3	Nightcycle	Baseline
4	DEN	Double	0.4	-50%	-50%	0	-50%	0	-50%	0	+0	+0	0.378	1	Nightcycle	Baseline
5	DEN	Double	0.4	-50%	-50%	0	-50%	0	-50%	0	+0	+0	0.219	0.5	Nightcycle	Baseline
6	DEN	Double	0.4	-50%	-50%	0	-50%	0	-50%	0.2	+0	+0	1.384	3	Nightcycle	deltaT
7	DEN	Double	0.4	-50%	-50%	0	-30%	0	-50%	0	+0	+0	1.384	3	Nightcycle	deltaT
8	DEN	Double	0.4	-50%	-50%	0	-30%	0	-50%	0	+0	+0	0.378	1	Nightcycle	deltaT
9	DEN	Double	0.3	-50%	-50%	0	-30%	0	-50%	0	+0	+0	0.378	1	Nightcycle	deltaT
10	DEN	Double	0.3	-50%	-50%	0	0%	0	-50%	0	+0	+0	0.219	0.5	Nightcycle	deltaT
11	DEN	Triple	0.4	-50%	-50%	0	-50%	0	-50%	0	+0	+0	1.384	3	Nightcycle	deltaT
12	DEN	Triple	0.4	-50%	-50%	0	-50%	0.2	-50%	0.2	+50	+0	0.378	1	Nightcycle	deltaT
13	DEN	Triple	0.4	-50%	-50%	0	-50%	0	-50%	0	+0	+0	0.378	1	Nightcycle	deltaT
14	DEN	Triple	0.4	-50%	-50%	0	-50%	0	-50%	0	+0	+0	0.219	0.5	Nightcycle	deltaT
15	DEN	Triple	0.3	-50%	-50%	0	-50%	0	-50%	0	+0	+0	0.219	0.5	Nightcycle	deltaT
16	DEN	Triple	0.3	0%	-30%	0	0%	0	-30%	0.2	+0	+0	0.219	0.5	Nightcycle	deltaT

(c) Parameters of optimised solution set for CS1 DEN.

#	Heating System	Glazing Type	SHGC	North WWR	South WWR	South Louvre D/H	East WWR	East Louvre D/H	West WWR	West Louvre D/H	IWI Ins. +mm	Roof Ins. mm	Frame U-value W/m ² .K	Infiltr. Rate m3/m ² .h	MVHR Control Strategy	NV Control Strategy
17	ASHP	Double	0.4	-50%	-50%	0	-50%	0	-50%	0.2	+80	+0	1.384	3	Nightcycle	Baseline
18	ASHP	Double	0.4	-50%	-50%	0	-50%	0	-50%	0	+0	+0	1.384	3	Nightcycle	Baseline
19	ASHP	Double	0.3	-50%	-50%	0	-50%	0	-50%	0	+0	+0	1.384	3	Nightcycle	Baseline
20	ASHP	Double	0.3	-50%	-30%	0	-50%	0	-50%	0	+0	+0	1.384	3	Nightcycle	Baseline
21	ASHP	Double	0.3	-50%	-30%	0	-30%	0	-50%	0	+0	+0	1.384	3	Nightcycle	Baseline
22	ASHP	Double	0.3	0%	-50%	0	-50%	0	-50%	0	+0	+0	1.384	3	Nightcycle	Baseline
23	ASHP	Double	0.3	0%	-50%	0	0%	0	-50%	0	+0	+0	0.219	0.5	Nightcycle	Baseline
24	ASHP	Double	0.4	0%	-30%	0	0%	0	0%	0	+0	+0	0.219	0.5	Nightcycle	Baseline
25	ASHP	Double	0.3	0%	0%	0	+30%	0	-50%	0	+0	+0	0.219	0.5	Nightcycle	Baseline
26	ASHP	Double	0.4	0%	0%	0	+30%	0	0%	0	+0	+0	0.219	0.5	Weekday	Nightpurge
27	ASHP	Double	0.3	0%	-30%	0	+30%	0	0%	0	+0	+0	0.219	0.5	Weekday	Nightpurge

(d) Parameters of optimised solution set for CS1 ASHP.

Figure 4.8: NSGA-ii optimisation results for CS1 scenario 1.

Relative Impact of Variables on LCCF and LCC

The relative impact of independent design measures on **LCCF** and **LCC** was assessed using linear regression analysis. Summation of unstandardised linear model coefficients across each level within a categorical variable, provides an overall weighted coefficient (β); this reflects the relative impact of changes in design parameters. In this context, a larger absolute β value indicates a stronger influence of that variable on the dependent outcome (**LCCF** or **LCC**), while the sign of β denotes the direction of the relationship - positive for an increase, negative for a reduction. The coefficients are therefore used to compare the relative importance of design parameters on model outputs. The weighted coefficient for each variable is shown in Figure 4.9. It is important to acknowledge the assumption of independence amongst changing parameters, inherent to linear regression analysis; despite this limitation, the method provides a straightforward approach to identifying significant predictors of **LCCF** and **LCC**, allowing for valuable insights into the primary drivers of building performance. Since heating system type emerged as the predominant predictor of **LCCF**, linear regression analysis was conducted independently for each heating system alternative.

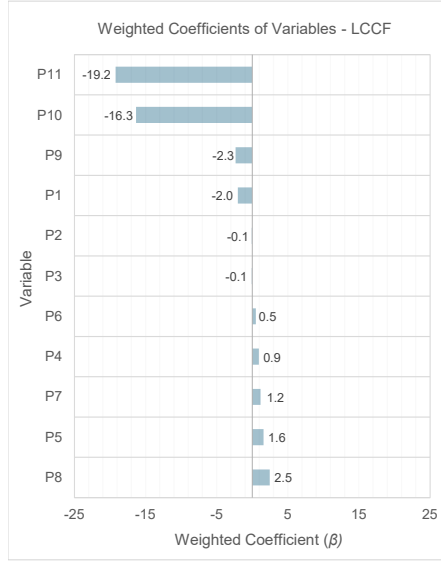
Heating System (P0)

Average **LCCF** among **ASHP** solutions was 346 kgCO_{2e}/m² less than that of the **DEN** group. This substantial reduction can be attributed to two primary factors. Firstly, the efficiency of the **ASHP** exceeds that of the **DEN** by approximately threefold (nominal **COP**:3.2), resulting in a 14 kWh/m² (63%) average decrease in heating operational energy consumption. Secondly, the **CEF** associated with the **ASHP** system is significantly lower than that of the **DEN** over the building's estimated life-cycle, as detailed in section 4.3.3. The cumulative impact results in an approximate 71% decrease in **OC** emissions over 60 years. Despite the **ASHP** system's considerable **EC** impact, approximately 372,507 kgCO_{2e} over 60 years (including two replacement cycles), the long-term **OC** savings outweigh the short-term **EC** costs by a factor of eight. This indicates substantial carbon savings potential.

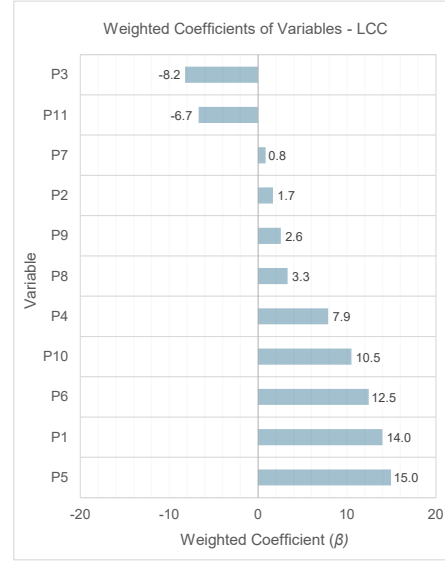
In contrast, the average **LCC** is approximately 9% (85 £/m²) lower amongst **DEN** solutions, primarily driven by the financial 'pay-back' resulting from the combined heat and power electricity by-product. Despite the much greater efficiency of **ASHPs**, the **LCC** results do indicate a marginal, sustained, cost-benefit of the **DEN** over **ASHP** heating systems. However, it is important to note that some costs should be taken into account for replacement cycles of the communal **DEN** network, potentially shifting **LCC** closer to that of the **ASHP**.

Variable		Variable	
P1	Glazing Type	P7	Internal Wall Insulation
P2	SHGC	P8	Roof Insulation
P3	North-WWR	P9	Frame U-value Infiltration Rate
P4	South-WWR D/H Ratio	P10	NV Operation
P5	East-WWR D/H Ratio	P11	MVHR Control
P6	West-WWR D/H Ratio		

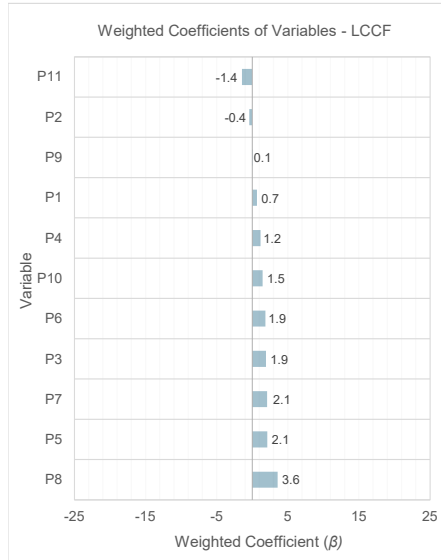
(a) Categorical variables.



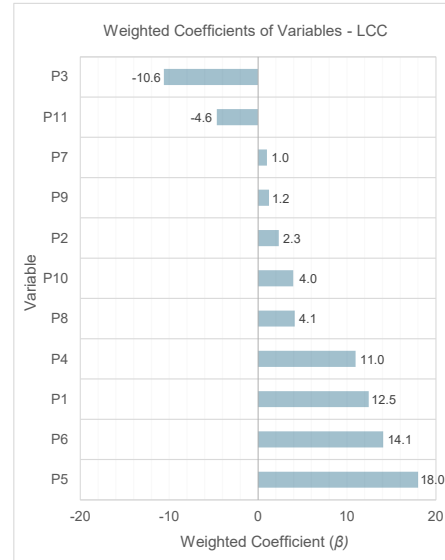
(b) t1 - Minimise LCCF (DEN)



(c) t2 - Minimise LCC (DEN)



(d) t1 - Minimise LCCF (ASHP)



(e) t2 - Minimise LCC (ASHP)

Figure 4.9: Weighted coefficients (β) of categorical variables in linear regression analysis for Scenario 1.

Glazing Type (P1, P2)

Upgrading to triple-glazed windows had a significant negative impact on model-predicted **LCCF** for designs reliant on the **DEN** (β : -2.0). However, when adopting the high-efficiency **ASHP**, the upgrade to triple glazing had a marginal positive impact on **LCCF** (β : +0.7), suggesting any additional **EC** was not offset by **OC** savings. In both scenarios, triple glazing had a strong positive impact on **LCC**, indicating that operational savings were insufficient to balance the higher capital costs. This implies that the suitability of triple glazing may be limited, even when reliant on an operationally carbon-intensive heating system, such as the **DEN**, and is subject to the efficacy of other conservation measures in place.

With respect to solar radiation, for **DEN** solutions, the impact of solar heat gain coefficient (**SHGC**) reductions on **LCCF** was statistically insignificant, suggesting the effect varied across design combinations. The impact on **ASHP** alternatives was stronger (**LCCF** β : -0.4), reflecting a greater focus on cooling loads to reduce **LCCF** under the operation of energy-efficient, low carbon heating systems. Limiting solar heat transmission appears to become a more effective design feature with equal **CEF** weightings assigned to both heating and cooling loads. Since no **EC**-penalty was attributed to the lower **SHGC** variant, the impact was driven solely by higher **OC** emissions. However, for both heating systems, **SHGC** reductions led to significant increases in **LCC**.

WWR | Louvre D/H Ratio (P3-P6)

Overall, **WWR** and louvre D/h ratio alternatives had relatively minor impacts on **LCCF** for both **DEN** (**LCCF** β : -0.1 to +1.6) and **ASHP** design combinations (**LCCF** β : +1.2 to +2.1). **WWR** reductions across **DEN** solutions showed weak but significant negative impacts on both **LCCF** and **LCC** across all facades, as shown in Appendix I.1. For **ASHP** solutions, **WWR** reductions led to marginally higher **LCCF** values, indicating that the preference for lower glazing ratios under **DEN** operation was driven by heat loss reduction rather than minimising solar heat gain. Reduced heat-related **OC** emissions associated with **ASHP** use resulted in less **LCCF** variance between glazing ratio alternatives, indicating greater design flexibility under optimised system performance.

The implementation of aluminum louvres for solar shading control generally demonstrated positive correlations with **LCCF** and **LCC**. The inefficacy of this measure indicates that, for the majority of design combinations, operational cost and carbon savings were counterbalanced by additional **EC** emissions and **CapEx**, ranging from 22,062 kgCO₂e to 165,692 kgCO₂e and £247,307 to £1,857,351 over the building's life-cycle. Larger depth to height ratios counterbalanced the impact of glazing area reductions on **LCCF** and **LCC** savings.

Insulation Thickness (P7, P8)

Internal wall insulation (IWI) and roof insulation additions resulted in significant positive correlations with both LCCF and LCC, irrespective of heating system type. This indicates that, for the majority of design combinations, the EC and CapEx associated with additional insulation layers outweigh any potential operational benefits (noting the already well-insulated baseline conditions). A comparison of solutions suggests that the predicted increase in cooling energy consumption with the addition of 50mm mineral wool insulation significantly outweighs heating load decreases. Due to the carbon-intensity of the DEN, this still results in marginal OC reductions over the buildings life-cycle. However, this is offset by greater EC emissions, resulting in a negligible net-effect on LCCF (+0.4%). A similar trend could be observed with additional extruded polystyrene (XPS) roof insulation, indicating limited benefits beyond that included in the existing build-up.

Frame U-value | Infiltration Rate (P9)

Additional PIR insulation demonstrated a negative correlation with LCCF when aligned with the baseline DEN heating system (β : -2.3). However, under the higher efficiency ASHP electricity-based heating system, the implementation of PIR closers and associated lower infiltration rates led to predicted increases in both LCCF and LCC. This suggests that the EC associated with the PIR insulation was not offset over the building's life-cycle due to lower OC emissions savings potential. In addition, for ASHP-based solutions, higher heating system efficiency relative to cooling can place disproportionate weighting on design iterations for reduced cooling demand, potentially favouring lower insulation levels.

Ventilation Strategy (P10, P11)

DeltaT and nightpurge NV strategies were advantageous in reducing OC emissions and operating costs, irrespective of other design features employed. DeltaT NV schedule had the strongest impact on LCCF reduction across DEN dependent solutions, whereas nightpurge ventilation was preferable for solutions reliant on the ASHP heating system, as depicted in Appendix I.3. This can be attributed to the high efficiency associated with heating energy consumption; nighttime cooling reduces the reliance on the mechanical cooling system, which is the dominating component of LCCF. Nightpurge NV was less effective under DEN operation since heating energy consumption is the predominant driver of LCCF, and will be greater upon implementation of this measure. Tighter NV regulation based on timestep temperature differences is a more effective strategy when a carbon-intensive heating system is in place. Adjustments to MVHR control strategies demonstrated the greatest impact on LCCF reductions (β : -1.4 to -19.2) across all measures, also resulting in large decreases in LCC (β : -4.6 to -6.7). Nightcycle MVHR control had the strongest negative impact on both metrics.

4.4.2 Scenario analysis

This section compares the ‘grid-average’ scenario (*S1*) detailed in the previous section, with results from the alternative decarbonisation pathway described in Table 3.4 and section 3.3.7.

Table 4.12: Summary of grid decarbonisation rate scenario alternatives; both S1 and S2 adopt the fluctuating fuel price pathways described in section 3.3.7.

Scenario Description	
S1	‘Best-case’: Electric grid carbon emissions decline rapidly from 2020 to 2030, plateauing at 2033.
S2	‘Worst-case’: Business-as-usual (BAU); incline in electric grid carbon emissions until 2025, thereafter declining gradually towards a plateau at 2042.

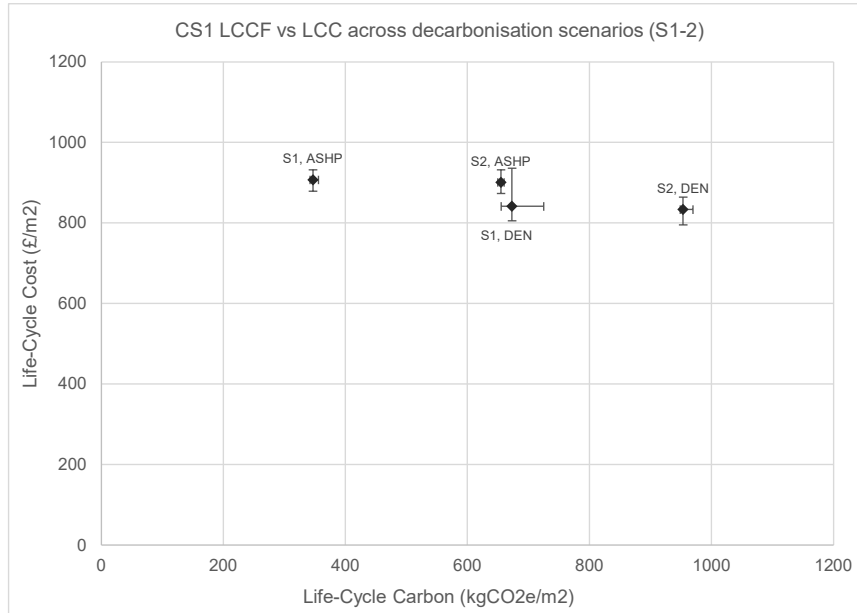


Figure 4.10: Comparison of pareto optimal solutions across decarbonisation scenarios. Points represent group averages; ranges depict variance of LCCF and LCC across pareto optimal solutions.

The LCCF and LCC across the decarbonisation pathways described in section 3.3.7 are shown in Figure 4.10. Across the baseline DEN scenarios, average LCCF values range from 655 kgCO₂e/m² to 970 kgCO₂e/m². For scenarios relying on the ASHP heating system, average LCCF varies from 342 kgCO₂e/m² to 660 kgCO₂e/m². These values correlate to average LCC ranges of 795 £/m² to 936 £/m² for the DEN and 874 £/m² to 932 £/m² for the ASHP group. The maximum given range within any single group is 70 kgCO₂e/m² for LCCF and 130 £/m² for LCC. Figure 4.10 clearly demonstrates how the heating system alternatives and decarbonisation pathways have a far greater influence on LCCF than the various design parameters across pareto solutions within the same group.

Amongst **ASHP** solutions, average **LCCF** increases by a factor of 1.9 (+308 kgCO₂e/m²) from S1 to S2. For **DEN** solutions, the relative increase across these scenarios is significantly less, rising by a factor of 1.4 (+281 kgCO₂e/m²). This difference can be attributed to the **CEF** assumptions relating to **ASHP** and **DEN** heating energy consumption. In the *S2:Worst-case* energy pathway, the average electricity **CEF** over the building's life-cycle increases by almost three fold (+0.043 kgCO₂e/kWh) compared to S1. By contrast, for the **DEN**, the average **CEF** actually decreases by 5% (-0.014 kgCO₂/kWh), since the combined heat and power electricity by-product becomes more carbon-valuable, contributing to a greater off-set of emissions from gas consumption, as described in section 4.3.3. Consequently, the difference in **LCCF** between **ASHP** and **DEN** solution sets becomes less distinct in S2 than in S1, although the **ASHP** solution is still substantially less than **DEN** alternatives.

As the electricity **CEF** increases from S1 to S2, **LCCF** becomes more sensitive to changes in operational energy consumption, reducing the spread of pareto-optimal solutions. For **DEN** solutions, two opposing factors are at play; carbon emissions associated with heating loads decrease, whilst the electricity **CEF** increases. Consequently, **LCCF** becomes more sensitive to changes in cooling operational energy and less sensitive to changes in heating operational energy. This adjustment leads to a ninefold reduction in the variance of **LCCF**, representing increased consistency among optimised design parameters. These findings underscore the enhanced design flexibility achievable under improved decarbonisation pathways without significantly impacting **LCCF**.

Despite implementation of identical assumptions relating to **CapEx** and **OpEx** in S1 and S2, marginal discrepancies were observed in **LCC**. For the **DEN** group, a decrease of 8 £/m² was noted from S1 to S2. Although the variances are minimal (<1%), their existence demonstrates the indirect effect of changing carbon emission pathways on **LCC**, through various optimised design parameters.

Embodied vs. operational carbon emissions

The impact of grid decarbonisation on the proportion of **LCCF** components is depicted in Figure 4.11. Across solution sets, **EC** is predominantly driven by emissions associated with initial and recurring replacement of components on the external envelope, such as glazing. For the **DEN** baseline, the predominant driver of **OC** shifts from heating and domestic hot water to lighting and power under slower rates of grid decarbonisation. Lighting and power remains the predominant driver of **OC** across all scenarios in the **ASHP** group.

The average **EC** associated with **ASHP** pareto solutions was approximately 1.3 times that of the **DEN** pareto front (DEN: 149 kgCO₂e/m², ASHP: 190 kgCO₂e/m²), owing to the high **EC** impact of the refrigerant, included within

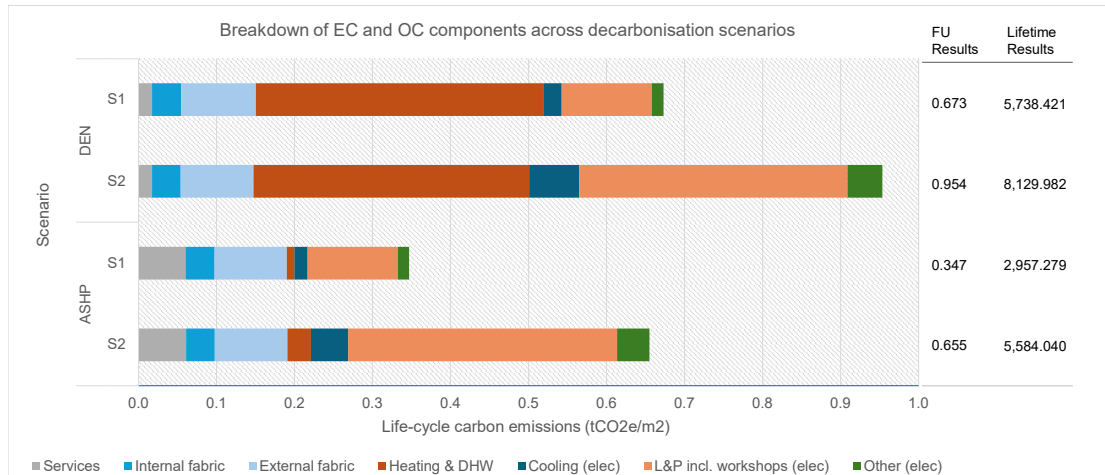


Figure 4.11: Average share of embodied versus operational carbon components across pareto solutions for scenarios 1 and 2.

the ‘services’ component. Whilst average **EC** remains relatively consistent across scenarios adopting the same heating system, average **OC** varies by 284 kgCO₂e/m² for the **DEN** scenarios and by 307 kgCO₂e/m² for the **ASHP** scenarios. For the **DEN** group, this shifts the ratio of **EC:OC** from 1:3 to 1:5 from S1 to S2. For the **ASHP** solutions, this ratio is much lower, ranging from 1:1 to 1:2 for S1 and S2 respectively. Under more rapid grid decarbonisation pathways and the uptake of energy efficient heating measures, results indicate that the share of **EC** could account for over half (55%) of the refurbished building’s **LCCF**.

Recurring Parameter Sets

Despite the large differences in **OC** resulting from varying decarbonisation pathways, 9% (n=6) of unique pareto optimal solutions appeared in both *S1:Best-case* and *S2:Worst-case* scenarios, presented in Table 4.13. Solutions present across both scenarios were primarily reliant on **ASHP** heating system operation and all implemented double glazing. The results indicate that it is feasible to provide **LCA**-optimised building redevelopment solutions that incorporate uncertainties relating to future grid decarbonisation pathways.

Time-dependency of carbon impact

The aggregated year-on-year **LCCF** over the building’s 60 year life-span is shown in Figures 4.12. Across scenarios, a step change can be observed at the 2052 time-point, reflecting the **EC** associated with the replacement of several building components, such as internal dry lining, partitions and spandrel panelling. This step change is more defined in S1 than S2, reflecting the reduced proportional impact of **EC** relative to **OC** when decarbonisation does not occur. For **ASHP**-based solutions, substantial step changes can be observed at 2044 and 2066, represent-

ing the 22-year replacement cycles of refrigerant-based ASHP systems. For S1, the cumulative LCCF impact appears to plateau at approximately 2043, whereas the DEN group continues to demonstrate a strong positive trajectory up to 2082. This indicates that, even under a faster rate of grid decarbonisation, the annual carbon intensity of CS1 will continue to increase beyond the building's life-span unless heating system replacement takes place. The results indicate that no other design alterations will be sufficient in achieving a relatively consistent year-on-year carbon impact by 2082.

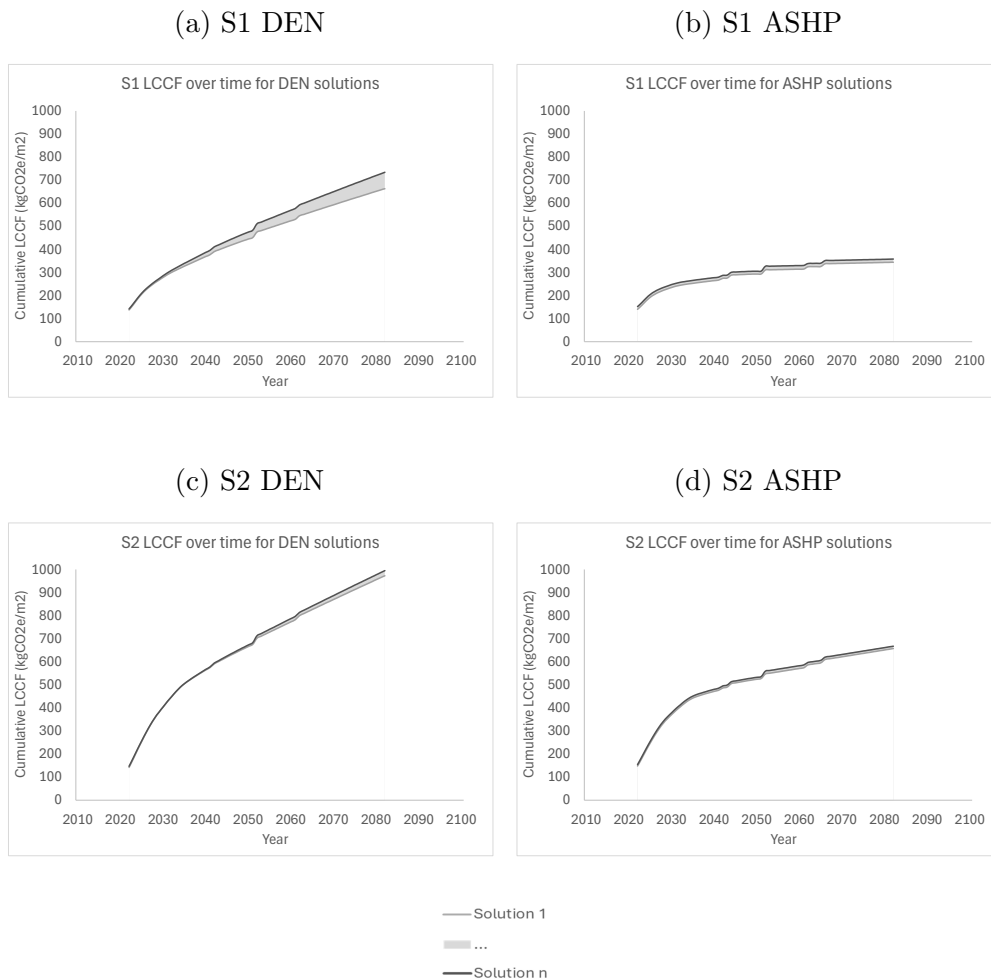


Figure 4.12: CS1 change in LCCF of pareto optimal solutions over time for S1 and S2.

Table 4.13: Recurring pareto optimal solutions across S1 and S2.

#	P0: Glazing type	P1: SHGC	P2: N-WWR (% change)	P3: S-WWR (% change)	P5: E-WWR (% change)	P8: W-WWR (% change)	P10: IWI Addition (mm)	P11: Roof Ins Addition (mm)	P12: Frame U-value (W/m ² k)	P13: Infiltration Rate (m ³ /(m ² h)@50Pa)	P14: NV Strategy	P15: Heating System	P16: MVHR Strategy
1	Double	0.4	-50%	-50%	-50%	-50%	0	0	0.219	0.5	Baseline	DEN	Nightcycle
2	Double	0.4	-50%	-50%	-50%	-50%	0	0	1.384	3	Baseline	DEN	Nightcycle
3	Double	0.3	0%	-50%	-50%	-50%	0	0	1.384	3	Baseline	ASHP	Nightcycle
4	Double	0.3	-50%	-50%	-50%	-50%	0	0	1.384	3	Baseline	ASHP	Nightcycle
5	Double	0.4	-50%	-50%	-50%	-50%	0	0	1.384	3	Baseline	ASHP	Nightcycle
6	Double	0.3	0%	-30%	30%	0%	0	0	0.219	0.5	Nightpurge	ASHP	Weekdays

CS1 Chapter Summary

This case study evaluates an architecture HE building typology, refurbished in 2016, with space functions including studios, workshops, offices and teaching rooms. Analysis demonstrates how a range of design interventions perform under diverse grid decarbonisation scenarios, based on achieving optimal life-cycle cost and life-cycle carbon performance. The following observations were made:

Heating Strategies:

- Heating system alternatives exhibited strong impacts on LCCF owing to the cumulative effect of electricity carbon emission factors over the building's lifetime.
- ASHP solutions achieved lower LCCF than the DEN baseline, despite a higher EC value from refrigerant leakage and end-of-life recovery. Services accounted for a significant proportion of embodied carbon in ASHP-based solutions.
- For ASHP solutions, additional design measures had minor impacts on further OC reductions, indicating greater design flexibility but a more nuanced trade-off between embodied and operational carbon.

Ventilation Strategies:

- MVHR and NV control strategies, and airtightness, emerged as the predominant predictors of LCCF for DEN-based solutions under the *S1:Best-case* scenario.
- MVHR control strategy adjustments exhibited a strong impact on LCC savings.

Façade Design:

- A 50% reduction in north façade WWR strongly influenced LCC savings, emphasising the importance of passive design measures.

General Observations:

- S1 ASHP solutions demonstrate a relatively consistent LCCF after 2052, whilst other scenarios continue to increase beyond the building's lifespan, irrespective of design alternatives.
- Higher LCCF values were observed under the *S2:Worst-case* scenario, largely driven by a steep initial incline to 2030.
- Optimised parameters reoccurred across various scenarios, indicating that grid decarbonisation uncertainties can be incorporated into design solutions.

Chapter 5

Case Study 2

5.1 Overview

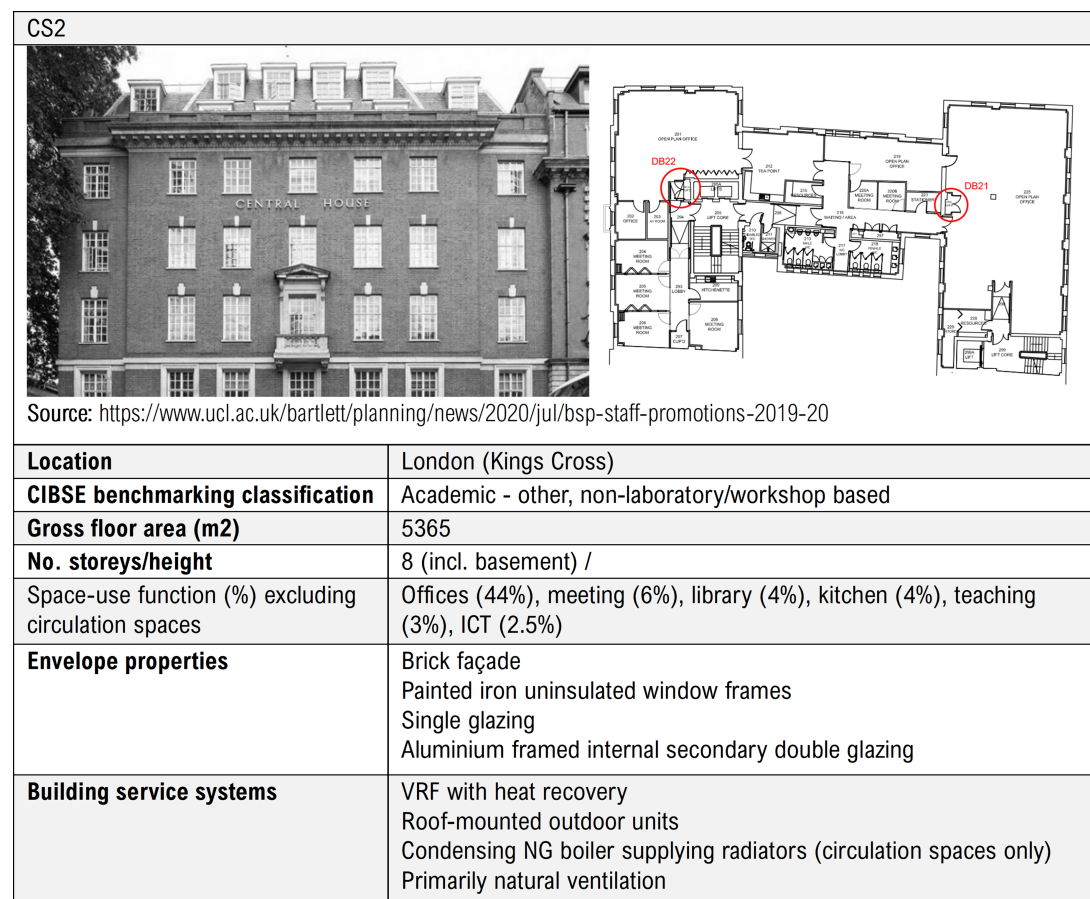


Figure 5.1: CS2 profile.

CS2: Post-Graduate Teaching and Offices

Refurbished in 2010, CS2 underwent internal retrofits to enhance the thermal insulation of its concrete and brick wall structure, whilst retaining original listed features, such as cast iron single glazed window frames. External walls were fitted internally with composite insulation boards, and secondary double glazing was installed inside existing single glazed windows. The building is primarily naturally ventilated, with heating and cooling provided by a VRF system, supplemented by a small contribution from a natural gas boiler (NGB) for some circulation spaces.

5.2 CS2: Model Development and Validation

5.2.1 Secondary Dataset Analysis

This section provides an overview of the data obtained from the sub-metering campaign and observations inferred from it's analysis, used to calibrate and validate the baseline building energy model.

Analysis of metered energy consumption and the detailed calibration and validation procedure for CS2 was the subject of prior research conducted by Jain et al. [175, 191]. As such, a succinct overview is provided here with further details available in the literature. A sub-metering campaign was carried out from August 2016 to July 2017, for which spatial and end-use disaggregated hourly electricity consumption data was available. This included separate metering of lighting and power, heating and cooling, and servers and lifts, by floor level. Since heating and cooling were supplied simultaneously to different building zones via the VRF system, it was not possible to further disaggregate these loads. Monthly energy consumption by end-use is depicted in Figure 5.2; heating and cooling, and lighting and power are the dominant energy end uses in the building. Operational-stage observations noted through analysis of the monitored dataset are summarised in Table 5.1, with further details available in [191].

Table 5.1: CS2 operational stage observations from sub-metering campaign.

Category	Observations
Occupancy profile	<ul style="list-style-type: none">• Monthly and seasonal occupancy variation based on term times• Higher out of hours use including weekends
HVAC operation	<ul style="list-style-type: none">• Systems operated throughout day and night, even during unoccupied periods• Non-functional AHU in the basement resulting in greater NV reliance• 2-3°C higher than typical set-point temperatures maintained
Lighting & power	<ul style="list-style-type: none">• High L+P baseload during unoccupied periods (~50%)

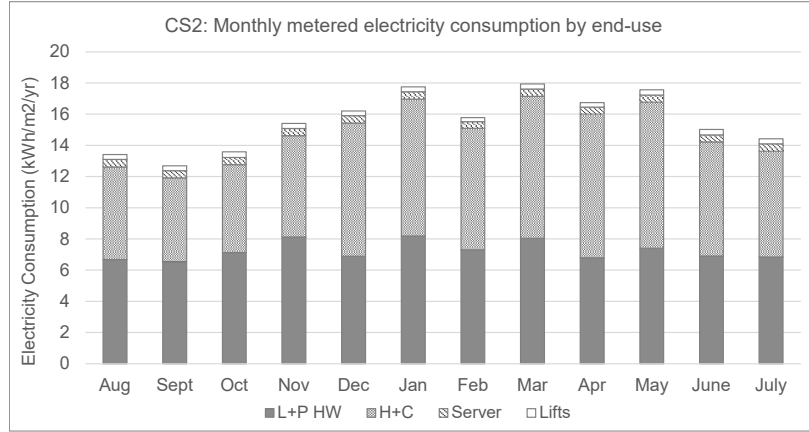


Figure 5.2: CS2: End-use disaggregated metered monthly electricity consumption data for Aug 2016 - Jul 2017.

5.2.2 Model development

The baseline model was developed according to specifications from available design-stage drawings, operation & maintenance manuals, on-site observations and stakeholder discussions. The predominant build-up consisted of external brick walls, fitted with composite board insulation during a recent refurbishment in 2010 to achieve an approximate U-value of $0.2 \text{ W/m}^2\text{K}$. Secondary double glazing was also installed on the inside of existing single glazed windows. An overview of the modelled constructions and their thermal properties is provided in Table 5.2. A baseline airtightness of $30 \text{ m}^3/\text{hr}/\text{m}^2 @ 50 \text{ Pa}$ was applied.

Table 5.2: CS2 primary constructions and thermal properties of existing building.

Construction	Description	Thickness (m)	U-value ($\text{W}/\text{m}^2\text{K}$)
External wall	200mm brick outer, 50mm air layer, 100mm brick, 10mm air gap, 40mm insulation board, 12mm plasterboard internal lining	0.412	0.20
External roof	10mm asphalt finish, 300mm cast concrete, 40mm insulation board, 12mm plasterboard	0.362	0.15
Internal partitions	25mm plasterboard, 25mm insulation, 25mm plasterboard	0.162	0.624
External glazing	Single glazed painted iron framing, aluminium-framed internal secondary glazing	-	1.40

In response to the dataset observations summarised in Table 5.1, the following updates were made to the baseline model.

- Occupancy, lighting and equipment schedules were updated to reflect term time monthly and seasonal variations.
- Lighting and equipment baseloads were increased by $\sim 60\%$ and $\sim 35\%$ respectively.

- Temperature set-point schedules were increased based on average monitored occupied and non-occupied zone temperatures.
- System and window operations were modified in response to the non-operational basement air-handling unit.

Detailed **HVAC** modelling incorporated the supply of heating and cooling to all main zones via **VRF** units. Plant was modelled as available 24/7 in line with evidence of out-of-hour system operation, as indicated by the sub-metered heating and cooling system energy data. Heating set-point (**SP**) temperatures were set to 23°C during occupied periods and 21°C during unoccupied periods. Heating was supplied to circulation areas via radiators, provided by two condensing boilers. The relative associated loads were very low by comparison to total building energy use and since granular metered data was not available for gas use, these were not assessed in the calibration process.

5.2.3 Calibration Results

The various sub-metering groupings are presented in Table 5.3, alongside monthly calibration results using 2016-17 weather data. Compliance with ASHRAE Guideline 14 criteria, which necessitates monthly **CVRMSE** to remain below 15% and **NMBE** within $\pm 5\%$, was achieved for lighting and power and hot water at each individual floor level. For other end uses, results were calibrated at the building-level. These findings demonstrate that the calibrated model sufficiently meets the ASHRAE Guideline 14 criteria, indicating a close proximity between monthly metered and simulated outputs.

Table 5.3: Calibration results for CS2. Target monthly validation criteria: $C_v(\text{RMSE})$ 15%, $\text{NMBE} \pm 5\%$ [176].

Level	End Use	$C_v(\text{RMSE})(\%)$	$\text{NMBE}(\%)$
Basement	L+P HW Ext	7.38	-3.83
Ground	L+P HW	12.53	-5.45
First	L+P HW	9.36	-3.84
Second	L+P HW	7.35	-4.06
Third	L+P HW	8.53	-4.19
Fourth	L+P HW	6.95	-1.22
Fifth	L+P HW	6.34	-3.65
Sixth	L+P HW	6.58	0.32
Building	H+C	4.16	-0.32
Building	Server	5.07	4.76
Building	Lift	0.02	-0.01

5.3 CS2: Framework Development

This chapter presents outputs from the implementation of various stages of the life-cycle optimisation framework on CS2 (outlined in Figure 3.8). Firstly, the included sub-set of ECMs are summarised. Normalised FU LCA calculation results are then presented for the refined ECM solution set and integrated into the NSGA-II GA. Section 5.4.1 discusses the life-cycle optimisation results for a single scenario. Finally, outputs are compared to findings from alternative grid decarbonisation and cost scenarios.

5.3.1 ECM selection

The final solution set included in the GA optimisation process is presented in Table 5.4. As a result of preliminary testing, the number of possible solution combinations reduced from 424,673,280 to 36,126,720. Details relating to CS2-specific ECMs are described in this section.

Table 5.4: Assigning genes and variable alterantives for implementation into the multi-objective optimisation framework.

Gene	Variable	Metric	CS2 Variants
x1.	Glazing U-value	W/m ² K	3, 1.5, 0.8
x2.	g-value	SHGC	0.4, 0.3
x3.	N-glazing area	%	0, -50
x4.	S-glazing area	%	0, -50, -30, +30
x5.	E-glazing area	%	0, -50, -30, +30
x6.	W-glazing area	%	0, -50, -30, +30
x7.	S-louvre	D/H ratio	0, 0.4, 0.6, 0.8
x8.	E-louvre	D/H ratio	0, 0.2, 0.4, 0.6
x9.	W-louvre	D/H ratio	0, 0.2, 0.4, 0.6
x10.	Wall Insulation (MW)	mm	0, 50, 80, 120
x11.	Roof Insulation (XPS)	mm	0, 120, 150, 180
x12.	Frame U-value	W/m ² K	9.5, 0.549, 0.287
x13.	Infiltration Rate	m ³ /(m ² .h)@50Pa	30, 7, 2
x14.	NV control	-	None, dT, nightpurge
x15.	HVAC system	-	VRF, ASHP
x16.	MVHR control	-	None, 7-19 weekdays, nightcycle, weekends

HVAC System Alternatives

HVAC system alternatives included in the optimisation framework consisted of the existing baseline VRF system and an ASHP alternative. Since both mechanisms operate in a similar way, based on refrigerant cycles, it was assumed that both heating and cooling will also be supplied by the ASHP, via the same distribution piping network. The presence of a NGB to accompany the VRF system was

retained for the baseline model. For the [ASHP](#), it was assumed that the [NGB](#) will be replaced with the [ASHP](#), to serve radiators in WCs and circulation spaces.

MVHR System and Controls

[MVHR](#) was not present in the existing building, with the exception of intended servicing to the lower ground floor. Since the basement air-handling unit was non-operational, the baseline was modelled as naturally ventilated only. Alternative scenarios assumed the addition of an [MVHR](#) system to supply mechanical ventilation at the zone-level via fan coil unit (FCU)s. [MVHR](#) scheduling alternatives included weekday, nightpurge and weekend operation.

Frame Insulation and Infiltration Rates

To improve the thermal performance of the thermally-bridged iron window frames, 0.05m and 0.1m [PIR](#) insulation closers were added, as detailed in Appendix [H.2](#). This intervention reduced the frame U-value from 9.5 W/m².K to 0.549 W/m².K and 0.287 W/m².K, respectively. Estimated infiltration rates were interpolated from a field study on the airtightness of nineteenth-century buildings, acknowledging that heritage buildings are anticipated to have higher air leakage rates than current industry standards, even after window frame upgrades [192]. The [PIR](#) closers correlated to estimated decreases in infiltration rates from 30 m³/hr/m² @ 50 Pa to 7 m³/hr/m² @ 50 Pa and 2 m³/hr/m² @ 50 Pa.

Material Choices for Paneling and Louvres

Replacement panelling and louvre additions were assumed to be manufactured in wood to align with the material pallet of the building. This also allowed for the comparison of the favourability of these [ECMs](#) when a lower carbon alternative is opted for - when reporting biogenic carbon - versus the high-carbon aluminium additions to CS1.

5.3.2 Modelling Inputs: Carbon Calculations

Life-cycle **EC** emissions were calculated on a **FU** basis, accounting for the various life-cycle stages as specified in BS EN 15978:2011 [17]. For building fabric, the **FU** was 1m² of the respective build-up. Where **HVAC** related **EC** emissions were included, the **FU** adopted was 1 unit of the relevant equipment.

EC: Fabric

The **EC** emissions associated with CS2 primary building elements are detailed in Table 5.5. These values were determined using the **LCA** stages and calculation methodology outlined in section 3.3.6. As per the RICS Professional Standard [19], assumptions were made concerning the usual manufacturing location, waste rate, and expected lifespan of each building material. All values in Table 5.5 are presented with respect to a functional unit of 1m² equivalent surface area of the relevant building material. For a comprehensive overview of **LCA** assumptions and results, along with the sources utilised to formulate these assumptions, please refer to Appendices F.4 and D.

Element	FU	Build-up	Volume/FU (m ³ /FU)	Manu- facture (L/N/E)	Waste rate (%)	Lifespan (yrs)	EC excl. biogenic (kgCO _{2e} /FU)	Biogenic (kgCO _{2e} /FU)	Total EC incl. biogenic (kgCO _{2e} /FU)
Roof	m ²	Asphalt finish	0.010	L	5	30	5.37	0.00	222.06-242.90
		RC cast concrete	0.300	L	5	75	112.45	0.00	
		Reinforcement mesh	0.003	N	15	75	44.07	0.00	
		EPS insulation	0.040	N	5	40	11.43	0.00	
		+/-XPS insulation	0.120-0.180	N	5	40	41.68-62.52	0.00	
		Plasterboard soffit	0.012	N	5	30	7.06	0.00	
External Wall	m ²	Brick and mortar	0.200	N	20	75	120.45	0.00	213.99-231.56
		Stainless steel brickties	1.2E-06	N	3	75	0.04	0.00	
		Brick and mortar	0.100	N	20	75	60.31	0.00	
		MW insulation	0.040	N	15	75	8.68	0.00	
		+/- MW insulation	0.050-0.120	N	15	75	10.85-26.04	0.00	
		+/-Gypframe	0.000	N	3	75	6.75-9.13	0.00	
		Gypsum plasterboard	0.012	N	5	30	6.91	0.00	
Spandrel panel	m ²	Timber cladding	0.026	E	5	30	59.25	-43.27	70.53
		MW insulation	0.170	N	15	75	36.89	0.00	
		Gypsum plasterboard	0.025	N	22.5	30	17.66	0.00	
Single glazing + secondary	m ²	-	0.003	E	5	40	25.31	0.00	25.31
Double glazing	m ²	-	0.003	E	5	40	24.72	0.00	24.72
Triple glazing	m ²	-	0.003	E	5	40	26.38	0.00	26.38
PIR closer	m ²	PIR insulation	0.05-0.1	N	15	75	12.56-25.12	0.00	35.67-48.23
		Gypsum plasterboard	0.039	N	5	30	23.11	0.00	
Louvre	m ²	Timber	0.05	E	1	30	109.34	-79.85	29.49

Table 5.5: Calculated EC of construction elements for CS2, including materials, volume per FU, assumptions impacting the calculations, and total EC for each element. Items shown in red are interventions. Waste rates obtained from [163]; expected lifespan from [77, 19]. Manufacture location: Local (L), National (N), European (E).

Since double and triple glazing casement units in non-residential applications typically incorporate aluminium window frames, it is assumed that the EC associated with framing was kept the same irrespective of the glazing alternatives. With respect to the single glazed units, this EC refers to emissions associated with the existing aluminium framed internal secondary glazing. The original, heritage painted cast iron window frame is assumed to be retained and thus no replacement cycles are included. Since frame EC was kept the same across scenarios, differences in the EC contribution of glazing alternatives were driven by the emissions associated with the glass panels. For single with secondary double glazing, this consisted of one pane of 3 mm glass to account for the internal glazed panel, with an ICE V3 value of 1.44 kgCO₂e/kg, compared to 1.63 kgCO₂e/kg and 1.75 kgCO₂e/kg for double and triple glazing respectively [59].

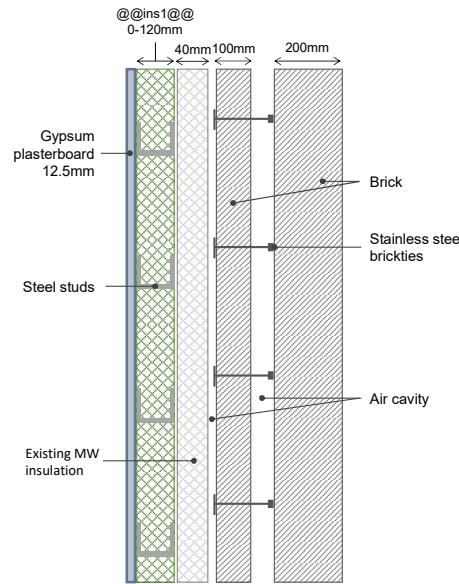


Figure 5.3: Assembly section: CS2 external wall build-up demonstrating the position of additional internal MW insulation (@@ins1@@).

The modelled external wall build-up is depicted in Figure 5.3, aligning with the baseline U-values specified in architectural plans, and typical materials as guided by industry standards [179]. Insulation and gypframe additions to the external wall were included in varying thicknesses of 0, 50, 80, 120mm and positioned internally to the existing insulation layer. Typical sizing, frequencies and spacing of metal elements were established through expert elicitation.

EC: Systems

The EC of the existing VRF system serving CS2 was calculated following a similar protocol as that in section 4.3.3. The overall procedure followed the life-cycle stages used for all other building materials, described in section 3.3.6. However, additional stages were incorporated to account for ‘in-use emissions’ (B1) and

‘refrigerant disposal’ (CSR) [19]. These stages reflect the substantial carbon emissions associated with refrigerant leakage during the use and end-of-life phases respectively [55]. A strong positive correlation between VRF system mass and rated capacity was established through manufacturers’ specifications ($R^2=0.84$) (see Appendix F). A1-A3 emissions associated with VRF material manufacture were extrapolated on this basis to achieve the industrial-scale rated capacity requirements for CS2. Refrigerant mass was also extrapolated from the linear correlation with system mass ($R^2=0.96$), shown in Figure 5.4b. The key differences in life-cycle calculation assumptions between ASHP and VRF systems are presented in Table 5.6, with further information on the selection of these inputs detailed in section 4.3.3. Note, EC associated with ASHP and VRF distribution pipe networks were not included in the calculation, as it was assumed that any minor discrepancies would have negligible impact on the optimisation process.

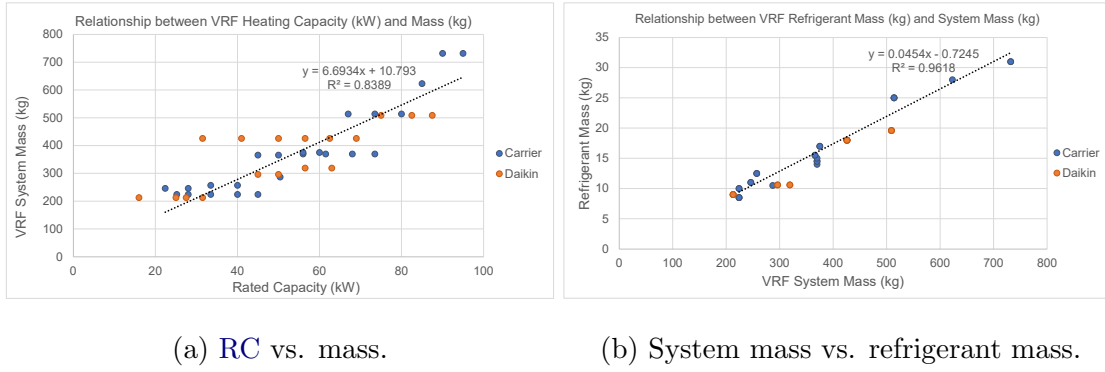


Figure 5.4: Correlation between RC, mass and refrigerant mass established from literature and VRF specifications by manufacturers Carrier and Daikin [193, 194].

Table 5.6: EC calculation assumptions for ASHP versus VRF, obtained from literature, manufacturers’ specifications and government guidelines [189, 195, 196].

System type	ASHP	VRF
FU	unit	unit
Manufacture	E	E
Expected lifespan	22 yrs	22 yrs
Refrigerant type	R-32	R-32
In-use refrigerant leakage rate	3.8% per yr	6% per yr
Refrigerant EOL recovery rate	98%	90%
GWP	675	675
Material recovery rate	96%	96%
Nominal COP	3.2	4.1

Natural Gas Boiler (NGB)

The EC of existing boiler replacement cycles were included in the baseline HVAC model, serving radiators in WCs and circulation spaces only. The calculations

followed the same methodology as that for [ASHP](#) and [VRF](#) systems. A1-A3 manufacturing emissions were scaled up from values obtained from literature, based on the simulated [NGB](#) rated capacity [55]. A strong positive linear correlation between system rated capacity and mass was observed from manufacturers' specifications ($R^2=0.91$), used to obtain values for additional life-cycle stages. Further details relating to the [NGB](#) carbon calculation assumptions can be found in Appendix [F.1](#). It should be noted that the relative contribution of the [NGB](#) system is minor in comparison to the refrigerant-based systems previously discussed, which supply heat to the majority of zones.

MVHR

The [EC](#) of the [MVHR](#) systems deployed in non-circulation spaces also followed the same EN 15978 guidance [17]. Manufacturers' specifications were scaled to meet commercial-scale requirements with a simulated design volumetric air flow rate of 14,690 m³/h (including a 10% safety factor). This was assumed to require scaled-out operation, with [EC](#) assumptions relating to three separate units, each with a maximum air flow rate of 4950 m³/h, as per available manufacturers' specifications [197]. Materials were scaled by weight to meet the 625 kg per unit estimation. Since existing ventilation duct-work serves basement zones only, the carbon associated with implementation of new duct-work was also approximated based on the design floor area. The [EC](#) related to duct-work manufacture and installation to serve approximately 4,105 m² conditioned internal area was scaled up from equivalent residential systems [198]. Assumptions include a single replacement cycle over a 50-year lifespan for PVC ductwork, and a recovery rate calculated based on materials weight-to-weight ratios. Drawing from ProAir's [EPDs](#), the study assumes 100% recycling of metals, plastics, aligning with assumptions from RICS guidance [77, 19, 198]. Further details are provided in Appendix [F.3](#).

OC emissions

[OC](#) emission pathways aligned with the grid electric and natural gas carbon emission factor pathways described in section 3.3.7. Both [VRF](#) and [ASHP](#) systems adopted the same electricity carbon emission factor pathways.

5.3.3 Modelling Inputs: Cost Calculations

CapEx

The [LCC](#) of various building components are summarised in Table 5.7, calculated following the ISO 15686-5:2017 protocol described in section 3.3.6 [18]. Costs for glazing include aluminium framed casement units; for single glazing, respective costs are attributed to the replacement of the aluminium framed internal secondary glazing. Double and triple glazing price ranges reflect adjustments for [SHGC](#) values from 0.4 to 0.3. All values were interpolated based on available data [167];

more extensive details of interpolations, including material and labour costs, are provided in F.6, F.7, F.9.

Element	FU	Build-up	Volume/FU (m ³ /FU)	Total Rate (£)	Replacement (yrs)	NPV- adjusted cost (£)	LCC (£)	Total LCC (£)
Roof	m ²	Asphalt finish	0.010	25.56	30	10.53	36.09	420.49-453.27
		RC cast concrete	0.300	142.21	-	142.21	284.42	
		Reinforcement mesh	0.003	-	-	-	-	
		EPS insulation	0.040	17.79	40	5.45	23.24	
		+/-XPS insulation	0.120-0.180	32.24-57.33	40	9.88-17.58	42.13-74.91	
External Wall	m ²	Plasterboard soffit	0.012	24.51	30	10.10	34.61	27154-276.19
		Brick and mortar	0.200	131.77	-	-	131.77	
		Stainless steel brickties	1.2E-06	1.85	-	-	1.85	
		Brick and mortar	0.100	90.87	-	-	90.87	
		MW insulation	0.040	4.03	-	-	4.03	
		+/- MW insulation	0.050-0.120	4.79-8.17	-	-	4.79-8.17	
		+/-Gypframe	0.000	3.62-4.89	-	-	3.62-4.89	
Spandrel panel	m ²	Gypsum plasterboard	0.0120	24.51	30	10.10	34.61	195.79
		Timber cladding	0.026	113.81	30	46.89	160.70	
		MW insulation	0.170	10.58	-	-	10.58	
Secondary glazing	m ²	Gypsum plasterboard	0.025	24.51	30	10.10	24.51	522.62
		Secondary glazing aluminium frame	-	400.00	40	122.62	522.62	
Double glazing	m ²	Double glazed casement aluminium window frame	-	609.07-652.06	40	186.71-199.89	795.78-851.95	795.78-851.95
Triple glazing	m ²	Triple glazed casement aluminium window frame	-	812.51-855.50	40	249.08-262.26	1061.59-1117.76	1061.59-1117.76
PIR closer	m ²	PIR insulation	0.05-0.10	43.56	-	-	43.56-52.25	152.23-160.92
		Gypsum plasterboard	0.0393	76.96	30	31.71	108.67	
Louvre	m ²	Timber	0.05	109.50	30	45.11	154.61	154.61

(a) Fabric

Element	FU	Total Rate (£)	Replacement (yrs)	NPV- adjusted cost (£)	Total LCC (£)
VRF	67 kW* unit	18,803	20, 40	16,175	34,978
ASHP	64 kW* unit	34,663	22, 44	29,208	63,871
NGB	19 kW* unit	2,471	22, 44	2,082	4,552
MVHR	14,690 m ³ /h unit	26,464	20, 40	22,765	49,230

(b) Systems *Extrapolated according to calculated rated capacity from each simulation run. Systems in black are present in the existing building.

Table 5.7: Calculated CapEx of construction elements for CS2, including materials, volume per FU and replacement costs. Items shown in red are interventions. Expected lifespan from [77, 19].

OpEx

Fuel price pathways followed the fluctuating fuel price assumptions outlined in section 3.3.7.

5.4 CS2: Framework Implementation

5.4.1 Life-cycle optimisation results

This section presents CS2 results of the life-cycle optimisation process for the ‘S1:Best-case’ scenario, described in chapter 3.3.7. Alternative decarbonisation pathways are explored in the following section 5.4.2.

Pareto Optimal Solutions

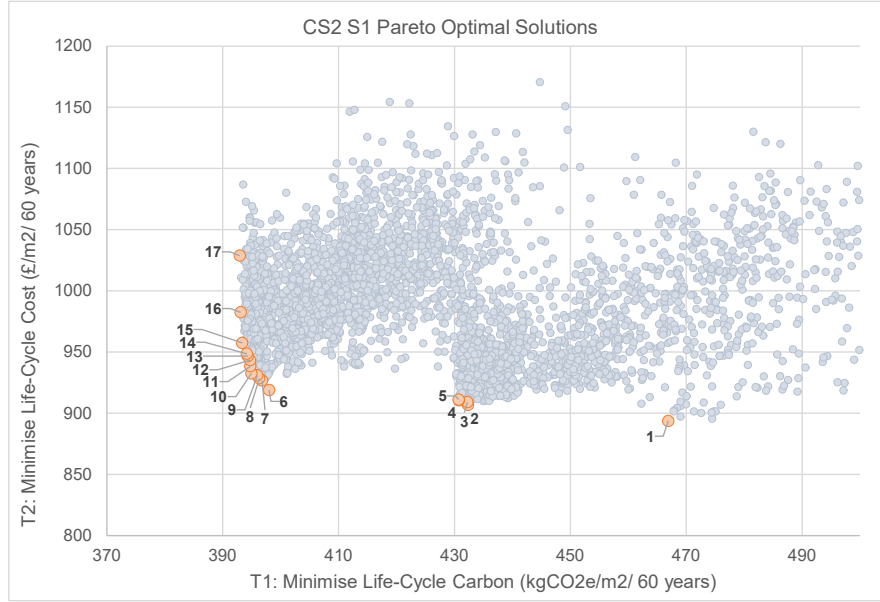
Characteristics of the pareto optimal solution set are shown in Table 5.5b, alongside LCCF and LCC values. The pareto front ranged from 894-1029 £/m² for LCC and from 393-467 kgCO₂e/m² for LCCF over the 60 year time frame. Two separate regions of the search space relating to the heating system alternatives can still be observed, albeit representing less distinct regions than those in CS1 and CS3. The LCCF of the VRF pareto group is on average 37.9 kgCO₂e/m² (+10%) greater than that of the ASHP. The differentiation between heating systems in terms of LCC is less apparent upon visual inspection, with an observable overlap between pareto solutions from different groups. Despite the relatively weak magnitude of impact of SHGC on LCCF and LCC, a preference for the lower SHGC value of 0.3 is seen across 88% of solutions. A reduction in WWR of 50% was most common amongst pareto solutions, particularly on the South, East and West facades. A variety of louvre D/h geometries were present. The use of MVHR weekday operation with NV deltaT appeared in almost all pareto optimal solutions when aligned with the VRF heating strategy. However, under ASHP operation, the implementation of MVHR was not present in any optimal solution.

Relative Impact of Variables on LCCF and LCC

The relative impact of independent ECM variables on LCCF and LCC was assessed through linear regression analysis. Aggregation of unstandardised linear model coefficients across each level within a categorical variable resulted in overall weighted coefficients (β), serving as a measure of the relative impact of changes in design parameters. The weighted coefficients for each variable are shown in Figure 5.6.

Heating System (P0)

The heating system appeared to be a significant predictor of both LCCF and LCC. Compared to VRF systems, ASHPs exhibited a notably lower carbon footprint, as evidenced by the negative weighted coefficient (β : -38.7), relative to the baseline. Both heating sources can be characterised as having high efficiencies (nominal COP: 3.2-4.1), with refrigerant leakage and recovery rates being the key determinant of LCCF differentiation. The lower ASHP emissions were associated with an increase in LCC (β : +10.3). The results suggest that buildings equipped



(a) Optimised LCCF and LCC values.

#	Heating System	Glazing Type	SHGC	North WWR	South WWR	South Louvre D/H	East WWR	East Louvre D/H	West WWR	West Louvre D/H	IWI Ins. mm	Roof Ins. mm	Frame U-value W/m ² .K	Infiltr. Rate ACH	MVHR Control Strategy	NV Control Strategy
1	VRF	Double	0.3	-50%	-50%	0.6	-50%	0	-50%	0.2	0	0	0.287	0.1	No MVHR	Nightpurge
2	VRF	Single	0.4	0%	-50%	0	-50%	0	-50%	0.4	0	0	0.287	0.1	Weekday	deltaT
3	VRF	Single	0.3	0%	-50%	0	-50%	0	-50%	0.2	0	0	0.287	0.1	Weekday	deltaT
4	VRF	Double	0.3	-50%	-50%	0.4	-50%	0	-50%	0	0	0	0.287	0.1	Weekday	deltaT
5	VRF	Double	0.3	-50%	-50%	0	-50%	0	-50%	0.4	0	0	0.287	0.1	Weekday	deltaT
6	ASHP	Single	0.3	0%	0%	0	0%	0	0%	0.2	0	0	0.287	0.1	No MVHR	Nightpurge
7	ASHP	Single	0.3	0%	0%	0.4	-50%	0	0%	0	0	0	0.287	0.1	No MVHR	Nightpurge
8	ASHP	Single	0.3	0%	-50%	0.6	-50%	0	-50%	0	0	0	0.287	0.1	No MVHR	Nightpurge
9	ASHP	Double	0.4	-50%	-50%	0.4	-50%	0	-50%	0	0	0	0.287	0.1	No MVHR	Nightpurge
10	ASHP	Double	0.3	-50%	-50%	0.4	-50%	0	-50%	0	0	0	0.287	0.1	No MVHR	Nightpurge
11	ASHP	Single	0.3	0%	-50%	0	-50%	0	-50%	0	0	0	0.287	0.1	Weekday	Baseline
12	ASHP	Single	0.3	0%	-30%	0.4	-50%	0.6	-50%	0.2	0	0	0.287	0.1	Weekday	Baseline
13	ASHP	Double	0.3	-50%	-50%	0.4	-50%	0.2	-50%	0	0	0	0.287	0.1	Weekday	Baseline
14	ASHP	Double	0.3	-50%	-30%	0	-50%	0.2	-50%	0	0	0	0.287	0.1	Weekday	Baseline
15	ASHP	Double	0.3	-50%	30%	0	-50%	0.4	-50%	0	0	0	0.287	0.1	Weekday	Baseline
16	ASHP	Single	0.3	0%	30%	0	-50%	0	30%	0	0	0	0.287	0.1	Weekday	Baseline
17	ASHP	Triple	0.3	0%	30%	0.4	-50%	0	30%	0	0	0	0.287	0.1	No MVHR	Nightpurge

(b) Parameters of optimised solution set for CS2.

Figure 5.5: NSGA-ii optimisation results for CS2 scenario 1.

Variable		Variable	
P0	Heating System	P6	West-WWR D/H Ratio
P1	Glazing Type	P7	Internal Wall Insulation
P2	SHGC	P8	Roof Insulation
P3	North-WWR	P9	Frame U-value Infiltration Rate
P4	South-WWR D/H Ratio	P10	MVHR NV Operation
P5	East-WWR D/H Ratio		

(a) Categorical variables.

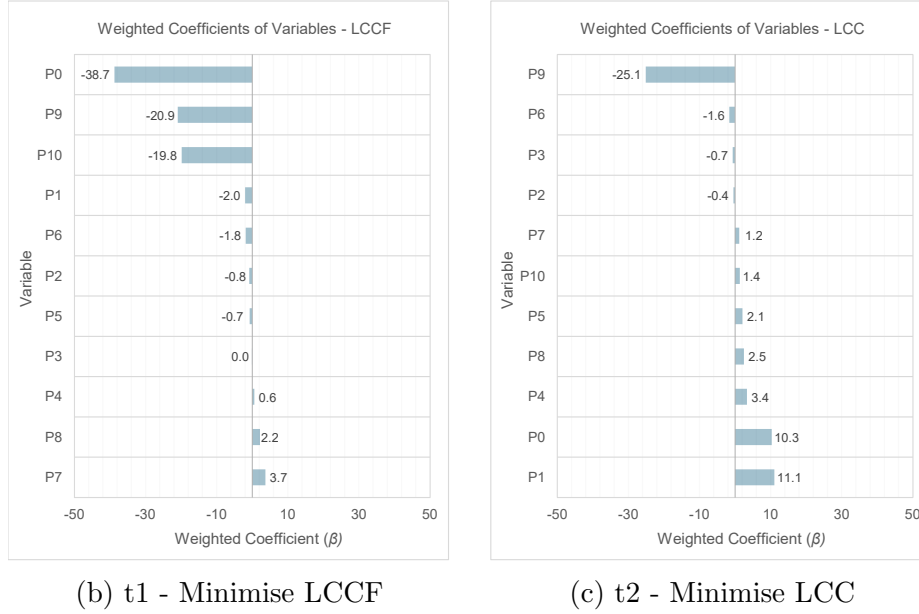


Figure 5.6: Weighted coefficients (β) of categorical variables in linear regression analysis for Scenario 1.

with [ASHP](#) systems contribute less to overall carbon emissions compared to those relying on [VRF](#) technology, but may incur greater costs over the building's life-cycle.

Glazing Type (P1, P2)

Glazing type also demonstrated a significant impact on both t1 and t2, although the magnitude of the coefficients varied. Transitioning from single (with secondary glazing) to double or triple-glazed windows led to a significant reduction in carbon emissions (β : -2.0) and increase in model predicted [LCC](#) (β : +11.1). The size of this impact was greater upon implementation of triple glazing over double glazing (see [Appendix J.1](#)), with respect to both [LCCF](#) and [LCC](#). However, the magnitude of impact on carbon savings suggests a relatively smaller influence compared to other factors. A decrease in [SHGC](#) from 0.4 to 0.3 had a marginal negative impact on both metrics, indicating that associated upfront carbon and costs were typically offset over the 60 year timeframe.

WWR | Louvre D/H Ratio (P3-P6)

Alterations in WWR and louvre D/H ratios showcased varying effects on both t1 and t2. Overall, these variables presented relatively nuanced impacts (LCCF β : -1.8 to +0.6; LCC β : -1.6 to +3.4), with some configurations leading to reductions and others to increases in carbon emissions and costs. Amongst these alternatives, the model indicates that 50% reduction in West facade glazing combined with West louvre 0.4 D/h ratio had the greatest significant impact on LCCF reduction. The magnitude of their coefficients indicates relatively modest contributions (see Appendix J.1), which may be substantial upon optimisation across all facade orientations. A 50% reduction in WWR on the East and West facades had the greatest impact across geometry alternatives, irrespective of associated D/H ratios.

Insulation Thickness (P7, P8)

By contrast, the addition of internal insulation to the external wall and roof resulted in significant positive correlations to both LCCF and LCC, indicating that the carbon and cost value of further additions to building envelope insulation were either ineffectual or counter-effective. For example, a comparison of two identical solutions with +80 mm and without IWI additions demonstrates the offset of OC savings (-4.8 kgCO₂e/m²) by the associated EC (+12.6 kgCO₂e/m²). Similarly, operating cost reductions (-4.2 £/m²) were outweighed by upfront costs of 5.2 £/m², indicating a limited benefit to insulation beyond that included in the existing build-up, with a U-value of 0.2 W/m².K.

Frame U-value | Infiltration Rate (P9)

The addition of PIR insulation closers to the cast iron window frame resulted in a significant reduction in both LCCF (β : -20.9) and LCC (β : -25.1), indicating that the EC and CapEx associated with the frame upgrades are substantially offset by OC savings. The most pronounced impact was observed under the highest insulation level of 100 mm, achieving a frame U-value of 0.287 W/m².K and infiltration rate of 0.1 ACH. This suggests that upgrading the window frames could yield significant financial and environmental benefits, although potential conflicts with listed building regulations should be considered.

Ventilation Strategy (P10)

Whilst the overall impact of ventilation strategies represented a large decrease in LCCF (β : -19.8) for marginal increases in LCC (β : +1.4), the magnitude of this impact was largely dependent on the NV and MVHR strategy combination. The operation of MVHR during weekday occupied hours, compounded with deltaT NV had the greatest magnitude of impact on LCCF reduction relative to the baseline (B: -43.3), and also resulted in a significant decrease in LCC (B: -23.9), indicating that the CapEx associated with MVHR implementation was sufficiently offset by

reductions in OpEx. MVHR weekend operation with deltaT NV offered the second lowest LCCF alternative (B: -19.3), as shown in Appendix J.1.

5.4.2 Scenario analysis

This section compares results from the ‘grid-average’ scenario (S1) presented in the previous section, with those from alternative decarbonisation pathways described in Table 5.8 and section 3.3.7.

Table 5.8: Summary of grid decarbonisation rate scenario alternatives; both S1 and S2 adopt the fluctuating fuel price pathways described in section 3.3.7.

Scenario Description	
S1	‘Best-case’: Electric grid carbon emissions decline rapidly from 2020 to 2030, plateauing at 2033.
S2	‘Worst-case’: BAU; incline in electric grid carbon emissions until 2025, thereafter declining gradually towards a plateau at 2042.

LCCF and LCC optimisation results for S1 and S2 are shown in Figure 5.7. For pareto optimal design interventions relying on the existing VRF and NGB systems, LCCF ranged from 426 kgCO₂e/m² to 774 kgCO₂e/m² across decarbonisation scenarios, with an average increase by a factor of 1.6 (+269 kgCO₂e/m²) from S1 to S2. Across ASHP solutions, LCCF values ranged from 395 kgCO₂e/m² to 747 kgCO₂e/m², with a slightly greater average relative increase between scenarios (x1.8). In S1, ASHP based solutions offered a lower LCCF alternative to VRF, despite a 17% increase in operational energy loads, driven by lower refrigerant-related emissions and the absence of gas-based technologies. The difference in LCCF between heating system alternatives is more substantial in S1 than S2, under a lower electricity CEF scenario, since the relative proportion of refrigerant emissions to overall LCCF is considerably higher (see section 5.4.2). In addition, greater differentiation between electricity and gas CEFs under a more optimistic energy outlook (S1) (as outlined in section 3.3.7) leads to a larger share of NGB OC emissions to overall LCCF, although this impact is marginal by comparison.

Whilst the impact of heating system alternatives remains the predominant driver of LCCF in S1, for S2, wider variances can be observed across pareto alternatives within each group than between ASHP and VRF solution sets. Intra-group variances in LCCF appeared to be largely impacted by the ventilation strategies adopted; variances are minimal in ‘S1 ASHP’ when ventilation strategies are consistent across all pareto solutions, whereas mixed ventilation control strategies led to wider ranges in EC and OC emissions. Pareto solutions with no MVHR and nightpurge ventilation controls resulted in approximately 3-7% (+23-49 kgCO₂e/m²) increase in LCCF compared to solutions with MVHR weekday operation and deltaT NV. Whilst the absence of MVHR led to lower EC emissions, this was off-set by increased electricity operational energy consumption and a greater reliance on NGB heating energy use as back-up during peak consumption periods. With respect to LCC, differences in average values from S1 to S2 of <10 £/m (1%) were observed, demonstrating minor discrepancies across optimal solution sets when the same fuel price projections were applied in both scenarios.

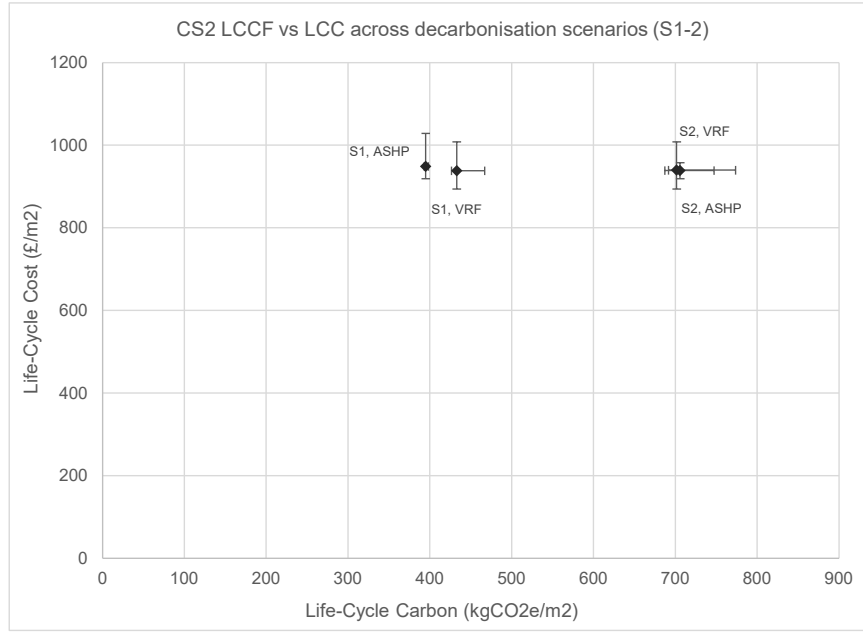


Figure 5.7: LCCF vs. LCC Comparison of pareto optimal solutions across decarbonisation scenarios. Points show group averages; error bars represent ranges.

Embodied vs. operational carbon emissions

The impact of grid decarbonisation and fuel price projections on the proportion of various **LCCF** components is depicted in Figure 5.8. Across all scenarios, **OC** accounts for a lower proportion of overall **LCCF** emissions (<65%) relative to values obtained from similar studies in the literature [76]. This reflects the implementation of electricity-based **VRF** and **ASHP** heating systems where, even under slower decarbonisation rates a much lower electricity **CEF** can be expected compared to the ‘2022 fixed’ value of 0.155 kgCO₂e/kWh (S2: 0.062 kgCO₂e/kWh, 60-yr average). Resulting **EC** emissions are estimated to account for approximately 60-68% of the refurbished building’s **LCCF** under the S1 ‘best-case’ scenario and 35-42% under the S2 ‘worst-case’ scenario.

Due to the high efficiency of both **VRF** and **ASHP** systems, lighting and power operational emissions account for a much greater proportion of overall **LCCF** relative to heating and cooling **OC** emissions. Since all main services are fueled by electricity, the ratio of each **OC** component changes proportionally under varying decarbonisation rates. With respect to **EC** emissions, the predominant driver across all solution sets is the emissions associated with the initial and recurring replacement of components on the external envelope, such as glazing. Services, which includes **EC** emissions related to **MVHR**, **NGB**, **VRF** and **ASHP** components, but largely driven by refrigerant leakage and **EOL** recovery, account for an average of 17% of the **LCCF** across **VRF** solutions and 7% across **ASHP** solutions.

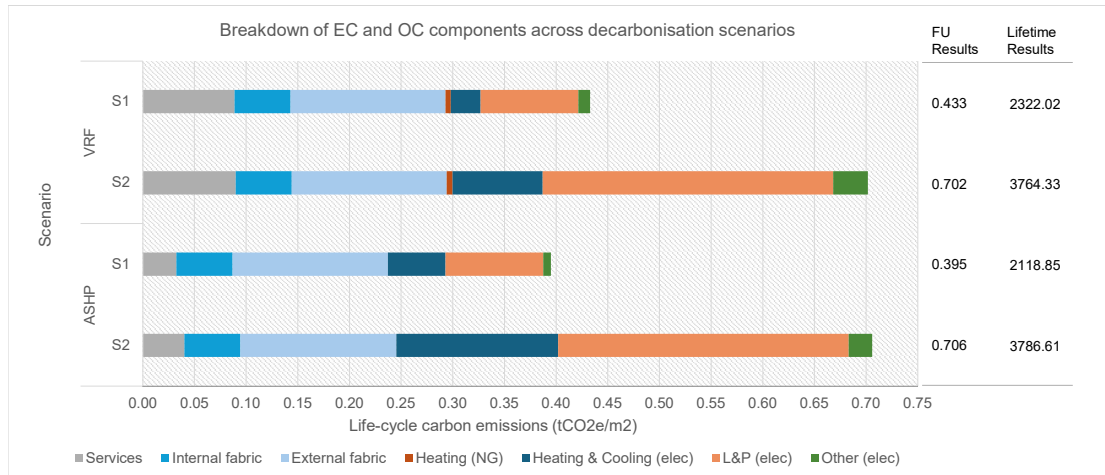


Figure 5.8: Average share of embodied versus operational carbon components across pareto solutions for scenarios 1 and 2.

Time-dependency of carbon impact

The aggregated year-on-year **LCCF** over the building's 60 year life-span is shown in Figure 5.9. A similar trend can be observed between pareto solutions relying on the baseline **VRF** and **NGB** systems and the replacement **ASHP**. The trends demonstrate steep positive trajectories until approximately 2033 and a step change at the 2052 time-point, reflecting the **EC** associated with the replacement of several building components, such as internal dry lining, partitions and spandrel panels. Minor step changes were also noted at 2044 and 2066, accounting for the replacement of the refrigerant based systems. These are slightly more pronounced across **VRF** solutions, due to the higher refrigerant mass and lower associated **EOL** recovery rate (90% vs. 98%). In addition, the higher expected in-use refrigerant leakage rate associated with **VRF** systems (6% vs. 3.8% per year) resulted in a greater incline across **VRF** solutions relative to **ASHP**.

Furthermore, a steeper incline can be observed amongst S2 solutions in comparison to S1, particularly until 2030, reflecting the slower rate of electricity decarbonisation. Across S1 **ASHP** solutions, a relatively consistent year on year impact can be observed from 2052, indicating that **LCCF** can be expected to be relatively stable by the end of the building's lifespan, with exceptions to step changes relating to replacement cycles. For all other scenarios, the annual carbon intensity of CS2 continues to increase beyond the building's life-span, irrespective of design alternatives.

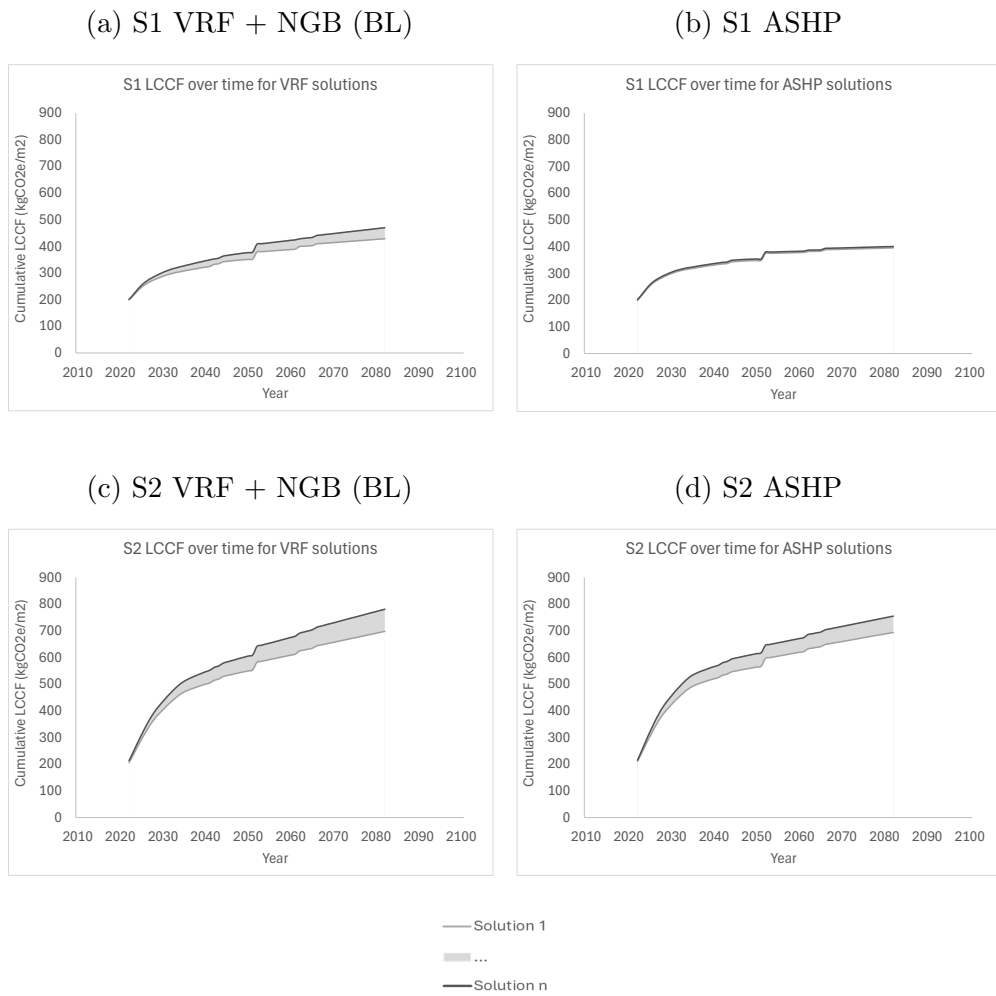


Figure 5.9: CS2 change in LCCF of pareto optimal solutions over time for scenario 1 and 2.

CS2 Chapter Summary

This case study examines an office **HE** building typology, refurbished in 2010, featuring a mix of retrofitted thermal upgrades and preserved listed architectural features. The space functions primarily as office areas. Results indicate how a range of design interventions, including heating, ventilation, and façade strategies, perform under diverse grid decarbonisation scenarios, focusing on optimising life-cycle cost and life-cycle carbon performance. The following observations were made:

Heating Strategies:

- Heating system type emerged as a key determinant of **LCCF**, particularly under the *S1:Best-case* scenario.
- **ASHP** solutions achieved lower **LCCF** values than the **VRF** baseline, despite higher operational energy loads, due to reduced refrigerant-related emissions and reliance on gas-based technologies.
- Services accounted for a considerable proportion of **EC** emissions, due to refrigerant leakage and end-of-life recovery.
- *S1 ASHP* solutions demonstrate a relatively consistent **LCCF** after 2052, whilst other scenarios continue to increase beyond the building's lifespan, irrespective of design alternatives.

Ventilation Strategies:

- Ventilation strategies, including airtightness measures, had a notable influence on **LCCF**, following heating systems as a key determinant of carbon reduction.
- Updating ventilation strategies (P10) was among the most impactful measures for reducing **LCCF** under *S1:Best-case*.

Façade Design:

- Window frame upgrades (P9) exhibited a strong impact on both **LCCF** and **LCC** savings, emphasising the importance of targeted façade improvements.

General Observations:

- The higher **LCCF** values observed under the *S2:Worst-case* scenario, relative to *S1*, were largely driven by a steep emissions incline to 2030.
- The relative contribution of **EC** to overall **LCCF** was high compared to studies found in literature, owing to the implementation of electricity-based heating systems and the quantification of grid-decarbonisation.

Chapter 6

Case Study 3

6.1 Overview

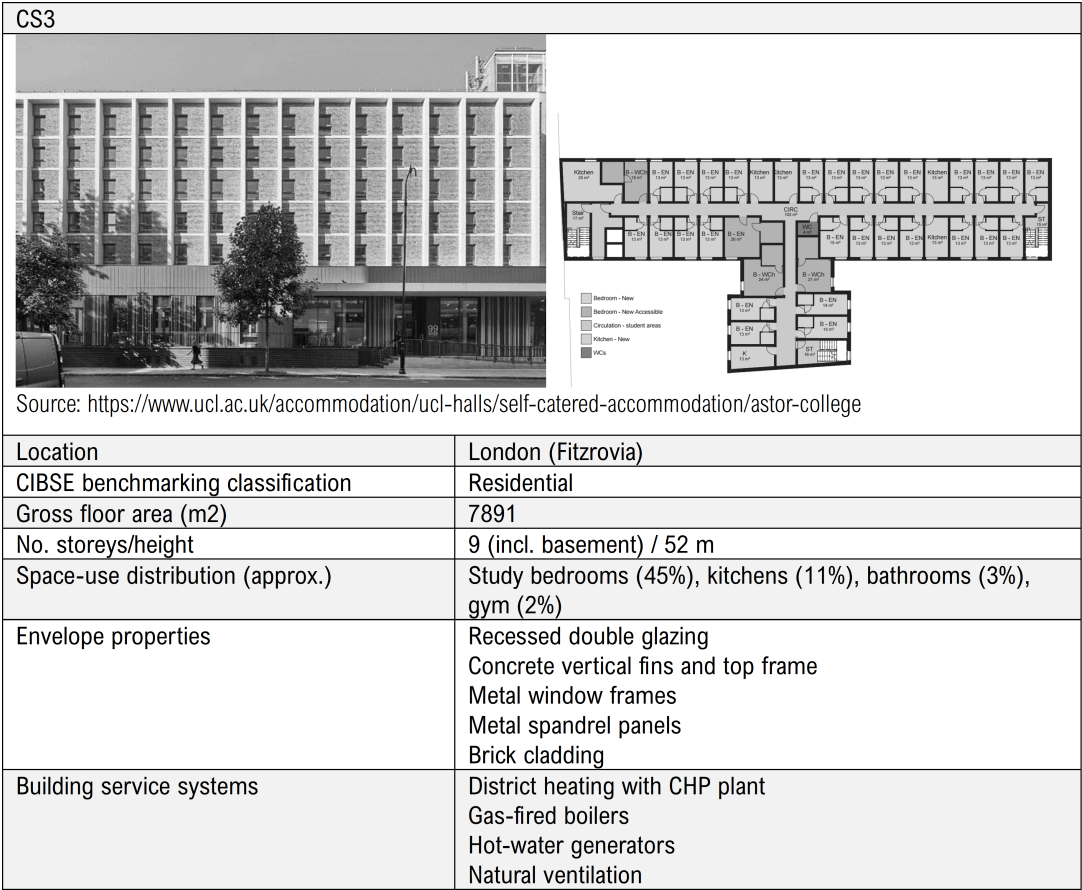


Figure 6.1: CS3 profile.

CS3: Student Accommodation

Refurbished in 2019, CS3 also experienced a significant expansion in floor area, leading to a substantial rise in the number of bedrooms provided, with a greater proportion of en-suite rooms. The refurbishment included the installation of metal windows and spandrel panels, as well as the addition of an insulated brick slip facade. Ceramic cladding, concrete vertical fins, and topframe components were also incorporated into the building's exterior. Primarily naturally ventilated, CS3 relies on natural gas boilers for heating and domestic hot water, with some boilers retained from the pre-refurbishment building as they were not yet at the end of their service life. The building does not provide mechanical cooling.

6.2 CS3: Model Development and Validation

6.2.1 Secondary Dataset Analysis

This section presents the pre-processing steps taken to prepare the secondary energy consumption datasets for use in model development and calibration.

A preliminary examination was carried out on the secondary dataset to evaluate data accuracy, replace missing data points, and address non-typical consumption and usage trends. Measured monthly energy consumption was obtained for an annual period from 2021-2022, following the completion of refurbishment construction works in 2019.

Data Analysis and Cleaning: Electric Loads

Based on the quality of raw hourly electricity consumption data, the annual period of May-21 to April-22 was selected for calibration of electricity consumption (data completeness 94.5%). The building is almost entirely naturally ventilated, and heating and domestic hot water is gas-supplied, thus electric loads relate to mains power, lighting, fans, pumps and switchboards. Missing hourly data points were extrapolated on the assumption of cyclic building occupancy behaviour patterns, following the protocol summarised in Table 6.1. Exceptions to this protocol were made to account for periods of reduced occupancy such as holidays. It should be noted that early-2021 consumption data may have non-typical usage patterns due to the impact of covid-19, however cross-validation against 2022 provided a reasonably close correlation and 2022 data was utilised for the months of January to April. High-resolution electricity consumption data was also available for various end use activities, including separate sub-metering for power, lighting, lifts, gym lighting and power, comms and plant.

Table 6.1: Data cleaning rules dependant on number of consecutive missing data points for the CS3 metered hourly dataset.

No. missing hourly data points	Rule
<4	Average calculated from previous and subsequent non-NA values.
4<x<24	Average calculated from same time points from previous and subsequent day.
>24	Values interpolated from previous or subsequent year.

Data Analysis and Cleaning: Thermal Loads

Thermal loads related to natural gas boiler supplied heating and domestic hot water usage. Metered fossil thermal energy consumption data for the building was invalid, thus necessitating approximation based on monthly energy bills. Since this approximation was a summation of both low-temperature hot water and domestic hot water energy consumption, heating and domestic hot water were calibrated on aggregate. For modelling purposes, the base load during occupied peak summer periods was utilized to approximate the portion of the fuel supply dedicated to domestic hot water, when heating was assumed to be mostly non-operational. In lieu of more accurate dissaggregated data availability, the simplified approach was considered a key limitation to the validity of the calibrated thermal model. The implications of calibration quality on the overall [LCA-CCA](#) framework are discussed in section 8.3.2. Resulting predicted monthly fuel use is shown in Figure 6.2, alongside end-use dissaggregated electric loads.

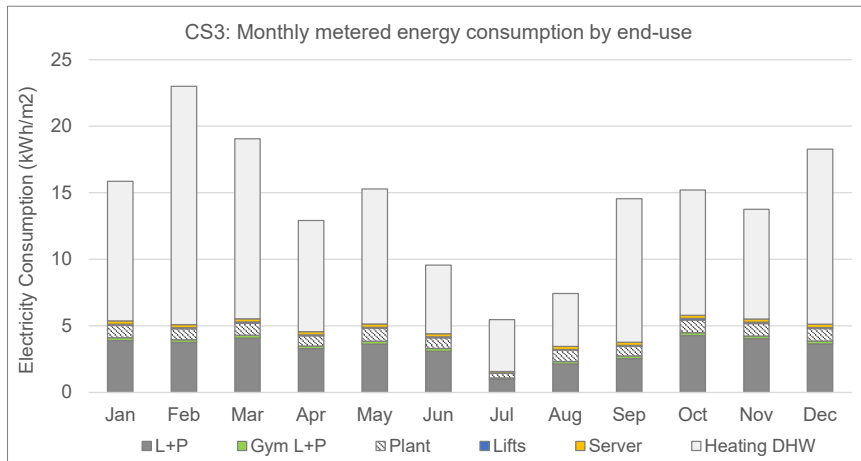


Figure 6.2: CS3: End-use dissaggregated metered monthly energy consumption data for 2021-2022.

6.2.2 Model development

The baseline model was developed according to specifications from available design-stage drawings, operation & maintenance manuals and on-site observations. The

primary modelled build-up consisted of an insulated brick-slip facade aligned with additional insulation and the concrete substrate retained from pre-refurbishment, achieving a U-value of 0.136 W/m².K. Double glazed windows were incorporated with an assumed U-value of 1.5 W/m².K. The aluminium frame U-value was modelled as 1.73 W/m².K accounting for the insulating thermal break. An overview of main modelled constructions and their thermal properties is provided in Table 6.2. A design airtightness of 5 m³/hr/m² @ 50 Pa was applied.

Table 6.2: CS3 primary constructions and thermal properties of existing building.

Construction	Description	Thickness (m)	U-value (W/m ² .K)
External wall	60mm insulated brickslip panel system, 120mm insulation infill, original concrete substrate	0.330	0.136
External roof	100mm roofing tiles, 160mm insulation board, 260mm cast concrete, 12mm plasterboard	0.533	0.181
Internal partitions	12.5mm plasterboard, air layer, 12.5mm plasterboard	0.162	0.624
External glazing	Double glazed aluminium casement	-	1.5

In response to the dataset observations summarised in Table 6.3, the following updates were made to the baseline model.

- Occupancy, lighting and equipment schedules were updated to reflect term time monthly and seasonal variations.
- Bedroom domestic hot water consumption rates were increased to reflect the relative GIA of en-suites.

Detailed HVAC modelling incorporated the supply of heating to all main zones via radiators. Combination boilers with a thermal efficiency of 0.92 supplied radiators. domestic hot water is also provided by the NGB plant. Bedroom heating SP temperatures were set to 20°C during occupied periods, with a setback temperature of 12°C during unoccupied periods. The building was modelled as predominantly naturally ventilated, for calibration purposes. However, for further investigation within the CCA-LCA optimisation process, mechanical cooling is integrated into the model.

Table 6.3: CS3 operational energy use dataset observations.

Category	Observations
Occupancy profile	<ul style="list-style-type: none"> • Monthly and seasonal occupancy variation based on term times • Indication of building operation over summer months • Indication of reduced capacity over summer months, particularly in July
HVAC operation	<ul style="list-style-type: none"> • Heating and domestic hot water account for significant proportion of energy end-use • Main zones supplied via NV only
Lighting & power	<ul style="list-style-type: none"> • High L+P baseload

6.2.3 Calibration Results

The various sub-metering groupings are presented in Table 6.4, alongside monthly calibration results using May 2021 to May 2022 climate data. Compliance with ASHRAE Guideline 14 criteria, which necessitates monthly [CVRMSE](#) to remain below 15% and [NMBE](#) within $\pm 5\%$, was achieved for all sub-metered end uses. For disaggregated electricity and gas fuel consumption, results were calibrated at the building-level. These findings demonstrate that the calibrated model sufficiently meets the ASHRAE Guideline 14 criteria, indicating a close proximity between monthly metered and simulated outputs.

Table 6.4: Calibration results for CS3. Target monthly validation criteria: $C_v(\text{RMSE})$ 15%, $\text{NMBE} \pm 5\%$ [176].

Level	End Use	$C_v(\text{RMSE})(\%)$	$\text{NMBE}(\%)$
Building	Electricity	11	5
Building	Natural Gas	15	1
Gym	L+P	8	-2
Building	Comms	2	0
Building	Plant	8	2
Building	Lift	11	-2
Building	All	10	2

6.3 CS3: Framework Development

This chapter presents outputs from the implementation of various stages of the life-cycle optimisation framework on CS3 (outlined in Figure 3.8). Firstly, the included sub-set of ECMs are described. Normalised FU LCA calculation results are then presented for the refined ECM solution set and integrated into the NSGA-ii GA. Section 6.4.1 discusses the life-cycle optimisation results for a single scenario. Finally, outputs are compared to findings from alternative grid decarbonisation and cost scenarios.

6.3.1 ECM selection

The final solution set included in the GA optimisation process is presented in Table 6.5. As a result of preliminary testing, the number of possible solution combinations reduced from 424,673,280 to 4,300,800. Details relating to CS3-specific ECMs are described in this section.

Table 6.5: Assigning genes and variable alterantives for implementation into the multi-objective optimisation framework.

Gene	Variable	Metric	CS2 Variants
x1.	Glazing U-value	W/m ² K	1.5, 0.8
x2.	g-value	SHGC	0.4, 0.3
x3.	NE-glazing area	%	0, -50
x4.	NW-glazing area	%	0, -50
x5.	SE-glazing area	%	0, -50, -30, +30
x6.	SW-glazing area	%	0, -50, -30, +30
x7.	SE-louvre	D/H ratio	0, 0.2, 0.4, 0.6, 0.8
x8.	SW-louvre	D/H ratio	0, 0.2, 0.4, 0.6, 0.8
x10.	Wall Insulation (MW)	mm	-50, 0, 50, 80
x11.	Roof Insulation (XPS)	mm	0, 50, 80, 120
x12.	Frame U-value	W/m ² K	1.735, 0.391, 0.223
x13.	Infiltration Rate	m ³ /(m ² .h)@50Pa	5, 3, 1
x14.	NV control	-	None, dT, nightpurge
x15.	HVAC system	-	NG, ASHP
x16.	MVHR control	-	None, 7-19 weekdays, nightcycle, weekends

Frame U-Values

The frame U-values were systematically calculated for each 50mm increment of PIR insulation and plasterboard, as demonstrated in Appendix H.2. The baseline U-value was set in accordance with the existing aluminum casements with a thermal break, measuring 1.735 W/m²K, equating to a baseline airtightness of 5 m³/hr/m² @ 50 Pa.

Night Purge Ventilation

Night purge ventilation was implemented in the kitchens and circulation spaces between the hours of 22:00 and 05:00, with a minimum outdoor temperature of 17°C and a maximum differential temperature of 2°C. Nightpurge [NV](#) control was not applied in bedrooms to allow for personal control of the environment.

MVHR

[MVHR](#) systems were added to supply all primary space use functions, including kitchens, bedrooms, and offices. Circulation spaces and similar areas were excluded. The air change rates applied aligned with [NCM](#) standards for each respective space type.

Spandrel Panels

Spandrel panels were introduced to replace glazed sections for [WWR](#) reductions. The new panels were assumed to be aluminum, consistent with the existing aluminum spandrel paneling in the baseline building.

Internal Wall Insulation

Considering the low indicative external wall U-value (already below Part L requirements), both the reduction and addition of mineral wool insulation were adopted as variable alternatives. In reducing the existing insulation build-up by 50 mm during future refurbishment cycles, the resulting external wall U-value remains below the Part L standard ($<0.18 \text{ W/m}^2\text{K}$) [[179](#)].

Material Choices

Wooden louvres were selected instead of aluminum louvres, due to their lower [EC](#) (when reporting biogenic carbon) and lower [CapEx](#).

6.3.2 Modelling Inputs: Carbon Calculations

EC: Fabric

The EC emissions associated with CS3 primary building elements are detailed in Table 5.5. These values were determined using the LCA stages and calculation methodology outlined in section 3.3.6. As per the RICS Professional Standard [19], assumptions were made concerning the usual manufacturing location, waste rate, and expected lifespan of each building material. All values in Table 6.6 are presented with respect to a functional unit of 1m² equivalent surface area of the relevant building material. For a comprehensive overview of LCA assumptions and results, along with the sources utilized to formulate these assumptions, please refer to Appendix G.1 and D.

Element	FU	Build-up	Volume/FU (m ³ /FU)	Manu- facture (L/N/E)	Waste rate (%)	Lifespan (yrs)	EC excl. biogenic (kgCO _{2e} /FU)	Biogenic (kgCO _{2e} /FU)	Total EC incl. biogenic (kgCO _{2e} /FU)
Roof	m ²	Roofing tile	0.100	L	5	75	17.42	0.00	245.84-270.15
		XPS insulation	0.160	N	5	40	55.58	0.00	
		RC cast concrete	0.260	L	5	75	104.05	0.00	
		Reinforcement mesh	0.003	N	15	75	44.07	0.00	
		+/-XPS insulation	0.050-0.120	N	5	40	17.37-41.68	0.00	
		Plasterboard soffit	0.013	N	5	30	7.35	0.00	
External Wall	m ²	Brick slip	0.017	N	20	75	10.22	0.00	91.1-134.11
		Stainless steel screw	1.87E-05	N	3	75	0.67	0.00	
		PUR insulation	0.043	N	15	75	10.80	0.00	
		MW insulation	0.120	N	15	75	26.04	0.00	
		Cast concrete	0.150	L	5	75	54.08	0.00	
		+/-MW insulation	-0.050-0.080	N	15	75	-10.85-17.49	0.00	
		+/-Gypframe	0.000	N	3	75	-6.77-7.90	0.00	
		Gypsum plasterboard	0.012	N	5	30	6.91	0.00	
Spandrel panel	m ²	Aluminium cladding	0.002	N	1	30	73.17	0.00	127.72
		MW insulation	0.170	N	15	75	36.89	0.00	
		Gypsum plasterboard	0.025	N	22.5	30	17.66	0.00	
Double glazing	m ²	-	0.003	E	5	40	24.72	0.00	24.72
Triple glazing	m ²	-	0.003	E	5	40	26.38	0.00	26.38
PIR closer	m ²	PIR insulation	0.05-0.1	N	15	75	12.56-25.12	0.00	35.67-48.23
		Gypsum plasterboard	0.039	N	5	30	23.11	0.00	
Louvre	m ²	Timber	0.05	E	1	30	109.34	79.85	29.49

Table 6.6: Calculated EC of construction elements for CS3, including materials, volume per FU and assumptions impacting the calculations. Items shown in red are interventions. Waste rates obtained from [163]; expected lifespan from [77, 19]. Manufacture location: Local (L), National (N), European (E).

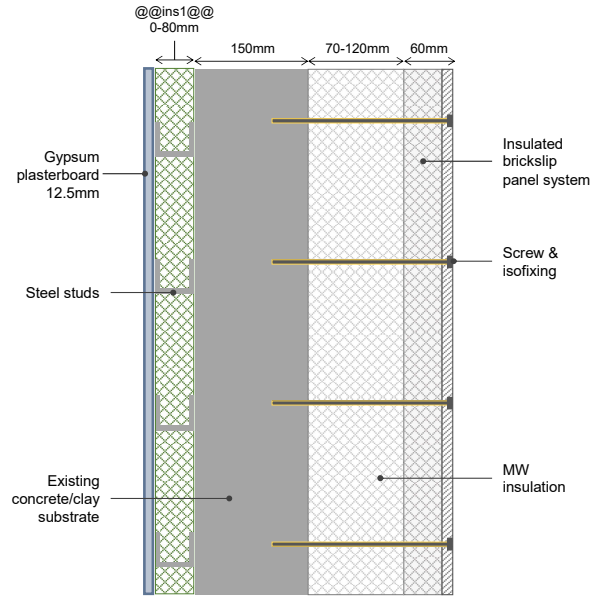


Figure 6.3: Assembly section: CS3 external wall build-up demonstrating all elements included in EC calculations and the position of additional internal MW insulation (@@IWI@@).

The modelled external wall build-up is depicted in Figure 6.3, aligning with the baseline U-values specified in architectural plans, and typical materials as guided by industry standards [179]. Insulation and gypframe additions to the external wall were included in varying thicknesses of 0, 50, 80mm and positioned internally to the existing concrete/clay substrate layer. An IWI reduction of 50mm from the baseline mineral wool thickness was also considered in the replacement. Typical sizing, frequencies and spacing of metal elements were established through expert elicitation.

EC: Systems

MVHR

The EC of the MVHR systems deployed in non-circulation spaces also followed the same EN 15978 guidance [17]. Manufacturers' specifications were scaled to meet commercial-scale requirements with a simulated design volumetric air flow rate of 43,416 m³/h (including a 10% safety factor). This was assumed to require scaled-out operation, with EC assumptions relating to four separate units, each with a maximum air flow rate of 11,000 m³/h, as per available manufacturers' specifications [197]. Materials were scaled by weight to meet the 1,421 kg per unit estimation. The carbon associated with implementation of new duct-work was also approximated based on the design floor area. The EC related to duct-work manufacture and installation to serve approximately 6,437 m² conditioned internal area was scaled up from equivalent residential systems [198]. Assumptions

include a single replacement cycle over a 50-year lifespan for PVC ductwork, and a recovery rate calculated based on materials weight-to-weight ratios. Drawing from ProAir’s EPDs, the study assumes 100% recycling of metals, plastics, aligning with assumptions from RICS guidance [77, 19, 198]. Further details are provided in Appendix F.3.

OC emissions

OC emission pathways aligned with the grid electric and natural gas carbon emission factor pathways described in section 3.3.7.

6.3.3 Modelling Inputs: Cost Calculations

CapEx

The LCC of various building components are summarised in Table 6.7, calculated following the ISO 15686-5:2017 protocol described in section 3.3.6 [18]. Values were interpolated based on available data [167]; more extensive details of interpolations, including material and labour costs, are provided in Appendices G.3, G.4, G.5.

OpEx

Fuel price pathways followed the fluctuating fuel price assumptions outlined in section 3.3.7.

Element	FU	Build-up	Volume/FU (m ³ /FU)	Total Rate (£)	Replacement (yrs)	NPV- adjusted cost (£)	LCC (£)	Total LCC (£)
Roof	m ²	Roofing tile	0.100	36.26	-	-	36.26	255.30–272.37
		XPS insulation	0.160	45.44	40	13.93	59.37	
		RC cast concrete	0.260	100	-	-	100	
		Reinforcement mesh	0.003	-	-	-	-	
		+/-XPS insulation	0.050-0.120	19.18-32.24	40	5.88-9.88	25.06-42.13	
		Plasterboard soffit	0.013	24.51	30	10.10	34.61	
External Wall	m ²	Brick slip	0.017	61.96	-	-	61.96	315.27–334.07
		Stainless steel screw	1.87E-05	1.85	-	-	1.85	
		PUR insulation	0.043	43.56	-	-	43.56	
		MW insulation	0.120	8.17	-	-	8.17	
		Cast concrete	0.150	173.53	-	-	173.53	
		+/-MW insulation	-0.050-0.080	-4.79-6.23	-	-	-4.79-6.23	
		+/-Gypframe	0.000	-3.62-4.16	-	-	-3.62-4.16	
		Gypsum plasterboard	0.012	24.51	30	10.10	34.61	
Spandrel panel	m ²	Aluminium cladding	0.002	202.35	30	83.37	285.72	320.81
		MW insulation	0.170	10.58	-	-	10.58	
		Gypsum plasterboard	0.025	24.51	30	10.10	24.51	
Double glazing	m ²	Double glazed casement aluminium window frame	-	609.07-652.06	40	186.71-199.89	795.78-851.95	795.78–851.95
Triple glazing	m ²	Triple glazed casement aluminium window frame	-	812.51-855.50	40	249.08-262.26	1061.59-1117.76	1061.59–1117.76
PIR closer	m ²	PIR insulation	0.05-0.10	43.56	-	-	43.56-52.25	152.23–160.92
		Gypsum plasterboard	0.0393	76.96	30	31.71	108.67	
Louvre	m ²	Timber	0.05	109.50	30	45.11	154.61	154.61

(a) Fabric

Element	FU	Total Rate (£)	Replacement (yrs)	NPV- adjusted cost (£)	Total LCC (£)
VRF	67 kW* unit	18,803	20, 40	16,175	34,978
ASHP	64 kW* unit	34,663	22, 44	29,208	63,871
NGB	19 kW* unit	2,471	22, 44	2,082	4,552
MVHR	14,690 m ³ /h unit	26,464	20, 40	22,765	49,230

(b) Systems *Extrapolated according to calculated rated capacity from each simulation run.

Table 6.7: Calculated CapEx of construction elements for CS3, including materials, volume per FU and replacement costs. Items shown in red are interventions. Expected lifespan from [77, 19].

6.4 CS3: Framework Implementation

6.4.1 Life-cycle optimisation results

This section presents the CS3 results from the life-cycle optimization process for the ‘best-case’ scenario (S1), as described in Chapter 3.3.7. Alternative decarbonisation pathways are examined in section 6.4.2.

Pareto Optimal Solutions

Characteristics of the pareto optimal solution set are shown in Table 6.5. As described in section 6.4.1, the two distinct regions represent the implementation of heating system alternatives. The pareto front ranged from 708-1357 £/m² for LCC and from 284-1159 kgCO₂e/m² for LCCF over the 60 year time frame, with NGB solutions presenting the cheaper, more carbon-intensive alternative. Within each search space, a region of higher LCC can be seen, representing the addition of MVHR systems. In general, the additional CapEx required for the implementation of MVHR outweighed OpEx benefits. The implementation of MVHR alongside the baseline NGB heating system resulted in a wide search space along the LCCF axis, indicating that for many design iterations, the combination of certain MVHR and NV control strategies led to increased heating loads. For ASHP-based design iterations, MVHR was not present in any pareto optimal solution, suggesting that the EC and CapEx associated with the implementation of MVHR and air distribution networks was not sufficiently offset by any operational savings. Further GA optimisation of control strategies could help to enhance operational benefits associated with MVHR adoption.

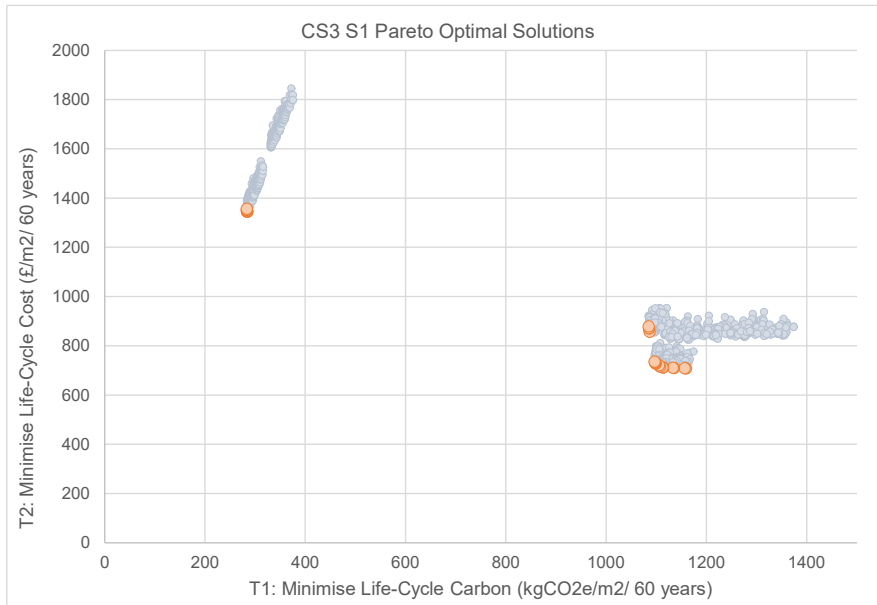
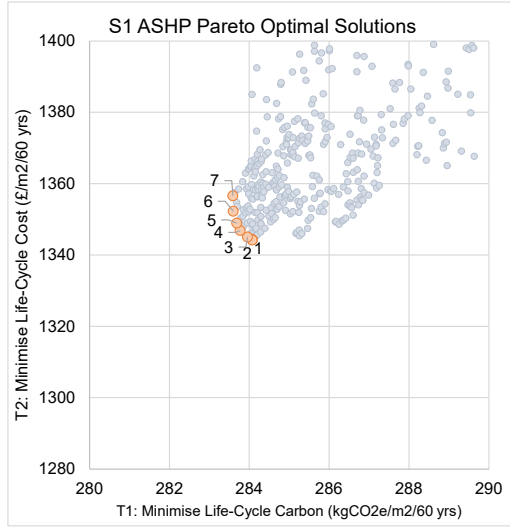
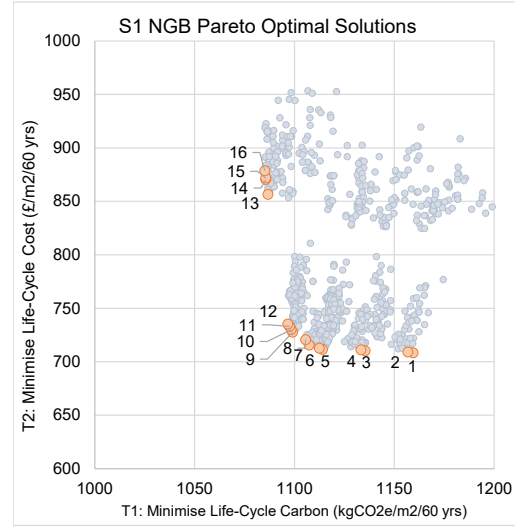


Figure 6.4: Optimised LCCF and LCC values.



(a) ASHP



(b) NGB

#	Heating System	Glazing Type	SHGC	North-West WWR	South-West WWR	South-West Louvre D/H	South-East WWR	South-East Louvre D/H	North-East WWR	IWI Ins. mm	Roof Ins. mm	Frame U-value W/m ² .K	Infiltr. Rate m3/m ² .h	MVHR Control Strategy	NV Control Strategy
1	NGB	Double	0.3	-50%	-50%	0	-50%	0.4	0%	-50	0	1.735	5	No MVHR	Nightpurge
2	NGB	Double	0.4	-50%	-50%	0	-50%	0.4	0%	-50	0	1.735	5	No MVHR	Nightpurge
3	NGB	Double	0.3	-50%	-50%	0	-50%	0.4	0%	-50	0	0.378	3	No MVHR	Nightpurge
4	NGB	Double	0.4	-50%	-50%	0	-50%	0.4	0%	-50	0	0.378	3	No MVHR	Nightpurge
5	NGB	Double	0.3	-50%	-50%	0	-50%	0.4	0%	-50	0	0.219	1	No MVHR	Nightpurge
6	NGB	Double	0.4	-50%	-50%	0	-50%	0.4	0%	-50	0	0.219	1	No MVHR	Nightpurge
7	NGB	Double	0.4	-50%	-50%	0	-50%	0.4	-50%	-50	0	0.219	1	No MVHR	Nightpurge
8	NGB	Double	0.4	-50%	-50%	0	-50%	0.4	-50%	0	0	0.219	1	No MVHR	Nightpurge
9	NGB	Triple	0.4	-50%	-50%	0	-50%	0.4	0%	-50	0	0.219	1	No MVHR	Nightpurge
10	NGB	Triple	0.4	-50%	-50%	0	-50%	0.4	-50%	-50	0	0.219	1	No MVHR	Nightpurge
11	NGB	Triple	0.4	-50%	-50%	0	-50%	0.4	0%	0	0	0.219	1	No MVHR	Nightpurge
12	NGB	Triple	0.4	-50%	-50%	0	-50%	0.4	-50%	0	0	0.219	1	No MVHR	Nightpurge
13	NGB	Double	0.3	-50%	-50%	0	-50%	0.4	0%	-50	0	0.378	3	Weekday	deltaT
14	NGB	Double	0.3	-50%	-50%	0	-50%	0.4	0%	-50	50	0.219	1	Weekday	deltaT
15	NGB	Double	0.3	-50%	-50%	0	-30%	0.4	0%	-50	50	0.219	1	Weekday	deltaT
16	NGB	Triple	0.4	-50%	-50%	0	-50%	0.4	0%	-50	0	0.378	3	Weekday	deltaT

(c) Parameters of optimised solution set for CS3 NGB.

#	Heating System	Glazing Type	SHGC	North-West WWR	South-West WWR	South-West Louvre D/H	South-East WWR	South-East Louvre D/H	North-East WWR	IWI Ins. mm	Roof Ins. mm	Frame U-value W/m ² .K	Infiltr. Rate m3/m ² .h	MVHR Control Strategy	NV Control Strategy
17	ASHP	Double	0.3	-50%	-50%	0	-50%	0.2	0%	-50	0	1.735	5	No MVHR	Nightpurge
18	ASHP	Double	0.3	-50%	-50%	0	-50%	0	0%	-50	0	1.735	5	No MVHR	Nightpurge
19	ASHP	Double	0.3	-50%	-50%	0	-30%	0	0%	-50	0	1.735	5	No MVHR	Nightpurge
20	ASHP	Double	0.3	-50%	-50%	0	0%	0	0%	-50	0	1.735	5	No MVHR	Nightpurge
21	ASHP	Double	0.3	-50%	-50%	0	30%	0.2	0%	-50	0	1.735	5	No MVHR	Nightpurge
22	ASHP	Double	0.3	-50%	-30%	0	30%	0.2	0%	-50	0	1.735	5	No MVHR	Nightpurge
23	ASHP	Double	0.3	-50%	0%	0	30%	0.2	0%	-50	0	1.735	5	No MVHR	Nightpurge

(d) Parameters of optimised solution set for CS3 ASHP.

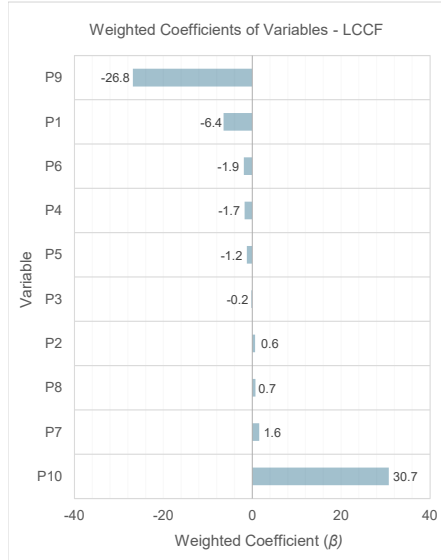
Figure 6.5: NSGA-ii optimisation results for CS3 scenario 1.

Relative Impact of Variables on LCCF and LCC

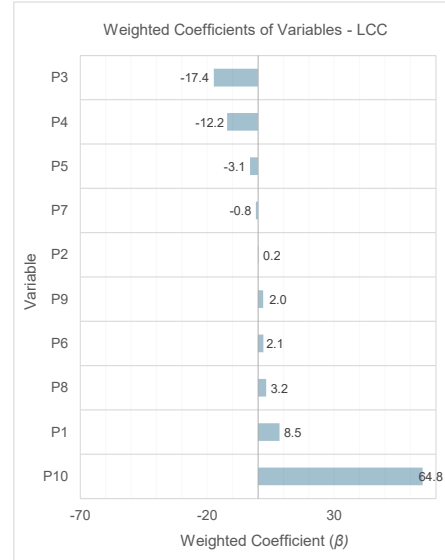
The relative impact of independent design measures on LCCF and LCC was evaluated using linear regression analysis. By aggregating the unstandardised linear model coefficients across each level within a categorical variable, an overall weighted coefficients (β) was derived, indicating the relative impact of changes in design parameters. The weighted coefficients for each variable are illustrated in Figure 6.6.

Variable		Variable	
P1	Glazing Type	P6	North East-WWR
P2	SHGC	P7	Internal Wall Insulation
P3	North West-WWR	P8	Roof Insulation
P4	South West-WWR D/H Ratio	P9	Frame U-value Infiltration Rate
P5	South East-WWR D/H Ratio	P10	MVHR NV Operation

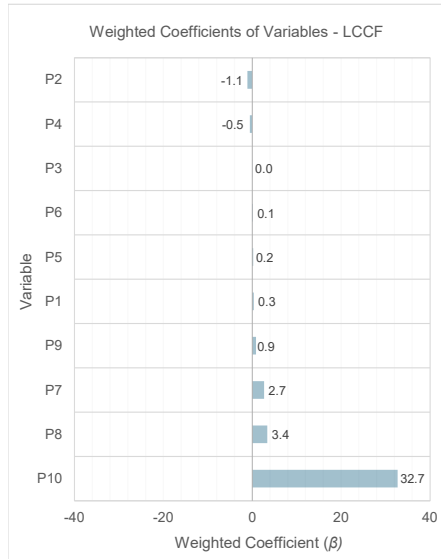
(a) Categorical variables.



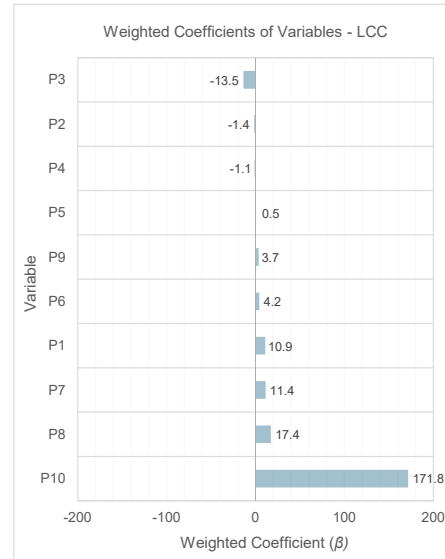
(b) t1 - Minimise LCCF (NGB)



(c) t2 - Minimise LCC (NGB)



(d) t1 - Minimise LCCF (ASHP)



(e) t2 - Minimise LCC (ASHP)

Figure 6.6: Weighted coefficients (β) of categorical variables in linear regression analysis for Scenario 1.

Heating System (P0)

The heating system emerged as the predominant predictor of both **LCCF** and **LCC**. The differentiation in **LCCF** and **LCC** resulting from heating system alternatives under the S1 scenario was significant, as shown in Figure 6.4. Consequently, linear regression analysis was conducted independently for each heating system alternative to avoid distorting the impacts of other variables. **ASHP**-based design iterations exhibited a substantially lower carbon footprint over the lifetime relative to the baseline **NGB** system. This was despite an approximate tenfold increase in estimated **EC** associated with **ASHP** heating systems due to system refrigerant leakage and recovery rates. However, the greater thermal efficiency (**NGB** η : 0.92; **ASHP** nominal COP: 3.2), combined with the lower electricity **CEF** over the building's lifetime compared to natural gas, resulted in an average 8-fold reduction in life-cycle **OC** emissions. These results suggest that buildings equipped with **ASHP** systems contribute considerably less to overall carbon emissions compared to those relying on **NGB** technology, although they may incur higher costs over the building's life cycle.

Glazing Type (P1, P2)

Transitioning from double to triple glazed windows led to a significant reduction in model-predicted **LCCF** for design combinations relying on the baseline **NGB** system (β : -6.4). However, when using **ASHP** as a more efficient electricity-based heating source, upgrading to triple glazing had a marginal positive impact on **LCCF** (β : +0.3), indicating that the additional **EC** was not offset by operational carbon savings. For both the baseline and **ASHP** alternatives, glazing type had a relatively strong positive impact on **LCC**, suggesting that **OpEx** savings were insubstantial to offset the higher **CapEx** associated with triple glazed casement units. A reduction in **SHGC** from 0.4 to 0.3 resulted in a marginal positive impact on **LCCF** (β : +0.6) and **LCC** (β : +0.2) for solutions relying on the baseline **NGB** system, but had a negative impact for **ASHP** alternatives (**LCCF** β : -1.1, **LCC** β : -1.4). This reflects the greater priority given to cooling loads in reducing **LCCF** under the operation of more efficient and less carbon-intensive heating systems.

WWR | Louvre D/H Ratio (P3-P6)

Alterations in **WWR** and louvre D/H ratios exhibited relatively minor impacts on t1 for both the **NGB** (**LCCF** β : -1.9 to -0.2) and **ASHP** design combinations (**LCCF** β : -0.5 to +0.2). Amongst **NGB** alternatives, the model predicts a 30% reduction in South-West facade glazing combined with a South-West louvre 0.6 D/H ratio had the largest, significant impact on **LCCF** reduction, as depicted in Appendix K.1; in general, glazing area reductions performed more favorably on all facades compared to the baseline **WWR**, in terms of both **LCCF** and **LCC**. For **ASHP** solutions, reductions in the South-West glazing area only had significant but weak negative impacts on **LCCF**. This indicates that the preference for lower

WWRs under NGB heating system operation was predominantly driven by heat loss reduction as opposed to minimising solar heat gain to the system. Similar to NGB systems, the reduction in glazing areas tended to demonstrate negative correlations with LCC despite implementation of replacement spandrel panels and, in many iterations, the addition of vertical shading components.

Insulation Thickness (P7, P8)

Unstandardised linear model coefficients were analysed for external wall insulation alternatives, since both reductions and additions to IWI were considered in this case study. For NGB-based systems, both reductions and increases to the mineral wool insulation thickness relative to the baseline led to greater LCCF values. This indicates that, across the majority of design combinations, the baseline intervention provides an optimal balance; EC savings associated with decreasing IWI thickness were offset by increased OC emissions, whereas further increases to IWI thickness beyond the baseline did not result in sufficient OC savings to offset the higher EC emissions. In contrast, a reduction in mineral wool insulation thickness of 0.05m led to a significant negative correlation with LCCF under ASHP-optimised design solutions, when the lifetime operational carbon emissions associated with the heating system are a less predominant driver of overall LCCF. Reducing the mineral wool insulation thickness also led to a strong negative correlation with LCC in both NGB and ASHP cases.

Frame U-value | Infiltration Rate (P9)

Additional PIR insulation demonstrated considerable efficacy in reducing LCCF when aligned with the baseline NGB heating system (β : -26.8), with relatively small associated increases in LCC. However, under the higher efficiency ASHP electricity-based heating system, the implementation of PIR closers and associated lower infiltration rates led to predicted increases in both LCCF and LCC. This suggests that the EC associated with the PIR insulation was not offset over the building's life-cycle due to the lower associated operational carbon emission savings potential. In addition, for ASHP-based solutions, the higher efficiency of the heating system relative to cooling may lead to a greater weighting on design iterations for reduced cooling demand, thus favouring lower insulation levels.

Ventilation Strategy (P10)

The overall impact of ventilation strategies represented a significant positive increase in both LCCF (β : +30.7 to +32.7) and LCC (β : +64.8 to +171.8), with the magnitude of this impact largely dependent on the NV and MVHR strategy combination. Under the NGB heating system operation, the combination of MVHR weekday operation with deltaT NV control had the strongest negative impact on LCCF, followed by NV night purge with no MVHR system. In contrast, the introduction of MVHR had a negative impact on LCCF across all ventilation

strategy combinations relying on the ASHP heating system, indicating that the EC associated with implementation was not offset by OC savings. For solutions relying on both NGB and ASHP systems, the introduction of MVHR correlated to significant increases in LCC due to substantial CapEx. The use of NV nightpurge ventilation without MVHR resulted in a weak negative correlation with model-predicted LCCF and LCC for both NGB and ASHP cases, as shown in Appendix K.1.

6.4.2 Scenario analysis

This section compares the ‘best-case’ scenario (S1) with alternative decarbonisation pathways described in Table 6.8 and Section 3.3.7.

Table 6.8: Summary of grid decarbonisation rate scenario alternatives; both S1 and S2 adopt the fluctuating fuel price pathways described in section 3.3.7.

	Scenario Description
S1	‘Best-case’: Electric grid carbon emissions decline rapidly from 2020 to 2030, plateauing at 2033.
S2	‘Worst-case’: BAU; incline in electric grid carbon emissions until 2025, thereafter declining gradually towards a plateau at 2042.

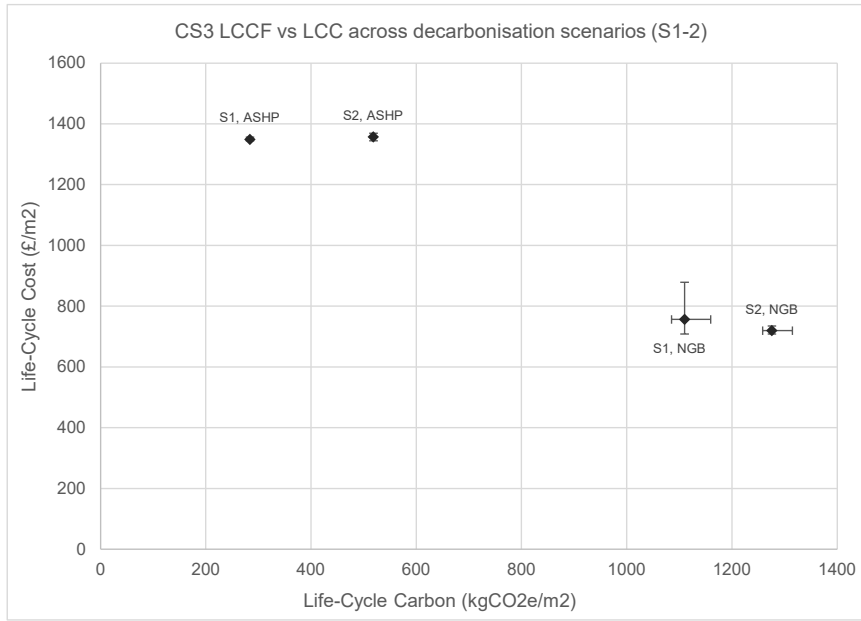


Figure 6.7: LCCF vs. LCC Comparison of pareto optimal solutions across decarbonisation scenarios. Points show group averages; error bars represent ranges.

LCCF and LCC optimisation results for S1 and S2 are shown in Figure 6.7. For Pareto optimal solutions reliant on the NGB system, LCCF ranged from 1085 kgCO₂e/m² to 1315 kgCO₂e/m², with an average increase of 15% (+166 kgCO₂e/m²) from S1 to S2. For ASHP solutions, the equivalent range was from 284 kgCO₂e/m² to 519 kgCO₂e/m² (x1.8). The wide ranges across decarbonisation scenarios relate to the rate of change in the electricity CEF, increasing by approximately 3-fold from S1 to S2, over the building’s estimated life-cycle. For solutions reliant on the NGB system, since electricity-based emissions constitute a smaller proportion of energy end-uses, the upward shift in LCCF was less notable than ASHP solutions. Consequently, the LCCF differentiation between ASHP and NGB solutions for S2 narrows relative to S1, although ASHP solutions still exhibit significantly lower LCCF than NGB alternatives.

The results indicate that the choice of heating system and decarbonisation scenario exerts a significantly greater impact on **LCCF** than other design alternatives within the same group. However, Figure 6.7 reveals notable differences in **LCCF** variances among Pareto solutions across different heating system groups. For **ASHP** groups, intragroup variances in **LCCF** were minimal, while **LCCF** varied by 57 kgCO₂e/m² and 74 kgCO₂e/m² for solutions within the **NGB** S1 and S2 groups, respectively. The reduced **LCCF** variances in **ASHP**-based design combinations highlight that the combination of low operational **CEF** and high-efficiency heating systems mitigates the impact of design alternatives on **OC** emissions and, consequently, on **LCCF**.

The average **LCC** ranges from 708 £/m² to 878 £/m² for the **NGB** alternatives and from 1344 £/m² to 1367 £/m² across **ASHP** groups, with the maximum range within any single group being 170 £/m². Wider intragroup variances were observed under the S1, **NGB** solution set, attributable to mixed ventilation control strategies, as described in Section 6.4.1. Despite identical assumptions for **CapEx** and **OpEx** in both S1 and S2, minor discrepancies were observed in **LCC**. For the **NGB** group, a decrease in the average **LCC** of 37 £/m² (5%) was noted. These variances, largely influenced by ventilation strategy selection, highlight the indirect effect of changing carbon emission pathways on **LCC** through different optimised design parameters.

Embodied vs. operational carbon emissions

The influence of grid decarbonisation and fuel price projections on the composition of various **LCCF** components is illustrated in Figure 6.8. Across all solution sets, **EC** is primarily driven by emissions related to the initial installation and recurring replacement of components on the external envelope, such as glazing. For baseline **NGB** solutions, heating and domestic hot water are the predominant sources of **OC** emissions, regardless of the decarbonisation pathway, accounting for 91% and 80% of total **OC** under S1 and S2, respectively. This predominance relates to the cumulative impact of the slower natural gas decarbonisation rate, which has a lower proportion of green gas penetration. Even under the ‘worst-case’ scenario, in which electricity is assumed to decarbonise much more slowly, the proportion of fossil thermal emissions remains significantly higher than that of electricity-related operational carbon emissions. Under the **ASHP**-dependent pathways, although heating and domestic hot water still accounting for a substantial proportion of **EUI** (approximately 34%), the relative proportion of **LCCF** decreased to only 14% and 23% of overall **LCCF** for S1 and S2, respectively, less than associated with lighting and power.

Across all scenarios, the average **EC** for **ASHP** Pareto solutions was about 1.19 times higher than that of **NGB** Pareto solutions (**NGB**: 140 kgCO₂e/m², **ASHP**:

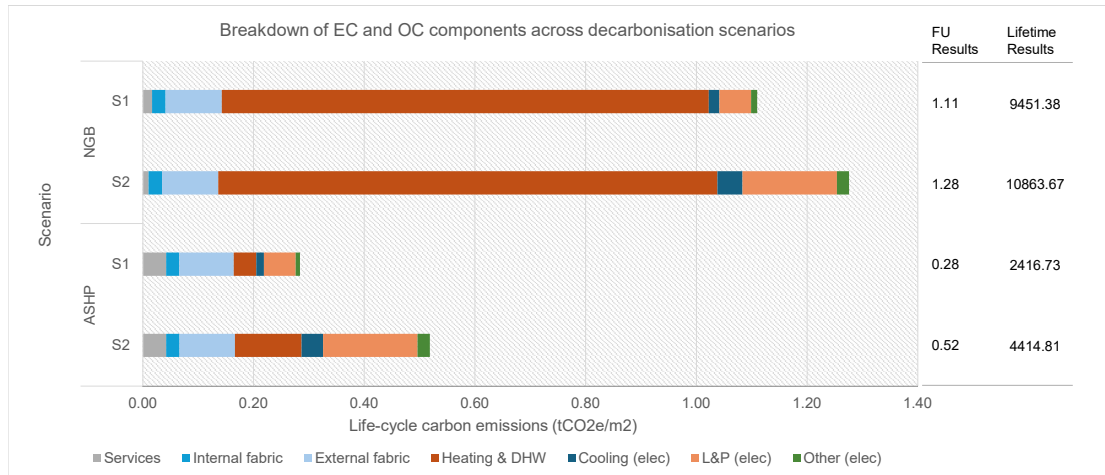


Figure 6.8: Average share of embodied versus operational carbon components across pareto solutions for scenarios 1 and 2.

165 kgCO₂e/m²), primarily due to the high EC impact of refrigerants. While the average EC remains relatively stable across scenarios using the same heating system, average OC varies by 257 kgCO₂e/m² for NGB scenarios and by 235 kgCO₂e/m² for ASHP scenarios. For the NGB group, this changes the EC:OC ratio from 1:7 in S1 to 1:8 in S2. For ASHP solutions, the ratio ranges from 1:1.4 in S1 to 1:2 in S2. Under more rapid grid decarbonisation pathways and with the adoption of energy-efficient heating measures, EC could account for over half (58%) of the refurbished building's LCCF.

Time-dependency of carbon impact

The aggregated year-on-year LCCF over the building's 60-year lifespan is illustrated in Figures 6.9. Across all scenarios, a notable step change is observed around the year 2052, corresponding to the EC associated with the replacement of various building components, including internal dry lining, partitions, and spandrel paneling. For ASHP-based solutions, additional step changes are evident in 2042 and 2066, reflecting the 22-year replacement cycles of refrigerant-based ASHP systems. Under scenario S1, the cumulative LCCF impact appears to plateau around 2043, whereas the NGB group continues to exhibit a pronounced upward trend extending to 2082. This trend indicates that despite a faster grid decarbonisation rate, the annual carbon intensity for CS1 will persistently increase beyond the building's lifespan unless there is a replacement of the heating system. The findings suggest that no other design modifications will suffice to achieve a relatively stable year-on-year carbon impact by 2082.

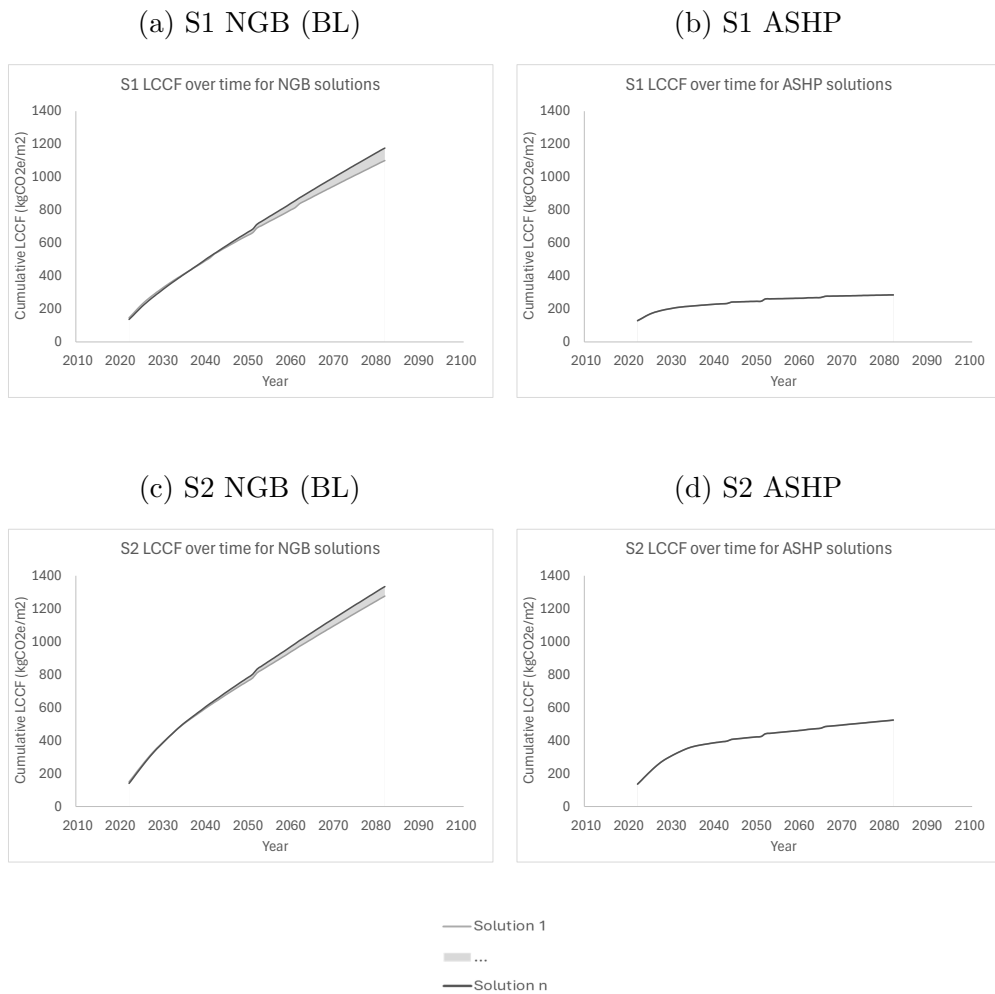


Figure 6.9: CS3 change in LCCF of pareto optimal solutions over time for scenario 1 and 2.

CS3 Chapter Summary

This case study explores a residential student accommodation, refurbished in 2019 and expanded to include additional en-suite rooms. The refurbishment introduced several building envelope upgrades, such as insulated brick slip façades, metal windows, and spandrel panels. Optimisation of life-cycle cost and life-cycle carbon under a range of alternative design and grid decarbonisation scenarios revealed:

Heating Strategies:

- Heating system alternatives had the strongest influence on **LCCF**, driven by cumulative **CEF** impacts over time.
- **ASHP** solutions maintained consistent **LCCF** stabilisation after 2052, whereas **NGB** solutions exhibited increasing emissions beyond the building's lifespan.
- For **ASHP** solutions, additional design measures had minimal impact on further **OC** reductions, indicating greater design flexibility but a more complex trade-off between embodied and operational carbon. This was exemplified through the preference for reduced **IWI** thicknesses.

Ventilation Strategies:

- **MVHR** contributed significantly to **LCC** due to high initial costs associated with unit installation and air distribution networks. This **CapEx** was justified for certain **NGB**-based solutions.

Façade Design:

- Window frame properties and glazing type were key predictors of **LCCF** reduction for **NGB**-based solutions under *S1: Best-case*.
- Triple glazing provided substantial **LCCF** savings for **NGB** solutions, though under **ASHP**-operation this measure resulted in a net increase in carbon.
- Reductions in South West **WWR** and **SHGC** were critical for optimising **LCCF** under **ASHP**-based scenarios.

Chapter 7

Discussion

7.1 Overview

The discussion is structured as follows: Section 7.2 synthesises findings across the three HE case study buildings, examining the trade-offs between key metrics such as LCCF and LCC and embodied and operational carbon. The impact of the LCA-CCA design pathway on present-day building performance is also presented and discussed. Section 7.3 directly addresses the research questions. The scaled-up impact and methodological development is considered. Subsequently, a suggested framework for integration of LCA-CCA within the wider design process is proposed.

7.2 Synthesis of case study findings

7.2.1 Future Energy, Carbon, and Cost in HE Building Design

The following sections compare the performance of baseline building design against the optimised design solutions. Baseline ‘non-adapted’ (NA) vs. optimised ‘adapted’ (A) outputs are depicted in Figure 7.1 for each case study, with reference to LCCF and LCC. The key findings are discussed below.

EUI Impacts

Operational energy outcomes across the case studies demonstrated changing proportional energy end-uses under future climate scenarios. All three building models predicted a reduction in overall EUI as average annual temperatures increase from 2022 to 2050, reflecting larger anticipated reductions in heating energy consumption than cooling load increases. The most significant decrease in energy consumption from 2022 to 2050 across baseline models was observed for CS2, with VRF systems operational for both heating and cooling end-uses. This demonstrates the significant future benefits of systems operating with high COP speci-

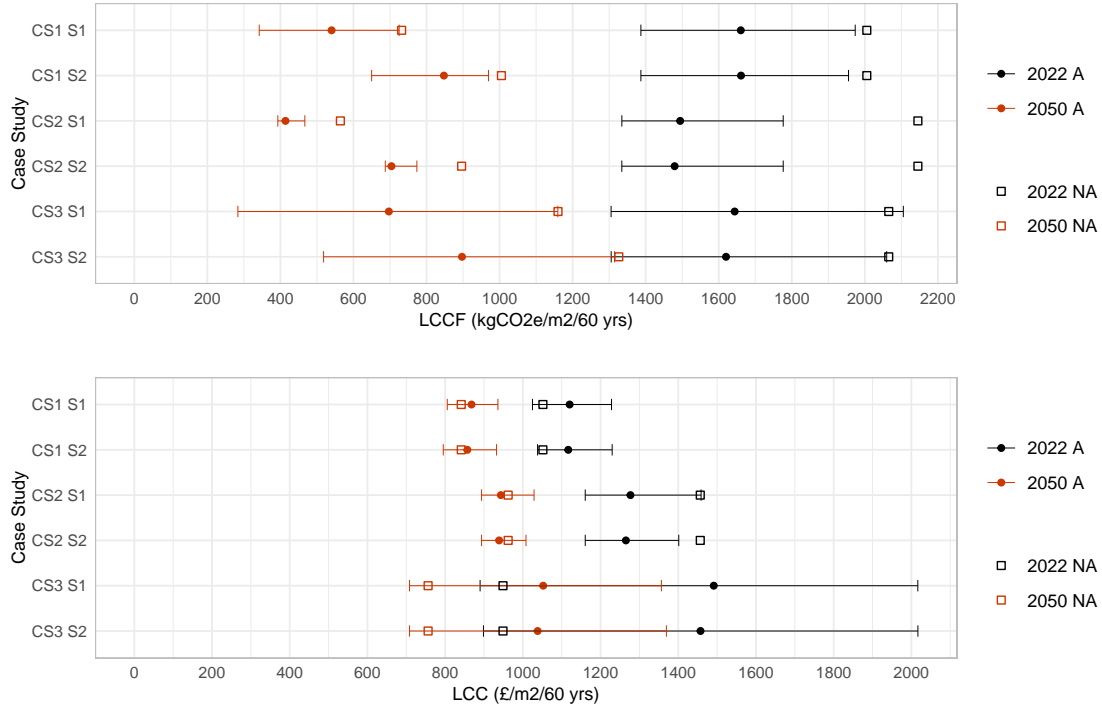


Figure 7.1: Case study comparison of metrics under current and future climates.

fications.

Across all case studies, the adapted solution sets (A) exhibited improved overall energy performance relative to non-adapted (NA) values, under both current (2022) and future (2050) climates. The optimisation for **LCCF** and **LCC** positively influenced **EUI**, despite the indirect assessment of operational loads through the **GA** optimisation process. The findings suggest that designing for future climates using the adopted **CCA-LCA** methodology is unlikely to have detrimental effects on present-day energy consumption. However, it is important to acknowledge the trade-off that **EUI** savings may not be maximised under current conditions when designing for future climates.

LCCF Impacts

Operational efficiency and fuel source can have a strong influence on operational carbon emissions of systems, dictating the suitability of subsequent design parameters. A visual comparison of **LCCF** for 2050 A solutions across case studies demonstrates substantially larger ranges for CS1 and CS3 when gas-based technologies are adopted as the baseline heating system. This variability relates to the uncertainties surrounding the decarbonisation rate of gas; the average **CEF** for electricity over the buildings' life-cycles is significantly lower than that for gas in both best-case (S1) and worst-case (S2) scenarios, despite an assumed lin-

ear annual increase in green gas penetration (see section 3.3.7) [157]. The technical, economic, and policy challenges associated with the widespread adoption of low-carbon hydrogen, CCS, and biomethane integration contribute to significant uncertainties regarding the pace and scale of green gas implementation [199]. Combined with the higher thermal efficiencies associated with electricity-based ASHP systems, these wide ranges represent potential for significant LCCF reduction when transitioning from gas-based technologies, even under slower rates of electricity sector decarbonisation. This is important as it highlights that the optimised models, while sensitive to grid decarbonisation assumptions, can still achieve lower LCCF. The findings underscore the necessity of making cautious assumptions about gas decarbonisation rates and relying on the relative predictability of electricity decarbonisation when assessing the long-term carbon impacts of building energy systems.

The research findings reinforce the limitations of employing fixed-rate CEFs in evaluating LCCF, resulting in notable disparities between present-day and projected future operational carbon scenarios. Figure 7.1 illustrates these discrepancies when fixed-rate decarbonisation assumptions are applied to 2022 A values. Incorporating grid decarbonisation pathways leads to substantial reductions in normalised LCCF, highlighting the risk of short-term perspectives associated with fixed operational carbon LCA models. Strategies deemed effective under current conditions may prove unsustainable as the electricity grid progressively decarbonises. This trend is particularly evident in CS1, where the carbon advantages of the combined heat and power-powered District Energy Network diminish over time. The findings highlight the need to integrating dynamic decarbonisation pathways into life-cycle assessments to reflect the long-term impacts of diverse energy systems and design strategies. There exists a critical trade-off between the short-term accuracy of measured, existing carbon emission factors and the long-term reliability of predicting evolving emission factors. Despite these challenges, the study suggests that solutions can be identified that perform effectively across varying decarbonisation assumptions. This capability enhances the resilience of design decisions, mitigating uncertainties associated with long-term carbon emission trajectories.

Embodied vs. Operational Carbon

The relationship between EC and OC emissions across the three case studies and varying decarbonisation pathways is illustrated in Figure 7.2. It should be noted that the EC/OC ratio is typically linked to the scale of refurbishment; buildings in poorer condition may require structural interventions or full facade replacements, leading to significantly higher EC. Nonetheless, the case study findings highlighted several contextual points concerning the interplay between embodied and operational carbon emissions, outlined below.

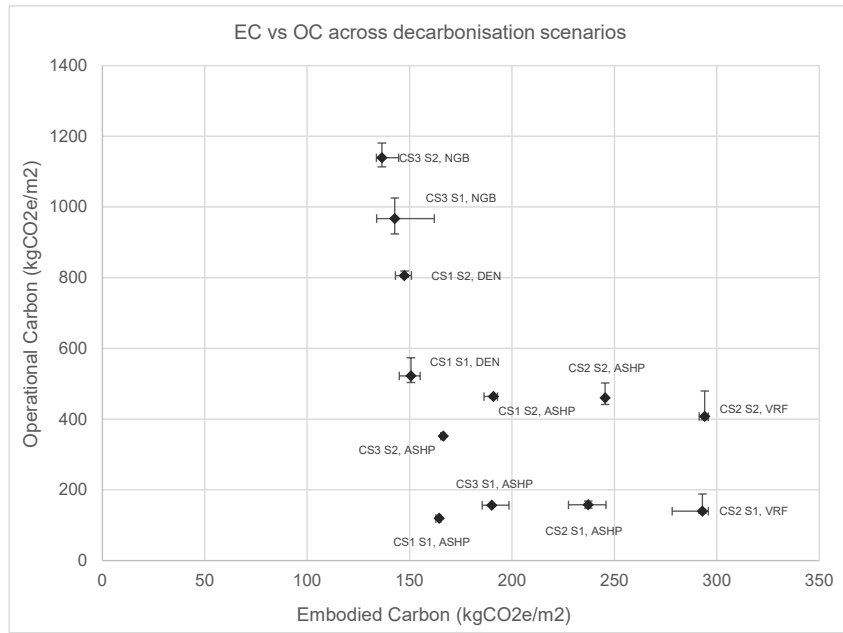


Figure 7.2: Ranges from Pareto-front values for EC and OC across three case studies and various decarbonisation pathways.

Balancing Embodied and Operational Carbon in Building Envelopes Considering the compliance of investigated case studies with modern building construction standards (regarding roof and wall U-values), an intricate trade-off exists between EC and OC for additional insulation measures. For CS3, with an external wall U-value better than Part L requirements, reducing the insulation thickness (relative to the pre-existing thickness) during replacement yielded EC savings that offset OC increases. Similarly, for CS1, low baseline frame U-values limited the subsequent benefit of additional PIR insulation, even when operating under a relatively carbon-intensive heating system. These findings highlight the importance of considering the contextual and nuanced impact of insulation on both embodied and operational carbon emissions; more insulation does not invariably reduce LCCF.

Renewable vs. Non-Renewable Construction Techniques Whilst direct comparisons between case studies are limited due to the distinct construction and operational characteristics of each building, the results indicate that lower EC construction materials afford greater design flexibility within the GA optimisation process. This analysis explicitly accounts for the biogenic carbon stored, sequestered, and released by organic materials, meaning that the results reflect both the emissions and the temporary carbon storage associated with organic materials. Conducting the same optimisation without including these biogenic carbon dynamics may yield different outcomes. The use of wooden louvres was prevalent across CS2 and CS3 pareto solutions in a range of D/h ratios. In contrast aluminium louvres adopted in CS1 appeared in only 14% of solutions

optimising towards a 0.2 D/h ratio. This indicates that renewable construction techniques could lead to a broader range of design alternatives within the optimisation framework, when accounting for biogenic carbon.

Impact of Refrigerant Embodied Carbon In CS1 and CS3, ASHP systems exhibited higher EC values than gas-based heating system alternatives, primarily due to refrigerant leakage and recovery rates. Despite this, the positive impact of refrigerant-related emissions on LCCF was minor by comparison to operational energy and carbon savings resulting from higher system efficiency and lower CEFs. Under the adopted assumptions, the overall benefits of ASHP systems in reducing operational carbon clearly justify their higher EC impact.

Enhanced Design Flexibility with Equal Heating and Cooling Operational Carbon Emission Distribution In the absence of high OC gas-dependent heating systems, glazing alternatives were more broadly represented across pareto solutions. Equally weighted OC emissions for heating and cooling resulted in a more diverse range of design solutions within the optimisation approach, avoiding an excessive focus on heating energy reduction strategies.

LCC Impacts

The research findings reveal that while the GA optimisation process effectively reduced EUI and LCCF, it did not yield substantial reductions in LCC relative to the baseline. The LCC for the existing building configuration remained lower than average values for CS1 and CS3 2050 A adapted solution sets and only slightly above the CS2 2050 A average. This upward shift in model-predicted LCC was primarily influenced by the higher operational costs associated with ASHP systems, particularly in CS1 and CS3, compared to gas-based heating technologies.

The retail energy price projections estimate substantially lower gas fuel prices compared to electricity, significant upon accumulation over the buildings lifetime [158]. In reality, the interaction between supply and demand is more nuanced; the continued uptake of gas-based technology could slow gas price reductions, whereas the rapid adoption of electricity-based systems could cause gas prices to fall rapidly due to declining demand. The volatility of the unabated natural gas market, historically impacted by global instabilities - such as the geopolitical tension of 2006 and the global financial crash of 2008 - introduces significant uncertainty to speculative life-cycle cost projections. The dynamic nature of economic change, particularly concerning energy-related price fluctuations, significantly impacts LCC decisions regarding fuel dependencies of technologies, with complex, interdependent system dynamics that drive market prices. The decoupling of electricity market price signals from highly-volatile gas prices could provide greater certainty in the building decision-making process.

Moreover, many Pareto optimal solutions with lower **LCCF** values entail higher **LCC** due to the elevated **CapEx** associated with newer technologies. While discount rates aim to capture the changing price of commodities over time, the attempt to quantify this economic relationship precisely overlooks the complexity of market dynamics, particularly in light of the fast-paced energy market where new technologies can rapidly penetrate the market. In this sense, treating the price of technologies, such as **ASHPs**, in the means of traditional supply vs. demand curves may disregard the broader, more intricate factors that influence market behavior. Overall, the results indicate that achieving significant cost savings alongside carbon reductions may remain a challenge, emphasising the need for careful consideration of the trade-offs between environmental and economic factors in building design and redevelopment.

Beyond fuel price trajectories, future operational costs will also depend on changing demand-side mechanisms and tariff structures. The increasing deployment of smart metering, flexible demand response, and time-of-use pricing could alter consumption patterns, allowing buildings to reduce their exposure to peak electricity tariffs [200, 201]. Similarly, the ongoing reform of the UK electricity market, including decoupling renewable generation from wholesale gas-linked prices and incentivising flexibility services, may reshape long-term operational cost profiles [202]. Incorporating these demand-side and market dynamics into future life-cycle cost modelling would enable a more representative evaluation of operational cost risks under net-zero energy transitions.

7.2.2 Aggregated Impact over Time

Across all case studies, a relatively stable year-on-year **LCCF** was observed only under S1 **ASHP** scenarios. In contrast, less-efficient gas-based heating technologies led to steep increases in **LCCF** that would be expected to continue beyond the buildings' life cycle. As a result, more pronounced **LCCF** ranges can be observed for CS1 and CS3, when gas-based heating technologies were included in design alternatives. This was notable even under the slower rates of electricity decarbonisation observed in S2, depicted in Figure 7.3. The higher **LCCF** values noted under the "S2:Worst-case" scenario were primarily driven by a steeper initial incline up to 2030. These findings highlight the importance of considering future grid decarbonisation in the assessment of heating technologies to achieve more realistic representations of design outcomes.

In all case studies, the findings indicate that the quality of building envelopes were sufficient to benefit from **ASHP** upgrades, when accounting for nominal **COP** adjustments according to time-step conditions. Whilst a context-specific approach is required to ensure systems can operate at a reasonable efficiency to reduce **OC** emissions, the findings support a balanced approach to **LCCF** management, prioritising immediate system upgrades, where advantageous, to achieve short-

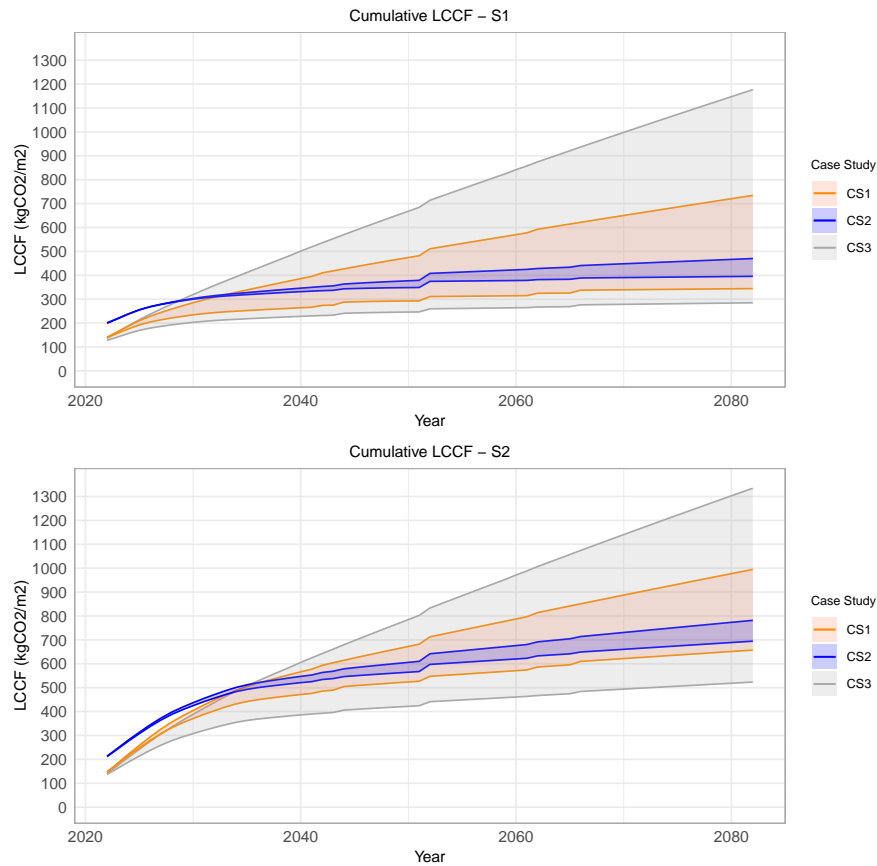


Figure 7.3: Aggregated LCCF over 60 year period across case studies for S1 and S2.

term carbon reductions, followed by gradual fabric enhancements to ensure long-term operational efficiency. A key concern with a system-first approach is the risk of mis-sizing systems, given the combined effects of future demand changes due to gradual fabric enhancements and climate change impacts. Further research is needed to determine the optimal timing of implementations and understand these trade-offs in the context of LCCF.

7.3 Responding to Research Questions

In light of the synthesis of case study findings provided in previous sections, the following research questions are addressed:

How do future climate projections impact the predicted operational energy performance of HE buildings?

Future climate projections had a strong impact on the predicted operational energy performance of the modelled HE buildings. The research findings indicated that, as average annual temperatures rise out to 2050, there would be a 10-25% reduc-

tion in overall **EUI** across the varying typologies under a high emission scenario, reflecting larger anticipated decreases in heating energy consumption compared to increases in cooling loads. Notably, substantial energy benefits were observed under the use of high **COP HVAC** systems, providing much greater **EUI** reductions under future climates compared to conventional gas-based technologies. Adapted solution sets -optimised under the adopted **CCA-LCA** methodology- demonstrated improved energy performance under both current and future climates.

Benchmarking against the wider UK **HE** building stock suggests that, if similar trends are observed across buildings within the same benchmarked categories, typical practice electricity benchmarks might increase from 70 to 76 kWh/m²/year for ‘Art and Design’ and from 64 to 68 kWh/m²/year for ‘Residential’. For fossil thermal **EUI**, there are substantial predicted reductions from 123 to 61 kWh/m²/year and from 199 to 152 kWh/m²/year, respectively. It is important to note that the uptake of electricity-based heating systems will further shift energy consumption from fossil fuels to electricity. However, the response to climate change will vary across different **HE** building typologies, emphasising the requirement for a contextual approach to climate change adaptation.

What are the life-cycle carbon and life-cycle cost implications of climate change adaptation strategies for urban HE building design?

Climate change adaptation strategies for urban HE buildings can result in significant **LCCF** reductions under the use of **GA** optimisation. Pareto-optimal solutions demonstrated substantial **LCCF** reductions under **ASHP** adoption relative to gas-based technologies. Consideration of changing carbon emission factors over time heightens the discrepancy in **LCCF** caused by electric and gas based systems, even under slower projected rates of grid decarbonisation.

Whilst heating system upgrades had the strongest impact on **LCCF** reduction across case studies, effective adaptation strategies require a balance between immediate system upgrades for short-term carbon reductions and gradual fabric enhancements to ensure long-term operational efficiency. However, the influence of climate change on changing heating and cooling demands requires evaluation of system sizing under various future climate scenarios. Overestimating or underestimating system capacity could compromise cost, efficiency and carbon savings, particularly as fabric enhancements would also alter building energy demands over time. This highlights the importance of testing and recalibrating design solutions to ensure adaptability and long-term efficiency under future climate conditions.

Whilst **EUI** and **LCCF** reductions were observed under implementation of the **CCA-LCA** framework, higher operational costs and capital expenditure associated with electricity-based systems may elevate **LCC**, particularly when fuel prices are projected based on current market conditions. However, substantial uncertainties

in gas decarbonisation and market dynamics complicate LCC projections.

The integration of LCA and CCA within a GA optimisation approach demonstrated its potential to balance energy efficiency, carbon reduction, and cost-effectiveness. The case studies revealed that optimised solutions could improve performance across multiple metrics while accommodating future climate impacts and decarbonisation pathways. The study underscored the importance of integrating dynamic decarbonisation pathways into LCA to provide a more realistic representation of long-term LCCF.

What are the trade-offs and synergies between embodied and operational carbon in HE building design?

The study demonstrated how trade-offs between EC and OC in HE building design can be complex and context-dependent. For example, whilst additional insulation can reduce OC, the associated EC may offset these gains, particularly in buildings already compliant with modern standards. This aligns with previous research indicating risks of ‘over-investment’ in the building envelope in cities with mild climates, low-carbon energy grids and high decarbonisation rates [203]. The choice of construction materials also plays a crucial role, with renewable materials like wood offering greater design flexibility across ‘optimal’ solution sets due to lower EC values compared to non-renewable materials like aluminium. It is important to note that these results account for the storage, sequestration, and release of biogenic carbon, which, if excluded, could lead to notably different outcomes.

Refrigerant leakage in ASHP systems contributes substantially to higher EC, but this is outweighed by their high operational efficiency and lower OC emissions. Furthermore, balancing OC emissions across heating and cooling end-uses increases design flexibility, allowing for a wider range of solution alternatives. Overall, optimising both EC and OC requires a nuanced approach that considers the tailored characteristics and operational demands of each building throughout its lifecycle.

How do uncertainties relating to grid decarbonisation impact the optimal selection of climate change adaptation strategies?

The research findings indicate that uncertainties relating to grid decarbonisation can significantly impact the selection of climate change adaptation strategies within the context of life cycle assessment frameworks for HE buildings.

Under slower decarbonisation scenarios, for design combinations relying on gas-based heating, the CCA-LCA methodology tends to place a disproportionate emphasis on strategies that reduce heating loads. This is because the carbon intensity of gas-based systems remains high, so reducing heating demand becomes

more critical to minimising **LCCF**. As a result, cooling load increases, which may also occur due to climate change, are given less priority in minimising **LCCF**. This imbalance can lead to suboptimal strategies that do not adequately address future cooling needs, potentially leading to higher overall carbon footprints and operational costs. The relationship between decarbonisation rates and **CCA** strategies is further complicated when considering the current use of gas-fired combined heat and power systems. These systems, which may initially offer carbon savings, see their “carbon pay-back” diminish over time as the grid becomes greener. Faster rates of electricity decarbonisation exacerbate this trend, making it more challenging to justify the continued use of combined heat and power systems as a viable **CCA** strategy in the long term.

When improved decarbonisation pathways are coupled with high-efficiency electric-based heating systems, the focus shifts. In these scenarios, cooling energy consumption becomes a more dominant component of the **LCCF**, dependent on the relative chiller efficiency. Under high-efficiency heating technologies, **CCA-LCA** optimised strategies tend to provide a more equal balance to heating and cooling load reductions. This highlights the importance of considering the long-term carbon intensity of specific energy end-uses in building design optimisation.

Furthermore, the study highlighted how **EC** becomes a more important factor during the optimisation process when faster rates of decarbonisation are assumed. When combined with the adoption of energy-efficient heating and cooling systems, the results suggested **EC** could account for over half of the refurbished buildings’ **LCCF**. In this situation, greater design flexibility with respect to impacts on operational energy use is provided, but a more significant weighting is given to the **EC** of design interventions. This can often lead to a more nuanced interplay between **EC** and **OC** emissions, as described in the previous research question.

Finally, some design solutions appeared optimal irrespective of decarbonisation scenario, indicating that certain **CCA** strategies and design parameters are robust enough to be effective under varying grid decarbonisation pathways. For example, for CS1, double glazing and S-facade **WWR** reductions were preferable regardless of decarbonisation assumptions. This suggests that incorporating grid decarbonisation uncertainties into the design process can lead to resilient and adaptable buildings.

7.4 Scaling-up and Methodological Development

7.4.1 Scaling-up

This section considers the consequences of extrapolating outputs from the perspective of scaled-up impact and methodological implications.

Extrapolated Impact

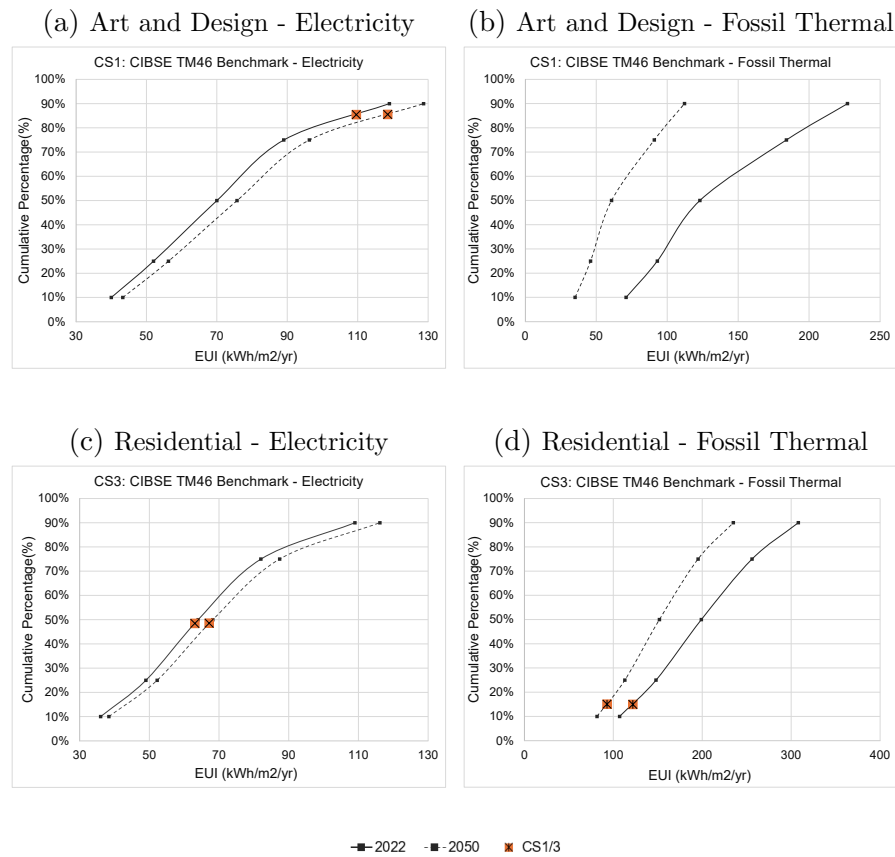
Benchmarking CS1 and CS3 EUIs against the wider UK HE building stock provides an indication of climate change impacts on scaled-up energy performance. CIBSE TM46 energy benchmarks provide up-to-date annual energy consumption data across a number of HE building typologies at a national level [190]. The analysis underpinning the development of these benchmarks is described by Hawkins et al. (2012) [173]. Aligning with case study results, the electricity and fossil thermal EUI for each building category is shown in Figure 7.4. The cumulative percentage (%) on the vertical axis represents how the buildings' energy performance compares to the wider dataset of benchmarked buildings of similar use types - effectively showing where it sits on the performance distribution curve. The graphs also illustrate how the entire distribution curve would shift if the wider HE building stock experienced proportional changes in energy use - due to climate change - to those observed in the case study building.

This demonstrates how, if future climate conditions drive some HE building typologies towards better overall energy performance, a reassessment of current benchmarks may be required. Across the three building categories, differences in spatial functions, operational profiles, internal gains, and envelope characteristics can influence the relative impact of external temperatures changes on thermal and energy performance. Indicative reductions in overall EUI benchmarks - 10% for 'art and design', 25% for 'other' and 13% for 'residential' - reflect the need to align future energy performance expectations with changing climate conditions. However, it is important to acknowledge that responses to climate change impacts will vary; sampling across the broader HE building stock could offer a clearer understanding of shifting energy end-uses across various typologies, as discussed in the subsequent section.

Methodological Impact

In the context of LCA-CCA framework implementation, the case study approach offers several methodological advantages and challenges.

Contextual Depth and Complexity The value of the case study approach lies in its ability to incorporate complex, real-world conditions of the buildings under study [204]. Each building's unique characteristics - ranging from its construction style to its operational patterns - are critical factors that influence the outcomes of the optimisation process. By focusing on these specific cases, the research captures a detailed understanding of how various interventions perform under realistic conditions, thereby enhancing the practical relevance of the findings. The approach allows for a rich, contextually grounded understanding of the complex interactions between building design, operational characteristics, and future climate and decarbonisation scenarios.



	Academic - art and design				Residential			
	Electricity		Fossil		Electricity		Fossil	
	2022	2050	2022	2050	2022	2050	2022	2050
Good practice - 25 th percentile	52	56	93	46	49	52	148	113
Typical practice - 50 th percentile	70	76	123	61	64	68	199	152

Figure 7.4: CIBSE TM46 current and predicted benchmarked EUI, simulated under 2022 and 2050 weather data [190].

Holistic Evaluation The use of multiple sources of evidence, including life-cycle carbon and cost impacts, and future climate projections, allows for a comprehensive evaluation of the building design strategies. In this study, the feedback process evaluating the impact of energy system decarbonisation assumptions further enriches the analysis, providing a robust methodology for assessing the sensitivity of the design strategies to various decarbonisation pathways. However, the process did not explicitly account for indoor environmental quality factors (e.g. lighting, air quality, noise). While building models aligned with relevant lighting and ventilation standards [174, 181, 205], direct optimisation of comfort parameters was beyond the scope of the analysis. In practice, design decisions are shaped by a balance between energy performance and occupant wellbeing, and improvements in one domain may compromise another [16].

Academic Rigor and Bias The complexity of LCA data pathways and the nu-

merous assumptions involved provide opportunity for heightened subjectivity and biases. This challenge is compounded by limited availability and variability of input data, particularly pertaining to embodied carbon data sources. Combined with inherent researcher biases, uncertainties and inconsistencies associated with detailed case study analysis can have a strong influence on the reliability and accuracy of conclusions drawn, necessitating a structured and objective research approach.

Generalisation of Findings One of the primary limitations of the case study approach is the difficulty in generalising findings to other contexts. The specific conditions and characteristics of the three university buildings mean that the results may not be directly applicable to other buildings with different contexts. By comparison, sampling approaches, which aim to achieve statistical generalisation through the study of representative subsets, offer a different set of strengths and weaknesses. In this research context, a sampling approach might involve studying a larger number of buildings to draw broader conclusions about optimal design strategies under varying decarbonisation pathways. This could provide statistically significant results that are more generalisable. However, sampling methods often require controlled conditions that may not fully capture the nuanced interactions present in actual operational settings, potentially overlooking important factors that influence building performance.

7.4.2 Methodological Development

This research introduces a novel methodological approach that integrates [LCA](#), [CCA](#), and multi-objective optimisation to evaluate long-term refurbishment strategies under evolving climate and energy system conditions. Existing [LCA](#) studies in the non-domestic building sector typically rely on static, short-term assumptions - often applying fixed carbon emission factors and steady-state climate conditions that overlook dynamic future uncertainties. By contrast, the methodology developed here embeds projected climate change, grid decarbonisation, and systems-fabric interactions within a unified optimisation framework, enabling a more realistic assessment of long-term performance trade-offs.

Furthermore, by employing a genetic algorithm (NSGA-II), the framework identifies non-obvious Pareto-optimal solutions across competing objectives of [LCC](#) and [LCCF](#). This approach enables exploration of thousands of design combinations, capturing non-linear and non-additive relationships between passive and active measures that are often oversimplified in traditional parametric or rule-of-thumb methods. Dynamic simulation modelling provides the necessary temporal resolution to correctly size systems (e.g. [ASHPs](#)) and evaluate performance under changing demand patterns.

The methodology therefore moves beyond static [LCAs](#), towards a dynamic

decision-support framework capable of handling uncertainty and complexity in future energy and climate conditions. Grounded in established standards (EN 15978, ISO 14040) and proven optimisation techniques [17, 56, 127], it redefines retrofit prioritisation by:

- Embedding long-term climate and energy system uncertainty into the [LCA](#) process;
- Challenging the continued use of fixed carbon factors in [LCA](#) and highlighting the growing dominance of embodied impacts;
- Revealing how systems–fabric trade-offs evolve over time as operational carbon declines;
- Providing a scalable, evidence-based framework for aligning carbon and cost decisions with future decarbonisation pathways.

The three case studies revealed both distinct challenges and common outcomes upon application of the [CCA-LCA](#) optimisation methodology. The introduction of high-efficiency, electric based heating systems had the most significant impact on [LCCF](#) reduction across all three case-studies. However, unique refurbishment solutions emerged due to the distinct characteristics of each building. In the architecture school (CS1), the need for flexible systems operations meant that optimisation prioritised ventilation control strategies, with additional insulation or glazing upgrades offering limited benefit once electric systems were introduced. The office building (CS2) balanced heritage preservation with improved thermal performance, where airtightness, and window frame improvements, paired with efficient ventilation control, yielded significant [LCCF](#) reductions. In the university residential accommodation (CS3), high domestic hot water demands influenced optimisation outcomes, with heating system type and glazing area reductions emerging as the most influential factors. This variability demonstrated the importance of tailoring interventions to typology-specific needs while identifying scalable strategies for the [HE](#) sector. This approach provides a robust foundation for evaluating design interventions and their long-term carbon and cost impacts. However, successful practical application requires integration with the wider design process, from concept through to facility management. In the following section, a framework is proposed for integrating [CCA-LCA](#) into the design process, aligning research outcomes from this study with best practice industry guidance.

7.5 Integrating CCA-LCA Framework into the Design Process

A high-level framework is proposed in Figure 7.5 to integrate the [CCA-LCA](#) genetic algorithm optimisation process into the design process, with focus on urban

HE estates. This framework intends to ensure that both climate adaptation and life cycle impacts are systematically addressed from the early design stages through to construction and facility management. The proposed framework builds on existing design protocols and emphasises the need for a multi-disciplinary approach. The key stages are outlined below.

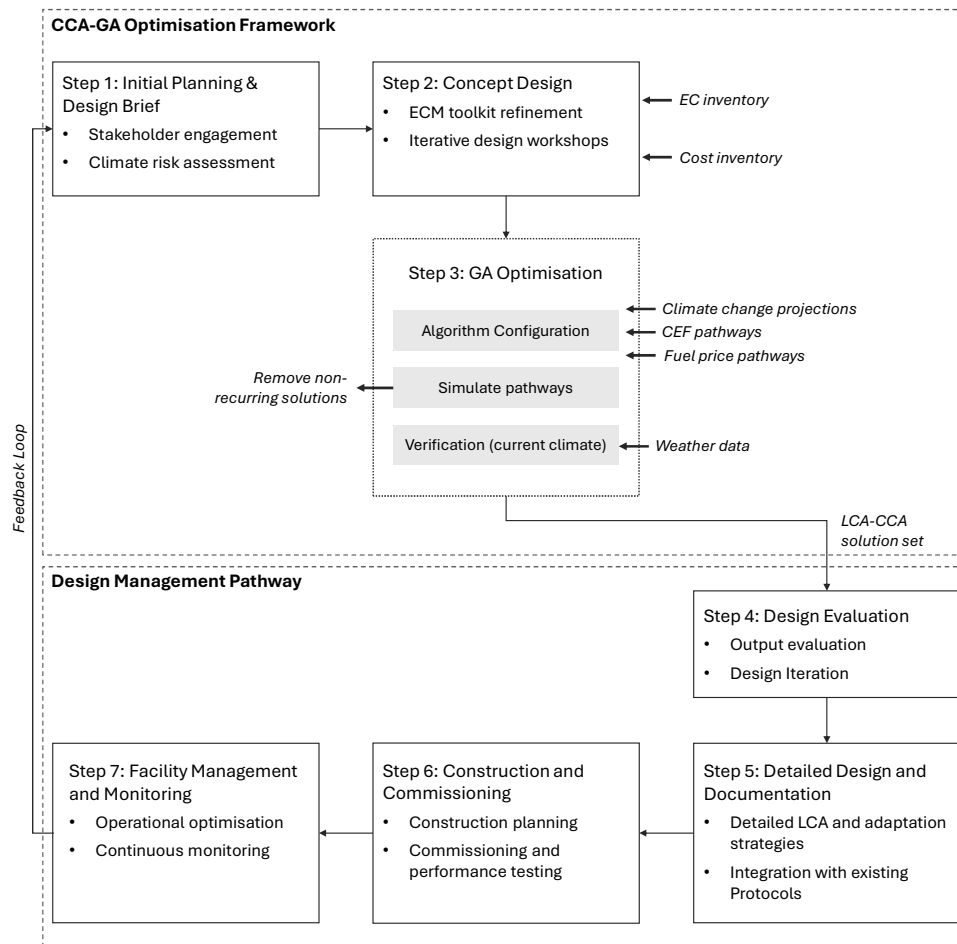


Figure 7.5: Suggested framework for integration of LCA-CCA into wider design process.

Step 1: Initial Planning and Design Brief

Stakeholder Engagement: Engage key stakeholders, such as architects, engineers, facility managers, and sustainability experts, to define the project's goals, constraints, and performance criteria.

Climate Risk Assessment: Conduct preliminary climate risk assessments to identify potential vulnerabilities in existing design.

Step 2: Concept Design

ECM Refinement: Use outcomes from initial assessment to refine/update **ECM** toolkit (see section 3.4.4).

Iterative Design Workshops: Develop initial design according to baseline analysis, ensuring that adaptation strategy options are integrated from the outset. This will serve as a starting point for the NSGA-II **GA** optimisation.

Step 3: **GA** Optimisation

Algorithm Configuration: Configure NSGA-II **GA** to optimise for **LCCF** and **LCC** under future climates and range of decarbonisation scenarios.

Run Simulations: Identify recurring Pareto-optimal solutions that balance performance criteria and perform well across a range of decarbonisation pathways.

Verification: Assess solution performance under present-day conditions.

Step 4: Design Evaluation

Output Evaluation: Evaluate NSGA-II outputs against project design requirements and identify potential conflicts, including assessment of trade-offs regarding **EC** vs. **OC** and **CapEx** vs. **OpEx**.

Design Iteration: Iterate the design based on feedback from evaluations, ensuring that the selected solutions align with overall project goals and stakeholder expectations.

Step 5: Detailed Design and Documentation

Detailed LCA and Adaptation Strategies: Develop detailed life cycle analyses and adaptation strategies for the selected design. Document the impacts and benefits of the proposed solutions.

Integration with Existing Protocols: Ensure compatibility with existing design frameworks, such as BREEAM, LEED, and WELL standards [CITE].

Step 6: Construction and Commissioning

Construction Planning: Incorporate **CCA-LCA** outputs into construction planning to minimize disruptions and ensure adherence to sustainability targets.

Commissioning and Performance Testing: Conduct thorough commissioning and performance testing to validate that design specifications are met and adaptation strategies implemented.

Step 7: Facility Management and Monitoring

Operational Optimisation: Implement facility management protocol to optimise

operational performance and maintain adaptation measures.

Continuous Monitoring: Establish a monitoring system to track energy use, carbon emissions, and climate impacts, facilitating ongoing performance improvements.

Chapter 8

Conclusion

This research investigated the integration of an [LCA-CCA](#) combined approach within the design process of [HE](#) buildings, focusing on impacts on energy, carbon, and cost metrics. A synthesis of findings from three detailed case studies [HE](#) buildings was provided, with distinct geometries, thermo-physical properties, and operational characteristics. The buildings were analysed under future climate and decarbonisation scenarios using multi-objective [GA](#) optimisation. The conclusion consolidates the main insights from this study and addresses the research questions, limitations and proposed directions for future work.

8.1 Summary of Key Findings

The synthesis of case study findings underscored several important points regarding the determinants of future energy, carbon, and cost impacts in [HE](#) building design:

Energy Use Intensity (EUI):

Future climates may lead to reductions in overall [EUI](#) due to larger anticipated decreases in heating energy relative to increases in cooling loads. Predicted reductions in overall [EUI](#) were 10% for ‘art and design’, 25% for ‘other’, and 13% for ‘residential’, indicating the need to reassess current benchmarks in light of evolving climate conditions. However, varying responses to climate change impacts across different building typologies highlight the importance of broader sampling to better understand these shifts in energy end-uses. Optimised adapted solutions generally demonstrated improved energy performance over non-adapted models for both present and future conditions, indicating the efficacy of the [CCA-LCA](#) approach in enhancing energy efficiency without adverse effects on present-day energy consumption.

Life Cycle Carbon Footprint (LCCF):

Operational efficiency and fuel source were found to significantly influence LCCF, with electricity-based systems like ASHPs showing potential for substantial LCCF reductions compared to gas-based systems over the buildings life-cycle, despite higher emissions associated with refrigerant use. The study found that cumulative year-on-year LCCF impact remained relatively consistent only for S1 ASHP scenarios, while slower decarbonisation rates and gas-based heating technologies led to significant LCCF increases beyond the building's life-cycle.

Upgrading to ASHPs before implementing gradual fabric improvements was shown to be a sensible approach where baseline thermal performance and airtightness were already sufficient for efficient heat pump operation. In these contexts, early system replacement leverages the benefits of grid decarbonisation and delivers greater carbon savings than immediate deep fabric retrofits. Subsequent, incremental fabric enhancements can then be targeted to optimise system performance. This challenges the traditional “fabric first” approach by demonstrating that, under evolving energy and emissions conditions, prioritising low-carbon systems can achieve greater and faster reductions in whole-life carbon impact. However, further research is needed to address potential system mis-sizing due to changing energy demands and climate impacts. The findings emphasise the importance of dynamic decarbonisation pathways over fixed-rate carbon emission factors for a more realistic representation of long-term carbon impacts.

Embodied vs. Operational Carbon:

The research revealed intricate trade-offs between embodied and operational carbon emissions in the context of the three HE buildings under study, particularly in relation to insulation and material choices. The key findings relating to the interplay between EC and OC were:

- The balance of embodied and operational carbon in the building envelope appeared to be relatively nuanced with respect to insulation thickness; trade-offs between EC and OC savings indicate insulation increases beyond current industry-standard U-values led to a higher LCCF.
- Low-carbon construction materials, such as wooden louvres, appeared to offer greater design flexibility amongst CCA-LCA optimised solutions compared to carbon-intensive materials like aluminium.
- Despite the higher embodied emissions from refrigerants in ASHP systems, their overall benefits in reducing operational carbon emissions justify EC increases.

- Equally weighting of OC emissions for heating and cooling energy use broadened CCA-LCA optimised design alternatives, avoiding a narrow focus on heating reduction strategies.

Life Cycle Cost (LCC):

While the CCA-LCA optimisation process effectively reduced EUI and LCCF, achieving significant LCC reductions remained challenging due to higher projected operational costs associated with electricity-based technologies. Extrapolating future fuel price projections from current market signals can lead to oversimplifications regarding the complex interplay between market dynamics, rapid low-carbon technology adoption and electricity energy prices. The volatility of unabated natural gas price signals adds significant uncertainty to life-cycle cost projections; decoupling electricity prices from gas may reduce this uncertainty, providing a clearer outlook with regards to the LCCF of refurbishment measures. The study highlighted challenges of balancing cost savings with carbon reductions and the need for careful consideration of environmental and economic trade-offs in HE building design.

8.2 Final Remarks

This research contributes to the growing body of knowledge on utilising GAs for building design optimisation by demonstrating the benefits of integrating LCA and CCA frameworks within the design process of HE buildings. The findings underscore the importance of a holistic approach to building design and refurbishment that balances life-cycle carbon with life-cycle cost, and operational carbon with embodied carbon impacts, under the face of future climate challenges. The future energy use and LCCF of HE buildings will likely be shaped by both building performance improvements and changing climatic conditions. The movement towards electric heating and cooling systems, combined with the improved thermal performance of building envelopes, indicates a trend towards lower operational carbon emissions. However, this also necessitates a focus on reducing embodied carbon in building materials and systems to balance overall LCCF. By providing a detailed methodological approach and identifying key trade-offs and synergies based on various decarbonisation pathways, this research provides valuable insights for practitioners and policymakers to improve the future climate resilience of the HE sector.

8.3 Limitations and Further Development

The research design makes use of available secondary datasets, databases and tools to ensure a viable time-frame for completion. These resources were selected to effectively respond to the aims identified, however, it is important to note several limitations that should be considered alongside research outcomes:

Data quality and availability Secondary data sources are used to develop and calibrate building energy models. The quality of datasets may impact the validity of the models being investigated, and the reliability of simulated outputs. A pre-processing step is carried out on secondary datasets included in this analysis to ensure reliability of model inputs. The selected time period for operational energy consumption analysis is considered to avoid irregular or extreme occupancy behaviour patterns, such as the 2020-21 building closures during the covid-19 pandemic.

Embodied carbon databases EPDs are not yet mandatory in industry; as such, data availability is still limited, particularly in relation to HVAC systems. The primary reference for EC data is the ICE v3 database, which selects peer-reviewed and verified values according to consistent criteria and professional feedback [60]. When specific information is not available in ICE v3, EPDs directly from manufacturers are used. EN 15804 aims to harmonise the assessment protocol of EPDs in the construction sector, enhancing transparency and comparability [58]. Regardless, questions of impartiality should still be considered, since process-related information may be provided by the manufacturers themselves. Additionally, since participation in the EPD process is voluntary, the data may not be representative of products at an industry-wide scale.

Operational carbon calculation Dynamic thermal simulation (DTS) modelling is used for the assessment of operational carbon impacts. The simulation tool adopted is industry-standard and widely used in building retrofit optimisation research, having undergone numerous reliability tests and been verified by third-parties to be within the level of accuracy required for building design. However, underlining calculations vary between DTS tool providers and provide a simplification of real-world phenomena that exist in practice.

Probabilistic climate projections The future climate projections used in this study are based on UKCP09, processed for application within building performance simulation [96]. UKCP09 has certain limitations, including lower spatial resolution and a narrower range of emission scenarios, relative to more recent models [99]. UKCP18 provides higher spatial resolution, more detailed regional data and updated emission scenarios [99]. Although UKCP18 was not available at the time of the study, its advancements offer more robust and up-to-date projections that better capture climate variability and

change at a finer scale.

Furthermore, the study adopts a high emission scenario, representative concentration pathway (RCP) 8.5, for the period 2061-2080, assessed at a 50th percentile projection [206]. Future studies should aim to capture the influence of a wider range of uncertainty in future weather projections on optimisation outputs.

Grid decarbonisation assumptions Incorporating long-term CEFs and fuel price projections associated with grid decarbonisation pathways introduces a high level of inherent uncertainty. While grid decarbonisation assumptions aim to capture broad trends in decarbonisation pathways, they are subject to significant variability due to fluctuations in energy pricing, grid properties, and the many factors influencing the uptake of renewable energy. Predicting the rate of grid decarbonisation and its subsequent impact on fuel prices remains challenging, as long-term forecasts are inherently volatile and sensitive to a range of uncertain variables. Although sensitivity analyses were employed to capture variations in pathways, only two decarbonisation scenarios (best-case and worst-case) were considered in detail. Expanding the range of scenarios may help better account for potential fluctuations in energy prices and decarbonisation trajectories. Additionally, grid decarbonisation was only considered for the operational aspect of the LCA, not embodied carbon, as incorporating future decarbonisation trends into manufacturing processes would require tracking complex, evolving supply chains. While beyond the scope of this study, integrating these factors could be valuable for future work.

ECM selection process The selection of design strategies for inclusion in the optimisation process is subjective in nature. Whilst steps were taken to justify any assumptions made, results may differ depending on geometric, fabric and system design specifications included in the optimisation process. Therefore, the design solutions are highly specific to the building in question and cannot be generalised across case studies. Several steps are taken to attempt to minimise subjectivity involved in the selection of energy conservation measures; a detailed discussion is provided in section 3.4.4.

Capturing non-quantifiable impacts in LCA LCA in building design typically focuses on quantitative metrics, such as energy consumption, emissions, and cost. However, broader environmental and social factors - like biodiversity or social equity - are difficult to capture quantitatively. Further research studies could aim to integrate multi-criteria assessment to combine quantitative and qualitative data. This would provide a more holistic view of environmental and economic impacts, reflecting a broader ethical commitment to sustainability.

Boundary Conditions for LCA This study focuses on building-level impacts, prioritising operational and direct emissions within the life-cycle boundary. While assumptions about green gas grid integration (e.g., hydrogen infrastructure) are included in terms of operational CEFs, the broader environmental and economic implications of constructing new energy infrastructure - such as the EC and CapEx associated with hydrogen grid development - are excluded. Incorporating these upstream factors would enhance the comprehensiveness of the life-cycle assessment but introduces substantial uncertainty, particularly given the speculative nature of large-scale infrastructure deployment.

8.3.1 Framework Development

In response to the research study outputs, the following areas of work are recommended for further development of the CCA-LCA framework.

Advancing the Dynamic Approach to CCA-LCA Optimisation Pathways

Investigating building design performance under future climate scenarios can significantly contribute to the “future-proofing” of buildings. However, in practice, climate change will occur gradually over a building’s lifespan. Ideally, building design characteristics should evolve correspondingly, adopting modular, interchangeable features that can be reused and repurposed to meet changing environmental demands at different climate stages. The current framework employs a single snapshot from a mid-range timepoint (2050, averaged from 2040-2069). Incorporating a more dynamic continuation of climate projections may yield greater insights into the optimisation of design progression over time.

Moreover, retrofit measures are often staggered, with fabric and systems being updated at different points in the building’s life cycle. It is important to investigate this impact, not only to understand the implications of sequential ‘one-by-one’ adjustments to optimal solution sets with respect to LCCF and LCC, but also to optimise the prioritisation of retrofits in line with evolving climatic conditions. For instance, the trade-off between EC and OC associated with insulation thickness will change over time with increasing average outdoor temperatures. Thus, the time-of-intervention within the 60-year LCA window should be addressed and optimised. This approach enables adaptation frameworks to incorporate future flexibility, allowing resilience to be incorporated at a later stage, when required.

Similarly, future framework developments should consider the dynamic nature of embodied carbon in construction materials and systems. Existing LCA frame-

works frequently utilise top-level assumptions regarding the life-cycle stages of products, applying the same assumptions across all material categories. As grid pathways decarbonise, the **EC** associated with the manufacture and distribution of specific products is also expected to decrease alongside operational carbon emissions. For example, research has demonstrated how future scenarios will likely impact the recycling rates of **ASHPs**, not just their operational emissions [55]. However, it is also important to acknowledge that overall **LCCF** is still typically most sensitive to operational emissions.

Comprehensive Analysis of Uncertainties and Sensitivities in CCA-LCA Frameworks

Uncertainties associated with the dynamic nature of climate change, carbon emissions, and cost pathways are inherent to studies projecting future scenarios. Typically, future climate uncertainties are addressed through the use of probabilistic climate projections, such as UKCP09 and UKCP18 [207]. Further investigation is required into the most effective methodologies for quantifying and addressing uncertainties related to grid decarbonisation scenarios and fuel price pathways. A robust approach to assessing these uncertainties could provide a more holistic assessment of potential impacts on **LCCF** and **LCC**.

In addition, further work can aim to assess the impact of policy implementation on optimised framework outputs. For instance, exploring the effect of carbon pricing could reveal the thresholds necessary to achieve specific carbon reduction scenarios and encourage increased uptake of energy efficiency measures. This approach can help to determine how expensive carbon would need to be to make a particular scenario feasible, providing valuable insights for policy development and economic planning.

Real-World Validation of LCA-CCA in HE Sector Building Design Frameworks

Effective integration of the **LCA-CCA** optimisation process within existing **HE** building design frameworks necessitates real-world validation. Computational models often fail to capture design conflicts and synergies, particularly in relation to the challenges and complexities of urban environments. Given the critical role of **IEQ** in **HE** design and its impact on productivity, potential conflicts between **GA** optimisation outputs and **IEQ** parameters, such as lighting, indoor air quality, and noise pollution, must be addressed.

Developing and testing the proposed **CCA-LCA** integration framework, detailed in Section 7.5, can help to evaluate its practical application. This includes assessing

outputs against design requirements and conflicts in urban [HE](#) estates, addressing practical barriers across the design, construction, and facility management chain (such as operational disruption), and ensuring compatibility with existing building design protocols.

Furthermore, it is crucial to understand how stakeholder perceptions and preferences influence the selection of climate adaptation strategies within the [HE](#) sector. Incorporating these human factors into the decision-making process, in harmony with the [CCA-LCA](#) optimisation process, is essential for tailoring the framework to the specific needs of the [HE](#) sector.

Multidimensionality of Decision Metrics

A limitation of this study lies in the evaluation of design iterations through a two-dimensional lens, focusing solely on [LCCF](#) and [LCC](#). Several design aspects may provide mutual benefits from a carbon and cost perspective but fall short when measured against alternative criteria. For example, previous research has indicated that [ASHPs](#) perform less favorably than [NGBs](#) with respect to other environmental impacts [55]. This underscores the importance of considering environmental factors beyond carbon emissions. Moreover, valuing climate change adaptation strategies based purely on economic and environmental perspectives may overlook crucial metrics influencing the in-use success or failure of a design. A comprehensive framework for climate change adaptation should encompass a wider range of evaluation metrics derived through a systems dynamic approach, such as student and staff satisfaction, productivity, and other socio-economic factors.

Expanding System Boundaries

Future research could explore a combined building-infrastructure approach to fully evaluate the interconnected impacts of decarbonisation pathways. Such an approach could expand the traditional life-cycle boundary of a building to include the [EC](#) and [CapEx](#) associated with the development of supporting energy infrastructures, such as hydrogen grids or large-scale renewable energy systems. By integrating these broader systemic factors, researchers could gain a more holistic understanding of the trade-offs and synergies between building-level interventions and wider energy network changes. This would allow for a more comprehensive assessment of how building designs interact with decarbonising energy grids, providing insights into optimal strategies for scaled-up sustainable infrastructure at a national level.

8.3.2 Case Study Application

Further research is required to understand the relative impacts of case study modelling approaches on [LCA-CCA](#) frameworks. For example, the level of calibration varied across the case studies according to the quality of available data. The importance of calibration robustness is a key consideration requiring further assessment. One argument posits that the uncertainties inherent in future climate data necessitate the use of highly calibrated models to mitigate additional uncertainty as much as possible. However, if future weather data introduces significant uncertainty, the relative impact of model error and uncertainty might diminish, making extremely detailed calibration less critical. Thus, the balance between the level of calibration detail and the overarching uncertainties from future climate projections must be carefully managed to ensure the practical applicability of the [LCA-CCA](#) framework.

References

- [1] Myles R Allen, Opha Pauline Dube, William Solecki, Fernando Aragón-Durand, Wolfgang Cramer, Stephen Humphreys, M Kainuma, J Kala, N Mahowald, Y Mulugetta, R Perez, M Wairiu, and K Zickfeld. *Framing and Context. In: Global Warming of 1.5° C. An IPCC Special Report on the impacts of global warming of 1.5° C above pre-industrial levels and related global greenhouse gas emission pathways, in the context of strengthening the global response to the.* Tech. rep. 2018. URL: https://www.ipcc.ch/site/assets/uploads/sites/2/2019/10/SR15_1SM_Low_Res.pdf.
- [2] NASA. *Carbon Dioxide — Vital Signs – Climate Change: Vital Signs of the Planet.* Nov. 2020. URL: <https://climate.nasa.gov/vital-signs/carbon-dioxide/>.
- [3] Thomas F Stocker, Dahe Qin, Gian-Kasper Plattner, Melinda M B Tignor, Simon K Allen, Judith Boschung, Alexander Nauels, Yu Xia, Vincent Bex, and Pauline M Midgley. *IPCC, 2013: Climate Change 2013: The Physical Science Basis. Contribution of Working Group I to the Fifth Assessment Report of the Intergovernmental Panel on Climate Change.* Tech. rep. Cambridge: IPCC, 2013. URL: www.cambridge.org.
- [4] Met Office. *UK Climate Projections: Headline Findings.* Tech. rep. 2022. URL: www.metoffice.gov.uk.
- [5] J M Murphy, G R Harris, D M H Sexton, E J Kendon, P E Bett, R T Clark, K E Eagle, G Fossler, F Fung, J A Lowe, R E McDonald, R N McInnes, C F McSweeney, J F B Mitchell, J W Rostron, H E Thornton, S Tucker, and K Yamazaki. *UKCP18 Land Projections: Science Report.* Tech. rep. Met Office, 2018. URL: <https://www.metoffice.gov.uk/pub/data/weather/uk/ukcp18/science-reports/UKCP18-Land-report.pdf>.
- [6] Lei Fang, David Wyon, Geo Clausen, and Povl Ole Fanger. “Sick Building Syndrome symptoms and performance in a field laboratory study at different levels of temperature and humidity”. In: (2002). URL: <https://orbit.dtu.dk/en/publications/sick-building-syndrome-symptoms-and-performance-in-a-field-labora>.

- [7] Keith Dear. “Modelling Productivity Loss from Heat Stress”. In: *Atmosphere* 9.7 (July 2018), p. 286. ISSN: 2073-4433. DOI: [10.3390/atmos9070286](https://doi.org/10.3390/atmos9070286). URL: <http://www.mdpi.com/2073-4433/9/7/286>.
- [8] Paraskevi Vivian Dorizas, Margarita Niki Assimakopoulos, and Mattheos Santamouris. “A holistic approach for the assessment of the indoor environmental quality, student productivity, and energy consumption in primary schools”. In: *Environmental Monitoring and Assessment* 187.5 (May 2015), pp. 1–18. ISSN: 15732959. DOI: [10.1007/s10661-015-4503-9](https://doi.org/10.1007/s10661-015-4503-9). URL: <https://pubmed.ncbi.nlm.nih.gov/25877649/>.
- [9] Li Lan, Lulu Xia, Rihab Hejjo, David P Wyon, and Pawel Wargocki. “Perceived air quality and cognitive performance decrease at moderately raised indoor temperatures even when clothed for comfort”. In: *Indoor Air* 30.5 (Sept. 2020), pp. 841–859. ISSN: 16000668. DOI: [10.1111/ina.12685](https://doi.org/10.1111/ina.12685). URL: <https://onlinelibrary.wiley.com/doi/abs/10.1111/ina.12685>.
- [10] Chryso Heracleous and Aimilios Michael. “Assessment of overheating risk and the impact of natural ventilation in educational buildings of Southern Europe under current and future climatic conditions”. In: *Energy (Oxford)* 165 (2018), pp. 1228–1239. ISSN: 0360-5442. DOI: [10.1016/J.ENERGY.2018.10.051](https://doi.org/10.1016/J.ENERGY.2018.10.051).
- [11] Pieter de Wilde and David Coley. *The implications of a changing climate for buildings*. 2012. DOI: [10.1016/j.buildenv.2012.03.014](https://doi.org/10.1016/j.buildenv.2012.03.014).
- [12] AUDE. *Higher Education Estates Management Report: Summary, insights and analysis of the 2021/22 academic year*. Tech. rep. 2023. URL: <https://www.aude.ac.uk/news-and-blogs/emr-report/>.
- [13] The Royal Anniversary Trust. “Accelerating the UK Tertiary Education Sector towards Net Zero A sector-led proposal for action and connected thinking”. In: (2023). URL: <https://royalanniversarytrust.org.uk/wp-content/uploads/2023/01/Accelerating-towards-Net-Zero.pdf>.
- [14] AUDE. *Higher Education estates statistics report 2014*. Tech. rep. 2014. URL: <https://www.aude.ac.uk/Resources/>.
- [15] Jie Dong, Yair Schwartz, Ivan Korolija, and Dejan Mumovic. “The impact of climate change on cognitive performance of children in English school stock: A simulation study”. In: *Building and Environment* 243 (2023), p. 110607. DOI: [10.1016/j.buildenv.2023.110607](https://doi.org/10.1016/j.buildenv.2023.110607). URL: <http://creativecommons.org/licenses/by/4.0/>.
- [16] CIBSE. *Integrated school design*. Tech. rep. 2015. URL: www.cibse.org.
- [17] BSI. *BS EN 15978:2011 - Sustainability of construction works. Assessment of environmental performance of buildings. Calculation method*. Tech. rep. BSI, 2011. URL: <https://shop.bsigroup.com/ProductDetail/?pid=000000000030256638>.

- [18] BSI. *BS ISO 15686-5:2017 - Buildings and constructed assets — Service life planning — Part 5: Life-cycle costing*. Tech. rep. Geneva: BSI, 2017. URL: <https://www.iso.org/standard/61148.html>.
- [19] RICS. *Whole life carbon assessment for the built environment, RICS professional statement, UK, 1st edition*. Tech. rep. London: Royal Institution of Chartered Surveyors, 2017. URL: www.rics.org.
- [20] X J Luo and Lukumon O Oyedele. “Life cycle optimisation of building retrofitting considering climate change effects”. In: *Energy and Buildings* 258 (2022), p. 111830. ISSN: 0378-7788. DOI: <https://doi.org/10.1016/j.enbuild.2022.111830>. URL: <https://www.sciencedirect.com/science/article/pii/S0378778822000019>.
- [21] Pengyuan Shen, William Braham, and Yunkyu Yi. “The feasibility and importance of considering climate change impacts in building retrofit analysis”. eng. In: *Applied energy* 233-234 (2019), pp. 254–270. ISSN: 0306-2619. DOI: [10.1016/j.apenergy.2018.10.041](https://doi.org/10.1016/j.apenergy.2018.10.041).
- [22] A T D Perera, Vahid M Nik, Deliang Chen, Jean-Louis Scartezzini, and Tianzhen Hong. “Quantifying the impacts of climate change and extreme climate events on energy systems”. In: *Nature Energy* 5.2 (2020), pp. 150–159. ISSN: 2058-7546. DOI: [10.1038/s41560-020-0558-0](https://doi.org/10.1038/s41560-020-0558-0).
- [23] Małgorzata Rymarzak and Alexi Marmot. “Higher Education Estate Data Accountability: The Contrasting Experience of UK and Poland”. In: *Higher Education Policy* 33 (2020), pp. 179–194. DOI: [10.1057/s41307-018-0109-5](https://doi.org/10.1057/s41307-018-0109-5). URL: www.palgrave.com/journals.
- [24] HESA. *Table 1 - Buildings and spaces — HESA*. Aug. 2021. URL: <https://www.hesa.ac.uk/data-and-analysis/estates/table-1>.
- [25] HESA. *Table 2 - Energy by HE provider and academic year*. Aug. 2021. URL: <https://www.hesa.ac.uk/data-and-analysis/estates/table-2>.
- [26] Ian Ward, Anthony Ogbonna, and Hasim Altan. “Sector review of UK higher education energy consumption”. In: *Energy Policy* 36.8 (Aug. 2008), pp. 2939–2949. ISSN: 0301-4215. DOI: [10.1016/J.ENPOL.2008.03.031](https://doi.org/10.1016/J.ENPOL.2008.03.031).
- [27] William Whyte. *Redbrick : A social and architectural history of Britain's civic universities*. June 2021. 2015, pp. 1–2. ISBN: 9780198716129. URL: <https://www.history.ox.ac.uk/publication/673921/manual>.
- [28] Christopher Beanland. “Concrete concept : brutalist buildings around the world / Christopher Beanland”. In: (2016). URL: https://discovery.upc.edu/iii/encore/record/C__Rb1479423?lang=cat.
- [29] Gov.uk. *Building Act 1984*. 1984. URL: <https://www.legislation.gov.uk/ukpga/1984/55>.

- [30] Martin Trow. “Reflections on the Transition from Elite to Mass to Universal Access: Forms and Phases of Higher Education in Modern Societies since WWII”. eng. In: *International Handbook of Higher Education*. Springer International Handbooks of Education. Dordrecht: Springer Netherlands, pp. 243–280. ISBN: 1402040113. DOI: [10.1007/978-1-4020-4012-2_13](https://doi.org/10.1007/978-1-4020-4012-2_13).
- [31] EAUC. *Sustainability Commitments*. URL: https://www.eauc.org.uk/sustainability_commitments.
- [32] Priestley Centre for Climate Futures. *Analysis reveals scale of tertiary education’s carbon emissions*. 2023. URL: <https://climate.leeds.ac.uk/news/analysis-reveals-scale-of-tertiary-educations-carbon-emissions/>.
- [33] Shaikh M.S.U. Eskander and Khandokar Istiak. “Energy efficiency and CO2 emissions: evidence from the UK universities”. In: *Applied Economics* 55.41 (2023), pp. 4727–4744. ISSN: 14664283. DOI: [10.1080/00036846.2022.2130872/ASSET/2A10B795-E3D4-4519-98F7-D009F168530B/ASSETS/IMAGES/RAEC_A_2130872_F0004_OC.JPG](https://doi.org/10.1080/00036846.2022.2130872/ASSET/2A10B795-E3D4-4519-98F7-D009F168530B/ASSETS/IMAGES/RAEC_A_2130872_F0004_OC.JPG). URL: <https://www.tandfonline.com/action/journalInformation?journalCode=raec20>.
- [34] Gov.uk. *The Building Regulations 2010*. URL: <https://www.legislation.gov.uk/uksi/2010/2214/contents>.
- [35] European Commission. *Energy Efficiency Directive*. URL: https://energy.ec.europa.eu/topics/energy-efficiency/energy-efficiency-targets-directive-and-rules/energy-efficiency-directive_en.
- [36] Official Journal of the European Union. *DIRECTIVE (EU) 2018/844 OF THE EUROPEAN PARLIAMENT AND OF THE COUNCIL of 30 May 2018 amending Directive 2010/31/EU on the energy performance of buildings and Directive 2012/27/EU on energy efficiency*. 2018. URL: <https://eur-lex.europa.eu/eli/dir/2018/844/oj/eng>.
- [37] Gov.uk. *Public Sector Decarbonisation Scheme: Phase 3*. URL: <https://www.gov.uk/government/publications/public-sector-decarbonisation-scheme-phase-3>.
- [38] Gov.uk. *CRC Energy Efficiency Scheme: closure guidance for participants*. URL: <https://www.gov.uk/guidance/crc-energy-efficiency-scheme-closure-guidance-for-participants>.
- [39] Gov.uk. *Climate Change Levy: detailed information*. URL: <https://www.gov.uk/government/collections/climate-change-levy-detailed-information>.
- [40] Gov.uk. *Climate Change Act 2008*. 2008. URL: <https://www.legislation.gov.uk/ukpga/2008/27/contents>.

- [41] Scottish Parliament. *Climate Change (Scotland) Act 2009*. 2009. URL: <https://www.legislation.gov.uk/asp/2009/12/contents>.
- [42] National Assembly of Wales. *Well-being of Future Generations (Wales) Act 2015*. 2015. URL: <https://www.legislation.gov.uk/anaw/2015/2/contents>.
- [43] BriteGreen. *Carbon management in the higher education sector: A guide to good practice*. Tech. rep. 2016. URL: https://www.sustainabilityexchange.ac.uk/carbon_management_in_the_higher_education_secto.
- [44] Gov.uk. *Emissions reduction pledge 2020: emissions reporting in public and higher education sectors*. 2020. URL: <https://www.gov.uk/government/publications/emissions-reduction-pledge-2020-emissions-reporting-in-public-and-higher-education-sectors>.
- [45] HECFE. *Carbon reduction target and strategy for higher education in England*. eng. 2010. URL: https://dera.ioe.ac.uk/id/eprint/10659/1/10_01a.pdf.
- [46] EAUC. *Public Bodies Climate Change Duties Reporting*. URL: <https://www.eauc.org.uk/reporting>.
- [47] BriteGreen. *2015/16 University Carbon Report*. Tech. rep. URL: <https://www.brite-green.co.uk/our-work/reports-publications/university-carbon-report>.
- [48] Chamara Panakaduwa, Paul Coates, and Mustapha Munir. “Identifying sustainable retrofit challenges of historical Buildings: A systematic review”. In: *Energy and Buildings* 313 (June 2024), p. 114226. ISSN: 0378-7788. DOI: [10.1016/J.ENBUILD.2024.114226](https://doi.org/10.1016/J.ENBUILD.2024.114226).
- [49] David A Waddicor, Elena Fuentes, Laura Siso, Jaume Salom, Berenger Favre, Christel Jimenez, and Marc Azar. “Climate change and building ageing impact on building energy performance and mitigation measures application: A case study in Turin, northern Italy”. In: *BUILDING AND ENVIRONMENT* 102 (June 2016), pp. 13–25. ISSN: 0360-1323. DOI: [10.1016/j.buildenv.2016.03.003](https://doi.org/10.1016/j.buildenv.2016.03.003).
- [50] Mehmet Aksoezen, Magdalena Daniel, Uta Hassler, and Niklaus Kohler. “Building age as an indicator for energy consumption”. In: *Energy and Buildings* 87 (Jan. 2015), pp. 74–86. ISSN: 0378-7788. DOI: [10.1016/J.ENBUILD.2014.10.074](https://doi.org/10.1016/J.ENBUILD.2014.10.074).
- [51] Maryam Zirak, Verena Weiler, Martin Hein, and Ursula Eicker. “Urban models enrichment for energy applications: Challenges in energy simulation using different data sources for building age information”. In: *Energy* 190 (Jan. 2020). ISSN: 03605442. DOI: [10.1016/J.ENERGY.2019.116292](https://doi.org/10.1016/J.ENERGY.2019.116292).

- [52] AbuBakr Bahaj and P James. “FUTURE ENERGY SOLUTIONS”. In: (2022). URL: https://www.researchgate.net/publication/268259548_FUTURE_ENERGY_SOLUTIONS.
- [53] Eleni Davidson, Yair Schwartz, Joe Williams, and Dejan Mumovic. “Resilience of the higher education sector to future climates: A systematic review of predicted building energy performance and modelling approaches”. In: *Renewable and Sustainable Energy Reviews* 191 (Mar. 2024), p. 114040. ISSN: 1364-0321. DOI: [10.1016/J.RSER.2023.114040](https://doi.org/10.1016/J.RSER.2023.114040).
- [54] GHG Protocol. *Scope 3 Calculation Guidance*. Tech. rep. URL: <https://ghgprotocol.org/scope-3-calculation-guidance-2>.
- [55] Selman Sevindik, Catalina Spataru, Teresa Domenech Aparisi, and Raimund Bleischwitz. “A Comparative Environmental Assessment of Heat Pumps and Gas Boilers towards a Circular Economy in the UK”. In: *Energies* 2021, Vol. 14, Page 3027 14.11 (May 2021), p. 3027. ISSN: 1996-1073. DOI: [10.3390/EN14113027](https://doi.org/10.3390/EN14113027).
- [56] ISO. *ISO 14040:2006(en), Environmental management — Life cycle assessment — Principles and framework*. 2006. URL: <https://www.iso.org/obp/ui/en/#iso:std:iso:14040:ed-2:v1:en>.
- [57] V. Venkatraj and M. K. Dixit. “Life cycle embodied energy analysis of higher education buildings: A comparison between different LCI methodologies”. In: *Renewable and Sustainable Energy Reviews* 144 (July 2021), p. 110957. ISSN: 1364-0321. DOI: [10.1016/J.RSER.2021.110957](https://doi.org/10.1016/J.RSER.2021.110957).
- [58] BSI. *BS EN 15804 - Sustainability of construction works. Environmental product declarations. Core rules for the product category of construction products*. Tech. rep. 2012. URL: <https://landingpage.bsigroup.com/LandingPage/Undated?UPI=000000000030279721>.
- [59] Geoffery Hammond and Craig Jones. *The Inventory of Carbon and Energy (ICE) V3.0*. Tech. rep. 2019. URL: <https://greenbuildingencyclopaedia.uk/wp-content/uploads/2014/07/Full-BSRIA-ICE-guide.pdf>.
- [60] Geoffrey P. Hammond and Craig I. Jones. “Embodied energy and carbon in construction materials”. In: *Proceedings of the Institution of Civil Engineers - Energy* 161.2 (May 2008), pp. 87–98. ISSN: 1751-4223. DOI: [10.1680/ENER.2008.161.2.87](https://doi.org/10.1680/ENER.2008.161.2.87). URL: <https://researchportal.bath.ac.uk/en/publications/embodied-energy-and-carbon-in-construction-materials/>.
- [61] Building Transparency. *The EC3 Tool*. URL: <https://www.buildingtransparency.org/tools/ec3/>.
- [62] One Click LCA. *LCA & EPDs for construction & manufacturing*. URL: <https://oneclicklca.com/en-gb/>.

- [63] Urban Development Federal Ministry for Housing and Building (BMWSB). *Ökobaudat*. URL: <https://www.oekobaudat.de/>.
- [64] Mayor of London. *The London Plan: Chapter 9 Sustainable Infrastructure*. Tech. rep. London, 2021. URL: <https://www.london.gov.uk/programmes-strategies/planning/london-plan/the-london-plan-2021-online/chapter-9-sustainable-infrastructure>.
- [65] Will Arnold. *Policy Position Paper Embodied carbon regulation – alignment of industry policy recommendations (Part Z)*. Tech. rep. Jan. 2024. URL: <https://part-z.uk/>.
- [66] Gov.uk. *Construction 2025: strategy*. 2013. URL: <https://www.gov.uk/government/publications/construction-2025-strategy>.
- [67] Ares and Elena. *The UK Emissions Trading Scheme*. Tech. rep. 2021. URL: www.parliament.uk/commons-library%7Cintranet.parliament.uk/commons-library%7Cpapers@parliament.uk%7C@commonslibrary.
- [68] BRE. *BREEAM Sustainable Building Certification*. URL: <https://breeam.com/>.
- [69] U.S. Green Building Council. *LEED rating system*. URL: <https://www.usgbc.org/leed>.
- [70] LETI. *Embodied Carbon Target Alignment*. Tech. rep. URL: <https://www.leti.uk/carbonalignment>.
- [71] Catherine De Wolf, Francesco Pomponi, and Alice Moncaster. “Measuring embodied carbon dioxide equivalent of buildings: A review and critique of current industry practice”. In: *Energy and Buildings* 140 (Apr. 2017), pp. 68–80. ISSN: 0378-7788. DOI: [10.1016/J.ENBUILD.2017.01.075](https://doi.org/10.1016/J.ENBUILD.2017.01.075).
- [72] Lottie Macnair, Pete Winslow, Bruce Martin, Ailsa Roberts, and Rachel De Matei. *The Embodied Biodiversity Impacts of Construction Materials*. Tech. rep. Nov. 2023. URL: <https://expedition.uk.com/project/embodied-biodiversity-impacts-of-construction-materials/>.
- [73] UKGBC. *Embodied Ecological Impacts*. Tech. rep. 2022. URL: <https://ukgbc.org/our-work/topics/embodied-ecological-impacts/#intro>.
- [74] Mohamad Monkiz Khasreen, Phillip F.G. Banfill, and Gillian F. Menzies. “Life-Cycle Assessment and the Environmental Impact of Buildings: A Review”. In: *Sustainability 2009, Vol. 1, Pages 674-701* 1.3 (Sept. 2009), pp. 674–701. ISSN: 2071-1050. DOI: [10.3390/SU1030674](https://doi.org/10.3390/SU1030674). URL: <https://www.mdpi.com/2071-1050/1/3/674/htm%20https://www.mdpi.com/2071-1050/1/3/674>.

- [75] Yair Schwartz, Rokia Raslan, and Dejan Mumovic. “Refurbish or Replace: Optimising Refurbished and New Building Designs for Life Cycle Carbon Footprint and Life Cycle Cost Minimisation”. In: *Building Simulation and Optimization 2018At: Cambridge, UK*. 2018. URL: [Refurbish%20or%20Replace:%20Optimising%20Refurbished%20and%20New%20Building%20Designs%20for%20Life%20Cycle%20Carbon%20Footprint%20and%20Life%20Cycle%20Cost%20Minimisation](#).
- [76] D Hawkins and D Mumovic. “Evaluation of life cycle carbon impacts for higher education building redevelopment: a multiple case study approach”. In: *Energy and Buildings* 150 (Sept. 2017), pp. 507–515. ISSN: 03787788. DOI: [10.1016/j.enbuild.2017.05.058](#).
- [77] C Scheuer, G A Keoleian, and P Reppe. “Life cycle energy and environmental performance of a new university building: modeling challenges and design implications”. In: *ENERGY AND BUILDINGS* 35.10 (Nov. 2003), pp. 1049–1064. ISSN: 0378-7788. DOI: [10.1016/S0378-7788\(03\)00066-5](#).
- [78] Seppo Junnila, Arpad Horvath, and Angela Acree Guggemos. “Life-Cycle Assessment of Office Buildings in Europe and the United States”. In: (2006). DOI: [10.1061/ASCE1076-0342200612:110](#).
- [79] David Hawkins. “LIFE CYCLE CARBON IMPACT OF HIGHER EDUCATION BUILDING REDEVELOPMENT”. PhD thesis. 2016. URL: [https://discovery.ucl.ac.uk/id/eprint/1476355/1/DH%20EngD%20thesis.pdf](#).
- [80] CIBSE. *TM65 Embodied carbon in building services: A calculation methodology*. Tech. rep. 2021. URL: [https://www.cibse.org/knowledge-research/knowledge-portal/embodied-carbon-in-building-services-a-calculation-methodology-tm65?id=a0q3Y00000IPZ0hQAP](#).
- [81] Karen Valls-Val and María D. Bovea. “Carbon footprint in Higher Education Institutions: a literature review and prospects for future research”. In: *Clean Technologies and Environmental Policy* 23.9 (Nov. 2021), pp. 2523–2542. ISSN: 16189558. DOI: [10.1007/S10098-021-02180-2/FIGURES/7](#). URL: [https://link.springer.com/article/10.1007/s10098-021-02180-2](#).
- [82] Douglas D Gransberg and Erin J Kelly. “Quantifying Uncertainty of Construction Material Price Volatility Using Monte Carlo”. eng. In: *Cost engineering (Morgantown, W. Va.)* 50.6 (2008), pp. 14–18. ISSN: 0274-9696. URL: [https://www.semanticscholar.org/paper/Quantifying-Uncertainty-of-Construction-Material-Gransberg-Kelly/0210cd7785f7df1e21b71fc96acc7ba0a7](#)
- [83] Sven Renner and Friedrich W. Wellmer. “Volatility drivers on the metal market and exposure of producing countries”. In: *Mineral Economics* 33.3 (Oct. 2020), pp. 311–340. ISSN: 21912211. DOI: [10.1007/S13563-019-](#)

- 00200-8/FIGURES/31. URL: <https://link.springer.com/article/10.1007/s13563-019-00200-8>.
- [84] Krishna P Kisi and Tulio Sulbaran. “Construction Cost and Schedule Impacts Due to COVID-19”. In: *Journal of Legal Affairs and Dispute Resolution in Engineering and Construction* 14.4 (Nov. 2022). ISSN: 1943-4162. DOI: [10.1061/\(ASCE\)LA.1943-4170.0000565](https://doi.org/10.1061/(ASCE)LA.1943-4170.0000565). URL: <https://orcid.org/0000>.
 - [85] FIEC. *Construction industry hit hard by war in Ukraine*. Tech. rep. European Construction Industry Federation, 2022. URL: <https://www.fiec.eu/library/fiec-media/article-construction-europe-construction-industry-hit-hard-war-ukraine>.
 - [86] European Commission. *EU Construction and Demolition Waste Management Protocol*. 2016. URL: <https://ec.europa.eu/docsroom/documents/20509/>.
 - [87] Tarja Häkkinen and Kaisa Belloni. “Barriers and drivers for sustainable building”. In: *Building Research & Information* 39.3 (May 2011), pp. 239–255. ISSN: 09613218. DOI: [10.1080/09613218.2011.561948](https://doi.org/10.1080/09613218.2011.561948). URL: <https://www.tandfonline.com/doi/abs/10.1080/09613218.2011.561948>.
 - [88] Jake Barnes and Sivapriya Mothilal Bhagavathy. “The economics of heat pumps and the (un)intended consequences of government policy”. In: *Energy Policy* 138 (Mar. 2020), p. 111198. ISSN: 0301-4215. DOI: [10.1016/J.ENPOL.2019.111198](https://doi.org/10.1016/J.ENPOL.2019.111198).
 - [89] John Barrett, Tim Cooper, Geoffrey P. Hammond, and Nick Pidgeon. “Industrial energy, materials and products: UK decarbonisation challenges and opportunities”. In: *Applied Thermal Engineering* 136 (May 2018), pp. 643–656. ISSN: 1359-4311. DOI: [10.1016/J.APPLTHERMALENG.2018.03.049](https://doi.org/10.1016/J.APPLTHERMALENG.2018.03.049).
 - [90] Bridgit. *How to calculate construction labor cost*. URL: <https://gobridgit.com/blog/how-to-calculate-construction-labor-cost/>.
 - [91] BCIS. *Construction labour costs - the latest trends according to BCIS/Hays index*. 2022. URL: <https://bcis.co.uk/news/construction-site-labour-costs-bcis-hays/>.
 - [92] GOV.UK. *New UK levy to level carbon pricing*. 2023. URL: <https://www.gov.uk/government/news/new-uk-levy-to-level-carbon-pricing>.
 - [93] UNFCCC. *Cap-and-trade programme*. URL: <https://unfccc.int/policy/cap-and-trade-programme>.
 - [94] Chris Giles and Leslie Hook. *Zero emissions goal: the mess of Britain’s carbon taxes*. 2020. URL: <https://www.ft.com/content/c4e7cf36-61f5-11ea-a6cd-df28cc3c6a68>.
 - [95] David Churcher and Peter Tse. *A BSRIA Guide: Life Cycle Costing (BG 67/2016)*. Tech. rep. BSRIA, Mar. 2016. URL: www.bsria.co.uk.

- [96] Anastasia Mylona. “The use of UKCP09 to produce weather files for building simulation”. In: *Building Services Engineering Research and Technology* (2012). ISSN: 01436244. DOI: [10.1177/0143624411428951](https://doi.org/10.1177/0143624411428951).
- [97] M Eames, T Kershaw, and D Coley. “On the creation of future probabilistic design weather years from UKCP09”. In: *Building Services Engineering Research and Technology* (2011). ISSN: 01436244. DOI: [10.1177/0143624410379934](https://doi.org/10.1177/0143624410379934).
- [98] Wei Tian and Pieter De Wilde. “Uncertainty and sensitivity analysis of building performance using probabilistic climate projections: A UK case study”. In: *Automation in construction* 20.8 (2011), pp. 1096–1109. ISSN: 0926-5805. DOI: [10.1016/j.autcon.2011.04.011](https://doi.org/10.1016/j.autcon.2011.04.011).
- [99] Jason A Lowe, Dan Bernie, Philip Bett, Lucy Bricheno, Simon Brown, Daley Calvert, Robin Clark, Karen Eagle, Tamsin Edwards, Giorgia Fossler, Fai Fung, Laila Gohar, Peter Good, Jonathan Gregory, Glen Harris, Tom Howard, Neil Kaye, Elizabeth Kendon, Justin Krijnen, Paul Maisey, Ruth McDonald, Rachel McInnes, Carol McSweeney, John F B Mitchell, James Murphy, Matthew Palmer, Chris Roberts, Jon Rostron, David Sexton, Hazel Thornton, Jon Tinker, Simon Tucker, Kuniko Yamazaki, and Stephen Belcher. *UKCP18 National Climate Projections*. 2018. URL: www.metoffice.gov.uk.
- [100] J. M. Murphy, D. M. Sexton, G. J. Jenkins, B. B. Booth, C. C. Brown, R. T. Clark, M. Collins, G. R. Harris, E. J. Kendon, R. A. Betts, S. J. Brown, K. A. Humphrey, M. P. McCarthy, R. E. McDonald, A. Stephens, C. Wallace, R. Warren, R. Wilby, and R. A. Wood. *UK Climate Projections Science Report: Climate Change projections*. 2009. URL: <https://research-portal.uea.ac.uk/en/publications/uk-climate-projections-science-report-climate-change-projections>.
- [101] D P Jenkins. “The importance of office internal heat gains in reducing cooling loads in a changing climate”. In: *International Journal of Low-Carbon Technologies* 4.3 (2009), pp. 134–140. DOI: [10.1093/ijlct/ctp019](https://doi.org/10.1093/ijlct/ctp019).
- [102] Detlef P. van Vuuren, Jae Edmonds, Mikiko Kainuma, Keywan Riahi, Allison Thomson, Kathy Hibbard, George C. Hurtt, Tom Kram, Volker Krey, Jean Francois Lamarque, Toshihiko Masui, Malte Meinshausen, Nebojsa Nakicenovic, Steven J. Smith, and Steven K. Rose. “The representative concentration pathways: An overview”. In: *Climatic Change* 109.1 (Nov. 2011), pp. 5–31. ISSN: 01650009. DOI: [10.1007/S10584-011-0148-Z/TABLES/4](https://doi.org/10.1007/S10584-011-0148-Z/TABLES/4). URL: <https://link.springer.com/article/10.1007/s10584-011-0148-z>.
- [103] Brian C. O’Neill, Elmar Kriegler, Keywan Riahi, Kristie L. Ebi, Stephane Hallegatte, Timothy R. Carter, Ritu Mathur, and Detlef P. van Vuuren. “A new scenario framework for climate change research: The concept of shared

- socioeconomic pathways”. In: *Climatic Change* 122.3 (Oct. 2014), pp. 387–400. ISSN: 01650009. DOI: [10.1007/S10584-013-0905-2/TABLES/2](https://doi.org/10.1007/S10584-013-0905-2/TABLES/2). URL: <https://link.springer.com/article/10.1007/s10584-013-0905-2>.
- [104] CIBSE. “TM59 Design methodology for the assessment of overheating risk in homes 2017”. In: (2017). URL: www.cibse.org.
 - [105] David M H Sexton and Glen R Harris. “The importance of including variability in climate change projections used for adaptation”. In: *Nature Climate Change* (2015). ISSN: 17586798. DOI: [10.1038/nclimate2705](https://doi.org/10.1038/nclimate2705).
 - [106] BEIS. *2020 UK Greenhouse Gas Emissions, Final Figures*. Tech. rep. 2022. URL: <https://assets.publishing.service.gov.uk/media/61f7fb418fa8f5389450212e/2020-final-greenhouse-gas-emissions-statistical-release.pdf>.
 - [107] DESNZ. “2022 UK greenhouse gas emissions: provisional figures”. In: (2023). URL: https://assets.publishing.service.gov.uk/media/6424b8b83d885d000fdade9b/2022_Provisional_emissions_statistics_report.pdf.
 - [108] Zeke Hausfather. “Analysis: Why the UK’s CO₂ emissions have fallen 38% since 1990”. In: *Carbon Brief* (2019). URL: <https://www.carbonbrief.org/analysis-why-the-uks-co2-emissions-have-fallen-38-since-1990/>.
 - [109] Jannik Giesekam, John Barrett, Peter Taylor, and Anne Owen. “The greenhouse gas emissions and mitigation options for materials used in UK construction”. In: *Energy and Buildings* 78 (2014), pp. 202–214. ISSN: 03787788. DOI: [10.1016/J.ENBUILD.2014.04.035](https://doi.org/10.1016/J.ENBUILD.2014.04.035).
 - [110] Jannik Giesekam, John Barrett, and Peter Taylor. “Scenario analysis of embodied greenhouse gas emissions in UK construction”. In: *Proceedings of the Institution of Civil Engineers. Engineering sustainability* 4 (June 2018), pp. 178–190. DOI: <https://doi.org/10.1680/jensu.16.00020>.
 - [111] Paul W. Griffin, Geoffrey P. Hammond, and Jonathan B. Norman. “Industrial energy use and carbon emissions reduction: a UK perspective”. In: *Wiley Interdisciplinary Reviews: Energy and Environment* 5.6 (Nov. 2016), pp. 684–714. ISSN: 2041840X. DOI: [10.1002/WENE.212](https://doi.org/10.1002/WENE.212).
 - [112] IEA. *Technology Roadmap - Low-Carbon Transition in the Cement Industry*. Tech. rep. 2018. URL: <https://www.iea.org/reports/technology-roadmap-low-carbon-transition-in-the-cement-industry>.
 - [113] Francesco Pomponi and Alice Moncaster. “Embodied carbon mitigation and reduction in the built environment – What does the evidence say?”. In: *Journal of Environmental Management* 181 (Oct. 2016), pp. 687–700. ISSN: 10958630. DOI: [10.1016/j.jenvman.2016.08.036](https://doi.org/10.1016/j.jenvman.2016.08.036).

- [114] Furqan Farooq, Xin Jin, Muhammad Faisal Javed, Arslan Akbar, Muhammad Izhar Shah, Fahid Aslam, and Rayed Alyousef. “Geopolymer concrete as sustainable material: A state of the art review”. eng. In: *Construction & building materials* 306 (2021), p. 124762. ISSN: 0950-0618. DOI: [10.1016/j.conbuildmat.2021.124762](https://doi.org/10.1016/j.conbuildmat.2021.124762).
- [115] Jannik Giesekam, John R. Barrett, and Peter Taylor. “Construction sector views on low carbon building materials”. In: *Building Research & Information* 44.4 (May 2016), pp. 423–444. ISSN: 14664321. DOI: [10.1080/09613218.2016.1086872](https://doi.org/10.1080/09613218.2016.1086872). URL: <https://www.tandfonline.com/doi/abs/10.1080/09613218.2016.1086872>.
- [116] Ember. *Energy Institute - Statistical Review of World Energy (2024) – with major processing by Our World in Data*. Tech. rep. 2024. URL: <https://ourworldindata.org/grapher/carbon-intensity-electricity?tab=chart&country=~GBR>.
- [117] IEA. *Energy Technology Perspectives 2020*. Tech. rep. 2020. URL: www.iea.org/t&c/.
- [118] DESNZ. *Heat and Buildings Strategy*. Tech. rep. 2021. URL: <https://www.gov.uk/government/publications/heat-and-buildings-strategy>.
- [119] Agneta Ghose, Sarah J. McLaren, David Dowdell, and Robyn Phipps. “Environmental assessment of deep energy refurbishment for energy efficiency-case study of an office building in New Zealand”. In: *Building and Environment* 117 (May 2017), pp. 274–287. ISSN: 0360-1323. DOI: [10.1016/J.BUILDENV.2017.03.012](https://doi.org/10.1016/J.BUILDENV.2017.03.012).
- [120] D González-Prieto, Y Fernández-Nava, E Marañón, and M M Prieto. “Environmental life cycle assessment based on the retrofitting of a twentieth-century heritage building in Spain, with electricity decarbonization scenarios”. In: (2021). DOI: [10.1080/09613218.2021.1952400](https://doi.org/10.1080/09613218.2021.1952400). URL: <https://doi.org/10.1080/09613218.2021.1952400>.
- [121] D Abbey, H Arbabi, C Gillott, W Ward, and D D Tingley. “Demolish or reuse? – The balance between operational and embodied emissions in the retrofit of commercial buildings”. eng. In: *IOP Conference Series: Earth and Environmental Science* 1078.1 (2022), p. 12016. ISSN: 1755-1307. DOI: [10.1088/1755-1315/1078/1/012016](https://doi.org/10.1088/1755-1315/1078/1/012016).
- [122] Ina Eileen Peukes, Francesco Pomponi, and Bernardino D’Amico. “Environmental impacts of upgrading gas to electric heating and cooling, considering decarbonisation of the electricity grid”. In: *Journal of Building Engineering* 68 (June 2023), p. 106066. ISSN: 2352-7102. DOI: [10.1016/J.JOBE.2023.106066](https://doi.org/10.1016/J.JOBE.2023.106066).

- [123] Anh-Tuan Nguyen, Sigrid Reiter, and Philippe Rigo. “A review on simulation-based optimization methods applied to building performance analysis”. eng. In: *Applied energy* 113 (2014), pp. 1043–1058. ISSN: 0306-2619. DOI: [10.1016/j.apenergy.2013.08.061](https://doi.org/10.1016/j.apenergy.2013.08.061).
- [124] Billy C.L. Wong, Zhaoji Wu, Vincent J.L. Gan, C.M. Chan, and Jack C.P. Cheng. “Parametric building information modelling and optimality criteria methods for automated multi-objective optimisation of structural and energy efficiency”. eng. In: *Journal of Building Engineering* 75 (2023), p. 107068. ISSN: 2352-7102. DOI: [10.1016/j.jobbe.2023.107068](https://doi.org/10.1016/j.jobbe.2023.107068).
- [125] Foad Asef, Vahid Majidnezhad, Mohammad-Reza Feizi-Derakhshi, and Saeed Parsa. “Heat transfer relation-based optimization algorithm (HTOA)”. In: *Soft Computing* 25.13 (2021), pp. 8129–8158. ISSN: 1433-7479. DOI: [10.1007/s00500-021-05734-0](https://doi.org/10.1007/s00500-021-05734-0). URL: <https://doi.org/10.1007/s00500-021-05734-0>.
- [126] Xin-She Yang. “Chapter 6 - Genetic Algorithms”. In: *Nature-Inspired Optimization Algorithms (Second Edition)*. Ed. by Xin-She Yang. Academic Press, 2021, pp. 91–100. ISBN: 978-0-12-821986-7. DOI: <https://doi.org/10.1016/B978-0-12-821986-7.00013-5>. URL: <https://www.sciencedirect.com/science/article/pii/B9780128219867000135>.
- [127] Kalyanmoy Deb, Amrit Pratap, Sameer Agarwal, and T Meyarivan. “A fast and elitist multiobjective genetic algorithm: NSGA-II”. In: *IEEE Transactions on Evolutionary Computation* 6.2 (Apr. 2002), pp. 182–197. ISSN: 1089778X. DOI: [10.1109/4235.996017](https://doi.org/10.1109/4235.996017).
- [128] Yi Zhang and Lubo Jankovic. “JEA, An Interactive Optimisation Engine for Building Energy Performance Simulation”. In: *Building Simulation Conference Proceedings* 15 (2017), pp. 2232–2241. ISSN: 25222708. DOI: [10.26868/25222708.2017.607](https://doi.org/10.26868/25222708.2017.607). URL: https://publications.ibpsa.org/conference/paper/?id=bs2017_607.
- [129] Ayat Osman, Bryan A Norman, and Robert Ries. “Life cycle optimization of building energy systems”. In: *Engineering optimization* 40.2 (2008), pp. 157–178. ISSN: 0305-215X. DOI: <https://doi.org/10.1080/03052150701646147>.
- [130] Tomás Méndez Echenagucia, Teresa Moroseos, and Christopher Meek. “On the tradeoffs between embodied and operational carbon in building envelope design: The impact of local climates and energy grids”. In: (2022). DOI: [10.1016/j.enbuild.2022.112589](https://doi.org/10.1016/j.enbuild.2022.112589). URL: <https://doi.org/10.1016/j.enbuild.2022.112589>.
- [131] Minjeong Sim and Dongjun Suh. “A heuristic solution and multi-objective optimization model for life-cycle cost analysis of solar PV/GSHP system: A case study of campus residential building in Korea”. eng. In: *Sustainable energy technologies and assessments* 47 (2021), p. 101490. ISSN: 2213-1388. DOI: [10.1016/j.seta.2021.101490](https://doi.org/10.1016/j.seta.2021.101490).

- [132] Bo Wang, Xiaohua Xia, and Jiangfeng Zhang. “A multi-objective optimization model for the life-cycle cost analysis and retrofitting planning of buildings”. eng. In: *Energy and buildings* 77 (2014), pp. 227–235. ISSN: 0378-7788. DOI: [10.1016/j.enbuild.2014.03.025](https://doi.org/10.1016/j.enbuild.2014.03.025).
- [133] Yuehong Lu, Shengwei Wang, Yang Zhao, and Chengchu Yan. “Renewable energy system optimization of low/zero energy buildings using single-objective and multi-objective optimization methods”. eng. In: *Energy and buildings* 89 (2015), pp. 61–75. ISSN: 0378-7788. DOI: [10.1016/j.enbuild.2014.12.032](https://doi.org/10.1016/j.enbuild.2014.12.032).
- [134] Omer T. Karaguzel, Rongpeng Zhang, and Khee Poh Lam. “Coupling of whole-building energy simulation and multi-dimensional numerical optimization for minimizing the life cycle costs of office buildings”. In: *Building Simulation* 7.2 (Apr. 2014), pp. 111–121. ISSN: 19968744. DOI: [10.1007/S12273-013-0128-5/METRICS](https://doi.org/10.1007/S12273-013-0128-5/METRICS). URL: <https://link.springer.com/article/10.1007/s12273-013-0128-5>.
- [135] Jamie Bull, Akshay Gupta, Dejan Mumovic, and Judit Kimpian. “Life cycle cost and carbon footprint of energy efficient refurbishments to 20th century UK school buildings”. In: *International journal of sustainable built environment* 3.1 (2014), pp. 1–17. ISSN: 2212-6090. DOI: <https://doi.org/10.1016/j.ijbsbe.2014.07.002>.
- [136] Nazanin Moazzen, Mustafa Erkan Karagüler, and Touraj Ashraffian. “Life Cycle Energy Assessment of a School Building under Envelope Retrofit: An Approach towards Environmental Impact Reduction”. In: *E3S web of conferences* 111 (2019), p. 3028. ISSN: 2267-1242. URL: <https://doi.org/10.1051/e3sconf/201911103028>.
- [137] Y. Hong, Collins I. Ezech, W. Deng, S-H. Hong, Y. Ma, Y. Tang, and Y. Jin. “Coordinated energy-environmental-economic optimisation of building retrofits for optimal energy performance on a macro-scale: A life-cycle cost-based evaluation”. eng. In: *Energy conversion and management* 243 (2021), p. 114327. ISSN: 0196-8904. DOI: [10.1016/j.enconman.2021.114327](https://doi.org/10.1016/j.enconman.2021.114327).
- [138] X. J. Luo and Lukumon O. Oyedele. “Assessment and optimisation of life cycle environment, economy and energy for building retrofitting”. In: *Energy for Sustainable Development* 65 (Dec. 2021), pp. 77–100. ISSN: 0973-0826. DOI: [10.1016/J.ESD.2021.10.002](https://doi.org/10.1016/J.ESD.2021.10.002).
- [139] Marta Gangolells, Katia Gaspar, Miquel Casals, Jaume Ferré-Bigorra, Nuria Forcada, and Marcel Macarulla. “Life-cycle environmental and cost-effective energy retrofitting solutions for office stock”. In: *Sustainable Cities and Society* 61 (Oct. 2020), p. 102319. ISSN: 2210-6707. DOI: [10.1016/J.SCS.2020.102319](https://doi.org/10.1016/J.SCS.2020.102319).

- [140] Mehrdad Rabani, Habtamu Bayera Madessa, Omid Mohseni, and Natasa Nord. “Minimizing delivered energy and life cycle cost using Graphical script: An office building retrofitting case”. In: *Applied Energy* 268 (June 2020), p. 114929. ISSN: 0306-2619. DOI: [10.1016/J.APENERGY.2020.114929](https://doi.org/10.1016/J.APENERGY.2020.114929).
- [141] Fanny Pernodet Chantrelle, Hicham Lahmidi, Werner Keilholz, Mohamed El Mankibi, and Pierre Michel. “Development of a multicriteria tool for optimizing the renovation of buildings”. eng. In: *Applied energy* 88.4 (2011), pp. 1386–1394. ISSN: 0306-2619. DOI: [10.1016/j.apenergy.2010.10.002](https://doi.org/10.1016/j.apenergy.2010.10.002).
- [142] Natasa Djuric, Vojislav Novakovic, Johnny Holst, and Zoran Mitrovic. “Optimization of energy consumption in buildings with hydronic heating systems considering thermal comfort by use of computer-based tools”. In: *Energy and Buildings* 39.4 (Apr. 2007), pp. 471–477. ISSN: 0378-7788. DOI: [10.1016/J.ENBUILD.2006.08.009](https://doi.org/10.1016/J.ENBUILD.2006.08.009).
- [143] Taehoon Hong, Jimin Kim, and Minhyun Lee. “A multi-objective optimization model for determining the building design and occupant behaviors based on energy, economic, and environmental performance”. In: *Energy* 174 (May 2019), pp. 823–834. ISSN: 0360-5442. DOI: [10.1016/J.ENERGY.2019.02.035](https://doi.org/10.1016/J.ENERGY.2019.02.035).
- [144] Tuomo Niemelä, Risto Kosonen, and Juha Jokisalo. “Cost-optimal energy performance renovation measures of educational buildings in cold climate”. In: *Applied Energy* 183 (Dec. 2016), pp. 1005–1020. ISSN: 0306-2619. DOI: [10.1016/J.APENERGY.2016.09.044](https://doi.org/10.1016/J.APENERGY.2016.09.044).
- [145] Fuad Mutasim Baba, Hua Ge, Radu Zmeureanu, and Liangzhu (Leon) Wang. “Optimizing overheating, lighting, and heating energy performances in Canadian school for climate change adaptation: Sensitivity analysis and multi-objective optimization methodology”. In: *Building and Environment* 237 (June 2023), p. 110336. ISSN: 0360-1323. DOI: [10.1016/J.BUILDENV.2023.110336](https://doi.org/10.1016/J.BUILDENV.2023.110336).
- [146] Anh Tuan Nguyen, David Rockwood, Minh Khoi Doan, and Thi Kim Dung Le. “Performance assessment of contemporary energy-optimized office buildings under the impact of climate change”. In: *Journal of Building Engineering* 35 (Mar. 2021), p. 102089. ISSN: 2352-7102. DOI: [10.1016/J.JOBE.2020.102089](https://doi.org/10.1016/J.JOBE.2020.102089).
- [147] Junjing Yang, Mattheos Santamouris, Siew Eang Lee, and Chirag Deb. “Energy performance model development and occupancy number identification of institutional buildings”. In: *Energy and buildings* 123 (2016), pp. 192–204. ISSN: 0378-7788. DOI: <https://doi.org/10.1016/j.enbuild.2015.12.018>.

- [148] T Shibuya and B Croxford. “The effect of climate change on office building energy consumption in Japan”. eng. In: (2016). DOI: <https://doi.org/10.1016/j.enbuild.2016.02.023>.
- [149] X.J. Luo and Lukumon O. Oyedele. “A data-driven life-cycle optimisation approach for building retrofitting: A comprehensive assessment on economy, energy and environment”. eng. In: *Journal of Building Engineering* 43 (2021), p. 102934. ISSN: 2352-7102. DOI: [10.1016/j.jobe.2021.102934](https://doi.org/10.1016/j.jobe.2021.102934).
- [150] William O Collinge, Amy E Landis, Alex K Jones, Laura A Schaefer, Melissa M Bilec, W O Collinge, M M Bilec, A E Landis, A K Jones, and L A Schaefer. “Dynamic life cycle assessment: framework and application to an institutional building”. In: (). DOI: [10.1007/s11367-012-0528-2](https://doi.org/10.1007/s11367-012-0528-2).
- [151] Alan R. Hevner, Salvatore T. March, Jinsoo Park, and Sudha Ram. “Design science in information systems research”. In: *MIS Quarterly: Management Information Systems* 28.1 (2004), pp. 75–105. ISSN: 02767783. DOI: [10.2307/25148625](https://doi.org/10.2307/25148625).
- [152] Pengyuan Shen, William Braham, Yunkyu Yi, and Eric Eaton. “Rapid multi-objective optimization with multi-year future weather condition and decision-making support for building retrofit”. In: *ENERGY* 172 (Apr. 2019), pp. 892–912. ISSN: 0360-5442. DOI: [10.1016/j.energy.2019.01.164](https://doi.org/10.1016/j.energy.2019.01.164).
- [153] Fabrizio Ascione, Nicola Bianco, Rosa Francesca De Masi, Gerardo Maria Mauro, and Giuseppe Peter Vanoli. “Resilience of robust cost-optimal energy retrofit of buildings to global warming: A multi-stage, multi-objective approach”. In: *Energy and Buildings* 153 (Oct. 2017), pp. 150–167. ISSN: 03787788. DOI: [10.1016/j.enbuild.2017.08.004](https://doi.org/10.1016/j.enbuild.2017.08.004). URL: <http://dx.doi.org/10.1016/j.enbuild.2017.08.004>.
- [154] Mohammad Hamdan and Osamah Qudah. “The initialization of evolutionary multi-objective optimization algorithms”. In: *Lecture Notes in Computer Science (including subseries Lecture Notes in Artificial Intelligence and Lecture Notes in Bioinformatics)*. Vol. 9140. Springer Verlag, 2015, pp. 495–504. ISBN: 9783319204659. DOI: [10.1007/978-3-319-20466-6_52](https://doi.org/10.1007/978-3-319-20466-6_52). URL: <https://researchportal.hw.ac.uk/en/publications/the-initialization-of-evolutionary-multi-objective-optimization-a>.
- [155] *EnergyPlus* — Department of Energy. URL: <https://www.energy.gov/eere/buildings/articles/energyplus>.
- [156] U.S. Department of Energy. *EnergyPlus Version 8.8.0 Documentation Input Output Reference*. Tech. rep. DoE, 2017. URL: https://energyplus.net/assets/nrel_custom/pdfs/pdfs_v9.6.0/InputOutputReference.pdf.

- [157] National Grid ESO. *Future Energy Scenarios (FES) 2021*. Tech. rep. National Grid ESO, 2021. URL: <https://www.neso.energy/publications/future-energy-scenarios-fes/fes-documents>.
- [158] Gov.uk. *Green Book supplementary guidance: valuation of energy use and greenhouse gas emissions for appraisal*. Oct. 2021. URL: <https://www.gov.uk/government/publications/valuation-of-energy-use-and-greenhouse-gas-emissions-for-appraisal>.
- [159] BRE. *Global Methodology for Environmental Profiles of Construction Products. SD6050 SD6050 Issue 1.0*. Tech. rep. 2013. URL: https://files.bregroup.com/bre-co-uk-file-library-copy/filelibrary/greenguide/PDF/Methodology_for_Environmental_Profiles_2008_SD6050.pdf.
- [160] Jake Hacker. *CIBSE TM49: 2014 Design Summer Years for London*. Tech. rep. London: CIBSE, 2014. URL: <https://www.cibse.org/knowledge-research/knowledge-portal/technical-memorandum-49-design-summer-years-for-london-2014-pdf/>.
- [161] Nicolas Francart, Torun Widström, and Tove Malmqvist. “Influence of methodological choices on maintenance and replacement in building LCA”. In: *International Journal of Life Cycle Assessment* 26.11 (Nov. 2021), pp. 2109–2126. ISSN: 16147502. DOI: [10.1007/S11367-021-01985-Z](https://doi.org/10.1007/S11367-021-01985-Z) / [FIGURES/4](https://link.springer.com/article/10.1007/s11367-021-01985-z). URL: <https://link.springer.com/article/10.1007/s11367-021-01985-z>.
- [162] Energy Industrial Strategy Department for Business. *Greenhouse gas reporting: conversion factors 2020*. 2020. URL: <https://www.gov.uk/government/publications/greenhouse-gas-reporting-conversion-factors-2020>.
- [163] Emma Burton and Nick Friedrich. *Net Waste Tool: Guide to Reference Data, Version 1.0*. Tech. rep. Arup, 2008.
- [164] Gov.uk. *List of registered landfill site operators - GOV.UK*. 2023. URL: <https://assets.publishing.service.gov.uk/media/650bfd5327d43b0014375a6f/LFT-Registered-Landfill-Sites-19-09-2023.ods/preview>.
- [165] Kathryn Bourke. *Life cycle costing 1st edition, April 2016*. Tech. rep. RICS professional guidance, 2016. URL: <https://www.rics.org/globalassets/rics-website/media/upholding-professional-standards/sector-standards/construction/black-book/life-cycle-costing-1st-edition-rics.pdf>.
- [166] Gov.uk. *The Green Book (2022) - GOV.UK*. 2022. URL: <https://www.gov.uk/government/publications/the-green-book-appraisal-and-evaluation-in-central-government/the-green-book-2020#:~:text=The%20Green%20Book%20is%20guidance,before%2C%20during%20and%20after%20implementation..>

- [167] AECOM. *Spon's Architects' and Builders' Price Book 2022*. Taylor & Francis, 2021. URL: <https://www.taylorfrancis.com/books/mono/10.1201/9781003196600/spon-architects-builders-price-book-2022-aecom>.
- [168] AECOM. *Spon's Mechanical and Electrical Services Price Book 2022*. CRC Press, Jan. 2022, pp. 1–832. ISBN: 9781000981841. DOI: [10.1201/9781003428831/SPON-MECHANICAL-ELECTRICAL-SERVICES-PRICE-BOOK-2024-AECOM-AECOM](https://doi.org/10.1201/9781003428831/SPON-MECHANICAL-ELECTRICAL-SERVICES-PRICE-BOOK-2024-AECOM-AECOM). URL: <https://www.taylorfrancis.com/books/mono/10.1201/9781003428831/spon-mechanical-electrical-services-price-book-2024-aecom-aecom>.
- [169] Gov.uk. *Energy trends - GOV.UK*. URL: <https://www.gov.uk/government/collections/energy-trends>.
- [170] Kathleen M Eisenhardt. “Building Theories from Case Study Research”. In: *The Academy of Management Review* 14.4 (1989), pp. 532–550. ISSN: 03637425. DOI: [10.2307/258557](https://doi.org/10.2307/258557). URL: <http://www.jstor.org/stable/258557>.
- [171] B Glaser and A Strauss. “The discovery of grounded theory: Strategies of qualitative research”. In: *Wiedenfeld and Nicholson* (1967). URL: http://www.sxf.uevora.pt/wp-content/uploads/2013/03/Glaser_1967.pdf.
- [172] CIBSE. “CIBSE TM46: ENERGY BENCHMARKS”. In: *Construction Research and Innovation* 1.2 (2010). URL: <https://www.cibse.org/knowledge-research/knowledge-portal/tm46-energy-benchmarks/>.
- [173] D Hawkins, S M Hong, R Raslan, D Mumovic, and S Hanna. “Determinants of energy use in UK higher education buildings using statistical and artificial neural network methods”. In: *International Journal of Sustainable Built Environment* 1.1 (June 2012), pp. 50–63. ISSN: 22126104. DOI: [10.1016/j.ijsbe.2012.05.002](https://doi.org/10.1016/j.ijsbe.2012.05.002).
- [174] UK Government. *National Calculation Methodology (NCM) modelling guide (for buildings other than dwellings in England)*. 2021. URL: https://www.uk-ncm.org.uk/filelibrary/NCM_Modelling_Guide_2021_Edition_England_15Dec2021.pdf.
- [175] Nishesh Jain, Esfand Burman, Dejan Mumovic, and Michael Davies. “IMPROVING MODEL CALIBRATION METHODS: A CASE STUDY APPLICATION OF INCORPORATING IEQ WITH ENERGY”. In: 2020. URL: <http://www.ibpsa.us>.
- [176] ASHRAE Guideline 14-2014. *Measurement of Energy, Demand, and Water Savings*. 2014. URL: https://upgreengrade.ir/admin_panel/assets/images/books/ASHRAE%20Guideline%2014-2014.pdf.
- [177] Germán Ramos Ruiz and Carlos Fernández Bandera. “Validation of calibrated energy models: Common errors”. In: *Energies* 10.10 (Oct. 2017). ISSN: 19961073. DOI: [10.3390/EN10101587](https://doi.org/10.3390/EN10101587).

- [178] Lia Webster, James Bradford, Dale Sartor, John Shonder, Erica Atkin, Steve Dunnivant, David Frank, Ellen Franconi, David Jump, Steve Schiller, Mark Stetz, and Bob Slattery. “M&V Guidelines: Measurement and Verification for Performance-Based Contracts Version 4.0”. In: (2015). URL: https://www.energy.gov/sites/prod/files/2016/01/f28/mv_guide_4_0.pdf.
- [179] Gov.uk. *Approved Document Part L: Conservation of fuel and power*. Tech. rep. 2021. URL: www.gov.uk/guidance/building-regulations-.
- [180] ASHRAE. “ANSI/ASHRAE Standard 55-2017 : Thermal Environmental Conditions for Human Occupancy”. In: *ASHRAE Inc.* (2017). ISSN: 1041-2336. URL: <https://www.ashrae.org/technical-resources/bookstore/standard-55-thermal-environmental-conditions-for-human-occupancy>.
- [181] CIBSE. *CIBSE Guide A: Environmental Design*. 2015. URL: <https://www.cibse.org/knowledge-research/knowledge-portal/guide-a-environmental-design-2015>.
- [182] CIBSE. *TM63 Operational performance: Building performance modelling*. Tech. rep. 2020. URL: <https://www.cibse.org/knowledge-research/knowledge-portal/operational-performance-building-performance-modelling-and-calibration-for-evaluation-of-energy-in-use-tm63>.
- [183] IPMVP. “IPMVP GENERALLY ACCEPTED M&V PRINCIPLES International Performance Measurement and Verification Protocol (October 2018)”. In: (2018). URL: https://evo-world.org/images/corporate_documents/IPMVP-Generally-Accepted-Principles_Final_26OCT2018.pdf.
- [184] CIBSE. “TM37 Design for improved solar shading control”. In: (2006). URL: <https://www.cibse.org/knowledge-research/knowledge-portal/tm37-design-for-improved-solar-shading-control/>.
- [185] P. J. Littlefair and BRE Trust. “Summertime solar performance of windows with shading devices”. In: (), p. 28. URL: <https://bregroup.com/store/bookshop/summertime-solar-performance-of-windows-with-shading-devices-downloadable-version->.
- [186] Zero Carbon Hub. *THERMAL BRIDGING GUIDE An introductory guide to thermal bridging in homes*. Tech. rep. 2016. URL: https://greenbuildingencyclopaedia.uk/wp-content/uploads/2016/10/ZCH-ThermalBridgingGuide-Screen_0.pdf.
- [187] Knauf Insulation. *Psi-value Calculator*. URL: <https://www.knaufinsulation.co.uk/psi-value-calculator>.
- [188] Carrier UK. *Air-to-Water heat pumps and chillers*. URL: <https://www.carrier.com/commercial/en/uk/products/heating-air-conditioning/air-to-water-heat-pumps/>.

- [189] Clara Bagenal George, Louise Hamot, and Rachel Levey. “Understanding the importance of Whole Life Carbon in the selection of heat-generation equipment”. In: *CIBSE Technical Symposium* (2019), pp. 25–26.
- [190] CIBSE. *Energy Benchmarking Tool*. URL: <https://www.cibse.org/Knowledge/Benchmarking>.
- [191] Nishesh Jain. “Reducing the performance gap using calibrated simulation models”. PhD thesis. 2020. URL: https://discovery.ucl.ac.uk/id/eprint/10119634/1/2021_01_21_Complete_PhD_V1.pdf.
- [192] Alexander Martín-Garín, José Antonio Millán-García, Juan María Hidalgo-Betanzos, Rufino Javier Hernández-Minguillón, and Abderrahmane Baïri. “Airtightness Analysis of the Built Heritage–Field Measurements of Nineteenth Century Buildings through Blower Door Tests”. In: *Energies* 2020, Vol. 13, Page 6727 13.24 (Dec. 2020), p. 6727. ISSN: 1996-1073. DOI: [10.3390/EN13246727](https://doi.org/10.3390/EN13246727).
- [193] Daikin. *UK Price Book*. 2023. URL: https://ultimateair.co.uk/wp-content/uploads/2023/10/DAIKIN_COMMERCIAL_PRICE_BOOK_OCT_23_WEB.pdf.
- [194] Carrier UK. *VRF outdoor units*. 2024. URL: <https://www.carrier.com/commercial/en/uk/products/vrf-systems/outdoor-units/>.
- [195] Barbara Rodriguez Droguett. “Embodied Carbon of Heating, Ventilation, Air Conditioning and Refrigerants (HVAC+R) Systems”. PhD thesis. 2019. URL: <https://digital.lib.washington.edu:443/researchworks/handle/1773/44736>.
- [196] Department for Environment Food and Rural Affairs. *F gas regulation in Great Britain Assessment report*. Tech. rep. 2022. URL: www.gov.uk/defra.
- [197] Airflow Developments. *Commercial MVHR Solutions*. Tech. rep. URL: <https://www.airflow.com/category/commercial-heat-recovery>.
- [198] ProAir. *EPD: ProAir Heat Recovery Ventilation Unit ProAir PA600LI and ProAir PA600PLI*. Tech. rep. 2022. URL: www.epdireland.org.
- [199] Climate Change Committee. *Net Zero - The UK’s contribution to stopping global warming*. Tech. rep. 2019. URL: <https://www.theccc.org.uk/publication/net-zero-the-uks-contribution-to-stopping-global-warming/>.
- [200] Shiyu Yang, H. Oliver Gao, and Fengqi You. “Demand flexibility and cost-saving potentials via smart building energy management: Opportunities in residential space heating across the US”. In: *Advances in Applied Energy* 14 (July 2024), p. 100171. ISSN: 2666-7924. DOI: [10.1016/J.ADAPEN.2024.100171](https://doi.org/10.1016/J.ADAPEN.2024.100171). URL: <https://www-sciencedirect-com.libproxy.ucl.ac.uk/science/article/pii/S266679242400009X>.

- [201] DESNZ. *Monitoring smart meter energy savings using the National Energy Efficiency Data-Framework*. Tech. rep. Nov. 2024. URL: https://www.google.com/search?q=smart+meter+cost+savings&rlz=1C10NGR_en-GBGB989GB989&oq=smart+meter+cost+savings&gs_lcrp=EgZjaHJvbWUyBggAEEUYOTIICAESourceid=chrome&ie=UTF-8.
- [202] DESNZ. *Review of electricity market arrangements (REMA): Summer update*. Tech. rep. July 2025. URL: <https://www.gov.uk/government/publications/review-of-electricity-market-arrangements-rema-summer-update-2025/review-of-electricity-market-arrangements-rema-summer-update-2025-accessible-webpage>.
- [203] Tomás Méndez Echenagucia, Teresa Moroseos, and Christopher Meek. “On the tradeoffs between embodied and operational carbon in building envelope design: The impact of local climates and energy grids”. In: *Energy and Buildings* 278 (Jan. 2023), p. 112589. ISSN: 0378-7788. DOI: [10.1016/J.ENBUILD.2022.112589](https://doi.org/10.1016/J.ENBUILD.2022.112589).
- [204] Esfandiar Burman. *Assessing the Operational Performance of Educational Buildings against Design Expectations - A Case Study Approach*. Tech. rep. 2015. URL: <https://discovery.ucl.ac.uk/id/eprint/1482161/>.
- [205] CIBSE. *KS17: Indoor Air Quality & Ventilation*. Tech. rep. 2011. URL: <https://www.cibse.org/knowledge-research/knowledge-portal/ks17-indoor-air-quality-ventilation/>.
- [206] Met Office. *HadCM3: Met Office climate prediction model*. URL: <https://www.metoffice.gov.uk/research/approach/modelling-systems/unified-model/climate-models/hadcm3>.
- [207] Met Office. *UK Climate Projections: Headline Findings*. Tech. rep. 2019. URL: www.metoffice.gov.uk.
- [208] A. L. Pisello. “High-albedo roof coatings for reducing building cooling needs”. In: *Eco-efficient Materials for Mitigating Building Cooling Needs: Design, Properties and Applications* (Feb. 2015), pp. 243–268. DOI: [10.1016/B978-1-78242-380-5.00009-1](https://doi.org/10.1016/B978-1-78242-380-5.00009-1).
- [209] Knauf. *AQUAPANEL® Cement Board Indoor EPD-USG-20190110-IAA1-EN*. Tech. rep. Aug. 2019. URL: <https://knauf.com/api/download-center/v1/assets/fba52cec-80e3-4a27-8e93-52e817cf4f4b?download=true>.
- [210] Mapei. *Mapetherm XPS EPD S-P-00914*. Tech. rep. Jan. 2017. URL: https://cdnmedia.mapei.com/docs/librariesprovider51/products-documents/epd-mapetherm-xps.pdf?sfvrsn=731338a_0.
- [211] LETI. *LETI Embodied Carbon Primer*. Tech. rep. 2020. URL: www.LETI.london.

- [212] Aecom. “Spon’s Mechanical and Electrical Services Price Book 2020”. In: *Spon’s Mechanical and Electrical Services Price Book 2020* (May 2021). DOI: [10.1201/9781003226000](https://doi.org/10.1201/9781003226000). URL: <https://www.taylorfrancis.com/books/mono/10.1201/9781003226000/spon-mechanical-electrical-services-price-book-2020-aecom>.
- [213] Worcester Bosch. *Greenstar 8000 Style Combi*. URL: <https://www.worcester-bosch.co.uk/products/boilers/directory/greenstar-8000-style-combi>.
- [214] Baxi. *Platinum Compact Combi Boiler — Gas Electric Combi Boilers*. URL: <https://www.baxi.co.uk/products/boilers/combi-boilers/baxi-platinum-compact-combi>.
- [215] Viessmann UK. *Vitodens Gas Condensing Combi Boilers*. URL: <https://www.viessmann.co.uk/en/products/gas/vitodens.html#product-range>.

Appendices

Appendix A

ASHP EMS script

```
! set plant design volumetric flow rate (m3/s) from InternalVariable
EnergyManagementSystem:InternalVariable,
Udesign,
HW Loop,
Plant Design Volume Flow Rate;
```

```
! Add temperature sensors to record outdoor dry-bulb temperature (ODBT) and HW loop temp
at the supply side inlet and outlet for each timestep (C)
EnergyManagementSystem:Sensor,
DBT,
,
Site Outdoor Air Drybulb Temperature;
```

```
EnergyManagementSystem:Sensor,
 $T_{in}$ ,
HW LOOP DEMAND SIDE INLET,
System Node Temperature;
```

```
EnergyManagementSystem:Sensor,
 $T_{out}$ ,
HW LOOP DEMAND SIDE OUTLET,
System Node Temperature;
```

```
! Extract actual mass flow rate at each timestep (kg/s)
EnergyManagementSystem:Sensor,
Uactual,
HW Loop Demand Side Outlet,
System Node Mass Flow Rate;
```



```

!Run program to calculate ASHP rated capacity
EnergyManagementSystem:ProgramCallingManager,
Calculate ASHP consumption,
EndOfSystemTimestepBeforeHVACReporting,
Calculate_ASHP_consumption;

EnergyManagementSystem:Program,
Calculate_ASHP_consumption,
SET nominal_cap = Udesign*10*4.184*992.25, ! Calculate heating rated capacity (kW)
SET rated_cap = nominal_cap*(0.9753899179+0.0204476869*DBT+0.0002900515*(DBT2)+
-0.0049160031 * Tin + 0.0000260904 * (Tin2) + 0.0000404003 * DBT * Tin),
! use ASHPHighTCAPFT curve to adjust nominal capacity to rated capacity due to current
outdoor air temp and loop water temperature
SET HD = Uactual * (Tin - Tout) * 4.184, ! Calculate actual heat demand (HD) of the system
at current timestep (kW)
SET PLR = HD/rated_cap, ! Calculate part-load ratio (PLR): heat demand/available heat
capacity
SET PLRout = 0.7500000000 + 0.2500000000 * PLR + 0.0000000000 * (PLR2), ! use HPWH-
PLFFPLR curve to find output fraction (y-axis) from input PLR (x-axis)
SET COP = 3.2*(1.9039959704+0.0359056033*DBT+0.0002757065*(DBT2)+-0.0342612220*
Tin + 0.0002211755 * (Tin2) + -0.0003068401 * DBT * Tin), ! call on ASHPHighTCOPFT curve
to adjust nominal COP based on current outdoor air temp and loop water temperature
SET ASHP_heat_electricity = HD/(COP * PLRout); !Calculate heating power requirements
(kW) at 10-minute timesteps

```

Appendix B

Preliminary Testing: Roof Albedo

The outermost layer of the baseline (BL) build-up was replaced with a surface presenting high albedo (HA) material properties. White clay tile with properties of solar reflectivity (SR) up to 80% and thermal emissivity (TE) up to 90% was implemented into the model, replacing the existing green roof and flat roof present in CS1 (see Table 4.3). Properties were derived from research by Pisello [208]. The SR and TE values shown in Table B.1 represent upper end of potential values for the material, selected to test the impact of the ‘best case’ scenario.

Table B.1: Metrics and values adopted to represent high albedo properties.

	BL	HA
Solar reflectance (SR) (%)	-	0.8
Thermal emissivity (TE) (%)	-	0.9

Table B.2: CS1 simulated annual energy consumption for baseline and high albedo roof.

Annual Energy Use (kWh/m ²)	BL	HA	Diff (%)
Fans	7.95	7.95	0.00%
Pumps	0.12	0.12	-0.43%
Cooling	14.02	13.96	-0.46%
District heating	35.48	35.48	-0.01%
Total electricity	116.56	116.50	-0.05%
Total energy use	152.04	151.98	-0.06%

Table B.2 modelling outputs suggest that, despite optimistic assumptions relating to SR and TE values, the impact of this measure on CS1 energy savings is marginal (<1% difference in total energy consumption). Assuming a high fixed-carbon emission scenario, the EC associated with manufacture alone (stage A1-A3) would substantially outweigh any OC benefits over the building’s 60 year time frame (EC: +4.7 kgCO_{2e}/m², OC: -0.6 kgCO_{2e}/m²). Whilst the accuracy of building performance modelling in simulating solar reflectance is may be limited, the results indicate the potential inefficacy of HA roofing materials as an ECM, particularly

from the perspective of [LCCF](#). As such, this measure was removed from the master [ECM](#) template in producing the final parameter list for inclusion in the [GA](#) optimisation process.

Appendix C

CS1 Preliminary Testing: North WWR

Initially WWRs of -50%, -30% and +30% relative to the baseline were considered for each orientation independently. However, since the N-facade typically receives very little direct solar gain, a preliminary study was conducted to validate the use of a reduced parameter sample set for this variable. The impact of varying the North facade WWR on annual operational energy demand and OC was tested under current conditions and using current CEFs.

Table C.1: Impact of varying the N-facade WWR on annual normalised energy consumption by end-use and total operational carbon.

N-WWR % change	Electricity kWh/m ² /yr	DEN kWh/m ² /yr	Cooling kWh/m ² /yr	Total Energy Consumption kWh/m ² /yr	Total OC kgCO _{2e}
BL	110.3	59.6	7.4	169.9	277,537
-50%	110.7	58.8	7.8	169.5	276,974
-30%	110.5	59.2	7.6	169.7	277,230
+30%	110.2	59.9	7.4	170.1	277,843

The results shown in Table C.1 indicate a marginal decrease in annual cooling electricity consumption of 0.09 kWh/m²/yr (0.01%) and marginal increase in heating loads of 0.3 kWh/m²/yr (<0.01%) as the WWR increases, relating to an overall increase of 0.19 kWh/m²/yr in total annual energy consumption when considering combined electric and DEN loads. This correlates to a positive increase in total annual OC emissions of 306 kgCO_{2e}, even under current-day CEF assumptions, where the DEN CEF is less than that of the electric grid (elec: 0.193 kgCO_{2e}/kWh, DEN: 0.189 kgCO_{2e}/kWh). As electricity is expected to decarbonise at a faster rate than DENs (see section 4.3.3, any OC savings resulting from a WWR increase would become even less ‘carbon-valuable’. As such, only the baseline and -50% WWRs were included within the GA optimisation.

Appendix D

Embodied Carbon (A1-A3) Material List

Table D.1: A1-A3 emissions per kg of material; most values modified by the densities provided.

Build-up	Emissions (A1-A3) kgCO ₂ e/kg	Biogenic (A1-A3) kgCO ₂ e/kg	Density kg/m ³	Source	Ref
A393 Reinforcement mesh	1.00	0	7800	CIBSE material data for "steel" quoted in ICE V3	[59]
Aluminium	6.67	0	2700	CIBSE material data for "aluminium" quoted in ICE V3	[59]
Asphalt finish	0.10	0	2330	ICE V3 value of 0.098 kgCO ₂ e/kg and 2330 kg/m ³	[59]
Brick	0.21	0	1920	Av. CIBSE material data for "Brick A" and "Brick B" quoted in ICE V3	[59]
Cast concrete	0.15	0	2400	ICE V3 value per m ³ for CEM1 based RC32/40 with 360 kg cementitious content	[59]
Cement board	0.53	0	750	EPD-USG-20190110-IAA1-EN	[209]
Double glazing	1.63	0	2500	ICE V3 value of 1.63 kgCO ₂ e/kg	[59]
Drainage retention layer	2.54	0	970		
EPS	6.75	0	20	Mapetherm EPS EPD S-P-00914	[210]
Glass	1.44	0	2500	ICE V3 value of 1.44 kgCO ₂ e/kg	[59]
Gypframe	2.76	0	7850	ICE V3 value of 2.76 kgCO ₂ e/kg	[59]
Gypsum plasterboard	0.39	0	640	ICE V3 value of 0.39 kgCO ₂ e/kg	[59]
Metal deck	NA	0	7850	EPD-TS-2018-009	
Mineral wool	1.28	0	140	CIBSE material data for "Glass fibre/wool" quoted in ICE V3	[59]
Mortar	0.14	0	1900	CIBSE material data for "cement mortar" quoted in ICE V3	[59]
PIR	5.30	0	40	LETI Embodied Carbon Primer Figure A.12.1	[211]
PVC	3.10	0	1380	ICE V3 value of 3.10 kgCO ₂ e/kg	[59]
Reinforcement steel	1.00	0	7800	CIBSE material data for "steel" quoted in ICE V3	[59]
Roofing Tile	0.09	0	1459	ICE V3 value for medium density concrete block at 100x215x440mm	[59]
Secondary glazing	1.44	0	2500	ICE V3 value of 1.44 kgCO ₂ e/kg	[59]
Stainless steel brickties	4.41	0	7850	CIBSE material data for "stainless steel, 5% Ni" quoted in ICE V3	[59]
Steel studs	2.76	0	7850	CIBSE material data for "steel" quoted in ICE V3	[59]
Timber	0.26	-1.55	510	CIBSE material data for "softwood" quoted in ICE V3	[59]
Triple glazing	1.75	0	2500	ICE V3 value of 1.75 kgCO ₂ e/kg	[59]
XPS	4.97	0	33	Mapetherm XPS EPD S-P-00914	[210]

Appendix E

CS1 LCA Calculations: Supplementary detail

Table E.1: [ASHP](#) specifications for various models manufactured by Carrier [\[188\]](#).

Model	Heating capacity (kW)	Mass (kg)	Mass Packaging (kg)
30RQP165R	178	1582	30
30RQP180R	197	1587	29
30RQP210R	237	1796	29
30RQP230R	256	1819	29
30RQP270R	275	1826	30
30RQP310R	317	2399	44
30RQP330R	336	2448	44
30RQP370R	387	2668	44
30RQP400R	406	2674	44
30RQP430R	441	3164	59
30RQP470R	467	3187	59
30RQP520R	537	3430	59

Table E.2: Calculated EC of construction elements for CS1, including materials, volume per FU and assumptions impacting the calculations. For manufacture, L=local, N=national, E=European.

Element	FU	Build-up	Volume m ³ /FU	Manuf- acture (L/N/E)	Waste rate %	Expected lifespan yrs	Total EC excl. biogenic kgCO ₂ e/FU	Total biogenic kgCO ₂ e/FU	Total EC incl. biogenic kgCO ₂ e/FU
Below grade wall	1m ²	XPS	0.079	N	5	75	13.81	0.00	13.81
	1m ²	Cast concrete	0.295	L	5	75	115.45	0.00	115.45
	1m ²	Reinforcement steel	0.005	N	15	75	45.75	0.00	45.75
	1m ²	Gypsum plasterboard	0.050	N	22.5	30	52.97	0.00	52.97
External sedum roof	1m ²	Sedum soil layer	0.250	L	10	75	4.24	0.00	-
	1m ²	Drainage retention layer	0.002	N	15	75	6.23	0.00	6.23
	1m ²	EPS	0.300	N	5	40	85.74	0.00	85.74
	1m ²	Metal deck	0.001	N	1	30	78.48	0.00	78.48
External flat roof	1m ²	Cast concrete	0.175	L	5	75	63.10	0.00	63.10
	1m ²	A393 Reinforcement mesh	0.003	N	15	75	43.07	0.00	43.07
	1m ²	EPS	0.300	N	5	40	85.74	0.00	85.74
	1m ²	Metal deck	0.001	N	1	30	78.48	0.00	78.48
RC150 roof	1m ²	Cast concrete	0.147	L	5	75	57.49	0.00	57.49
	1m ²	A393 Reinforcement mesh	0.003	N	15	75	44.07	0.00	44.07
	1m ²	EPS	0.300	N	5	40	85.74	0.00	85.74
	1m ²	Metal deck	0.001	N	1	30	78.48	0.00	78.48
Roof insulation	1m ²	120mm XPS	0.120	N	5	40	41.68	0.00	41.68
	1m ²	150mm XPS	0.150	N	5	40	52.10	0.00	52.10
	1m ²	180mm XPS	0.180	N	5	40	62.52	0.00	62.52
External walls	1m ²	Brick slip	0.070	N	20	75	41.83	0.00	41.83
	1m ²	Mortar	0.000	N	5	75	0.16	0.00	0.16
	1m ²	Mineral wool	0.050	N	15	75	10.85	0.00	10.85
	1m ²	Stainless steel brickties	0.000	N	3	75	0.04	0.00	0.04
	1m ²	Mineral wool	0.120	N	15	75	26.04	0.00	26.04
	1m ²	Gypframe	0.000	N	3	75	9.13	0.00	9.13
	1m ²	Cement board	0.013	N	5	75	5.61	0.00	5.61
	1m ²	Steel studs	0.000	N	3	75	3.85	0.00	3.85
	1m ²	Gypsum plasterboard	0.013	N	5	30	7.20	0.00	7.20

Table E.3: E.2 (continued)

Element	FU	Build-up	Volume m ³ /FU	Manuf- acture (L/N/E)	Waste rate %	Expected lifespan yrs	Total EC excl. biogenic kgCO _e /FU	Total biogenic kgCO _{2e} /FU	Total EC incl. biogenic kgCO _e /FU
External walls, exposed concrete	1m ²	Brick slip	0.070	N	20	75	41.83	0.00	41.83
	1m ²	Mortar	0.000	N	5	75	0.16	0.00	0.16
	1m ²	Mineral wool	0.050	N	15	75	10.85	0.00	10.85
	1m ²	Stainless steel brickties	0.000	N	3	75	0.04	0.00	0.04
	1m ²	Mineral wool	0.120	N	15	75	26.04	0.00	26.04
	1m ²	Gypframe	0.000	N	3	75	9.13	0.00	9.13
	1m ²	Cast concrete	0.173	L	5	75	67.58	0.00	67.58
	1m ²	Reinforcement steel	0.002	N	3	75	18.71	0.00	18.71
External walls, timber clad	1m ²	Timber	0.026	E	5	30	59.25	-43.27	15.98
	1m ²	Mineral wool	0.120	N	15	75	26.04	0.00	26.04
	1m ²	Gypframe	0.000	N	3	75	9.13	0.00	9.13
	1m ²	Cement board	0.013	N	5	75	16.84	0.00	16.84
	1m ²	Steel studs	0.000	N	3	75	11.54	0.00	11.54
	1m ²	Gypsum plasterboard	0.013	N	5	30	7.20	0.00	7.20
IWI + gypframe	1m ²	50mm mineral wool	0.050	N	15	75	10.85	0.00	10.85
	1m ²	Gypframe	0.000	N	3	75	6.75	0.00	6.75
IWI + gypframe	1m ²	80mm mineral wool	0.080	N	15	75	17.36	0.00	17.36
	1m ²	Gypframe	0.000	N	3	75	7.77	0.00	7.77
IWI + gypframe	1m ²	120mm mineral wool	0.120	N	15	75	26.04	0.00	26.04
	1m ²	Gypframe	0.000	N	3	75	9.13	0.00	9.13
Wooden panel	1m ²	Timber	0.026	E	1	30	56.85	-41.52	15.33
	1m ²	Mineral wool	0.120	N	15	75	26.04	0.00	26.04
	1m ²	Gypsum plasterboard	0.025	N	22.5	30	17.66	0.00	17.66
Aluminium spandrel panel	1m ²	Aluminium cladding	0.002	N	1	30	73.17	0.00	73.17
	1m ²	Mineral wool	0.170	N	15	75	36.89	0.00	36.89
	1m ²	Gypsum plasterboard	0.025	N	22.5	30	17.66	0.00	17.66
Glass spandrel panel	1m ²	Glass	0.006	E	5	35	50.62	0.00	50.62
	1m ²	Mineral wool	0.150	N	15	75	32.55	0.00	32.55
	1m ²	Gypsum plasterboard	0.025	N	22.5	30	17.66	0.00	17.66

Table E.4: E.3 (continued)

Element	FU	Build-up	Volume m ³ /FU	Manuf- acture (L/N/E)	Waste rate %	Expected lifespan yrs	Total EC excl. biogenic kgCO _e /FU	Total biogenic kgCO _{2e} /FU	Total EC incl. biogenic kgCO _e /FU
Internal partitions	1m ²	Gypsum plasterboard	0.025	N	22.5	30	17.66	0.00	17.66
	1m ²	Gypframe	0.000	N	3	75	3.85	0.00	3.85
	1m ²	Gypsum plasterboard	0.025	N	22.5	30	17.66	0.00	17.66
Glazing	1m ²	Double glazing	0.003	E	5	40	24.72	0.00	24.72
Glazing	1m ²	Triple glazing	0.003	E	5	40	26.38	0.00	26.38
Al/timber composite frame 1	1m ²	Aluminium	0.005	N	5	40	190.62	0.00	190.62
	1m ²	PVC	0.005	N	5	40	45.58	0.00	45.58
	1m ²	Timber	0.097	E	5	40	221.04	-161.43	59.61
Al/timber composite frame 2	1m ²	Aluminium	0.005	N	5	40	190.62	0.00	190.62
	1m ²	PVC	0.005	N	5	40	45.58	0.00	45.58
	1m ²	Timber	0.200	E	5	40	455.75	-332.84	122.91
PIR closer	1m ²	0.05m PIR	0.050	N	15	75	12.56	0.00	12.56
	1m ²	Gypsum plasterboard	0.039	N	5	30	23.11	0.00	23.11
PIR closer	1m ²	0.10m PIR	0.100	N	15	75	25.12	0.00	25.12
	1m ²	Plasterboard	0.039	N	5	30	23.11	0.00	23.11
Al louvre	1m ²	Aluminium	0.002	N	1	30	73.17	0.00	73.17

Table E.5: Cost of two stage air-to-water heat pump for low-temperature hot water use, based on data from [212] and extrapolated based on calculated output capacity from each simulation run. Initial price discounted by two years to reflect estimated costs for 2022 starting year.

Heat output & cooling capacity	Heat capacity kW	Net Price £	Material £	Labour hours	Labour £	Unit	Total rate £	Replacement Cycles	Replacement years	Replacement NPV-adjusted cost £	Life-cycle cost £
17 kW heating, 18 kW cooling	17	12995	16446	12	404.29	nr	16851				
24 kW heating, 24 kW cooling	24	15338	19442	12	404.29	nr	19846				
32 kW heating, 31 kW cooling	32	16132	20417	12	404.29	nr	20821				
64 kW heating, 62 kW cooling	64	28737	36370	12	404.29	nr	36774				
387 kW heating	387		174086	12	404.29	nr	164473*	2	22, 44	130635	295109
Rate for 2 units (£)	590,218										

* Extrapolated.

Table E.6: MVHR unit and ductwork costs, discounted based on price from Stage D appendices from 2014. Life-spans obtained from [77].

Airflow rate (m ³ /h)	Unit	Total rate (£)	Replacement Cycles	Replacement years	Replacement NPV-adjusted cost (£)	Life-cycle cost £
10800	nr	25000				
26640	nr	60000				
11880	nr	27000				
3960	nr	10000				
30204	nr	53502*	2	20, 40	46024	99525

(a) MVHR Unit Costs. Description: AHU, complete with control dampers, attenuators, panel and bag filters, frost coil, thermal wheel, cooling and heating coil and hygroscopic wheel.

Floor Area (m ²)	Unit	Total rate (£)	Replacement Cycles	Replacement years	Replacement NPV-adjusted cost (£)	Life-cycle cost £
6170	m ²	462750				
578	m ²	43350				
711	m ²	53325				
5655		334819*	1	50	76375	411194
Rate for MVHR + ductwork		175900.2				

(b) Ductwork Distribution Costs. Description: Supply and extract ductwork distribution (£75/m²). Replacement only.

* Total rate discounted by 8 years to match the 2022 timeframe of the rest of the data.

Appendix F

CS2 LCA Calculations: Supplementary detail

Table F.1: **VRF** specifications for various models manufactured by (1) Daikon and (2) Carrier [194, 193].

Manufacturer	Model	Horse Power (HP)	Capacity (kW)	Mass (kg)	Refrigerant Mass (kg)
1	REMA5A	5	16	213	9
1	REYA8A	8	25	213	9
1	REYA10A	10	31.5	213	9
1	REYA12A	12	27.5	213	9
1	REYA14A	14	45	296	10.6
1	REYA16A	16	50	296	10.6
1	REYA18A	18	56.5	319	10.6
1	REYA20A	20	63	319	10.6
1	REMA5A+REMA5A	10	31.5	426	18
1	REMA5A+REYA8A	13	41	426	18
1	REYA8A+REYA8A	16	50	426	18
1	REYA8A+REYA10A	18	56.5	426	18
1	REYA8A+REYA12A	20	62.5	426	18
1	REYA10A+REYA12A	22	69	426	18
1	REYA8A+REYA16A	24	75	509	19.6
1	REYA12A+REYA14A	26	82.5	509	19.6
1	REYA12A+REYA16A	28	87.5	509	19.6
2	38VT008173HQEE	8	25.2	224	8.5
2	38VT010173HQEE	10	28	224	8.5
2	38VT012173HQEE	12	33.5	224	8.5
2	38VT014173HQEE	14	40	224	10
2	38VT016173HQEE	16	45	224	10
2	38VT018173HQEE	18	50.4	287	10.5
2	38VT020173HQEE	20	56	370	14
2	38VT022173HQEE	22	61.5	370	14.5
2	38VT024173HQEE	24	68	370	14.5
2	38VT026173HQEE	26	73.5	370	15
2	38VT008173RQEE	8	22.4	246	11
2	38VT010173RQEE	10	28	246	11
2	38VT012173RQEE	12	33.5	257	12.5
2	38VT014173RQEE	14	40	257	12.5
2	38VT016173RQEE	16	45	366	15.5
2	38VT018173RQEE	18	50	366	15.5
2	38VT020173RQEE	20	56	375	17
2	38VT022173RQEE	22	60	375	17
2	Combination	24	67	514	25
2	Combination	26	73.5	514	25
2	Combination	28	80	514	25
2	Combination	30	85	623	28
2	Combination	32	90	732	31
2	Combination	34	95	732	31

Table F.2: NGB specifications for various models manufactured by [213, 214, 215].

Model	Design Cap (kW)	Total Mass (kg)	Package Mass (kg)	Appliance Mass (kg)
GR8700iW 30	30	55.0	8.0	47.0
GR8700iW 35	35	55.0	8.0	47.0
GR8700iW 40	40	55.0	8.0	47.0
GR8700iW 45	45	57.0	8.0	49.0
GR8700iW 50	50	57.0	8.0	49.0
Baxi Platinum Compact 25 Combi	20	37.0	5.7	31.3
Baxi Platinum Compact 30 Combi	20	37.0	5.7	31.3
Baxi Platinum Compact 36 Combi	25	37.5	6.0	31.5
Baxi 224 Combi 2	20	32.6	6.1	26.5
Baxi 228 Combi 2	20	33.7	6.2	27.5
Baxi 424 Combi 2	20	34.3	6.3	28.0
Baxi 430 Combi 2	20	35.4	6.4	29.0
Baxi 624 Combi 2	20	34.3	6.3	28.0
Baxi 630 Combi 2	25	35.4	6.4	29.0
Baxi 636 Combi 2	25	36.6	6.6	30.0
Baxi 824 Combi 2	20	34.3	6.3	28.0
Baxi 830 Combi 2	25	35.4	6.4	29.0
Baxi 836 Combi 2	25	36.6	6.6	30.0
VITOCROSSAL100, SINGLE UNIT	74	288.0	50.0	238.0
VITOCROSSAL100, SINGLE UNIT	110	345.0	50.0	295.0
VITOCROSSAL100, SINGLE UNIT	146	345.0	50.0	295.0
VITOCROSSAL100, SINGLE UNIT	184	390.0	50.0	340.0
VITOCROSSAL100, SINGLE UNIT	220	390.0	50.0	340.0
VITOCROSSAL100, SINGLE UNIT	258	435.0	50.0	385.0
VITOCROSSAL100, SINGLE UNIT	291	435.0	50.0	385.0
VITOCROSSAL100, TWIN UNIT	240	590.0	76.0	666.0
VITOCROSSAL100, TWIN UNIT	318	590.0	76.0	666.0
VITOCROSSAL100, TWIN UNIT	400	680.0	87.3	767.3
VITOCROSSAL100, TWIN UNIT	480	680.0	87.3	767.3
VITOCROSSAL100, TWIN UNIT	560	770.0	98.6	868.6
VITOCROSSAL100, TWIN UNIT	636	770.0	98.6	868.6
VITODENS 050-W	17	42.3	7.3	35.0
VITODENS 050-W	22	42.3	7.3	35.0
VITODENS 050-W	29	44.6	7.6	37.0
VITODENS 100-W	10	40.0	7.0	33.0
VITODENS 100-W	18	40.0	7.0	33.0
VITODENS 100-W	23	40.0	7.0	33.0
VITODENS 100-W	29	40.0	7.0	33.0
VITODENS 111-W	23	80.0	12.0	68.0
VITODENS 111-W	29	80.0	12.0	68.0
VITODENS 200-W	23	41.7	7.2	34.5
VITODENS 200-W	29	41.7	7.2	34.5
VITOCROSSAL 300 (Typ CM3C)	80	437.7	56.7	381.0
VITOCROSSAL 300 (Typ CM3C)	105	444.6	57.6	387.0
VITOCROSSAL 300 (Typ CM3C)	130	446.9	57.9	389.0
VITOCROSSAL 300 (Typ CM3C)	170	497.1	64.1	433.0
VITOCROSSAL 300 (Typ CM3C)	225	514.3	66.3	448.0
VITOCROSSAL 300 (Typ CM3C)	285	529.1	68.1	461.0
VITOCROSSAL 200-W Gas condensing boiler	45	76.6	11.6	65.0
VITOCROSSAL 200-W Gas condensing boiler	55	76.6	11.6	65.0
VITOCROSSAL 200-W Gas condensing boiler	74	97.2	14.2	83.0
VITOCROSSAL 200-W Gas condensing boiler	91	97.2	14.2	83.0
VITOCROSSAL 200-W Gas condensing boiler	111	150.9	20.9	130.0
VITOCROSSAL 200-W Gas condensing boiler	136	150.9	20.9	130.0
VITOCROSSAL 200 TYPE CRU	727	1642.2	207.2	1435.0
VITOCROSSAL 200 TYPE CRU	909	1707.4	215.4	1492.0
VITOCROSSAL 200 TYPE CM2	370	684.6	87.6	597.0
VITOCROSSAL 200 TYPE CM2	460	787.4	100.4	687.0
VITOCROSSAL 200 TYPE CM2	575	868.5	110.5	758.0
VITOCROSSAL 200 TYPE CM2C	80	437.7	56.7	381.0
VITOCROSSAL 200 TYPE CM2C	105	444.6	57.6	387.0
VITOCROSSAL 200 TYPE CM2C	130	446.9	57.9	389.0
VITOCROSSAL 200 TYPE CM2C	170	497.1	64.1	433.0
VITOCROSSAL 200 TYPE CM2C	225	514.3	66.3	448.0
VITOCROSSAL 200 TYPE CM2C	285	529.1	68.1	461.0

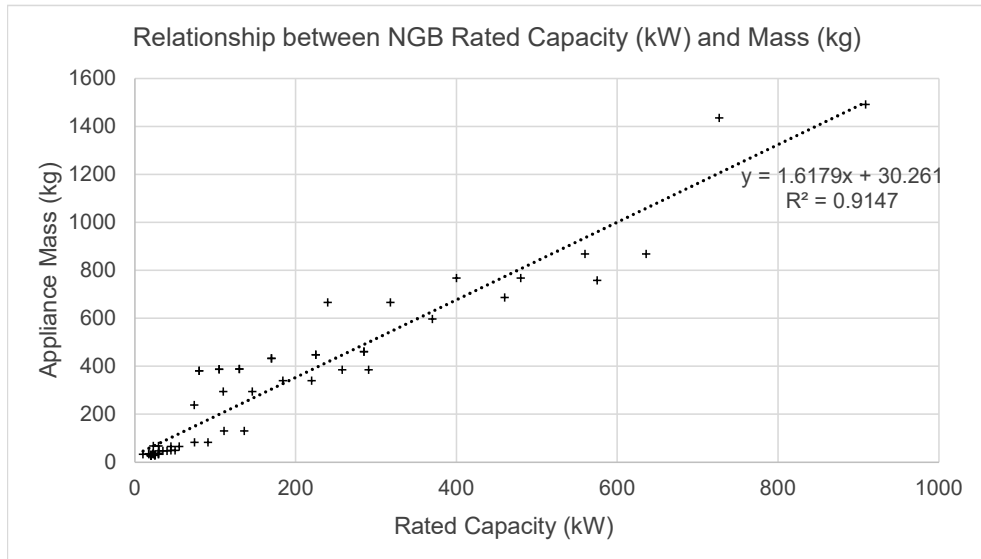


Figure F.1: Relationship between natural gas boiler capacity and mass, extrapolated from manufacturers specifications [213, 214, 215].

Table F.3: MVHR components by weight, according to [198]. From ProAir PA600PLI EPD: “C3. Waste processing: In the C3 phase, it is assumed that the HRV units and the installed components (such as: ducting, wiring, switches, etc.) are shredded for recycling or landfilling. It is assumed that 100% of the metals, plastics and PCBs are recycled. The remaining materials are assumed to be landfilled. C4. Disposal: In C4, the mass of material per unit that goes to landfill is the mass of the HRV units, less the mass of recyclable materials (metals, plastic and PCBs) per unit” [198].

Material	kg per FU			Proportion of total (kg/kg)	Recovered or Landfill (R/L)
	Lower limit	Upper limit	Middle estimate		
PE foam	4	7	5.5	0.200507	L
PVC and PVC fixings	1	2	1.5	0.055	R
Silicone sealant	0.5	1.5	1	0.036	L
Galvanised steel	3	5	4	0.146	R
Hydrocarbon sealant	1	2	1.5	0.055	L
Electric motor	2	3	2.5	0.091	R
Steel	0.05	0.15	0.1	0.003	R
Mild steel	0.1	0.4	0.25	0.009	R
Copper	0.1	0.2	0.15	0.005	R
Brass	0.01	0.04	0.025	0.001	R
Aluminium	3	5	4	0.146	R
Cardboard	0.1	0.4	0.25	0.009	R
LDPE	0.5	0.9	0.7	0.026	L
PCB	0.2	0.5	0.35	0.013	R
Neoprene	0.1	0.2	0.15	0.005	L
Polycarbonate	0.001	0.01	0.0055	0.000	R
PP synthetic fibre	0.1	0.3	0.2	0.007	L
Polypropylene	4.5	6	5.25	0.191	R
Packaging	0	0	0	0	L

Table F.4: Calculated EC of construction elements for CS2, including materials, volume per FU and assumptions impacting the calculations. For manufacture, L=local, N=national, E=European.

Element	FU	Build-up	Volume m ³ /FU	Manuf- acture (L/N/E)	Waste rate %	Expected lifespan yrs	Total EC excl. biogenic kgCO _e /FU	Total biogenic kgCO _{2e} /FU	Total EC incl. biogenic kgCO _e /FU
External flat roof	m2	Asphalt finish	0.010	L	5	30	5.37	0.00	5.37
	m2	Concrete, cast	0.300	L	5	75	112.45	0.00	112.45
	m2	A393 Reinforcement Mesh	0.003	N	15	75	44.07	0.00	44.07
	m2	EPS Expanded Polystyrene	0.040	N	5	40	11.43	0.00	11.43
	m2	Gypsum plasterboard	0.012	N	5	30	7.06	0.00	7.06
Roof insulation	m2	120mm XPS	0.120	N	5	40	41.68	0.00	41.68
	m2	150mm XPS	0.150	N	5	40	52.10	0.00	52.10
	m2	180mm XPS	0.180	N	5	40	62.52	0.00	62.52
External walls	m2	Brick	0.200	N	20	75	120.29	0.00	120.29
	m2	Mortar	0.000	N	5	75	0.16	0.00	0.16
	m2	Stainless steel brickties	0.000	N	3	75	0.04	0.00	0.04
	m2	Brick	0.100	N	20	75	60.15	0.00	60.15
	m2	Mortar	0.000	N	5	75	0.16	0.00	0.16
	m2	Mineral wool	0.040	N	15	75	8.68	0.00	8.68
	m2	Gypsum plasterboard	0.012	N	5	30	6.91	0.00	6.91
External walls, timber clad	m2	Woods-timber	0.026	E	5	30	59.25	-43.27	15.98
	m2	Mineral wool	0.170	N	15	75	36.89	0.00	36.89
	m2	Gypsum plasterboard	0.025	N	22.5	30	17.66	0.00	17.66
IWI + gypframe	m2	50mm mineral wool	0.050	N	15	75	10.85	0.00	10.85
	m2	Gypframe	0.000	N	3	75	6.77	0.00	6.77
IWI + gypframe	m2	80mm mineral wool	0.080	N	15	75	17.49	0.00	17.49
	m2	Gypframe	0.000	N	3	75	7.80	0.00	7.80
IWI + gypframe	m2	120mm mineral wool	0.120	N	15	75	26.23	0.00	26.23
	m2	Gypframe	0.000	N	3	75	9.16	0.00	9.16

Table F.5: F.4 (continued)

Element	FU	Build-up	Volume m ³ /FU	Manuf- acture (L/N/E)	Waste rate %	Expected lifespan yrs	Total EC excl. biogenic kgCO _e /FU	Total biogenic kgCO _{2e} /FU	Total EC incl. biogenic kgCO _e /FU
Internal partitions	m2	Gypsum plasterboard	0.025	N	22.5	30	17.66	0.00	17.66
	m2	Gypframe	0.000	N	3	75	3.85	0.00	3.85
	m2	Mineral wool	0.025	N	15	75	5.43	0.00	5.43
	m2	Gypsum plasterboard	0.025	N	22.5	30	17.66	0.00	17.66
Glazing	m2	Secondary glazing	0.003	E	5	40	25.31	0.00	25.31
Glazing	m2	Double glazing	0.003	E	5	40	24.72	0.00	24.72
Glazing	m2	Triple glazing	0.003	E	5	40	26.38	0.00	26.38
Aluminium frame	m2	Aluminium	0.005	N	5	40	190.62	0.00	190.62
PIR closer	m2	0.05m PIR	0.050	N	15	75	12.56	0.00	12.56
	m2	Gypsum plasterboard	0.039	N	5	30	23.11	0.00	23.11
PIR closer	m2	0.1m PIR	0.100	N	15	75	25.12	0.00	25.12
	m2	Plasterboard	0.039	N	5	30	23.11	0.00	23.11
Wooden louvre	m2	Woods-timber	0.050	E	1	30	109.34	-79.85	29.49

Table F.6: Extrapolation of two stage air-to-water heat pump for low-temperature hot water use, based on data from [212], and extrapolated based on calculated output capacity from each simulation run. Initial price discounted by two years to reflect estimated costs for 2022 starting year.

Heat output & cooling capacity	Heat capacity kW	Net Price £	Material £	Labour hours	Labour £	Unit	Total rate £	Replacement Cycles	Replacement years	Replacement NPV-adjusted cost £	Life-cycle cost £
17 kW heating, 18 kW cooling	17	12995	16446	12	404.29	nr	16851				
24 kW heating, 24 kW cooling	24	15338	19442	12	404.29	nr	19846				
32 kW heating, 31 kW cooling	32	16132	20417	12	404.29	nr	20821				
64 kW heating, 62 kW cooling	64	28737	36370	12	404.29	nr	36774				
396 kW cooling		396	188000	12	404.29	nr	177589*	2	22, 44	149643	327231
Rate for 1 unit (£)	327,231										

* Extrapolated.

Table F.7: MVHR unit and ductwork costs, discounted based on price from Stage D appendices from 2014. Life-spans obtained from [77].

Airflow rate (m ³ /h)	Unit	Total rate (£)	Replacement Cycles	Replacement years	Replacement NPV-adjusted cost (£)	Life-cycle cost £
10800	nr	25000				
26640	nr	60000				
11880	nr	27000				
3960	nr	10000				
14690	nr	26464*	2	20, 40	22765	49230

(a) MVHR Unit Costs. Description: AHU, complete with control dampers, attenuators, panel and bag filters, frost coil, thermal wheel, cooling and heating coil and hygroscopic wheel.

Floor Area (m ²)	Unit	Total rate (£)	Replacement Cycles	Replacement years	Replacement NPV-adjusted cost (£)	Life-cycle cost £
6170	m ²	462750				
578	m ²	43350				
711	m ²	53325				
4105		243058*	1	50	55443	298501
Rate for MVHR + ductwork		347730				

(b) Ductwork Distribution Costs. Description: Supply and extract ductwork distribution (£75/m²). Replacement only.

* Total rate discounted by 8 years to match the 2022 timeframe of the rest of the data.

Table F.8: VRF unit costs obtained from manufacturers specifications [193], and extrapolated based on calculated output capacity from each simulation run.

Heat output & cooling capacity	Heat Capacity kW	Cool Capacity kW	Material £	Labour hours	Labour £	Unit	Total rate £	Replacement Cycles	Replacement years	Replacement NPV-adjusted cost £	Life-cycle cost £
REMA5A	16	14	7299	12	381.08	nr	7680.082				
REYA8A	25	22.4	7430	12	381.08	nr	7811.082				
REYA10A	31.5	28	8161	12	381.08	nr	8542.082				
REYA12A	27.5	33.5	9897	12	381.08	nr	10278.08				
REYA14A	45	40	11667	12	381.08	nr	12048.08				
REYA16A	50	45	13746	12	381.08	nr	14127.08				
REYA18A	56.5	50.4	15283	12	381.08	nr	15664.08				
REYA20A	63	55.9	16984	12	381.08	nr	17365.08				
REMA5A+REMA5A	31.5	28	14598	12	381.08	nr	14979.08				
REMA5A+REYA8A	41	36.4	14729	12	381.08	nr	15110.08				
REYA8A+REYA8A	50	44.8	14860	12	381.08	nr	15241.08				
REYA8A+REYA10A	56.5	50.4	15591	12	381.08	nr	15972.08				
REYA8A+REYA12A	62.5	55.9	17327	12	381.08	nr	17708.08				
REYA10A+REYA12A	69	61.5	18058	12	381.08	nr	18439.08				
REYA8A+REYA16A	75	67.4	21176	12	381.08	nr	21557.08				
REYA12A+REYA14A	82.5	73.5	21564	12	381.08	nr	21945.08				
REYA12A+REYA16A	87.5	78.5	23643	12	381.08	nr	24024.08				
67.4 kW		67.4	18422.2	12	381.08	nr	18803.28*	2	20,40	16175.19	34978.47

* material and labour price extrapolated, total rate discounted by 2 years to match 2022 timeframe of rest of data.

Table F.9: NGB unit costs obtained from [212], and extrapolated based on rated capacity from each simulation run. Description: Commercial; Condensing Gas boiler; Low Nox floor standing condensing boiler with high efficiency modulating premix burner; Stainless steel heat exchanger.

Max. Output kW	Net Price £	Material £	Labour hours	Labour £	Unit	Total rate £	Replac- ement Cycles	Replac- ement years	Replacement NPV-adjusted cost £	Life- cycle cost
12	648	820	8.59	289.41	nr	1109				
15	682	863	8.59	289.41	nr	1152				
18	726	919	8.88	299.17	nr	1218				
21	843	1067	9.92	334.21	nr	1402				
23	935	1183	10.66	359.14	nr	1542				
29	1213	1535	11.81	397.88	nr	1933				
37	1434	1815	11.81	397.88	nr	2213				
41	1492	1888	12.68	427.19	nr	2315				
12	809	1024	9.16	308.6	nr	1333				
15	842	1066	10.95	368.91	nr	1435				
18	906	1147	11.98	403.61	nr	1551				
21	1068	1352	12.78	430.56	nr	1782				
23	1232	1559	12.78	430.56	nr	1990				
29	1570	1987	15.45	520.52	nr	2508				
37	3019	3820	17.65	594.63	nr	4415				
50	4462	5647	8	269.52	nr	5917				
70	4929	6238	8	269.52	nr	6508				
100	5334	6751	8	269.52	nr	7020				
125	5508	6971	10	336.91	nr	7308				
150	6144	7776	10	336.91	nr	8113				
200	7072	8950	10	336.91	nr	9287				
250	8108	10261	10	336.91	nr	10598				
300	9041	11442	10	336.91	nr	11779				
350	10201	12910	10	336.91	nr	13247				
400	11478	14527	10	336.91	nr	14863				
450	12744	16129	10	336.91	nr	16466				
500	13908	17602	10	336.91	nr	17939				
575	15647	19803	10	336.91	nr	20140				
650	16693	21127	10	336.91	nr	21464				
720	19473	24645	10	336.91	nr	24982				
850	24052	30440	12	404.29	nr	30845				
1000	26804	33923	12	404.29	nr	34327				
1150	27890	35298	12	404.29	nr	35702				
1300	35322	44704	14	471.67	nr	45175				
1440	40189	50863	14	471.67	nr	51335				
1700	49928	63189	14	471.67	nr	63661				
2000	56010	70886	14	471.67	nr	71358				
2300	58221	73685	14	471.67	nr	74156				
18.68		1907		375.6416	nr	2152*	2	22, 44	1813	3965
Rate for 1 units (£)		3965								

* material and labour price extrapolated, total rate discounted by 2 years to match 2022 timeframe of rest of data.

Appendix G

CS3 LCA Calculations: Supplementary detail

Table G.1: Calculated EC of construction elements for CS3, including materials, volume per FU and assumptions impacting the calculations. For manufacture, L=local, N=national, E=European.

Element	FU	Build-up	Volume m ³ /FU	Manuf- acture (L/N/E)	Waste rate %	Expected lifespan yrs	Total EC excl. biogenic kgCO _e /FU	Total biogenic kgCO _{2e} /FU	Total EC incl. biogenic kgCO _e /FU
External flat roof	m2	Roofing Tile	0.100	L	5	75	17.42	0.00	17.42
	m2	XPS Extruded Polystyrene	0.160	N	5	40	55.58	0.00	55.58
	m2	A393 Reinforcement Mesh	0.003	N	15	75	44.07	0.00	44.07
	m2	Concrete, cast	0.260	L	5	75	104.05	0.00	104.05
	m2	Gypsum plasterboard	0.013	N	5	30	7.35	0.00	7.35
Roof insulation	m2	50mm XPS	0.050	N	5	40	17.37	0.00	17.37
	m2	80mm XPS	0.080	N	5	40	27.79	0.00	27.79
	m2	120mm XPS	0.120	N	5	40	41.68	0.00	41.68
External walls	m2	Brick	0.017	N	20	75	10.22	0.00	10.22
	m2	Mortar	0.000	N	5	75	0.16	0.00	0.16
	m2	Screw and isofixing	0.000	N	3	75	0.67	0.00	0.67
	m2	PUR insulation	0.043	N	15	75	10.80	0.00	10.80
	m2	Mineral wool	0.120	N	15	75	26.04	0.00	26.04
	m2	Cast concrete	0.150	L	5	75	54.08	0.00	54.08
	m2	Gypsum plasterboard	0.012	N	5	30	6.91	0.00	6.91
Aluminium spandrel panel	m2	Aluminium cladding	0.002	N	1	30	73.17	0.00	73.17
	m2	Mineral wool	0.170	N	15	75	36.89	0.00	36.89
	m2	Gypsum plasterboard	0.025	N	22.5	30	17.66	0.00	17.66
IWI + gypframe	m2	-50mm mineral wool	-0.050	N	15	75	-10.85	0.00	-10.85
	m2	Gypframe	0.000	N	3	75	6.75	0.00	6.75
IWI + gypframe	m2	50mm mineral wool	0.050	N	15	75	10.85	0.00	10.85
	m2	Gypframe	0.000	N	3	75	6.75	0.00	6.75
IWI + gypframe	m2	80mm mineral wool	0.080	N	15	75	17.36	0.00	17.36
	m2	Gypframe	0.000	N	3	75	7.77	0.00	7.77

Table G.2: G.1 (continued)

Element	FU	Build-up	Volume m ³ /FU	Manuf- acture (L/N/E)	Waste rate %	Expected lifespan yrs	Total EC excl. biogenic kgCO _e /FU	Total biogenic kgCO _{2e} /FU	Total EC incl. biogenic kgCO _e /FU
Internal partitions	m2	Gypsum plasterboard	0.013	N	22.5	30	8.83	0.00	8.83
	m2	Gypframe	0.000	N	3	75	3.85	0.00	3.85
	m2	Gypsum plasterboard	0.013	N	22.5	30	8.83	0.00	8.83
Glazing	m2	Double glazing	0.003	E	5	40	24.72	0.00	24.72
Glazing	m2	Triple glazing	0.003	E	5	40	26.38	0.00	26.38
Aluminium frame	m2	Aluminium	0.005	N	5	40	190.62	0.00	190.62
PIR closer	m2	0.05m PIR	0.050	N	15	75	12.56	0.00	12.56
	m2	Gypsum plasterboard	0.039	N	5	30	23.11	0.00	23.11
PIR closer	m2	0.1m PIR	0.100	N	15	75	25.12	0.00	25.12
	m2	Plasterboard	0.039	N	5	30	23.11	0.00	23.11
Wooden louvre	m2	Woods-timber	0.050	E	1	30	109.34	-79.85	29.49

Table G.3: Cost of two stage air-to-water heat pump for low-temperature hot water use, based on data from [212], and extrapolated based on calculated output capacity from each simulation run. Initial price discounted by two years to reflect estimated costs for 2022 starting year.

Heat output & cooling capacity	Heat capacity kW	Net Price £	Material £	Labour hours	Labour £	Unit	Total rate £	Replacement Cycles	Replacement years	Replacement NPV-adjusted cost £	Life-cycle cost £
17 kW heating, 18 kW cooling	17	12995	16446	12	404.29	nr	16851				
24 kW heating, 24 kW cooling	24	15338	19442	12	404.29	nr	19846				
32 kW heating, 31 kW cooling	32	16132	20417	12	404.29	nr	20821				
64 kW heating, 62 kW cooling	64	28737	36370	12	404.29	nr	36774				
396 kW cooling		396	188000	12	404.29	nr	177589*	2	22, 44	149643	327231
Rate for 1 unit (£)	327,231										

* Extrapolated.

Table G.4: MVHR unit and ductwork costs, discounted based on price from Stage D appendices from 2014. Life-spans obtained from [77].

Airflow rate (m ³ /h)	Unit	Total rate (£)	Replacement Cycles	Replacement years	Replacement NPV-adjusted cost (£)	Life-cycle cost £
10800	nr	25000				
26640	nr	60000				
11880	nr	27000				
3960	nr	10000				
43416	nr	76527*	2	20, 40	65831	142358

(a) MVHR Unit Costs. Description: AHU, complete with control dampers, attenuators, panel and bag filters, frost coil, thermal wheel, cooling and heating coil and hygroscopic wheel.

Floor Area (m ²)	Unit	Total rate (£)	Replacement Cycles	Replacement years	Replacement NPV-adjusted cost (£)	Life-cycle cost £
6170	m ²	462750				
578	m ²	43350				
711	m ²	53325				
6437		381093*	1	50	86930	468023
Rate for MVHR + ductwork		610381				

(b) Ductwork Distribution Costs. Description: Supply and extract ductwork distribution (£75/m²). Replacement only.

* Total rate discounted by 8 years to match the 2022 timeframe of the rest of the data.

Table G.5: NGB unit costs obtained from [212], and extrapolated based on rated capacity from each simulation run. Description: Commercial; Condensing Gas boiler; Low Nox floor standing condensing boiler with high efficiency modulating premix burner; Stainless steel heat exchanger.

Max. Output kW	Net Price £	Material £	Labour hours	Labour £	Unit	Total rate £	Replac- ement Cycles	Replac- ement years	Replacement NPV-adjusted cost £	Life- cycle cost
12	648	820	8.59	289.41	nr	1109				
15	682	863	8.59	289.41	nr	1152				
18	726	919	8.88	299.17	nr	1218				
21	843	1067	9.92	334.21	nr	1402				
23	935	1183	10.66	359.14	nr	1542				
29	1213	1535	11.81	397.88	nr	1933				
37	1434	1815	11.81	397.88	nr	2213				
41	1492	1888	12.68	427.19	nr	2315				
12	809	1024	9.16	308.6	nr	1333				
15	842	1066	10.95	368.91	nr	1435				
18	906	1147	11.98	403.61	nr	1551				
21	1068	1352	12.78	430.56	nr	1782				
23	1232	1559	12.78	430.56	nr	1990				
29	1570	1987	15.45	520.52	nr	2508				
37	3019	3820	17.65	594.63	nr	4415				
50	4462	5647	8	269.52	nr	5917				
70	4929	6238	8	269.52	nr	6508				
100	5334	6751	8	269.52	nr	7020				
125	5508	6971	10	336.91	nr	7308				
150	6144	7776	10	336.91	nr	8113				
200	7072	8950	10	336.91	nr	9287				
250	8108	10261	10	336.91	nr	10598				
300	9041	11442	10	336.91	nr	11779				
350	10201	12910	10	336.91	nr	13247				
400	11478	14527	10	336.91	nr	14863				
450	12744	16129	10	336.91	nr	16466				
500	13908	17602	10	336.91	nr	17939				
575	15647	19803	10	336.91	nr	20140				
650	16693	21127	10	336.91	nr	21464				
720	19473	24645	10	336.91	nr	24982				
850	24052	30440	12	404.29	nr	30845				
1000	26804	33923	12	404.29	nr	34327				
1150	27890	35298	12	404.29	nr	35702				
1300	35322	44704	14	471.67	nr	45175				
1440	40189	50863	14	471.67	nr	51335				
1700	49928	63189	14	471.67	nr	63661				
2000	56010	70886	14	471.67	nr	71358				
2300	58221	73685	14	471.67	nr	74156				
18.68		1907		375.6416	nr	2152*	2	22, 44	1813	3965
Rate for 1 units (£)		3965								

* material and labour price extrapolated, total rate discounted by 2 years to match 2022 timeframe of rest of data.

Appendix H

Build-up schematics and calculations

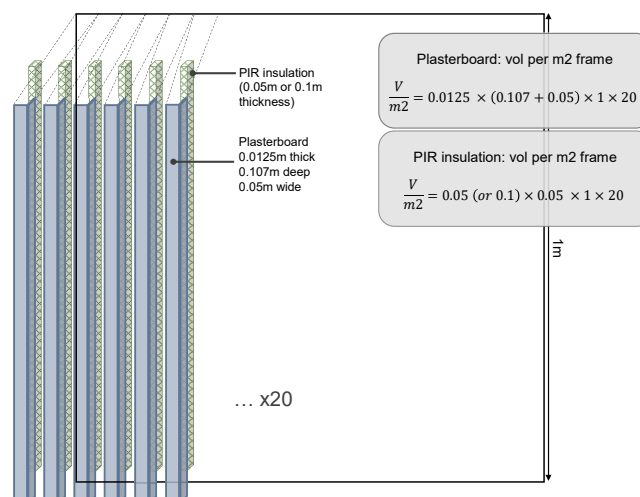


Figure H.1: Schematic demonstrating the calculation of volumes per FU used in EC calculations for PIR insulation and plasterboard.

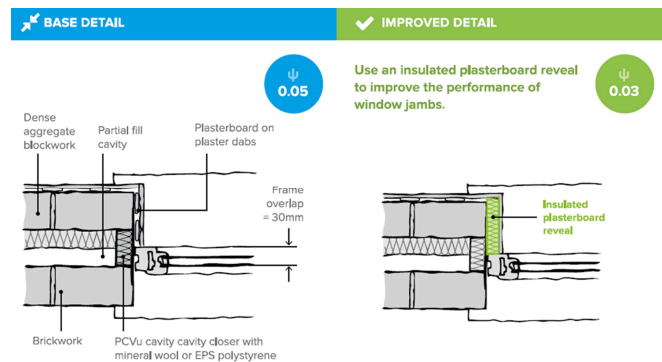


Figure H.2: Assembly section: PIR insulated plasterboard reveal detailing from the Zero Carbon Hub thermal bridging guide [186].

Appendix I

CS1 results

I.0.1 Scenario 1: Linear Regression Statistical Output

```

Call:
lm(formula = t1 ~ P0 + P1 + P2 + P3 + P4 + P5 + P6 + P7 + P8 +
    P9 + P10, data = data)

Residuals:
    Min       1Q   Median       3Q      Max
-7.6147 -1.6637 -0.6777  1.4550 13.1677

Coefficients:
              Estimate Std. Error t value Pr(>|t|)
(Intercept)  740.06996   0.35915   2060.6 < 2.00E-16 ***
P0 Triple    -7.08528   0.16256   -43.585 < 2.00E-16 ***
P1 SHGC 0.3   -0.18563   0.15286   -1.214   0.224744
P2 WWR-50% N  -0.11629   0.15275   -0.761   0.446586
P3 WWR-30% S | BL D/h  0.00645   0.31003    0.021   0.983404
P3 WWR-30% S | 0.4 D/h  1.06626   0.36923    2.888   0.003921 **
P3 WWR-30% S | 0.6 D/h  1.13026   0.40068    2.821   0.004837 **
P3 WWR-30% S | 0.8 D/h  2.20025   0.41811    5.262   1.58E-07 ***
P3 WWR-50% S | BL D/h  0.10514   0.29089    0.361   0.717799 |
P3 WWR-50% S | 0.4 D/h  0.43819   0.37644    1.164   0.244552
P3 WWR-50% S | 0.6 D/h  0.88168   0.33971    2.595   0.009518 **
P3 WWR-50% S | 0.8 D/h  1.07144   0.35832    2.99   0.002822 **
P3 WWR+30% S | BL D/h  0.35687   0.43835    0.814   0.415669
P3 WWR+30% S | 0.4 D/h  1.58172   0.44653    3.542   0.000406 ***
P3 WWR+30% S | 0.6 D/h  2.99335   0.40357    7.417   1.76E-13 ***
P3 WWR+30% S | 0.8 D/h  3.79783   0.41463    9.159 < 2.00E-16 ***
P3 WWR BL S | 0.4 D/h  0.38922   0.41754    0.932   0.351363
P3 WWR BL S | 0.6 D/h  1.62594   0.39682    4.097   4.35E-05 ***
P3 WWR BL S | 0.8 D/h  3.07555   0.38781    7.931   3.61E-15 ***
P4 WWR-30% E | BL D/h  -0.04043   0.33864   -0.119   0.904982
P4 WWR-30% E | 0.2 D/h  1.27485   0.39727    3.209   0.001353 **
P4 WWR-30% E | 0.4 D/h  2.54224   0.40179    6.327   3.07E-10 ***
P4 WWR-30% E | 0.6 D/h  4.74482   0.42983   11.039 < 2.00E-16 ***
P4 WWR-50% E | BL D/h  0.07438   0.28222    0.264   0.79215
P4 WWR-50% E | 0.2 D/h  0.50585   0.34916    1.449   0.147561
P4 WWR-50% E | 0.4 D/h  1.38501   0.32605    4.248   2.26E-05 ***
P4 WWR-50% E | 0.6 D/h  2.71286   0.36171    7.5   9.56E-14 ***
P4 WWR+30% E | BL D/h  0.47446   0.3309    1.434   0.151768
P4 WWR+30% E | 0.2 D/h  2.55088   0.34276    7.442   1.47E-13 ***
P4 WWR+30% E | 0.4 D/h  5.82347   0.37179   15.663 < 2.00E-16 ***
P4 WWR BL E | 0.2 D/h  2.20111   0.33696    6.532   8.20E-11 ***
P4 WWR BL E | 0.4 D/h  5.0674   0.35477   14.284 < 2.00E-16 ***
P5 WWR-30% W | BL D/h  -0.94991   0.40308   -2.357   0.01854 *
P5 WWR-30% W | 0.2 D/h  -0.19954   0.37068   -0.538   0.590427
P5 WWR-30% W | 0.4 D/h  1.67607   0.40497    4.139   3.64E-05 ***
P5 WWR-30% W | 0.6 D/h  4.93584   0.54347    9.082 < 2.00E-16 ***
P5 WWR-50% W | BL D/h  -1.75556   0.22818   -7.694   2.24E-14 ***
P5 WWR-50% W | 0.2 D/h  -1.20846   0.34611   -3.492   0.000491 ***
P5 WWR-50% W | 0.4 D/h  -0.5926   0.36993   -1.602   0.109327
P5 WWR-50% W | 0.6 D/h  1.53082   0.45692    3.35   0.000822 ***
P5 WWR+30% W | BL D/h  0.40109   0.49189    0.815   0.414937
P5 WWR+30% W | 0.2 D/h  2.83658   0.52895    5.363   9.15E-08 ***
P5 WWR+30% W | 0.4 D/h  8.39443   0.3843   21.844 < 2.00E-16 ***
P5 WWR BL W | 0.2 D/h  1.51249   0.28744    5.262 < 2.00E-16 ***
P5 WWR BL W | 0.4 D/h  5.43006   0.31591   17.189 < 2.00E-16 ***
P6 IWI 0.05   2.50023   0.20477   12.21 < 2.00E-16 ***
P6 IWI 0.08   3.43643   0.30469   11.278 < 2.00E-16 ***
P6 IWI 0.12   5.06137   0.23455   21.579 < 2.00E-16 ***
P7 Roof XPS 0.12  6.19754   0.20422   30.348 < 2.00E-16 ***
P7 Roof XPS 0.15  7.36695   0.29189   25.239 < 2.00E-16 ***
P7 Roof XPS 0.18  9.6794   0.23704   40.834 < 2.00E-16 ***
P8 0.219 | 0.5 m3/(m2.h) -4.78277   0.182   -26.279 < 2.00E-16 ***
P8 0.378 | 1 m3/(m2.h) -4.28666   0.16478   -26.015 < 2.00E-16 ***
P9 NV deltaT -27.12377   0.16346  -165.937 < 2.00E-16 ***
P9 NV Nightpurge -7.1891   0.24567   -29.263 < 2.00E-16 ***
P10 MVHR Nightcycle -43.00054   0.19662  -218.697 < 2.00E-16 ***
P10 MVHR Weekend  39.15006   0.22334   175.297 < 2.00E-16 ***

---
Signif. codes:  0 *** 0.001 ** 0.01 * 0.05 . 0.1

Residual standard error: 3.089 on 1987 degrees of freedom
Multiple R-squared:  0.9936, Adjusted R-squared:  0.9935
F-statistic: 5541 on 56 and 1987 DF, p-value: < 2.2e-16

```

Figure I.1: CS1 DEN scenario 1 linear regression model statistics for LCCF.

```

Call:
lm(formula = t2 ~ P0 + P1 + P2 + P3 + P4 + P5 + P6 + P7 + P8 +
    P9 + P10, data = data)

Residuals:
    Min       1Q   Median       3Q      Max
-23.4814  -3.6693  -0.0806   3.7250  21.3502

Coefficients:
(Intercept)          Estimate Std. Error t value Pr(>|t|)
P0 0.8|1003          853.9262    0.6349 1344.99 <2e-16 ***
P1 0.3                49.3976    0.2874 171.89 <2e-16 ***
P2 N-WWR-30%         5.1325    0.2702 18.99 <2e-16 ***
P3 S-WWR-30%         -16.7612    0.2700 -62.07 <2e-16 ***
P3 S-WWR-30% | BL D/h -3.9459    0.5481  -7.20 8.51e-13 ***
P3 S-WWR-30% | 0.4 D/h 5.1578    0.6527   7.90 4.50e-15 ***
P3 S-WWR-30% | 0.6 D/h 10.8946    0.7083 15.38 <2e-16 ***
P3 S-WWR-30% | 0.8 D/h 17.6790    0.7391 23.92 <2e-16 ***
P3 S-WWR-50% | BL D/h -9.8899    0.5142 -19.23 <2e-16 ***
P3 S-WWR-50% | 0.4 D/h -3.7229    0.6655  -5.59 2.52e-08 ***
P3 S-WWR-50% | 0.6 D/h 1.3797    0.6005   2.30 0.0217 *
P3 S-WWR-50% | 0.8 D/h 5.9657    0.6334   9.42 <2e-16 ***
P3 S-WWR+30% | BL D/h 7.7112    0.7749   9.95 <2e-16 ***
P3 S-WWR+30% | 0.4 D/h 28.7739    0.7894 36.45 <2e-16 ***
P3 S-WWR+30% | 0.6 D/h 39.5632    0.7134 55.46 <2e-16 ***
P3 S-WWR+30% | 0.8 D/h 53.9388    0.7330 73.59 <2e-16 ***
P3 S-WWR BL | 0.4 D/h 16.6459    0.7381 22.55 <2e-16 ***
P3 S-WWR BL | 0.6 D/h 23.6869    0.7015 33.77 <2e-16 ***
P3 S-WWR BL | 0.8 D/h 34.1839    0.6855 49.86 <2e-16 ***
P4 E-WWR-30% | BL D/h -4.3979    0.5986  -7.35 2.95e-13 ***
P4 E-WWR-30% | 0.2 D/h 6.9014    0.7023   9.83 <2e-16 ***
P4 E-WWR-30% | 0.4 D/h 24.7527    0.7103 34.85 <2e-16 ***
P4 E-WWR-30% | 0.6 D/h 43.0472    0.7598 56.65 <2e-16 ***
P4 E-WWR-50% | BL D/h -8.9154    0.4989 -17.87 <2e-16 ***
P4 E-WWR-50% | 0.2 D/h -3.3190    0.6172  -5.38 8.46e-08 ***
P4 E-WWR-50% | 0.4 D/h 9.1820    0.5764 15.93 <2e-16 ***
P4 E-WWR-50% | 0.6 D/h 19.8721    0.6394 31.08 <2e-16 ***
P4 E-WWR+30% | BL D/h 4.2507    0.5849   7.27 5.26e-13 ***
P4 E-WWR+30% | 0.2 D/h 35.5047    0.6059 58.60 <2e-16 ***
P4 E-WWR+30% | 0.4 D/h 72.7408    0.6572 110.68 <2e-16 ***
P4 E-WWR BL | 0.2 D/h 30.4390    0.5957 51.10 <2e-16 ***
P4 E-WWR BL | 0.4 D/h 59.6460    0.6271 95.11 <2e-16 ***
P5 W-WWR-30% | BL D/h -4.3230    0.7126  -6.07 1.56e-09 ***
P5 W-WWR-30% | 0.2 D/h 6.0883    0.6553   9.29 <2e-16 ***
P5 W-WWR-30% | 0.4 D/h 32.2691    0.7159 45.08 <2e-16 ***
P5 W-WWR-30% | 0.6 D/h 50.4981    0.9607 52.56 <2e-16 ***
P5 W-WWR-50% | BL D/h -7.8789    0.4034 -19.53 <2e-16 ***
P5 W-WWR-50% | 0.2 D/h -6.6941    0.6118 -10.94 <2e-16 ***
P5 W-WWR-50% | 0.4 D/h 4.4471    0.6539   6.80 1.37e-11 ***
P5 W-WWR-50% | 0.6 D/h 18.4141    0.8077 22.80 <2e-16 ***
P5 W-WWR+30% | BL D/h 6.3094    0.8695   7.26 5.69e-13 ***
P5 W-WWR+30% | 0.2 D/h 41.9377    0.9351 44.85 <2e-16 ***
P5 W-WWR+30% | 0.4 D/h 90.7499    0.6793 133.585 <2e-16 ***
P5 W-WWR BL | 0.2 D/h 27.1615    0.5081 53.455 <2e-16 ***
P5 W-WWR BL | 0.4 D/h 69.7635    0.5584 124.924 <2e-16 ***
P6 IWI 0.05          2.4045    0.3620   6.643 3.97e-11 ***
P6 IWI 0.08          2.2635    0.5386   4.202 2.76e-05 ***
P6 IWI 0.12          3.0005    0.4146   7.237 6.54e-13 ***
P7 Roof XPS 0.12      7.6521    0.3610 21.197 <2e-16 ***
P7 Roof XPS 0.15      9.8324    0.5160 19.055 <2e-16 ***
P7 Roof XPS 0.18     13.9094    0.4190 33.194 <2e-16 ***
P8 0.219 |22GS_Infil_0.5.idf 4.9650    0.3217 15.432 <2e-16 ***
P8 0.378 |22GS_Infil_1.idf 4.9690    0.2913 17.059 <2e-16 ***
P9 NV dt             21.6828    0.2890 75.039 <2e-16 ***
P9 NV Nightpurge     -10.9226    0.4343 -25.151 <2e-16 ***
P10 MVHR Nightcycle  -10.2062    0.3476 -29.364 <2e-16 ***
P10 MVHR Weekend     -3.1396    0.3948  -7.952 3.04e-15 ***
---
Signif. codes:  0 '***' 0.001 '**' 0.01 '*' 0.05 '.' 0.1
Residual standard error: 5.461 on 1987 degrees of freedom
Multiple R-squared:  0.9895,    Adjusted R-squared:  0.9892
F-statistic: 3351 on 56 and 1987 DF,  p-value: < 2.2e-16

```

Figure I.2: CS1 DEN scenario 1 linear regression model statistics for LCC.

```

Call:
lm(formula = t1 ~ P0 + P1 + P2 + P3 + P4 + P5 + P6 + P7 + P8 +
    P9 + P10, data = data)

Residuals:
    Min       1Q   Median       3Q      Max
-3.5697 -0.7275 -0.1475  0.5933  4.2163

Coefficients:
              Estimate Std. Error t value Pr(>|t|)
(Intercept)  347.17339    0.1416 2451.722 < 2.00E-16 ***
P0 Triple    2.56104      0.06614   38.722 < 2.00E-16 ***
P1 SHGC 0.3  -0.9623      0.05685  -16.928 < 2.00E-16 ***
P2 N-WWR-50% 3.36039      0.06002   55.991 < 2.00E-16 ***
P3 S-WWR-30% 0.28965      0.12784    2.266    0.0236 *
P3 S-WWR-30% 0.4 D/h 1.05549      0.16353    6.454    1.43E-10 ***
P3 S-WWR-30% 0.6 D/h 1.5035      0.14975    10.04 < 2.00E-16 ***
P3 S-WWR-30% 0.8 D/h 2.06881      0.16844    12.282 < 2.00E-16 ***
P3 S-WWR-50% BL D/h 0.65074      0.12461    5.222    2.00E-07 ***
P3 S-WWR-50% 0.4 D/h 1.16485      0.15056    7.737    1.78E-14 ***
P3 S-WWR-50% 0.6 D/h 1.17639      0.16783    7.01    3.50E-12 ***
P3 S-WWR-50% 0.8 D/h 1.5118      0.1866     8.102    1.06E-15 ***
P3 S-WWR+30% BL D/h -0.27071      0.1504    -1.8    0.07205 .
P3 S-WWR+30% 0.4 D/h 1.46469      0.15775    9.285 < 2.00E-16 ***
P3 S-WWR+30% 0.6 D/h 2.20109      0.13883    15.854 < 2.00E-16 ***
P3 S-WWR+30% 0.8 D/h 3.20418      0.14085    22.749 < 2.00E-16 ***
P3 S-WWR BL 0.4 D/h 1.21831      0.14395    8.464 < 2.00E-16 ***
P3 S-WWR BL 0.6 D/h 1.84005      0.16214    11.348 < 2.00E-16 ***
P3 S-WWR BL 0.8 D/h 2.36388      0.15778    14.982 < 2.00E-16 ***
P4 E-WWR-30% BL D/h 0.98778      0.14389    6.865    9.46E-12 ***
P4 E-WWR-30% 0.2 D/h 1.80855      0.12594    14.361 < 2.00E-16 ***
P4 E-WWR-30% 0.4 D/h 3.44428      0.15139    22.75 < 2.00E-16 ***
P4 E-WWR-30% 0.6 D/h 5.07861      0.15811    32.12 < 2.00E-16 ***
P4 E-WWR-50% BL D/h 1.45532      0.11665    12.476 < 2.00E-16 ***
P4 E-WWR-50% 0.2 D/h 2.07473      0.13982    14.838 < 2.00E-16 ***
P4 E-WWR-50% 0.4 D/h 2.80053      0.15337    18.26 < 2.00E-16 ***
P4 E-WWR-50% 0.6 D/h 3.93849      0.16328    24.121 < 2.00E-16 ***
P4 E-WWR+30% BL D/h -0.67591      0.13049    -5.18    2.50E-07 ***
P4 E-WWR+30% 0.2 D/h 1.90458      0.11986    15.889 < 2.00E-16 ***
P4 E-WWR+30% 0.4 D/h 4.89766      0.12937    37.859 < 2.00E-16 ***
P4 E-WWR BL 0.2 D/h 2.23      0.14164    15.744 < 2.00E-16 ***
P4 E-WWR BL 0.4 D/h 4.78259      0.14458    33.08 < 2.00E-16 ***
P5 W-WWR-30% BL D/h 0.61859      0.1546     4.001    6.59E-05 ***
P5 W-WWR-30% 0.2 D/h 1.62413      0.11704    13.877 < 2.00E-16 ***
P5 W-WWR-30% 0.4 D/h 3.79589      0.16814    22.576 < 2.00E-16 ***
P5 W-WWR-30% 0.6 D/h 5.32522      0.16735    31.821 < 2.00E-16 ***
P5 W-WWR-50% BL D/h 1.05737      0.09547    11.075 < 2.00E-16 ***
P5 W-WWR-50% 0.2 D/h 0.99768      0.13624    7.323    3.81E-13 ***
P5 W-WWR-50% 0.4 D/h 1.8981      0.18021    10.533 < 2.00E-16 ***
P5 W-WWR-50% 0.6 D/h 3.48096      0.17325    20.092 < 2.00E-16 ***
P5 W-WWR+30% BL D/h -0.57171      0.17921    -3.19    0.00145 **
P5 W-WWR+30% 0.2 D/h 2.23921      0.1424    15.724 < 2.00E-16 ***
P5 W-WWR+30% 0.4 D/h 6.54157      0.12863    50.856 < 2.00E-16 ***
P5 W-WWR BL 0.2 D/h 1.79557      0.12166    14.758 < 2.00E-16 ***
P5 W-WWR BL 0.4 D/h 5.79096      0.14185    40.825 < 2.00E-16 ***
P6 IWI 0.05  3.71775      0.0856    43.43 < 2.00E-16 ***
P6 IWI 0.08  4.97074      0.10519    47.254 < 2.00E-16 ***
P6 IWI 0.12  7.00002      0.0796    87.939 < 2.00E-16 ***
P7 Roof XPS 0.12 6.82478      0.08151    83.731 < 2.00E-16 ***
P7 Roof XPS 0.15 8.44911      0.10447    80.88 < 2.00E-16 ***
P7 Roof XPS 0.05 10.26275      0.07854   130.674 < 2.00E-16 ***
P8 0.219 | 0.5 m3/(m2.h) 0.10105      0.06521    1.55    0.12141
P8 0.378 | 1 m3/(m2.h) 0.12179      0.07217    1.687    0.09171
P9 NV dt 6.77964      0.06912    98.082 < 2.00E-16 ***
P9 NV Nightpurge -2.127      0.0826   -25.752 < 2.00E-16 ***
P10 MVHR Nightcycle -3.11362      0.07759   -40.129 < 2.00E-16 ***
P10 MVHR Weekend 0.24085      0.07726    3.117    0.00186 **
---
Signif. codes:  0 '***' 0.001 '**' 0.01 '*' 0.05 '.' 0.1 ' ' 1

Residual standard error: 1.115 on 1618 degrees of freedom
Multiple R-squared:  0.9833,    Adjusted R-squared:  0.9828
F-statistic: 1704 on 56 and 1618 DF, p-value: < 2.2e-16

```

Figure I.3: CS1 ASHP scenario 1 linear regression model statistics for LCCF.

```

Call:
lm(formula = t2 ~ P0 + P1 + P2 + P3 + P4 + P5 + P6 + P7 + P8 +
    P9 + P10, data = data)

Residuals:
    Min       1Q   Median       3Q      Max
-25.422  -3.182   0.311   3.188  20.977

Coefficients:
              Estimate Std. Error t value Pr(>|t|)
(Intercept)    939.4879     0.6413 1465.003 < 2e-16 ***
P0 0.8|1003    47.5257     0.2995  158.670 < 2e-16 ***
P1 0.3         5.3850     0.2574   20.917 < 2e-16 ***
P2 N-WWR-50%  -18.2985     0.2718  -67.323 < 2e-16 ***
P3 S-WWR-30% | BL D/h -5.2680     0.5790  -9.099 < 2e-16 ***
P3 S-WWR-30% | 0.4 D/h  4.1885     0.7406   5.656 1.83e-08 ***
P3 S-WWR-30% | 0.6 D/h  9.2074     0.6782  13.576 < 2e-16 ***
P3 S-WWR-30% | 0.8 D/h 16.9500     0.7628  22.220 < 2e-16 ***
P3 S-WWR-50% | BL D/h -10.4318     0.5643 -18.486 < 2e-16 ***
P3 S-WWR-50% | 0.4 D/h -5.0473     0.6818  -7.403 2.14e-13 ***
P3 S-WWR-50% | 0.6 D/h -0.7639     0.7600  -1.005 0.315
P3 S-WWR-50% | 0.8 D/h  4.5676     0.8451   5.405 7.45e-08 ***
P3 S-WWR+30% | BL D/h  7.7694     0.6811  11.407 < 2e-16 ***
P3 S-WWR+30% | 0.4 D/h 27.6915     0.7144  38.762 < 2e-16 ***
P3 S-WWR+30% | 0.6 D/h 39.7669     0.6287  63.250 < 2e-16 ***
P3 S-WWR+30% | 0.8 D/h 53.0725     0.6379  83.204 < 2e-16 ***
P3 S-WWR BL | 0.4 D/h 15.9133     0.6519  24.411 < 2e-16 ***
P3 S-WWR BL | 0.6 D/h 25.2473     0.7343  34.382 < 2e-16 ***
P3 S-WWR BL | 0.8 D/h 32.3576     0.7145  45.285 < 2e-16 ***
P4 E-WWR-30% | BL D/h -4.8962     0.6516  -7.514 9.47e-14 ***
P4 E-WWR-30% | 0.2 D/h  7.0401     0.5703  12.344 < 2e-16 ***
P4 E-WWR-30% | 0.4 D/h 26.3888     0.6856  38.489 < 2e-16 ***
P4 E-WWR-30% | 0.6 D/h 43.8630     0.7161  61.257 < 2e-16 ***
P4 E-WWR-50% | BL D/h -9.3449     0.5283 -17.689 < 2e-16 ***
P4 E-WWR-50% | 0.2 D/h -4.9076     0.6332  -7.750 1.61e-14 ***
P4 E-WWR-50% | 0.4 D/h  8.3273     0.6946  11.989 < 2e-16 ***
P4 E-WWR-50% | 0.6 D/h 19.6972     0.7395  26.638 < 2e-16 ***
P4 E-WWR+30% | BL D/h  5.8522     0.5910   9.903 < 2e-16 ***
P4 E-WWR+30% | 0.2 D/h 36.2092     0.5428  66.704 < 2e-16 ***
P4 E-WWR+30% | 0.4 D/h 73.4088     0.5859 125.299 < 2e-16 ***
P4 E-WWR BL | 0.2 D/h 30.0846     0.6414  46.901 < 2e-16 ***
P4 E-WWR BL | 0.4 D/h 58.7000     0.6547  89.652 < 2e-16 ***
P5 W-WWR-30% | BL D/h -6.1105     0.7001  -8.728 < 2e-16 ***
P5 W-WWR-30% | 0.2 D/h  5.8800     0.5300  11.093 < 2e-16 ***
P5 W-WWR-30% | 0.4 D/h 30.4337     0.7614  39.968 < 2e-16 ***
P5 W-WWR-30% | 0.6 D/h 48.4402     0.7579  63.915 < 2e-16 ***
P5 W-WWR-50% | BL D/h -10.1986     0.4324 -23.588 < 2e-16 ***
P5 W-WWR-50% | 0.2 D/h -9.2012     0.6170 -14.913 < 2e-16 ***
P5 W-WWR-50% | 0.4 D/h  1.7308     0.8161   2.121 0.034
P5 W-WWR-50% | 0.6 D/h 18.7924     0.7846  23.951 < 2e-16 ***
P5 W-WWR+30% | BL D/h  3.5112     0.8116   4.326 1.61e-05 ***
P5 W-WWR+30% | 0.2 D/h 38.4861     0.6449  59.677 < 2e-16 ***
P5 W-WWR+30% | 0.4 D/h 89.0983     0.5825 152.950 < 2e-16 ***
P5 W-WWR BL | 0.2 D/h 25.3834     0.5510  46.069 < 2e-16 ***
P5 W-WWR BL | 0.4 D/h 70.2327     0.6424 109.328 < 2e-16 ***
P6 IWI 0.05    2.2945     0.3877   5.919 3.95e-09 ***
P6 IWI 0.08    1.5078     0.4764   3.165 0.00158 **
P6 IWI 0.12    3.2797     0.3605   9.098 < 2e-16 ***
P7 Roof XPS 0.12 7.1352     0.3691  19.330 < 2e-16 ***
P7 Roof XPS 0.15 8.7072     0.4731  18.405 < 2e-16 ***
P7 Roof XPS 0.18 10.0505     0.4934  20.367 < 2e-16 ***
P8 0.219 | 0.5 m3/(m2.h) -2.5262     0.5884  -4.293 1.78e-05 ***
P8 0.378 | 1 m3/(m2.h) -1.9736     0.5736  -3.440 0.000592 ***
P9 NV dT       -11.4766     0.6226 -18.438 < 2e-16 ***
P9 NV Nightpurge -6.5781     0.5212 -12.622 < 2e-16 ***
P10 MVHR Nighcycle -10.8441     0.6243 -17.374 < 2e-16 ***
P10 MVHR Weekend  2.2235     0.6198   3.587 0.000338 ***
---
Signif. codes:  0 '***' 0.001 '**' 0.01 '*' 0.05 '.'

Residual standard error: 5.048 on 1618 degrees of freedom
Multiple R-squared:  0.9914, Adjusted R-squared:  0.9911
F-statistic: 3322 on 56 and 1618 DF, p-value: < 2.2e-16

```

Figure I.4: CS1 ASHP scenario 1 linear regression model statistics for LCC.

Appendix J

CS2 Results

J.0.1 Scenario 1: Linear Regression Statistical Output


```

Call:
lm(formula = t1 ~ P0 + P1 + P2 + P3 + P4 + P5 + P6 + P7 + P8 +
    P9 + P10, data = data)

Residuals:
    Min       1Q   Median       3Q      Max
-40.418  -5.109  -1.352    3.013   62.017

Coefficients:
(Intercept)          512.72969      1.66332    308.256 < 2e-16 ***
P0 ASHP             -71.55699      0.53210   -134.480 < 2e-16 ***
P1 Triple           -4.64958      0.50852    -9.143 < 2e-16 ***
P1 Double           -2.61399      0.47393    -5.516 3.69e-08 ***
P2 SHGC 0.3         -1.26054      0.42568    -2.961 0.003082 **
P3 N-WWR-50%        -0.04182      0.40996    -0.102 0.918749
P4 S-WWR-30% | BL D/h 0.94848      1.13373    0.837 0.402866
P4 S-WWR-30% | 0.4 D/h -1.16129     1.19085   -0.975 0.329531
P4 S-WWR-30% | 0.6 D/h 0.99651      1.20657    0.826 0.408908
P4 S-WWR-30% | 0.8 D/h 1.39061      1.23591    1.125 0.260583
P4 S-WWR-50% | BL D/h -0.64655     1.00248   -0.645 0.518995
P4 S-WWR-50% | 0.4 D/h 2.11286      1.04010    2.031 0.042280 *
P4 S-WWR-50% | 0.6 D/h 0.46729     1.07352    0.435 0.663379
P4 S-WWR-50% | 0.8 D/h -0.75893     1.20270   -0.631 0.528063
P4 S-WWR+30% | BL D/h 0.64698      1.18977    0.544 0.586620
P4 S-WWR+30% | 0.4 D/h 1.50135      1.13802    1.319 0.187157
P4 S-WWR+30% | 0.6 D/h 0.98553      1.25671    0.784 0.432958
P4 S-WWR+30% | 0.8 D/h 0.44912      1.23115    0.365 0.715285
P4 S-WWR BL | 0.4 D/h 0.81377       1.11528    0.730 0.465647
P4 S-WWR BL | 0.6 D/h 1.41838       1.19676    1.185 0.236016
P4 S-WWR BL | 0.8 D/h 0.85877       1.20627    0.712 0.476557
P5 E-WWR-30% | BL D/h 0.17473       1.18203    0.148 0.882489
P5 E-WWR-30% | 0.2 D/h -2.42719     1.13657   -2.136 0.032776 *
P5 E-WWR-30% | 0.4 D/h -0.99002     1.06992   -0.925 0.354856
P5 E-WWR-30% | 0.6 D/h -0.85241     1.05454   -0.808 0.418953
P5 E-WWR-50% | BL D/h -1.89158     0.88471   -2.138 0.032570 *
P5 E-WWR-50% | 0.2 D/h -1.20788     0.99294   -1.216 0.223878
P5 E-WWR-50% | 0.4 D/h -1.71061     1.08642   -1.575 0.115440
P5 E-WWR-50% | 0.6 D/h -0.16062     1.10838   -0.145 0.884789
P5 E-WWR+30% | BL D/h -0.81570     1.08243   -0.754 0.451142
P5 E-WWR+30% | 0.2 D/h 1.19123      1.12745    1.057 0.290770
P5 E-WWR+30% | 0.4 D/h 3.10824      1.25602    2.475 0.013377 *
P5 E-WWR BL | 0.2 D/h -0.65337     1.02228   -0.639 0.522776
P5 E-WWR BL | 0.4 D/h 0.50714       1.04166    0.487 0.626388
P6 W-WWR-30% | BL D/h -2.34092     1.10848   -2.112 0.034762 *
P6 W-WWR-30% | 0.2 D/h -0.64718     1.11900   -0.578 0.563053
P6 W-WWR-30% | 0.4 D/h -2.14240     1.12085   -1.911 0.056023 .
P6 W-WWR-30% | 0.6 D/h -0.62247     1.05175   -0.592 0.553989
P6 W-WWR-50% | BL D/h -1.87037     0.94707   -1.975 0.048348 *
P6 W-WWR-50% | 0.2 D/h -2.89381     0.94797   -3.053 0.002283 **
P6 W-WWR-50% | 0.4 D/h -3.54718     0.97957   -3.621 0.000297 ***
P6 W-WWR-50% | 0.6 D/h -1.98252     1.06606   -1.860 0.063005 .
P6 W-WWR+30% | BL D/h -0.31488     1.07915   -0.292 0.770462
P6 W-WWR+30% | 0.2 D/h -2.87607     1.06772   -2.694 0.007097 **
P6 W-WWR+30% | 0.4 D/h -3.25038     1.14395   -2.841 0.004515 **
P6 W-WWR BL | 0.2 D/h -1.57658     1.11199   -1.418 0.156325
P6 W-WWR BL | 0.4 D/h -0.02452     1.06672   -0.023 0.981659
P7 IWI 0.05         7.55473      0.64233   11.761 < 2e-16 ***
P7 IWI 0.08        10.25044      0.74174   13.820 < 2e-16 ***
P7 IWI 0.12        14.82616      0.61938   23.937 < 2e-16 ***
P8 Roof XPS 0.12     3.89698      0.60450    6.447 1.28e-10 ***
P8 Roof XPS 0.15     5.86221      0.69655    8.416 < 2e-16 ***
P8 Roof XPS 0.18     8.25494      0.61486   13.426 < 2e-16 ***
P9 0.287 | 0.1 ACH  -26.93086     0.59807   -45.030 < 2e-16 ***
P9 0.549 | 0.4 ACH  -15.17826     0.70165   -21.632 < 2e-16 ***
P10 MVHR Nightcycle | NV BL -14.43326     1.40823   -10.249 < 2e-16 ***
P10 MVHR Nightcycle | NV dT -16.09182     1.16967   -13.758 < 2e-16 ***
P10 MVHR Weekday | NV BL -18.59483     0.97450   -19.081 < 2e-16 ***
P10 MVHR Weekday | NV dT -43.25070     0.97490   -44.364 < 2e-16 ***
P10 MVHR Weekday | NV Nightpurge 13.04287     1.18940   10.966 < 2e-16 ***
P10 MVHR Weekend | NV BL -12.54418     1.30876    -9.585 < 2e-16 ***
P10 MVHR Weekend | NV dT -19.26123     1.46947   -13.108 < 2e-16 ***
P10 MVHR Weekend | NV Nightpurge 18.00306     1.35874   13.250 < 2e-16 ***
P10 No MVHR | NV Nightpurge -13.16416     0.93060   -14.146 < 2e-16 ***
---
Signif. codes:  0 '***' 0.001 '**' 0.01 '*' 0.05 '.'

Residual standard error: 12.37 on 4036 degrees of freedom
Multiple R-squared:  0.9001,    Adjusted R-squared:  0.8986
F-statistic: 577.3 on 63 and 4036 DF,  p-value: < 2.2e-16

```

Figure J.1: CS2 scenario 1 linear regression model statistics for LCCF.

```

Call:
lm(formula = t2 ~ P0 + P1 + P2 + P3 + P4 + P5 + P6 + P7 + P8 +
    P9 + P10, data = data)

Residuals:
    Min       1Q   Median       3Q      Max
-68.636 -13.739  -1.214  11.568  125.407

Coefficients:
              Estimate Std. Error t value Pr(>|t|)
(Intercept)    987.200349    3.001402   328.913 < 2e-16 ***
P0 ASHP         19.087740    0.958236    19.920 < 2e-16 ***
P1 Triple       35.297223    0.917087    38.488 < 2e-16 ***
P1 Double        8.205154    0.855179     9.595 < 2e-16 ***
P2 SHGC 0.3     -0.658052    0.767638    -0.857 0.391362
P3 N-WWR-50%    -1.445623    0.739349    -1.955 0.050621 .
P4 S-WWR-30%    | BL D/h      0.006875    2.044368     0.003 0.997317
P4 S-WWR-30%    | 0.4 D/h     -2.354906    2.149277    -1.096 0.273287
P4 S-WWR-30%    | 0.6 D/h      4.542104    2.176751     2.087 0.036983 *
P4 S-WWR-30%    | 0.8 D/h      2.599056    2.222237     1.170 0.242244
P4 S-WWR-50%    | BL D/h      0.894238    1.808738     0.494 0.621051
P4 S-WWR-50%    | 0.4 D/h     -2.198084    1.876865    -1.171 0.241609
P4 S-WWR-50%    | 0.6 D/h     -0.261967    1.934572    -0.135 0.892292
P4 S-WWR-50%    | 0.8 D/h     -1.316579    2.170643    -0.607 0.544191
P4 S-WWR+30%    | BL D/h     12.334626    2.147241     5.744 9.90e-09 ***
P4 S-WWR+30%    | 0.4 D/h     14.815991    2.053765     7.214 6.45e-13 ***
P4 S-WWR+30%    | 0.6 D/h     15.395722    2.264004     6.800 1.20e-11 ***
P4 S-WWR+30%    | 0.8 D/h     15.630377    2.217652     7.048 2.12e-12 ***
P4 S-WWR BL    | 0.4 D/h      2.612797    2.012680     1.298 0.194303
P4 S-WWR BL    | 0.6 D/h      4.092515    2.157573     1.897 0.057924 .
P4 S-WWR BL    | 0.8 D/h      2.636375    2.174162     1.213 0.225356
P5 E-WWR-30%    | BL D/h      1.383288    2.130258     0.649 0.516148
P5 E-WWR-30%    | 0.2 D/h     -0.489009    2.051326    -0.238 0.811593
P5 E-WWR-30%    | 0.4 D/h      4.612417    1.928121     2.392 0.016794 *
P5 E-WWR-30%    | 0.6 D/h      1.962588    1.903437     1.031 0.302567
P5 E-WWR-50%    | BL D/h     -10.705046    1.595802    -6.708 2.24e-11 ***
P5 E-WWR-50%    | 0.2 D/h     -8.096562    1.791866    -4.519 6.41e-06 ***
P5 E-WWR-50%    | 0.4 D/h     -6.720278    1.956024    -3.436 0.000597 ***
P5 E-WWR-50%    | 0.6 D/h     -2.857163    2.000325    -1.428 0.153269
P5 E-WWR+30%    | BL D/h     19.375854    1.951274     9.930 < 2e-16 ***
P5 E-WWR+30%    | 0.2 D/h     23.884985    2.031670    11.756 < 2e-16 ***
P5 E-WWR+30%    | 0.4 D/h     31.511788    2.261004    13.937 < 2e-16 ***
P5 E-WWR BL    | 0.2 D/h      6.751175    1.845121     3.659 0.000256 ***
P5 E-WWR BL    | 0.4 D/h     13.232263    1.877958     7.046 2.15e-12 ***
P6 W-WWR-30%    | BL D/h     -4.476417    1.999653    -2.239 0.025236 *
P6 W-WWR-30%    | 0.2 D/h     -1.672168    2.019000    -0.828 0.407597
P6 W-WWR-30%    | 0.4 D/h     -3.715178    2.024700    -1.835 0.066590 .
P6 W-WWR-30%    | 0.6 D/h     -2.460374    1.899861    -1.295 0.195384
P6 W-WWR-50%    | BL D/h    -10.884551    1.709636    -6.367 2.15e-10 ***
P6 W-WWR-50%    | 0.2 D/h    -10.316160    1.711701    -6.027 1.82e-09 ***
P6 W-WWR-50%    | 0.4 D/h     -9.483356    1.769362    -5.360 8.80e-08 ***
P6 W-WWR-50%    | 0.6 D/h     -6.969338    1.924060    -3.622 0.000296 ***
P6 W-WWR+30%    | BL D/h     12.647960    1.944593     6.504 8.76e-11 ***
P6 W-WWR+30%    | 0.2 D/h     14.958688    1.927152     7.762 1.05e-14 ***
P6 W-WWR+30%    | 0.4 D/h     18.863094    2.066315     9.129 < 2e-16 ***
P6 W-WWR BL    | 0.2 D/h      3.338557    2.006165     1.664 0.096160 .
P6 W-WWR BL    | 0.4 D/h      2.680807    1.925349     1.392 0.163886
P7 IWI 0.05     4.052111    1.158197     3.499 0.000473 ***
P7 IWI 0.08     3.473002    1.337273     2.597 0.009436 **
P7 IWI 0.12     2.868941    1.116357     2.570 0.010208 *
P8 Roof XPS 0.12 6.791206    1.089998     6.230 5.13e-10 ***
P8 Roof XPS 0.15 4.503639    1.255517     3.587 0.000338 ***
P8 Roof XPS 0.18 8.641484    1.108223     7.798 7.97e-15 ***
P9 0.287 | 0.1 ACH -32.208650    1.078056   -29.877 < 2e-16 ***
P9 0.549 | 0.4 ACH -18.667768    1.263950   -14.769 < 2e-16 ***
P10 MVHR Nightcycle | NV BL 37.801620    2.535416    14.909 < 2e-16 ***
P10 MVHR Nightcycle | NV dT 22.888665    2.108246    10.857 < 2e-16 ***
P10 MVHR Weekday | NV BL   8.431408    1.757001     4.799 1.65e-06 ***
P10 MVHR Weekday | NV dT  -23.856326    1.756641   -13.581 < 2e-16 ***
P10 MVHR Weekday | NV Nightpurge 42.882245    2.143966    20.001 < 2e-16 ***
P10 MVHR Weekend | NV BL  47.455253    2.357482    20.130 < 2e-16 ***
P10 MVHR Weekend | NV dT  21.251099    2.643993     8.038 1.19e-15 ***
P10 MVHR Weekend | NV Nightpurge 66.786877    2.447483    27.288 < 2e-16 ***
P10 No MVHR | NV Nightpurge -8.932245    1.677937    -5.323 1.07e-07 ***
---
Signif. codes:  0 *** 0.001 ** 0.01 * 0.05 .

Residual standard error: 22.34 on 4046 degrees of freedom
Multiple R-squared:  0.7869,    Adjusted R-squared:  0.7836
F-statistic: 237.1 on 63 and 4046 DF,  p-value: < 2.2e-16

```

Figure J.2: CS2 scenario 1 linear regression model statistics for LCC.

Appendix K

CS3 Results

K.0.1 Scenario 1: Linear Regression Statistical Output

```

Call:
lm(formula = t1 ~ P1 + P2 + P3 + P4 + P5 + P6 + P7 + P8 + P9 +
    P10, data = data)

Residuals:
    Min       1Q   Median       3Q      Max
-39.972  -2.837   0.167   3.440  38.989

Coefficients:
              Estimate Std. Error t value Pr(>|t|)
(Intercept)    1163.0062     3.8553  301.667 < 2e-16 ***
P1 Triple      -14.2094     0.6763  -21.009 < 2e-16 ***
P2 SHGC 0.3      1.4592     0.6431   2.269  0.02350 *
P3 NW-WWR-50%   -0.2436     0.7592  -0.321  0.74844
P4 SW-WWR-30%    0.8856     3.6280   0.244  0.80722
P4 SW-WWR-30%    0.4 D/h    -0.7241     3.5387  -0.205  0.83790
P4 SW-WWR-30%    0.6 D/h   -10.3850     3.8645  -2.687  0.00733 **
P4 SW-WWR-30%    0.8 D/h    -5.7994     3.9646  -1.463  0.14387
P4 SW-WWR-30%    BL D/h    -5.1367     3.7152  -1.383  0.16712
P4 SW-WWR-50%    0.2 D/h    -4.2894     2.9126  -1.473  0.14117
P4 SW-WWR-50%    0.4 D/h    -2.3283     3.1254  -0.745  0.45648
P4 SW-WWR-50%    0.6 D/h    -2.4492     3.3871  -0.723  0.46981
P4 SW-WWR-50%    0.8 D/h    -4.6197     3.3572  -1.376  0.16913
P4 SW-WWR-50%    BL D/h    -3.4327     2.6940  -1.274  0.20291
P4 SW-WWR+30%    BL D/h     6.5706     3.2048   2.050  0.04062 *
P4 SW-WWR+30%    0.2 D/h     7.9496     3.1938   2.489  0.01298 *
P4 SW-WWR+30%    0.4 D/h     5.3687     3.4112   1.574  0.11587
P4 SW-WWR+30%    0.6 D/h     8.2408     3.8231   2.156  0.03138 *
P4 SW-WWR+30%    0.8 D/h     6.1183     3.4497   1.774  0.07647 .
P4 SW-WWR BL     0.2 D/h     2.1908     3.8771   0.565  0.57216
P4 SW-WWR BL     0.4 D/h     5.6887     3.8749   1.468  0.14242
P4 SW-WWR BL     0.6 D/h     1.1677     4.2347   0.276  0.78281
P4 SW-WWR BL     0.8 D/h     2.9394     3.0258   0.971  0.33158
P5 SE-WWR-30%    0.2 D/h    -2.6296     3.3425  -0.787  0.43164
P5 SE-WWR-30%    0.4 D/h    -2.4396     3.1682  -0.770  0.44149
P5 SE-WWR-30%    0.6 D/h    -1.9003     3.5400  -0.537  0.59153
P5 SE-WWR-30%    0.8 D/h    -4.4474     3.5301  -1.260  0.20804
P5 SE-WWR-30%    BL D/h    -2.5445     3.2178  -0.791  0.42928
P5 SE-WWR-50%    0.2 D/h    -2.1377     2.8537  -0.749  0.45399
P5 SE-WWR-50%    0.4 D/h    -1.0763     2.5368  -0.424  0.67147
P5 SE-WWR-50%    0.6 D/h    -0.2982     2.7586  -0.108  0.91394
P5 SE-WWR-50%    0.8 D/h    -2.5908     3.1586  -0.820  0.41230
P5 SE-WWR-50%    BL D/h     0.3731     3.1924   0.117  0.90700
P5 SE-WWR+30%    BL D/h    -1.3656     3.1765  -0.430  0.66736
P5 SE-WWR+30%    0.2 D/h    -4.2621     3.1670  -1.346  0.17870
P5 SE-WWR+30%    0.4 D/h    -0.3174     3.1162  -0.102  0.91890
P5 SE-WWR+30%    0.6 D/h    -2.8802     3.3854  -0.851  0.39512
P5 SE-WWR+30%    0.8 D/h    -0.7152     3.0898  -0.231  0.81700
P5 SE-WWR BL     0.2 D/h    -3.3055     3.4274  -0.964  0.33508
P5 SE-WWR BL     0.4 D/h    -1.4907     2.8961  -0.515  0.60686
P5 SE-WWR BL     0.6 D/h     8.7586     3.5334   2.479  0.01336 *
P5 SE-WWR BL     0.8 D/h     0.3678     3.0725   0.120  0.90473
P6 NE-WWR -50%   -3.7088     0.6656  -5.572  3.3e-08 ***
P7 IWI -0.05     2.5228     0.7959   3.170  0.00158 **
P7 IWI 0.05      1.0625     0.9789   1.085  0.27799
P7 IWI 0.08      3.5436     1.2666   2.798  0.00525 **
P8 Roof XPS 0.05  1.5341     0.8473   1.811  0.07053 .
P8 Roof XPS 0.08  0.1677     0.8877   0.189  0.85022
P8 Roof XPS 0.12  1.9650     0.9756   2.014  0.04429 *
P9 0.219 | 1 m3/h-m2 NCM at 50 Pa -45.6313     0.7938  -57.484 < 2e-16 ***
P9 0.378 | 3 m3/h-m2 NCM at 50 Pa -24.8756     0.8566  -29.039 < 2e-16 ***
P10 MVHR Nightcycle | NV BL 164.6142     1.1519  142.901 < 2e-16 ***
P10 MVHR Nightcycle | NV dT 142.6218     1.8532   76.958 < 2e-16 ***
P10 MVHR Weekday | NV BL 12.0942     1.1701   10.336 < 2e-16 ***
P10 MVHR Weekday | NV dT -35.3772     1.1614  -30.461 < 2e-16 ***
P10 MVHR Weekday | NV Nightpurge 58.6891     1.2420   47.253 < 2e-16 ***
P10 No MVHR | NV Nightpurge -2.2564     0.9416  -2.396  0.01676 *
---
Signif. codes:  0 '***' 0.001 '**' 0.01 '*' 0.05 '.'

Residual standard error: 9.5 on 925 degrees of freedom
Multiple R-squared:  0.9836,    Adjusted R-squared:  0.9826
F-statistic: 988.6 on 56 and 925 DF, p-value: < 2.2e-16

```

Figure K.1: CS3 NGB scenario 1 linear regression model statistics for LCCF.

```

Call:
lm(formula = t2 ~ P1 + P2 + P3 + P4 + P5 + P6 + P7 + P8 + P9 +
    P10, data = data)

Residuals:
    Min       1Q   Median       3Q      Max
-14.4156  -2.2956   0.2392   1.8650  26.0805

Coefficients:
(Intercept)              761.3439      1.7150 443.943 < 2e-16 ***
P1 Triple              18.6918      0.3009  62.128 < 2e-16 ***
P2 SHGC 0.3              0.5010      0.2861   1.751 0.080268 .
P3 NW-WWR-50%          -23.3891      0.3377 -69.252 < 2e-16 ***
P4 SW-WWR-30% | 0.2 D/h  -11.5000      1.6139  -7.126 2.08e-12 ***
P4 SW-WWR-30% | 0.4 D/h   -8.5578      1.5741  -5.437 6.95e-08 ***
P4 SW-WWR-30% | 0.6 D/h  -12.1782      1.7191  -7.084 2.77e-12 ***
P4 SW-WWR-30% | 0.8 D/h   -7.2078      1.7636  -4.087 4.75e-05 ***
P4 SW-WWR-30% | BL D/h   -11.4007      1.6527  -6.898 9.75e-12 ***
P4 SW-WWR-50% | 0.2 D/h  -17.7438      1.2956 -13.695 < 2e-16 ***
P4 SW-WWR-50% | 0.4 D/h  -16.6239      1.3903 -11.957 < 2e-16 ***
P4 SW-WWR-50% | 0.6 D/h  -15.5927      1.5067 -10.349 < 2e-16 ***
P4 SW-WWR-50% | 0.8 D/h  -13.3622      1.4934  -8.948 < 2e-16 ***
P4 SW-WWR-50% | BL D/h  -18.1654      1.1984 -15.158 < 2e-16 ***
P4 SW-WWR+30% | BL D/h    8.2779      1.4256   5.807 8.76e-09 ***
P4 SW-WWR+30% | 0.2 D/h    8.9307      1.4207   6.286 5.01e-10 ***
P4 SW-WWR+30% | 0.4 D/h    7.7184      1.5174   5.086 4.42e-07 ***
P4 SW-WWR+30% | 0.6 D/h   11.5841      1.7007   6.812 1.74e-11 ***
P4 SW-WWR+30% | 0.8 D/h   12.1763      1.5346   7.935 6.08e-15 ***
P4 SW-WWR BL | 0.2 D/h   -0.7865      1.7247  -0.456 0.648466
P4 SW-WWR BL | 0.4 D/h    3.8501      1.7237   2.234 0.025743 *
P4 SW-WWR BL | 0.6 D/h   -0.5183      1.8837  -0.275 0.783286
P4 SW-WWR BL | 0.8 D/h    4.0900      1.3460   3.039 0.002443 **
P5 SE-WWR-30% | 0.2 D/h   -2.8396      1.4868  -1.910 0.056470 .
P5 SE-WWR-30% | 0.4 D/h   -3.6416      1.4093  -2.584 0.009921 **
P5 SE-WWR-30% | 0.6 D/h   -2.3745      1.5747  -1.508 0.131934
P5 SE-WWR-30% | 0.8 D/h   -3.6953      1.5703  -2.353 0.018817 *
P5 SE-WWR-30% | BL D/h   -3.7182      1.4314  -2.598 0.009536 **
P5 SE-WWR-50% | 0.2 D/h   -6.0469      1.2694  -4.763 2.21e-06 ***
P5 SE-WWR-50% | 0.4 D/h   -4.9587      1.1285  -4.394 1.24e-05 ***
P5 SE-WWR-50% | 0.6 D/h   -4.9087      1.2271  -4.000 6.83e-05 ***
P5 SE-WWR-50% | 0.8 D/h   -3.1803      1.4051  -2.263 0.023841 *
P5 SE-WWR-50% | BL D/h   -4.2567      1.4201  -2.997 0.002795 **
P5 SE-WWR+30% | BL D/h    3.7954      1.4130   2.686 0.007361 **
P5 SE-WWR+30% | 0.2 D/h    1.9616      1.4088   1.392 0.164136
P5 SE-WWR+30% | 0.4 D/h    3.1325      1.3862   2.260 0.024064 *
P5 SE-WWR+30% | 0.6 D/h    2.1821      1.5059   1.449 0.147669
P5 SE-WWR+30% | 0.8 D/h    3.8688      1.3744   2.815 0.004984 **
P5 SE-WWR BL | 0.2 D/h   -3.0952      1.5246  -2.030 0.042630 *
P5 SE-WWR BL | 0.4 D/h    0.5813      1.2883   0.451 0.651936
P5 SE-WWR BL | 0.6 D/h    3.2258      1.5718   2.052 0.040420 *
P5 SE-WWR BL | 0.8 D/h    1.1638      1.3668   0.851 0.394722
P6 NE-WWR-50%           4.1630      0.2961 14.061 < 2e-16 ***
P7 IWI -0.05          -5.0412      0.3540 -14.239 < 2e-16 ***
P7 IWI 0.05           4.0512      0.4354   9.304 < 2e-16 ***
P7 IWI 0.08           5.6485      0.5634 10.025 < 2e-16 ***
P8 Roof XPS 0.05       4.0887      0.3769 10.848 < 2e-16 ***
P8 Roof XPS 0.08       5.0675      0.3949 12.833 < 2e-16 ***
P8 Roof XPS 0.12       6.3385      0.4340 14.605 < 2e-16 ***
P9 0.219 | 1 m3/h-m2 NCM at 50 Pa 3.7637      0.3531 10.659 < 2e-16 ***
P9 0.378 | 3 m3/h-m2 NCM at 50 Pa 1.4856      0.3811   3.899 0.000104 ***
P10 MVHR Nightcycle | NV BL 121.7383      0.5124 237.572 < 2e-16 ***
P10 MVHR Nightcycle | NV dT 122.1164      0.8244 148.130 < 2e-16 ***
P10 MVHR Weekday | NV BL 112.1468      0.5205 215.464 < 2e-16 ***
P10 MVHR Weekday | NV dT 150.8932      0.5166 292.076 < 2e-16 ***
P10 MVHR Weekday | NV Nightpurge 113.8355      0.5525 206.038 < 2e-16 ***
P10 No MVHR | NV Nightpurge -3.1400      0.4189  -7.496 1.54e-13 ***
---
Signif. codes:  0 '***' 0.001 '**' 0.01 '*' 0.05 '.'

Residual standard error: 4.226 on 925 degrees of freedom
Multiple R-squared:  0.9963,    Adjusted R-squared:  0.996
F-statistic: 4416 on 56 and 925 DF, p-value: < 2.2e-16

```

Figure K.2: CS3 NGB scenario 1 linear regression model statistics for LCC.